The Republic of Iraq
Ministry of Higher Education and Scientific Research
University of Babylon - College of Science
Department of Chemistry

Synthesis of New Tin Compounds and Study their Applications as Photo Stabilizers for Poly (vinyl chloride) and Antioxidant

A Thesis

Submitted to the College of Science / University of Babylon

As a partial fulfillment of the Requirements for

The Degree of Philosophic Doctoral in Chemistry

BY

Rafid Rayyis Arraq Thahy

B.Sc. Chemistry Science- Babylon University (2007)

M.Sc. Chemistry Science- Babylon University (2019)

Supervisor

Asst. Prof. ***Angham Ghanim Hadi*** (Ph.D.)

2023 AD ***1445 AH***

بِسْمِ اللّهِ الرَّحْمَنِ الرَّحِيمِ

وَلَسَوْفَ يُعْطِيكَ رَبُّكَ فَتَرْضَىٰٓ ﴿٥﴾

صَدقَ الله العَلي العَظيم

سُورَةُ الضُّحَىٰ

Certification

I'm certify that this thesis was prepared under my supervision at the Department of Chemistry, the College of Science at the University of Babylon as a partial requirement for the degree of Doctor of Philosophy in Science of Chemistry and this work has never been published anywhere else.

Signature:

Name: **Dr. Angham G. Hadi**

Scientific order: Assistant Professor

Address: University of Babylon

Collage of Science, Department of Chemistry

Date: / /2023

In the view of the available recommendation, I forward this thesis for debate by the examining committee.

Signature:

Name: **Dr. Abbas Jasim Atiyah**

Scientific order: Professor

Address: University of Babylon

College of Science, Department of Chemistry

Date: / / 2023

Dedication

This effort is respectively dedicated to whom never hesitated to provide me with what consolidates advance in my life, the soul of my father ,to the precious heart and paradise on earth , my mother, , to my lovely brothers and sisters, to the secret of my happiness, who have emotionally supported me and been enduring me throughout the period of my PhD., my wife, and my children. May Allah bless them all and keep them safe.

Acknowledgements

Praise and thanks are first due to Allah Almighty for blessing me with patience and endurance to accomplish the present study.

My profoundest gratitude is to my supervisor **Asst.prof. Dr. Angham Ghanim Hadi** for her extremely intellectual and stimulating generosity, discussions, encouragements, comments, and the time she spent in helping me to enrich this work.

I would like to extend my sincere gratitude to the Department of Chemistry in the University of Babylon.

My thanks are owed to Head of Chemistry Department **Prof. Dr. Abbas Jassim Atiyah.**

I have been fortunate enough to receive help from some excellent people especially my great teacher **Prof. Dr. Mahmood Hussein Hadwan.**

A special thanks go to anyone who gave me help in my study.

Rafid Rayyis Arraq

Summary

Twelve organotin (IV) complexes were successfully synthesized by condensation reactions of ligand (Cephalexin, Tyrosine) with aromatic and aliphatic organotin (IV) compounds dissolved in methanol. FTIR spectroscopy, nuclear magnetic resonance (^{1}H, ^{13}C, ^{119}Sn-NMR) and elemental analysis were used to characterize these compounds. The prepared complexes are used as stabilizers to inhibit photo degradation of poly (vinyl chloride) films (40 μm thickness) when exposed to ultraviolet radiation, leading to weight loss, growth of specific functional groups (I_{OH}, $I_{C=O}$, and $I_{C=C}$), as well as changes in the chemical structure. The surface morphology of the PVC films was observed using a microscope, atomic force microscopy and a scanning electron microscopy. PVC containing organotin (IV) complexes exhibited fewer surface cracks and damage than blank film. The most effective photo stabilizer for poly (vinyl chloride) films was Me_2SnL_2-Cephalexin complex due to the presence of more methyl groups that have less steric hindrance and heteroatoms that allow polar interactions with PVC. The roughness factor for the PVC (pure) after 300 hours of irradiation was significant (Rq =316.2) compared to the one for the Me_2SnL_2 complex (Rq = 67.2). The study of antioxidant activity to organotin (IV) complexes compares with tannic acid using DPPH and CUPRAC methods. Organotin (IV) complexes exhibit greater antioxidant activity than a ligand against the stable free radical DPPH because of the metal moiety present in the complexes. The reported IC_{50} values of the complexes remained lower than those of tannic acid (a reference antioxidant). The complex Me_3SnL-Cephalexin has a high antiradical power (ARP) and low IC_{50}, as shown by the results of the DPPH and Cuprac tests. So, at low concentrations of 40 and 50 μg/mL, exhibits a larger percentage of scavenging activity.

List of Contents

Chapter One- Introduction

Chapter Two- Experimental

List of Abbreviations

Descriptions	*Abbreviations*
Antiradical Power	*ARP*
Atomic Force Microscope	*AFM*
Butyl	*Bu*
Carbonyl Index	$I_{C=O}$
Coupling Constant	*J*
Fourier Transformed Infrared Spectroscopy	*FTIR*
2, 2-Diphenyl-1-Picrylhydrazyl	*DPPH*
Hydroxyl Index	I_{OH}
Inhibitory Concentration Value 50%	IC_{50}
Ligand	*L*
Methyl	*Me*
Phenyl	*Ph*
Polyene Index	$I_{C=C}$
Poly (vinyl chloride)	*PVC*
Q panel company- ultraviolet radiation	*Q-UV*
Reactive oxygen species	*ROS*
Roughness Factor	*Rq*
Scanning Electron Microscopy	*SEM*
Tetramethyl Silane	*TMS*

List of Tables

List of Figures

List of schemes

1.1 Tin Chemistry

Tin is listed in group fourteen of the periodic table, among the elements carbon, silicon, germanium, and lead. Tin (Sn, Stannum) is the forty-nine most abundant element in the earth's crust. It contains a soft, silvery white mineral that is relatively inert to air and water at ambient temperature but oxidizes to tin dioxide (SnO_2) above 200°C. It has four electrons in the outer electronic shell as the following electronic arrangement: [Kr] $_{36}$ $4d^{10}$ $5s^2$ $5p^2$. Therefore, tin exists in two stable oxidation states: Sn^{+2} (Stannous) and Sn^{+4} (Stannic). It appears that practically all organotin compounds have a tetravalent structure because tin (II) compounds are easily oxidized to tin (IV). Hence, tetravalent tin atoms have tetrahedral geometry and undergo sp^3 hybridization [1, 2]. As shown in Fig. 1.1.

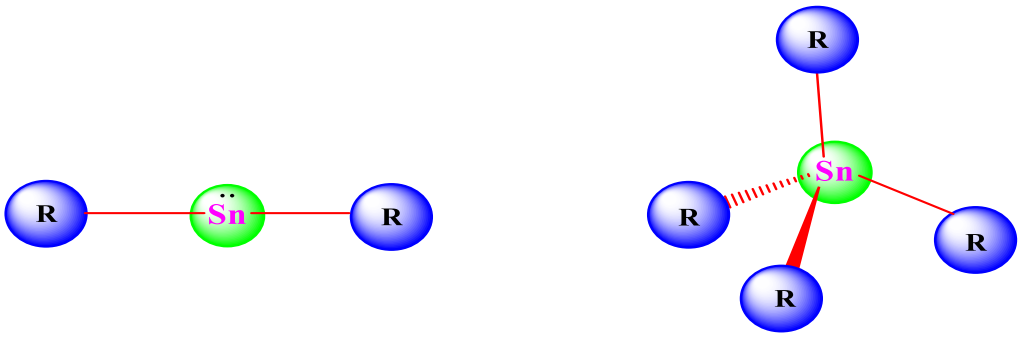

(a) (b)

Figure 1.1 Two Possible Structures of Tin: (a) Bivalent and (b) Tetravalent where R can be any atom or group.

There are two types of tin allotropes. The white tin, often known β-tin, is an electrically conducting silvery metal having a distorted cubic crystal structure at room temperature. It progressively changes below around 13.2 °C to grey tin or called α –tin it is a semiconductor and has a diamond structure. Tin has ten stable isotopes that produce different mass spectra, as illustrated in Table1.1 The isotope ^{119}Sn is mostly used in nuclear magnetic resonance spectroscopy because it has high sensitivity [3].

Table 1.1 Isotopes of Tin.

Isotopes	Mass	Abundance (%)	Spin
112	111.90494	0.95	0
114	113.90296	0.65	0
115	114.90353	0.34	½
116	115.90211	14.24	0
117	116.90306	7.57	½
118	117.90179	24.01	0
119	118.90339	8.58	½
120	119.90213	32.97	0
122	121.90341	4.17	0
124	123.90524	5.98	0

1.2 Organometallic Compounds

Organometallic compounds are chemical compounds that have at least one covalent bond between a metallic element and the carbon atom of organic molecules. Organometallic complexes are divided into two types: those with sigma bonds, which are formed by donating an electron pair from the ligand into an unfilled orbital on the metal center and those with pi bonds, which are formed by moving electrons from an atomic orbital on one atom to an anti-bonding orbital on another atom or ligand, relieving the metal of excess negative charge and increasing the bond order of the M-C bond [4,5].Fig.1.2 depicts one example of CO (ligand donating and accepting) and M (metal).

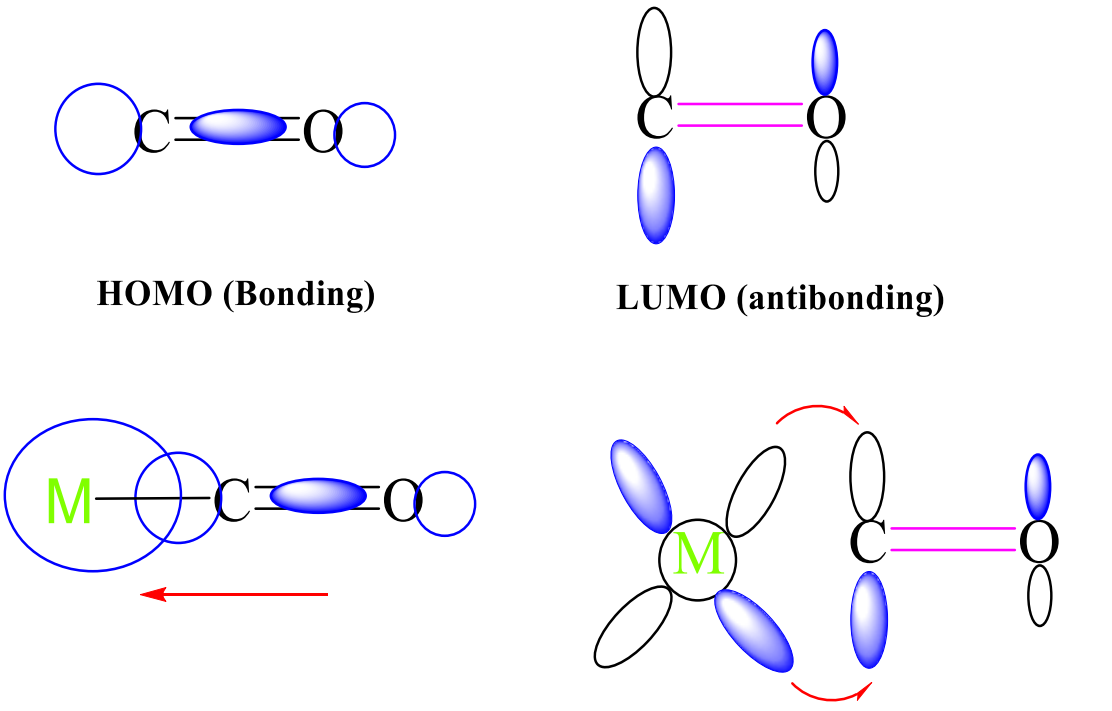

Figure 1.2 Showed Sigma and Pi Bonding between the Metal and Ligand.

The metallic component of organometallic complexes can be transition metals, including commonly occurring d-block elements and some elements involving the lanthanides as Lanthanum (La), Hafnium (Hf) and Osmium (Os) or can be a non-transition metal such as boron (B), aluminum (Al), tin (Sn) and antimony (Sb) [6]. Organometallics have a common structural range from linear to octahedral and even beyond [7]. Organometallic compounds may undergo ligand exchange, which has applications in many disciplines of medical chemistry, particularly in the development of novel chemotherapeutic drugs and in biological activity [8].

1.2.1 Organotin (IV) Compounds

Organotin chemistry is a subfield of organometallic chemistry [9]. Organotin compounds are tetravalent in general and include at least one covalent carbon -tin bond [10]. Edward Frankland discovered the first of these compounds in 1849 and named it diethyltindiiodide ($(C_2H_5)_2SnI_2$) [11]. Lowich discovered in 1852 that alkyl halides react with a tin-sodium alloy to produce tin-alkyl compounds. In 1903, Pope and Peachey published a report on the synthesis of tetra alkyl or tetra aryl stannes using Grignard reagents and alkyl tin halides. This method became the standard for synthesizing organotin compounds [12]. A typical formula for organotin (IV) complexes is $R_xSn\ (L)_{4-x}$, where L is either an organic or inorganic ligand and R is either an aryl or an alkyl group this type of complex includes a tin center link to the anion, usually chloride, oxide, thiolate, hydroxide, and carboxylate [13]. The kind of aryl or alkyl substituents attached to the tin central result in the formation of one or more covalent C-Sn bonds. The biological activities of organotin (IV) compounds have been significantly altered through the addition of these substituents [14].

Organotin (IV) compounds are classified into four types based on the number of organic groups they contain: mono ($RSnX_3$), di (R_2SnX_2), tri (R_3SnX) and tetra (R_4Sn) organotin. These compounds can also be divided into aromatic and aliphatic types [15]. Organotin (IV) compounds have tetrahedral, trigonal bipyramidal and octahedral structures. R_3SnX species have more trigonal bipyramidal five-coordinated structures, whereas R_2SnX_2 complexes have more octahedral six-coordinated structures. They are easily coordinated to appropriate ligands, in contrast to carbon coordination mechanisms, leading to highly coordinated species. Derivatives of organotin (IV) have shown promise as physiologically active metallopharmaceuticals with anticancer activity against a variety of human tumour cell lines. Tributyltin, trimethyltin and triphenyltin are only a few examples of triorganotin (IV) compounds with significant biological activity that are frequently used as biocides. Due to their strong reactivity, diorganotin compounds are used in many applications, including silicon elastomer cold-curing agents, polyurethane foam catalysts and PVC stabilizers [16-18].

1.2.1.1 Organotin (IV) Carboxylates

Organotin (IV) carboxylates are one of the most important types of organotin (IV) compounds. Organotin (IV) carboxylates have attracted increasing attention due to their broad applications in a variety of fields, including biological activity, PVC stabilizers, anti-tumor medications and polymer catalysts. This substance can be monomeric or polymeric. It has three general types: $R_3SnOCOR'$, $R_2Sn\ (OCOR')_2$ and $RSn\ (OCOR')_3$, where R and R' might be the same or different groups [19, 20]. The ability to coordinate through the electron-donating oxygen atoms is one of the unique properties of carboxylic acid precursors, which enables it to serve as a multidentate or bridge-building component in structural materials [21]. The coordination number and environment of the tin atom in organotin (IV) carboxylates can be modified by changing the steric and electronic characteristics of the carboxylic acid ligands and substituents linked to the tin atom [22]. Numerous organotin (IV) carboxylates may be used to scavenge free radicals and lessen oxidative stress on the body. Organotin (IV) carboxylate's biological activity is regulated by the shape, oxidation states, coordination number and kinetic stability of the metal atoms. It is generally known that tin metal, which ranges in coordination number from four to eight forms stable bonds with heteroatoms and carbon atoms [23-25]. Higher coordination numbers can result from intra- or intermolecular interactions, especially in complexes where tin connects to electronegative ligand atoms like oxygen, nitrogen, and sulfur [26].

1.2.2 Geometry of Organotin (IV) Carboxylate

When the effective nuclear charge of tin is high, and an electronegative carboxylate substituent is present, organotin (IV) carboxylate complexes produce a wide variety of structural types. Tetrahedral, trigonal pyramidal and octahedral are the most common tin (IV) structures. Tetraorganotin (IV) compounds were unable to explain the ability to increase the coordination number due to the poor acceptor properties of the tin present, which were based on a decrease in Lewis acidity and the presence of more organic groups at the tin central. Triorganotin (IV) carboxylate prefers tin atom structures with five coordinative trigonal bipyramidal geometries, the organic groups at the equatorial site and the donor atom at the axial sites [27, 28]. The carboxylate ligands bind to the tin atom in six coordinated tin atoms, resulting in an octahedral geometry. Organotin (IV) carboxylates are easily coordinated to suitable ligands, resulting in highly coordinated species because of the ability of the unoccupied orbitals (5d) suitable energy that is shared in tetravalent tin hybridizations illustrated in Fig.1.3. The biological activity of organotin compounds is strongly influenced by the chemical components of the molecule and the coordination number of the tin atom [29].

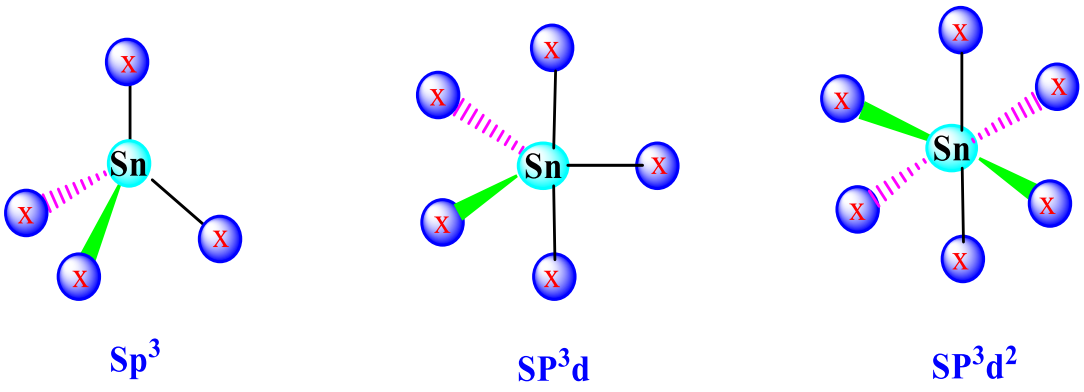

Figure 1. 3 The Principal Coordination Geometries of Tetravalent Tin.

1.3 The Search in literatures for Synthesis Organotin (IV) Complexes.

Farina *et al*. created the diorganotin (IV) carboxylate by mixing organotin derivatives with the ligand N-methyl-m-nitrobenzohydroxamic acid. The ligand formed a five-member ring chelate when it bonded to the tin atom through oxygen atoms as shown in Fig.1.4. The complexes were studied using physicochemical methods (elemental analysis and electrolytic conductance) as well as spectral methods including UV-Visible, IR, (^{1}H, ^{13}C and ^{119}Sn-NMR). Monomer structures, bidentate and octahedral geometries were suggested for the compounds produced [30].

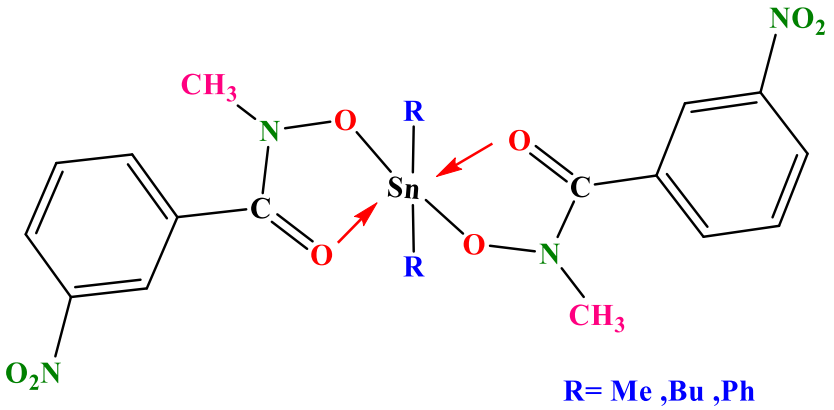

Figure 1.4 Diorganotin (IV)-N-methyl-M-nitrobenzohydroxamic acid Complexes.

Yousif E. *et al*. created complexes of the type R_2SnL_2, where R was phenyl, butyl and methyl and Ligand was 2-thioacetic-5-phenyl-1, 3, 4-oxadiazole. These complexes were identified via spectral techniques including UV-Visible, IR, and (^{1}H, ^{13}C, ^{119}Sn-NMR). Also used physicochemical methods (elementary analysis, electrolytic conductance). The complexes that were produced, monomer structures, bidentate and octahedral geometries were proposed [31]. As shown in Fig. 1.5.

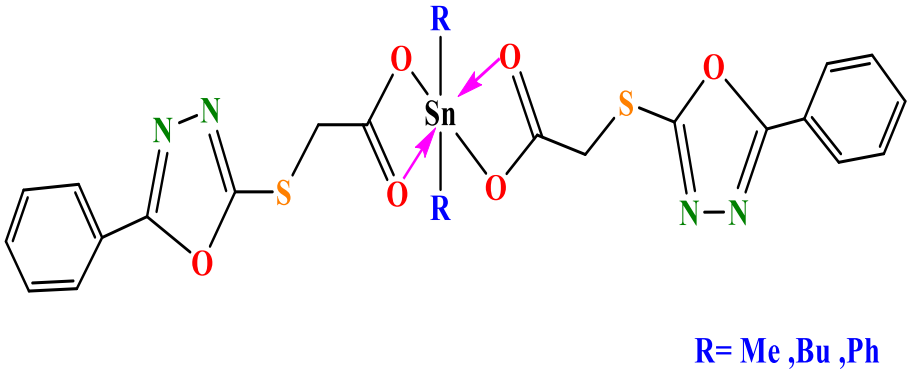

Figure 1.5 Diorganotin (IV) - 2-Thioacetic-5-Phenyl-1, 3, 4-Oxadiazole Complexes.

Angham G. *et al*. synthesized the diorganotin (IV) complexes in 79-86% yield by reacting excess naproxen with organotin (IV) chlorides. Complexes were identified via elemental analysis, infrared radiation, and nuclear magnetic resonance (^{1}H, ^{13}C, ^{119}Sn) techniques [32]. An octahedral geometry was proposed for the synthesized organotin (IV) complexes. As displayed in Fig.1.6.

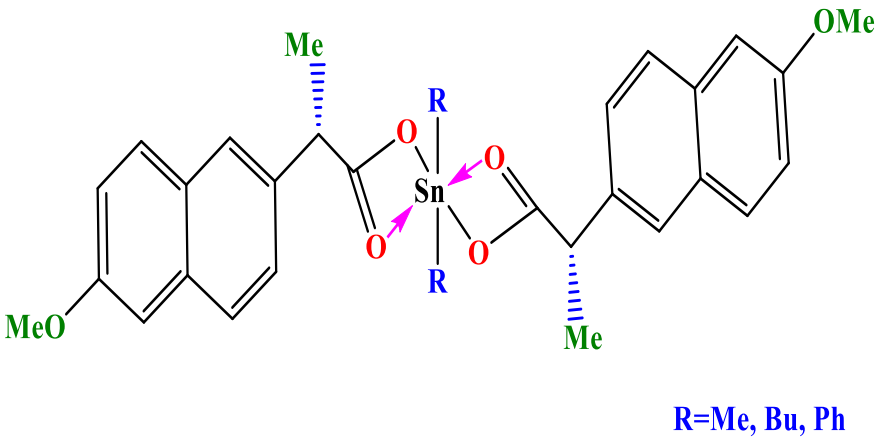

Figure 1.6 Diorganotin (IV) Naproxen Complexes.

Shaheen F. *et al*. created triorganotin (IV) complexes by refluxing the sodium salt of 3- (1H-indol-3-yl) propanoic acid with triorganotin (IV) chloride in dry toluene for 6-7 hours. The solvent was evaporated in a vacuum. Elemental analysis (CHN), FTIR, ^{1}H, ^{13}C and ^{119}Sn NMR spectroscopies were used to characterize the formed complexes [33]. The triorganotin (IV) complexes propose a trigonal bipyramidal geometry, as shown in Fig. 1.7.

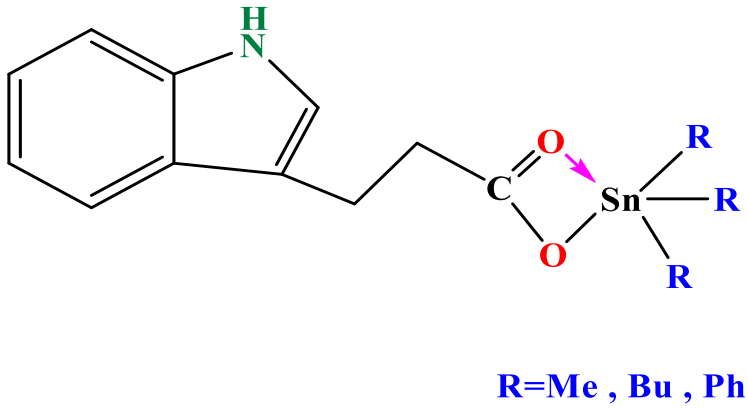

Figure 1.7 Triorganotin (IV) - 3- (1H-indol-3-yl) Propanoate Complexes.

Baraa w. *et al*. created the organotin (IV) complex by reacting triorganotin (IV) chlorides with Ibuprofen as a ligand in the presence of methanol under reflux conditions. The resultant complexes were identified using FTIR, nuclear magnetic resonance (^{1}H, ^{119}Sn) and energy dispersive X-ray techniques [34]. Fig.1.8 depicts the prepared complexes trigonal bipyramidal geometry.

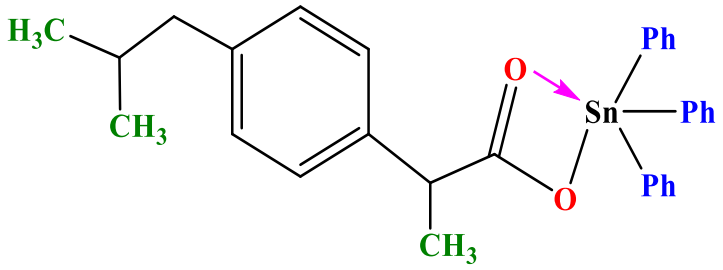

Figure 1.8 Triorganotin (IV) - Ibuprofen Complexes.

Ahmed A. *et al*. synthesized triorganotin (IV) complexes by reacting mefenamic acid as a ligand with several substituted tin (IV) chlorides in boiling methanol, giving the corresponding tin (IV) complexes in 70–77% yields. The complexes were identified by elemental analysis (CHN), FTIR and proton-NMR spectroscopies [35]. The complexes exhibited five coordinated geometries as explained in Fig. 1.9.

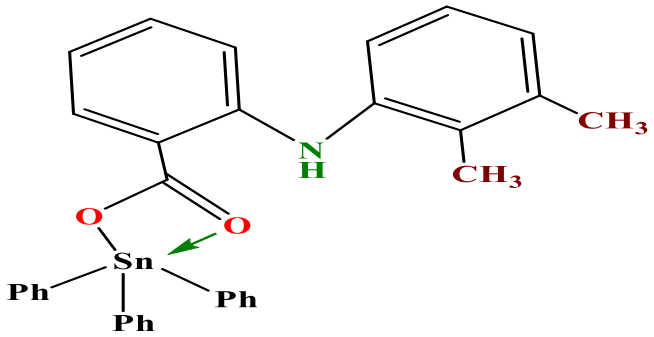

Figure 1.9 Triorganotin (IV) - Mefenamic acid Complexes.

1.4 Poly (Vinyl Chloride)

Poly (vinyl chloride), or write in short PVC, is one of the most important thermoplastic polymers generated on a large scale in the world. PVC can be manufactured as a rigid material with excellent resistance to chemicals and weather or as a flexible material with a low degree of crystallinity [36]. Poly (vinyl chloride) has attracted considerable attention because of its low production cost, simplicity of molding and good physical, mechanical and chemical properties [37]. Baumann was the first person to accidentally produce poly (vinyl chloride) when he created a white solid material from vinyl chloride monomer (VCM) that could resist heat up to 130 °C without decomposing as shown in Fig.1.10 [38]. Plastics output has considerably increased every year. Poly(vinyl chloride) plays a significant role in the industrial production of building materials (e.g., frames for doors, windows, pipes, cables, flooring and wall coverings), electronics (e.g., computers, keyboards, laptops, cellular phones and wires), medical supplies (e.g., bags for plasma and blood, tubing and infusion kits), packaging (cling film, bottles and food bags), plastic cards, apparel, office supplies and sporting equipment [39].

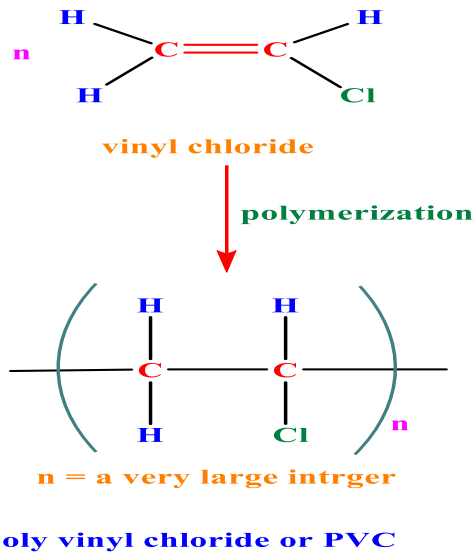

Figure 1.10 Poly (vinyl chloride) Productions.

1.4.1 The Poly (Vinyl Chloride) Stereo Regularity

When discussing the arrangement of side groups around the asymmetric segment of vinyl-type repeat units -CH_2CHR, stereo regularity (also known as tacticity) is used to characterize spatial isomerism in vinyl polymers. As a result, thermoplastics have three distinct polymer chain forms: tactic, isotactic and syndiotactic .The random attachment of the side groups around the backbone chain is described by a tactic form, while side groups that change regularly on both sides of the chain are described in syndiotactic forms and the normal configuration of the side group chloral in Poly(vinyl chloride) polymer has side groups that are all on the same side of the polymer chain in isotactic forms [40, 41]. As shown in Fig.1.11.

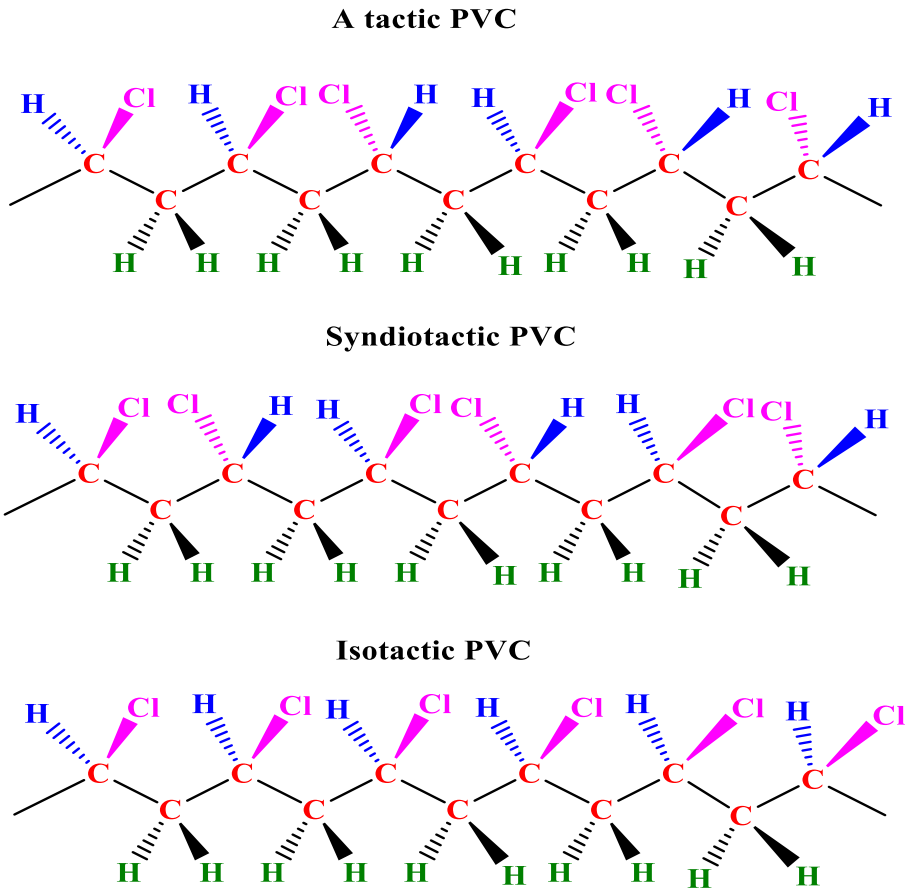

Figure 1.11 The Regular arrangement of Poly (Vinyl Chloride).

1.4.2 Degradation of Poly (Vinyl Chloride)

In general, the term degradation refers to a complicated process in which a polymeric substance exposed to environmental conditions such as moisture, high temperatures and UV radiation undergoes several chemical and physical changes. All industrially produced organic polymers degrade when exposed to sunlight. Bond-breaking reactions are caused by the absorption of near-ultraviolet wavelengths [42, 43]. Poly (vinyl chloride) suffers a very rapid dehydrochlorination and peroxidation process in the presence of oxygen and moisture when exposed to ultraviolet light. Degradation also produces a significant change in mechanical characteristics such as strength, flexibility, colour changes, loss of transparency, bleaching and surface erosion, which are followed by a reduction or elevation in average molecular weight because of chain scission or crosslinking of the polymer molecules. In simple terms, polymer degradation refers to the process of cleaving macromolecules into fragments of diverse structures and sizes. Weathering-related the free-radical process that causes PVC breakdown may be described when enough energy is absorbed to disrupt chemical bonds and expose weak regions to degradation [44, 45].

1.4.3 Types of Polymers Degradation

Polymer degradation frequently starts at the materials surface and progresses within. Multiple mechanisms, such as thermal degradation, photodegradation, radioactive decay, ionizing radiation, and mechanical action, can cause polymers to degrade [46].

1.4.3.1 Thermal Degradation

Thermal degradation is the loss of physical, mechanical, or electrical features caused by the effect of increased temperature on a polymer. The unsaturated form that occurs in a PVC chain after the loss of the first HCl molecule is an allylic chlorine molecule. This allylic chlorine on the other hand, causes the next loss of an HCl molecule and repeated processes results in conjugated double bonds as shown in Scheme 1.1. The elimination of hydrogen chloride, the main volatile product, starts at the glass transition temperature (70°C) [47, 48].

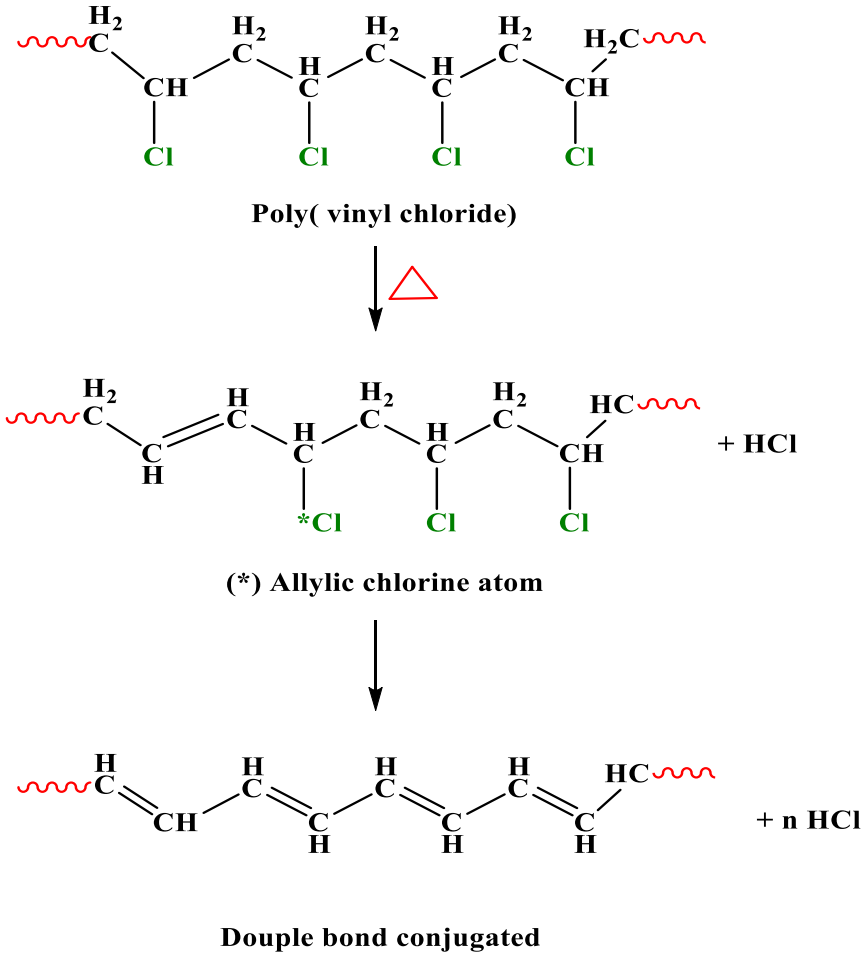

Scheme 1.1 Thermal degradation of Poly (Vinyl Chloride).

1.4.3.2 Photodegradation

Photodegradation is the degradation of a polymeric molecule induced by photon absorption, specifically wavelengths present in sunlight such as infrared, visible, and ultraviolet irradiations. As a result, the polymer chains are broken, radicals are created and the molecular weight was lowered, causing mechanical and physical properties decrease. Photodegradation can occur both in the absence of oxygen (chain breaking or cross-linking) and in the presence of oxygen (photooxidative). In the presence of sunlight, the cleavage of the (C-Cl) bond in PVC chains leads to the generation of the ($Cl^{\bullet}$) radical and the polyene radical [49, 50]. Therefore, excited states will dissipate via several pathways. As shown in Scheme 1.2.

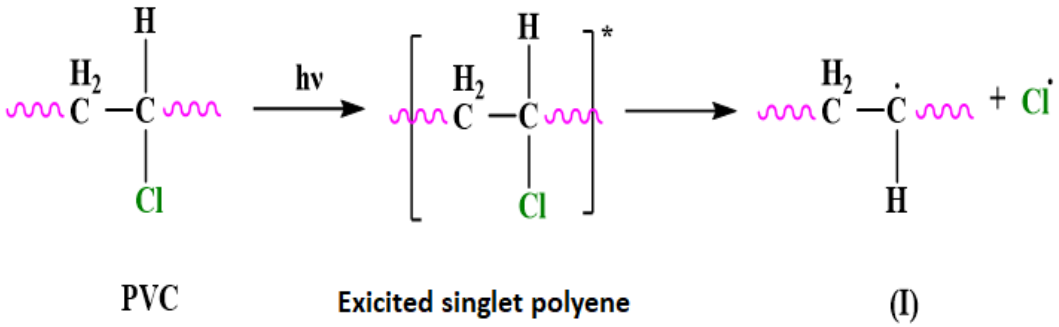

Scheme 1.2 Formation of Polyene Radical.

Polyene radical is very likely to be scavenged by air oxygen to give peroxy radical as illustrated in Scheme 1.3.

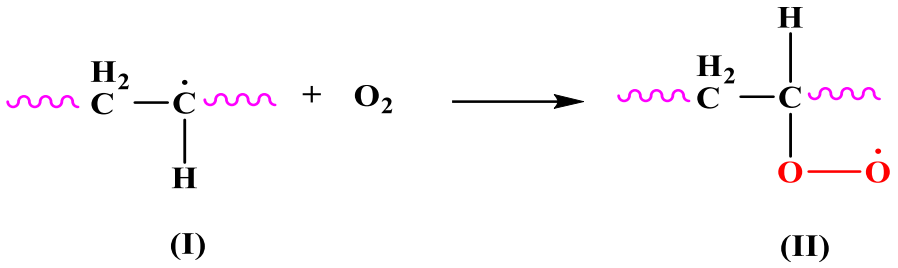

Scheme 1.3 Formation of Peroxy Radical.

The peroxy radical reacts with the CH_2 group in poly vinyl chloride to form hydroperoxide (through hydrogen extraction from PVC) and the poly (vinyl chloride) radical (III) to produce an alkene Scheme1.4. When the peroxy radical reacts with the CH-Cl group, it produces a hydroperoxide group and β-chlorine as shown in Scheme 1.5. The β-chlorine radical is unstable and reacts with oxygen to produce a γ-chloroalkyl peroxy radical (V). As explained in Scheme 1.6.

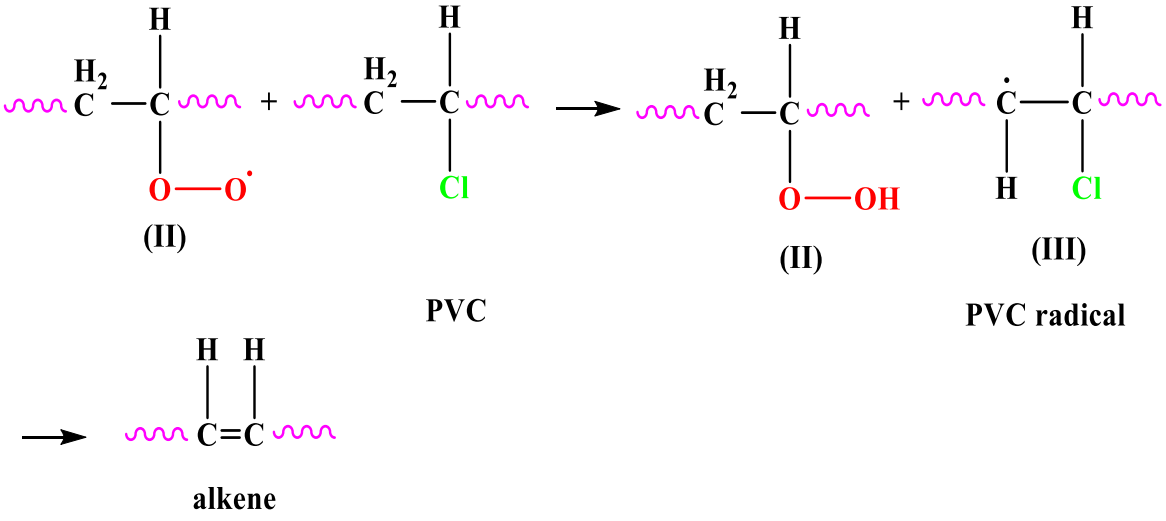

Scheme 1.4 Formation of PVC Radical.

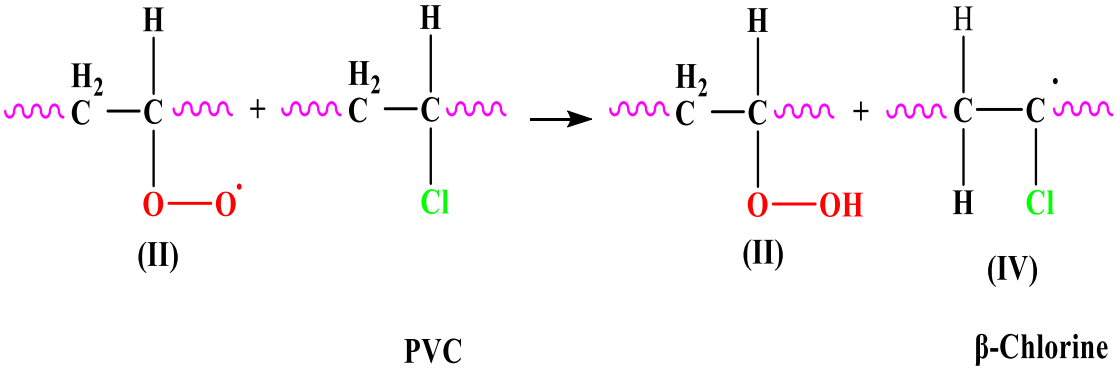

Scheme 1. 5 Formation of β-Chlorine Radical.

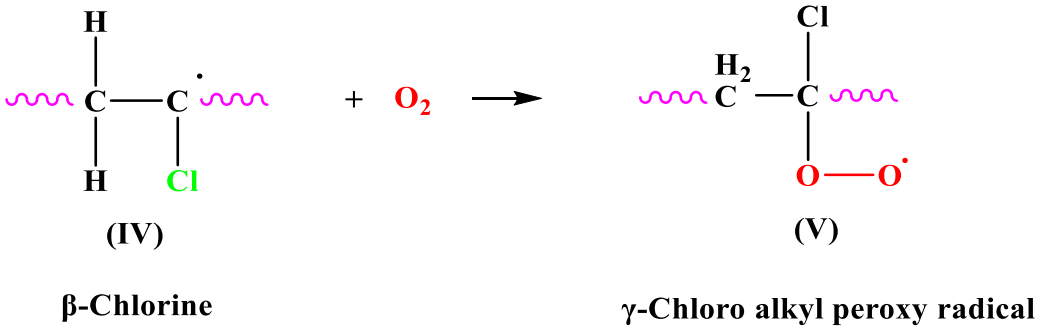

Scheme 1.6 Formation of γ-Chloroalkyl Peroxy Radical.

The bimolecular contact results in the development of a peroxide bridge (termination reaction) are shown in Scheme 1.7.

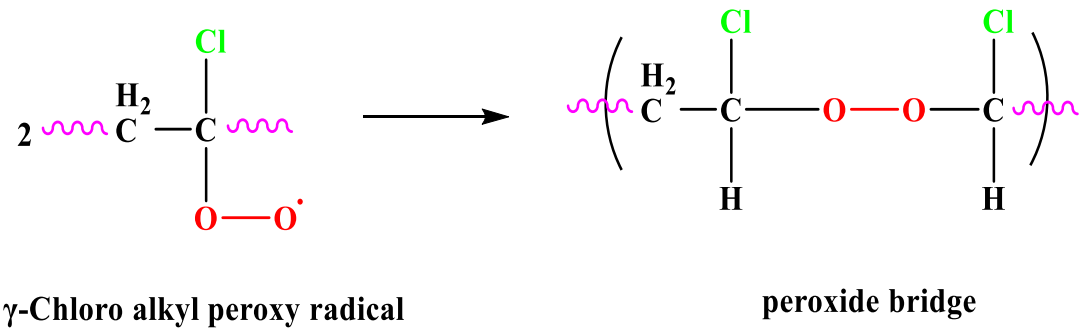

Scheme 1.7 Formation of Peroxide Bridge.

The peroxy (O-O) bond is weak rapidly break lead to formation alkoxy radical (VI) as explained in Scheme 1.8.

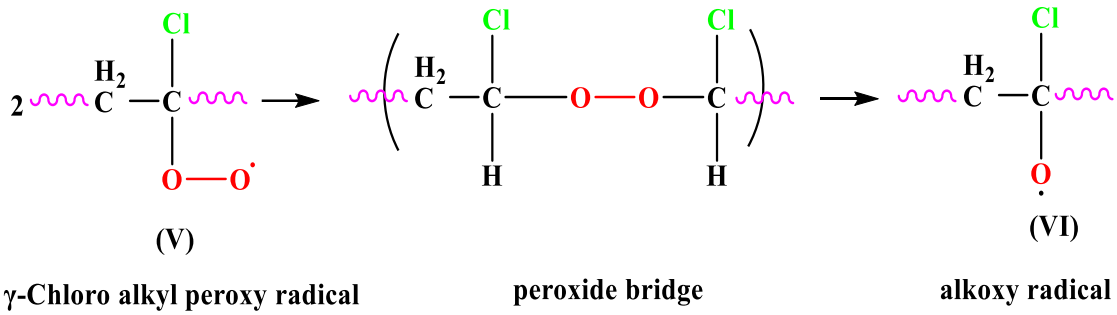

Scheme 1.8 Formation of alkoxy Radicals.

As indicated in Scheme 1.9, an alkoxy radical (VI) is formed by removing hydrogen from PVC to generate α-chloroalcohol, which decomposes rapidly into the appropriate ketone. Tertiary alkoxy radicals are also stabilized by β-scission, which can involve C-Cl bond cleavage to form ketone and alkene via chlorine radical elimination [51, 52].

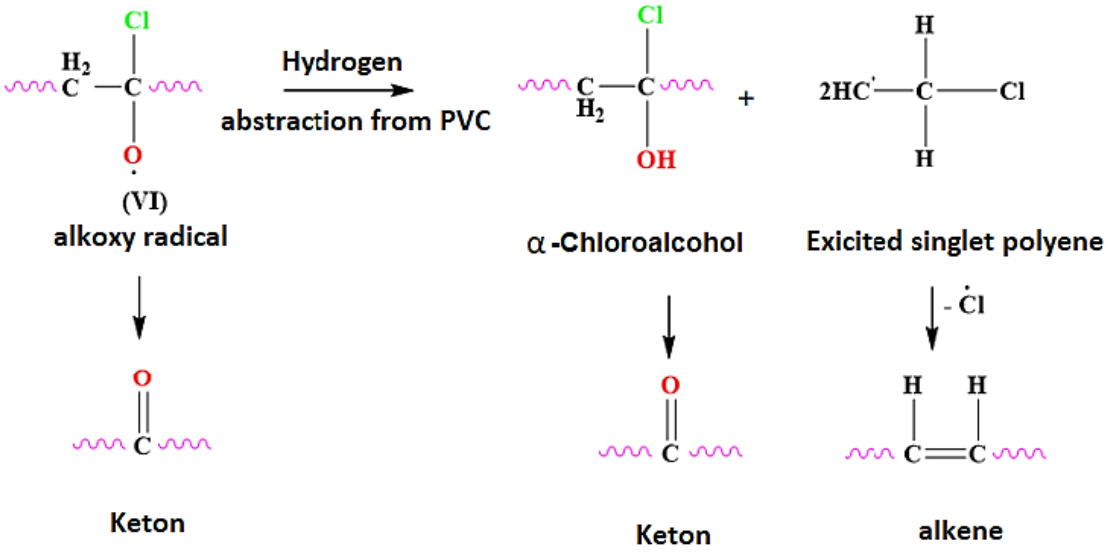

Scheme 1.9 Formation of Ketone and alkene groups.

1.4.4 Classification of Stabilizers for Poly (Vinyl Chloride)

1.4.4.1 Primary Stabilizers

The primary stabilizers prevent further dehydro-chlorination by interacting with allylic chlorine atoms, intermediates in the degradation chain. This process should be faster than chain propagation, requiring a highly active nucleophile. However, the nucleophile's reactivity should not be so strong that it reacts with the secondary chlorine of the PVC chain, which rapidly depletes the stabilizer to be effective; the stabilizer must form complexes with the polymer chlorine atoms, indicating that it has a Lewis acid property [53]. As shown in Scheme 1.10.

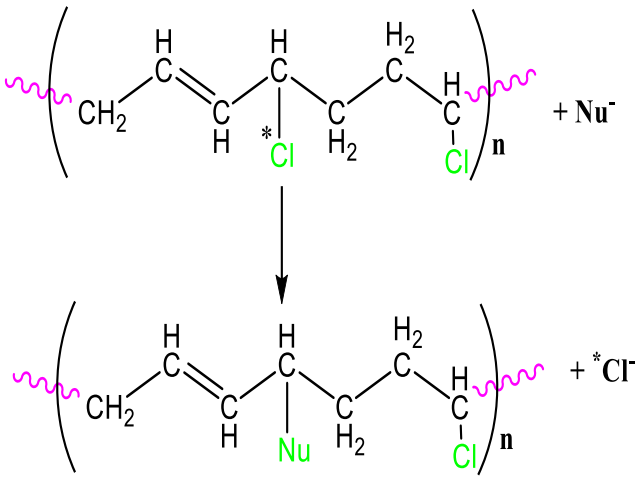

Scheme 1.10 Thermal Stabilizer Mechanism of Poly (Vinyl Chloride) as a Primary Stabilizer.

1.4.4.2 Secondary Stabilizers

Secondary stabilizers function by scavenging the hydrogen chloride radical that is generated by the dehydrochlorination process. Hydrogen chloride scavenging reduces the rate of degradation and prevents the very rapid process that probably results in poly (vinyl chloride) deterioration. Secondary stabilizers should be added to support the primary stabilizers interactions with the allylic chlorine atom of poly (vinyl chloride). In general, the stabilizer is usually added at a quantity of 0.5–2% of the polymer's weight [54]. An example used to describe the mechanism of organotin compounds as primary and secondary stabilizers as shown in Scheme 1.11and eq.1.1. First, the Organotin compound interacts at the polymers allylic defect sites, replacing Cl with an alkyl thiyl group that is less prone to removal.

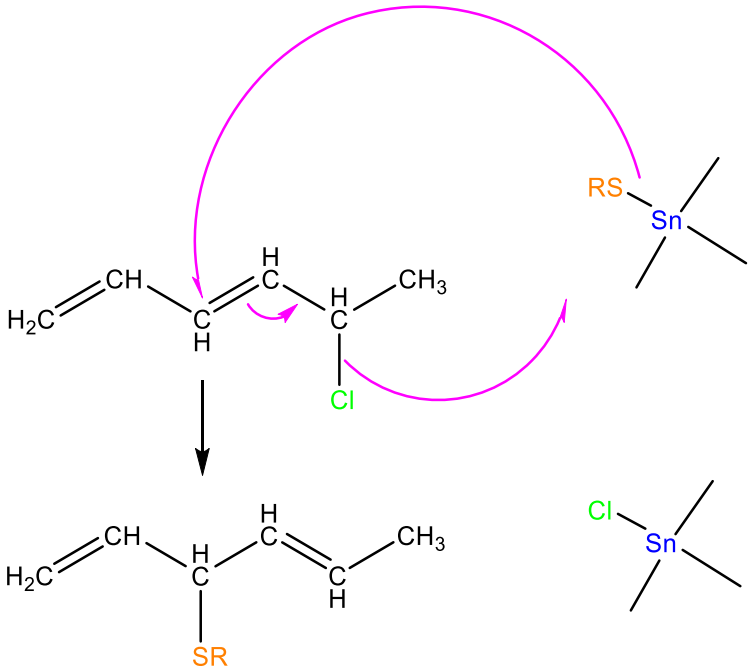

Scheme 1.11 The Mechanism of Organotin Compounds as Primary Stabilizers.

The second effect is the removal of hydrogen chloride, which would normally accelerate the removal process. The stabilizer behavior in this process is described as a secondary stabilizer according to equation (1.1) [55].

$R_2Sn(SR)_2 + HCl \rightarrow R_2Sn(SR)Cl + HSR$ ..... (1.1)

1.4.5 Stabilization of Poly (Vinyl Chloride)

When PVC is exposed to sunlight over a prolonged period, it loses hydrogen chloride from the polymer by autocatalytic dehydrochlorination, leading to defect sites in the polymer chain [56, 57]. To prevent the possibility of degradation, suitable additives are added to poly (vinyl chloride), resulting in a complex polymer with behavior and properties that differ significantly from PVC alone. Polymer stabilizers should be non-volatile and chemically stable, have lower manufacturing costs, be suitable with the polymer and be employed in small quantities [58, 59]. The most common PVC additives include organotin compounds, polyphosphates, Schiff bases and heterocyclic compounds. The skeleton of additives, which contains aromatic residues, is important for improving resistance to oxidants and acting as UV absorbers. Organotin (IV) compounds are common photo stabilizers that assist in the protection of polymers. Since 1940, stabilizers consisting of organotin chemicals have been utilized to prevent this degradation, such as dibutyltin dilaurate, dibutyltin maleate and dibutyltin methyl maleate [60-62]. Organotin (IV) complexes have been evaluated for their effectiveness as photodegradation and photooxidation inhibitors of poly (vinyl chloride). The Table 1.2 displays some additives that were added to the poly (vinyl chloride) to stabilize, modify, or enhance its performance [63].

Table 1.2 The Effect of Additives on Poly (Vinyl Chloride) [64].

Additives	Function	Example
Plasticizers	To soften poly (vinyl chloride) by reducing its glass transition temperature.	phthalates, phosphates, polyesters
Lubricants	To inhibit poly (vinyl chloride) adhesion.	lead and calcium stearates
Stabilizers	Are used to minimize poly (vinyl chloride) photodegradation and it maintain strength, flexibility, and toughness.	fatty acids, Organotin compounds
Fillers	To lower poly (vinyl chloride) manufacturing costs and increase toughness.	metal carbonates, sulfates

1.4.6 Organotin (IV) Complexes as Poly (Vinyl Chloride) Stabilizers

Organotin (IV) compounds act as heat and light stabilizers. Several suggestions have been offered to explain the role of organotin (IV) complexes in stabilized poly (vinyl chloride) films. Tin (IV) a strong Lewis acid, interacting with the allylic chlorine atoms in the PVC, acts as a primary stabilizer and inhibits the dehydrochlorination process by hydrogen chloride scavenging, which is also known as a secondary stabilizer. Organotin (IV) complexes are frequently used as photo stabilizers for PVC by decomposing peroxide ($POO^{\bullet}$) and quenching excited states by complexing with radicals and additives of the π-system [65]. Yousif *et al*. described the diorganotin (IV) complexes of the ligand benzamide-doacetic acid complexes in PVC polymers as shown in Fig.1.12.

These stabilizers behave as radical scavengers for peroxide decomposers, UV absorbers and HCl scavengers to stabilize PVC films [66, 67].

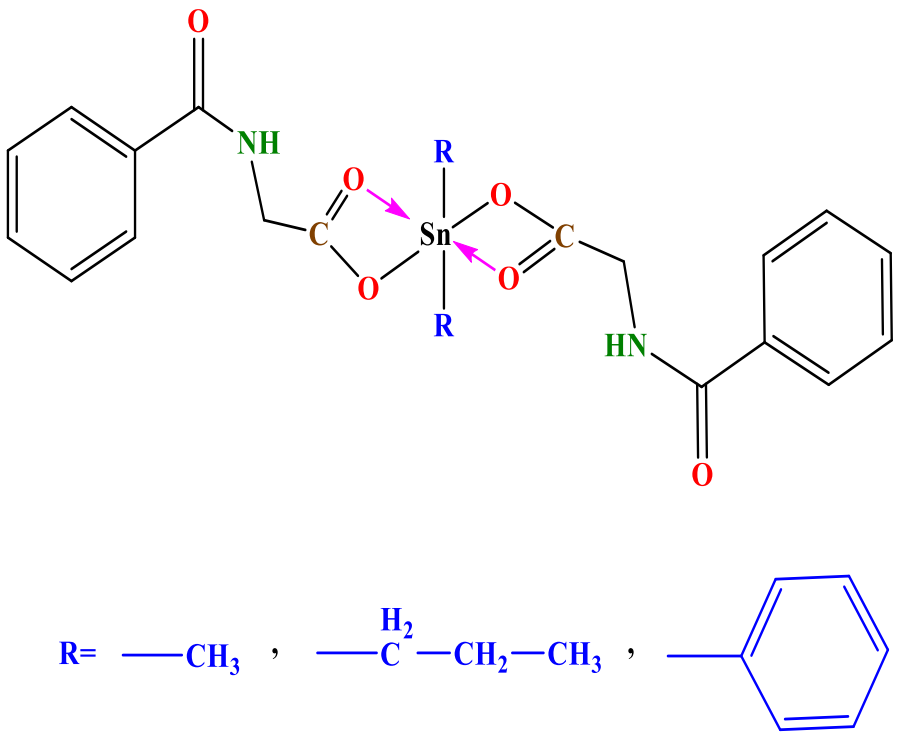

Figure 1.12 Diorganotin (IV) Complexes.

Tin (IV) carboxylates stabilize poly (vinyl chloride) via two mechanisms, depending on the metal that acts as a strong Lewis acid and strongly basic carboxylates, which have little or no Lewis acidity, are mostly hydrogen chloride scavengers. As displayed in Scheme 1.12.

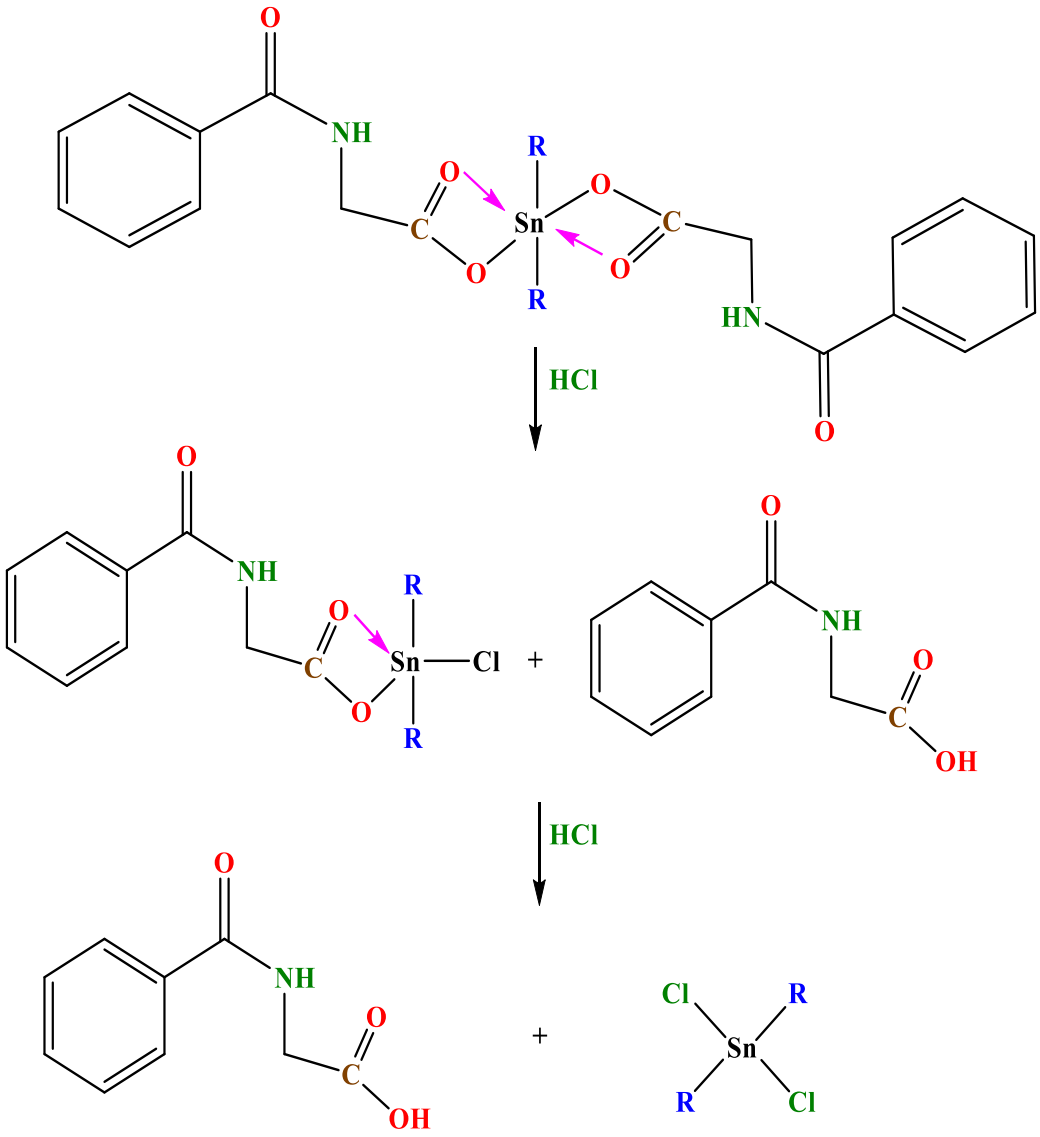

Scheme 1.12 Mechanism of Photostabilization of Complexes as HCl Scavengers.

The high efficiency of PVC stabilization is explained by the association of the tin (IV) ion with chlorine atoms at the surface of poly (vinyl chloride) [68]. The stabilizer is classified as the primary stabilizer in this mechanism as explained in Scheme 1.13.

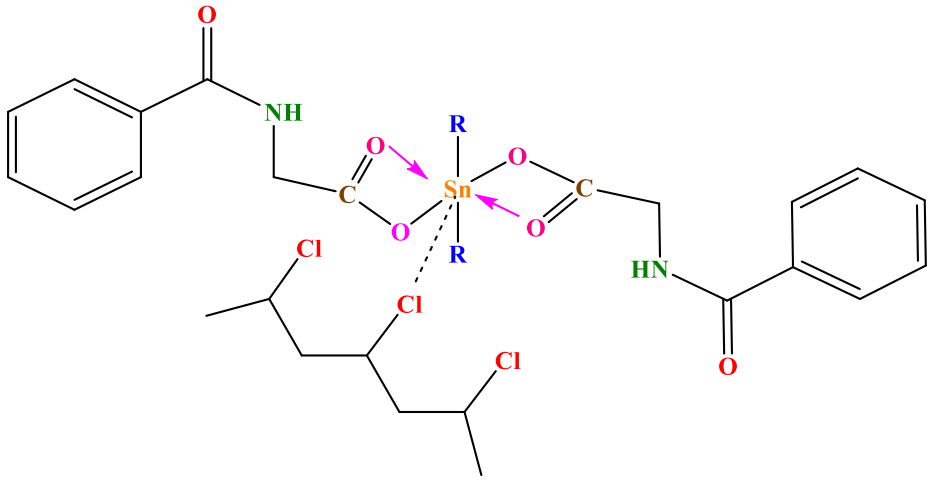

Scheme 1.13 Photostabilization Mechanisms of Complexes as Primary Stabilizers.

Metal chelate complexes are commonly used as photo stabilizers for poly (vinyl chloride). As a result, it is presumed that these complexes will act as peroxide decomposers via the suggested mechanism in Scheme 1.14.

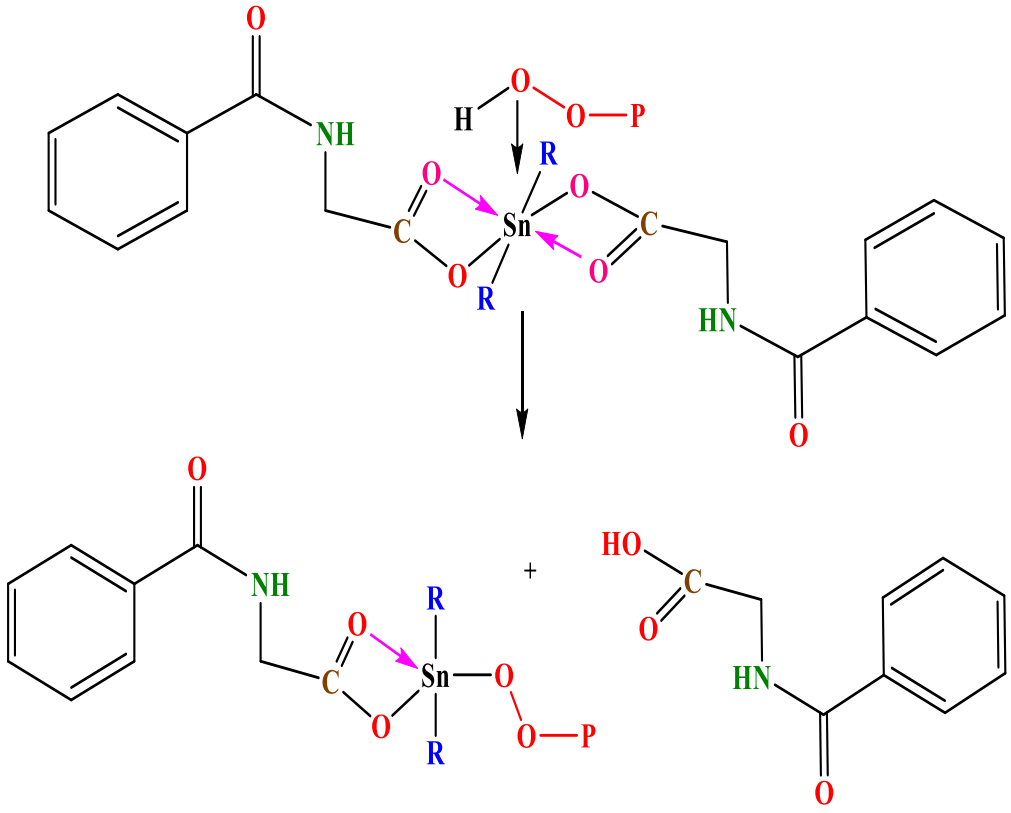

Scheme 1.14 Mechanism of Photostabilization of Complexes as Peroxide decomposer.

1.5 Free Radicals

A free radical is any chemical species that contains an unpaired electron in an atomic orbital and may exist independently. When an unpaired electron is present, most radicals have similar properties. Many radicals are highly reactive and unstable [69]. They function as oxidants or reductants by accepting or donating electrons from other molecules. Among the most common free radicals in biological systems are reactive oxygen species (ROS), which include both radical and non-radical species such as the superoxide anion radical $O_2^{\bullet -}$, hydroxyl radical HO$^{\bullet}$, hydrogen peroxide H_2O_2, lipid hydroperoxides and peroxyl radicals. By starting destructive chain radical reactions, ROS attack intracellular structures such as proteins, nucleic acids, lipids, and membranes, causing cell damage and disrupting homeostasis [70, 71].

1.5.1 Concept of Oxidative Stress

The expression oxidative stress refers to a state of oxidative damage caused by an imbalance between free radical generation and antioxidant defenses, as shown in Fig.1.13. It is related to damage to a wide range of molecule species, including lipids, nucleic acids, and proteins [72]. Oxidative stress can develop in tissues that have been damaged by excessive exercise, heat injury, illness, or toxins. Oxidative stress produces more radical-generating enzymes such as xanthine oxidase and lipoxygenase, which activate phagocytes, release free iron, and copper ions or disrupt the electron transport chains, resulting in an excess of ROS and changing the redox state [73-75].

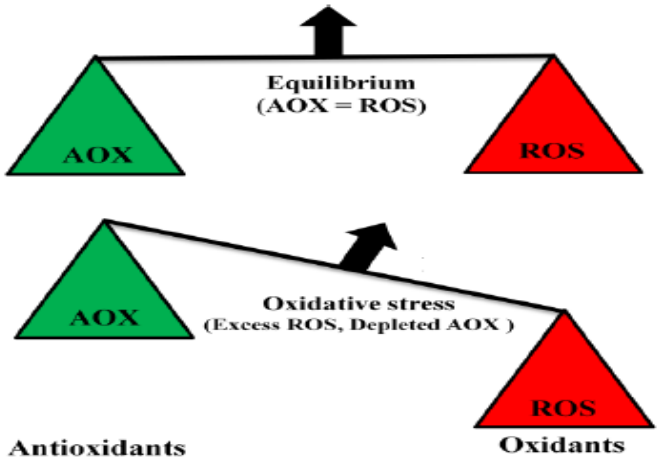

Figure 1.13 Balance and imbalance between Oxidant and Antioxidant.

1.5.2 The Biochemical Basis of Free Radical Production in the Body

At the end of the mitochondrial respiratory chain, where oxygen is completely reduced to water during aerobic metabolism, oxygen acts as the final electron acceptor [76, 77]. A portion of the electrons do not make it to the end of the electron transport chain in the mitochondrial membrane; instead, they escape and interact directly with oxygen in the early section of the chain, generating superoxide anion radicals. According to research on isolated brain mitochondria, 1–2 percent of the electrons that go down the respiratory chain escapes and converts oxygen to superoxide and hydrogen peroxide, which is their dismutation product. Although hydrogen peroxide itself is not a radical, the presence of iron ions causes it to act as a precursor to the formation of the hydroxyl radical ($OH^{\bullet}$) [78, 79]. Superoxide is also created endogenously in postischemic tissues by oxidase enzymes, e.g., xanthine oxidase. Superoxide is produced naturally by soluble oxidases, including nicotinamide adenine dinucleotide phosphate (NADPH) oxidase in phagocyte cells [80].

1.5.3 Inorganic Interpretation of Free Radical production in the Body

Most diatomic molecules have electrons that spin in an antiparallel direction, allowing electrons from the two atoms to share a single orbital and so form a covalent bond. According to the Pauli Exclusion Principle, antiparallel spinning allows for energy reduction. Each electron's spin reduces the energy of the others and consequently, the total spin energy of the electrons in the orbital is zero [81, 82]. While oxygen molecules existed in single and triple states, as illustrated by their molecular orbitals as shown in Figs. 1.14 and 1.15. The total spin quantum number of singlet oxygen, which has all its electron's spin-paired, is zero. While the spin quantum number is one in the triplet oxygen, because found two unpaired electrons. Under normal conditions, the unpaired bi radical state of oxygen predominates. The oxygen molecule is more stable in its triplet state ($^3O_2$) than in its singlet state ($^1O_2$) [83, 84]. Table 1.3 displays some of the chemical characteristics of singlet and triplet oxygen.

Table 1. 3 Some Chemical Properties of Single and Triplet Oxygen.

	$^3O_2$	$^1O_2$
Amount of Energy	0 Kcal/mole	22.5 Kcal/mole
Nature	Diradical	Electrophilic, non-radical
Reaction	Radical Substance	Compounds rich in electrons

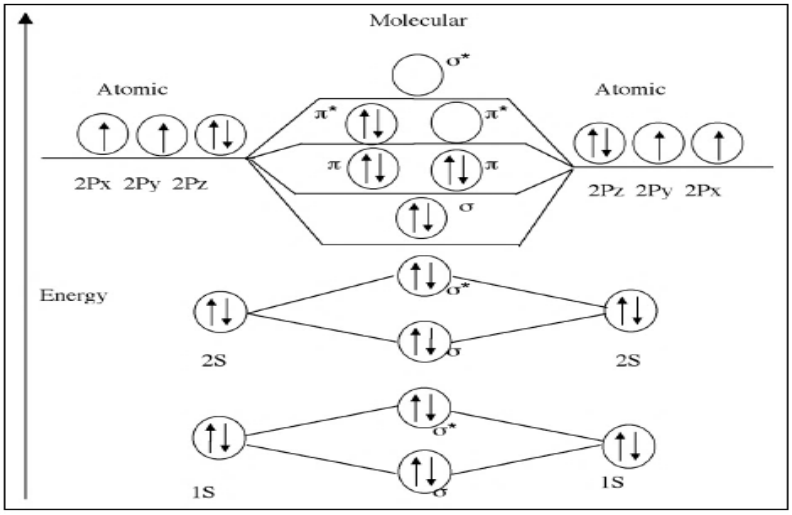

Figure 1.14 Molecular Orbital of Singlet Oxygen.

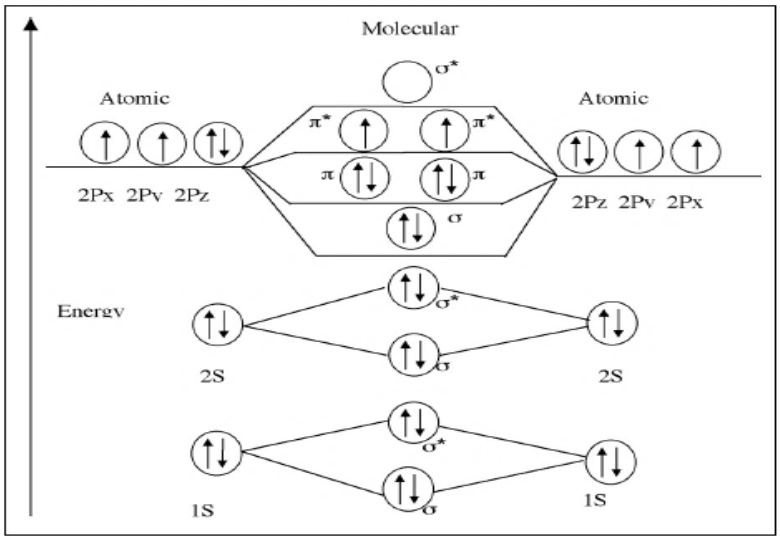

Figure 1.15 Molecular Orbital of Triplet Oxygen.

Spin quantum number of paired electrons S= +1/2 (+) -1/2 = 0

Spin quantum number of unpaired electrons S= +1/2 (+) +1/2 =1

By applied of Hound rules to calculate multiplicity of oxygen getting:

M=2S+1 …… ……Multiplicity of Hound

M= 2 × 0+1 = 1 Singlet state

M= 2 × 1+1 = 3 Triplet state

Except for oxygen, which has excellent unpaired electron stability, the triplet state is frequently assumed to be more energetic than the singlet state in other biomolecules. [85]. The reactivity of ROS is caused by this discrepancy in oxygen behavior. As a result, the paired electrons of energetic oxygen are thought to be chemically strongly oxidative; therefore, the singlet state for oxygen reacts easily with an external electron provided by another molecule to form the superoxide radical ($O^{\bullet -}_2$). As shown in Fig. 1.16, while the triplets form of oxygen is more stable than the singlet state because it is difficult to find a molecule that interacts with antiparallel electrons [86].

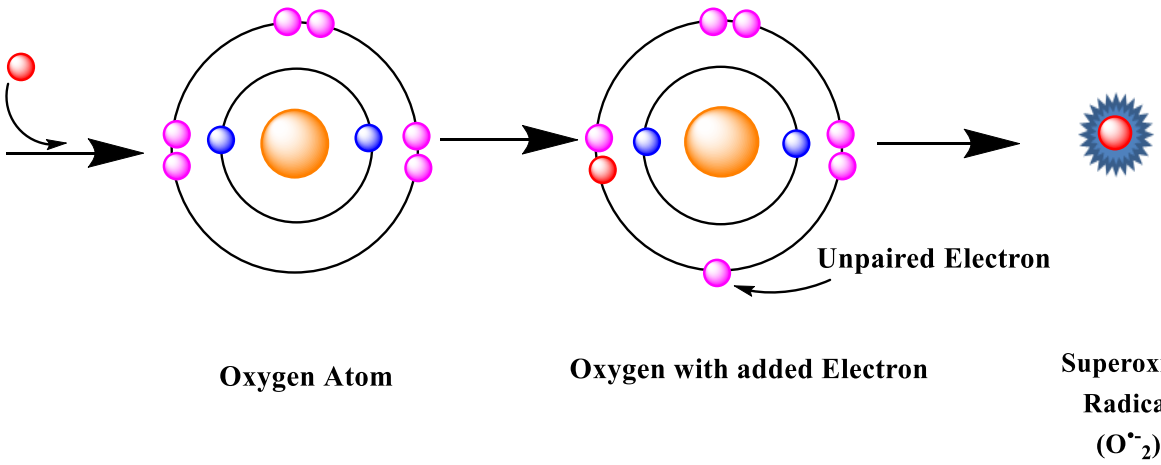

Figure 1.16 Oxygen in a Single State accepts Electron to generate a Superoxide Radical ($O^{\bullet -}_2$).

Although the superoxide radical is localized, temporary, and difficult to pass across cellular membranes, it may be converted by the enzyme superoxide dismutase into H_2O_2, which is membrane-diffusible and has a longer half-life [87]. Moreover, the superoxide radical can undergo the Haber-Weiss reaction with body metals [88, 89].

In this process, iron catalyst is employed to generate hydroxyl radicals from superoxide and H_2O_2. Other major ROS produced by peroxides include alkoxy radicals (RO•) and peroxyl radicals (ROO•) [90]. As seen in Scheme 1.15.

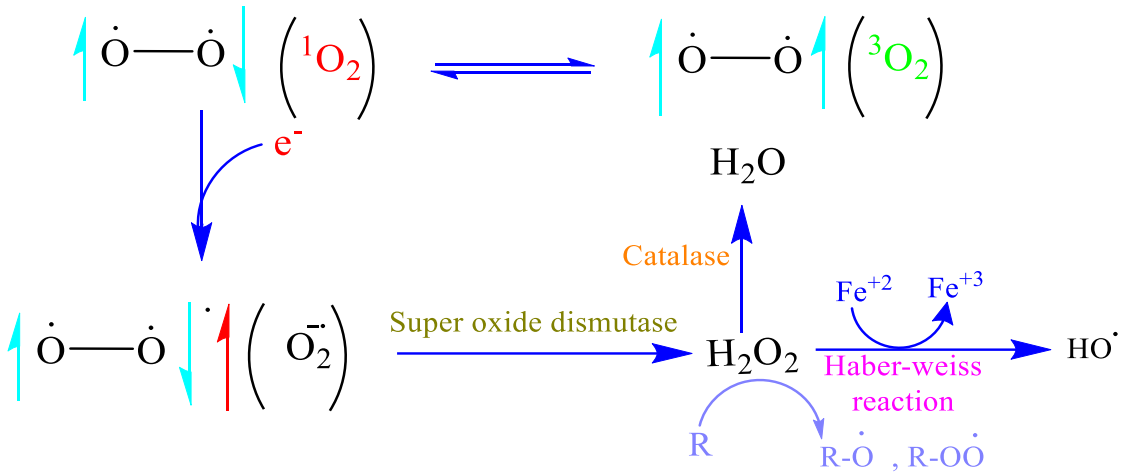

Scheme 1.15 Shown the Conversion of Multiple ROS from one Oxygen Molecule.

1.6 Antioxidant

Antioxidants are molecules that inhibit or reduce free radical reactions and delay or prevent cellular damage. Oxidation is a chemical process in which electrons are transferred from a material to an oxidizing agent [91]. Free radicals, which are generated during processes, can cause a chain of reactions that damages cells. Antioxidants terminate the chain reactions by reducing the free radical intermediates and they also prevent more oxidation processes by being oxidized themselves [92]. Antioxidants exist in the intracellular and extracellular environments in both enzymatic and non-enzymatic forms. These antioxidants with low molecular weight can safely interact with free radicals to prevent the chain reaction before important molecules are damaged. Every living organism contains antioxidant defense to deal with reactive oxygen species. Low antioxidant levels reduced oxidative stress, which can harm or kill cells [93].

1.6.1 Classification of Antioxidants

Antioxidants can be classified in several ways depending on the following parameters:

1. They are classified as enzymatic or nonenzymatic antioxidants based on their action. In the presence of cofactors such as copper, zinc, manganese and iron, antioxidant enzymes convert harmful oxidative products to hydrogen peroxide and subsequently to water in a multistep process. Non-enzymatic antioxidants such as ascorbic acid, α-tocopherol and plant polyphenols operate by interfering with free radical chain reactions [94].

2. The ability to dissolve in lipids or water the antioxidants fall into two categories: lipid-soluble antioxidants and water-soluble antioxidants. Antioxidants that are water soluble, like vitamin C, are found in cellular fluids like the cytosol and cytoplasmic matrix. Cell membranes hold many of the lipid-soluble antioxidants, such as vitamin E and carotenoids [95].

3. The differences between small- and large-molecule antioxidants in terms of size. Small-molecule antioxidants neutralize and eliminate reactive oxygen species via a process known as "radical scavenging." Glutathione, vitamin C and vitamin E are the principal antioxidants in this category. Large-molecule antioxidants are surface proteins (albumin) and enzymes (catalase, superoxide dismutase and glutathione peroxidase) that absorb ROS and prevent them from damaging other critical proteins [96, 97].

1.6.2 Organotin (IV) Carboxylates Biological Properties

The scientific study of organotin biological activity began in 1950. Van der Kerk and Luijten discovered in 1954 that various organotin compounds with the general formula R_3SnX are effective fungicides [98]. Organotin (IV) carboxylates have considerable antioxidant and antibacterial activities as well as antitumor and anticancer characteristics [99]. The type and number of organic groups R directly linked to the tin atom, as well as the amount of carboxylate groups linked to the tin atom through Sn-O bonds, determine the applications of organotin (IV) carboxylates for any biological activity. These parameters determine the efficiency of organotin (IV) compounds for the specified objectives. When organotin (IV) binds to several places in the body, including carbohydrates, nucleic acid derivatives, amino acids, and proteins [100]. The type of the R group determines the site of attacks. Hetero atoms presence such as oxygen, nitrogen and sulfur in the ligand plays a major role in the geometry and therefore effect the biological activity of these complexes. Organotin (IV) compounds' potent biological activity motivates its use in medications [101].

1.7 Aims of the Project

The project's objective is to increase knowledge about the importance of organotin (IV) compounds from both an industrial and a biological standpoint. Details can be explained as follows:

1- Synthesizing organotin (IV) complexes by condensation reactions of ligand (cephalexin, tyrosine) with tri- and di-organotin (IV) compounds dissolved in methanol.
2- Characterizing the obtained complexes physically by elemental analysis, color, and melting point determination, as well as chemically by infrared spectroscopy and nuclear magnetic resonance spectroscopy.
3- Studying the industrial applications of the prepared complexes as stabilizers to inhibit photodegradation of polyvinyl chloride films (40 μm thicknesses) and evaluation of weight loss and photostabilizing Efficiency of all complexes by FTIR Spectroscopy.
4- Studying the surface morphology of the PVC films by using a microscope, atomic force microscopy and a scanning electron microscopy.
5- Studying the biological applications via the study of the antioxidant activity of organotin (IV) complexes and comparing them with tannic acid through measuring by DPPH and CUPRAC methods.

Chapter Two

Experimental

2.1 Materials and Reagents

High-purity chemicals were utilized in the present study without any additional purification. as shown in Table 2.1.

Table 2.1: Information on the purity and source of the test chemicals used by different companies.

Compounds	Formula	M.wt.	State	Purity	Company
Cephalexin	$C_{16}H_{17}O_4N_3S$	347.39	Solid	98%	BDH
Dibutyiltindichloride	$SnC_8H_{18}Cl_2$	303.84	Solid	97%	Alfa- Aesar
Diethyl ether	$C_4H_{10}O$	74.07	liquid	99.5%	BDH
Dimethylltindichloride	$SnC_2H_6Cl_2$	219.68	Solid	98%	Sigma
Diphenyltindichloride	$SnC_{12}H_{10}Cl_2$	343.82	Solid	98%	Fluka
L-Tyrosine	$C_9H_{11}NO_3$	181.19	Solid	98%	Reagent World
Methanol	CH_3OH	32.04	liquid	99%	GCC
Poly (vinyl chloride)	(C_2H_3Cl) n	(62.5) n	solid	97%	Petkim
Tetrahydrofuran (THF)	C_4H_8O	72.11	liquid	99.5%	Romil
Tributyltinchloride	$SnC_{12}H_{27}Cl$	325.50	liquid	97%	Qinmu
Trimethyltin chloride	SnC_3H_9Cl	199.27	Solid	98%	Dideu
Triphenyltinchloride	$SnC_{18}H_{15}Cl$	385.47	Solid	97%	Fluka

2.2 Instruments

2.2.1 Melting Point Apparatus

The Stuart SMP30 melting point apparatus, which can take three samples simultaneously within the optimum heating block and has a maximum temperature of 400°C, was employed to identify complexes and ligands. The measurements were performed at Chemistry Department, College of Science, Babylon University.

2.2.2 Elemental Analysis CHNS

Using the EM-017mth instrument, the percentage contents of the elements (CHNS) for the ligand and the produced complexes were calculated. These were completed in the Ibn Sina State Company's laboratories.

2.2.3 Fourier Transformed Infrared Spectroscopy (FTIR)

FTIR spectra are utilized to identify distinct functional groups of materials obtained by the Shimadzu 8400 spectrophotometer (4000–400 cm^{-1}) using the KBr discs. The measurements were occurred at the Chemistry Department, the College of Science, Babylon University.

2.2.4 ^{1}H, ^{13}C and ^{119}Sn Nuclear Magnetic Resonance

The spectra of nuclear magnetic resonance were recorded using a Bruker spectrophotometer (^{1}H, ^{13}C, ^{119}Sn-NMR in frequencies 300.81, 75.65 and 149.21 MHz respectively) using deuterated DMSO-d_6 as a solvent and tetramethyl silane as an internal standard reference. These were conducted in Mashhad, Ferdowsi Square, Boali Research, Iran.

2.2.5 Accelerated UV-Weathering

Using a Q-UV sample from an accelerated weather meter (Germany, Saarbrucken, Philips.), which was fitted with UV-B313 nm lamps, the polyvinyl chloride films were subjected to ultraviolet light for a duration of 300 hours at a temperature of 25 °C. These experiments were carried out at the Chemistry Department of Al-Mustansiriyah University. The UV-weathering acceleration process is depicted in diagram form in Fig. 2.1.

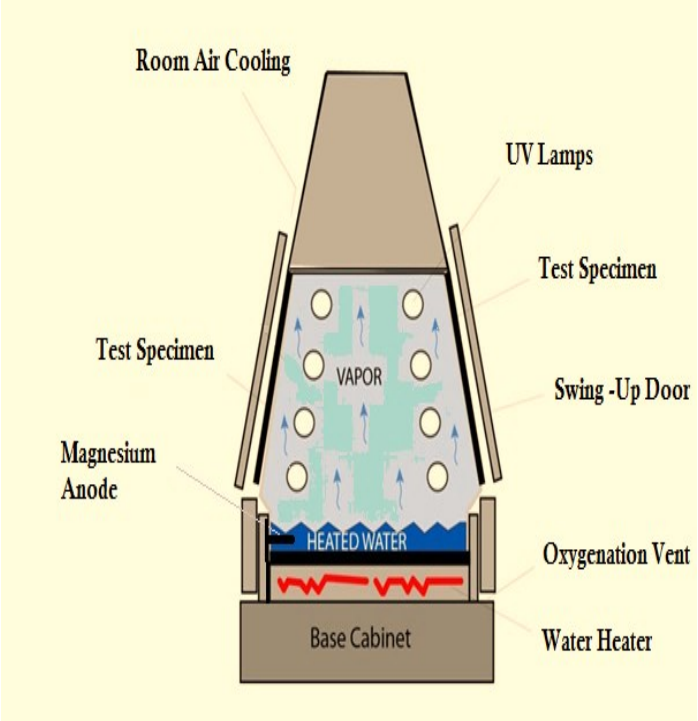

Figure 2.1 Schematic diagram of Accelerating UV-Weathering.

2.2.6 Microscope

The morphology of polyvinylchloride films was tested using a microscope with a power magnification 400 times (Meiji Techno, Tokyo, Japan). The measurements were performed at the Department of Chemistry, College of Science, Al-Nahrain University.

2.2.7 Atomic Force Microscopy (AFM)

The principle of AFM is that a sharp tip at the end of a cantilever generates a spring that is scanned in axles X and Y across a sample put on a piezo crystal. Changes in height (Z direction) caused by tip interactions with the sample, resulting in bending of the cantilever caused by attractive or repulsion forces. This bending is detected using a laser beam and a split photodetector, which produces a topographical picture of the sample under study [102,103]. The surface morphology investigated by the irradiated polymer films using AFM (Type AA2000, Angstrom Advanced Inc, USA). The measurements were performed in the Department of Chemistry, College of Science, Al-Nahrain University. The atomic force microscope principle was depicted in Fig. 2.2.

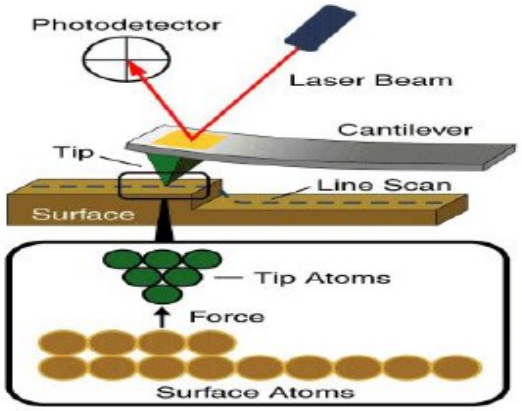

Figure 2.2 Principal of Atomic Force Microscope.

2.2.8 Scanning Electron Microscope (SEM)

SEM is the preferred method for analyzing specimen surfaces. Fig. 2.3 depicts a typical SEM configuration, which includes an electron gun (electron source and accelerating anode), electromagnetic lenses to focus the electrons, a vacuum chamber containing the specimen stage and a variety of detectors to collect the signals generated by the specimen [104, 105]. To achieve high resolution, it is essential for SEM to operate in a vacuum to prevent interactions between electrons and gas molecules. Heating or applying high energy in the range of 1– 40 keV accelerates the primary electrons generated from the electron gun. These released electrons are focused by electromagnetic lenses and restricted to a monochromatic beam (with a width of 100 nm or less). When the main electron beam strikes the sample surface, it gives off atomic electron energy that leads to the generation of secondary electrons and therefore many signals [106, 107]. The signals are gathered by electron collectors (detectors), which are manipulated by the computer to form the required image [108]. The measurements were achieved in the Department of physical, College of Science, Al-Mustansiriyah University.

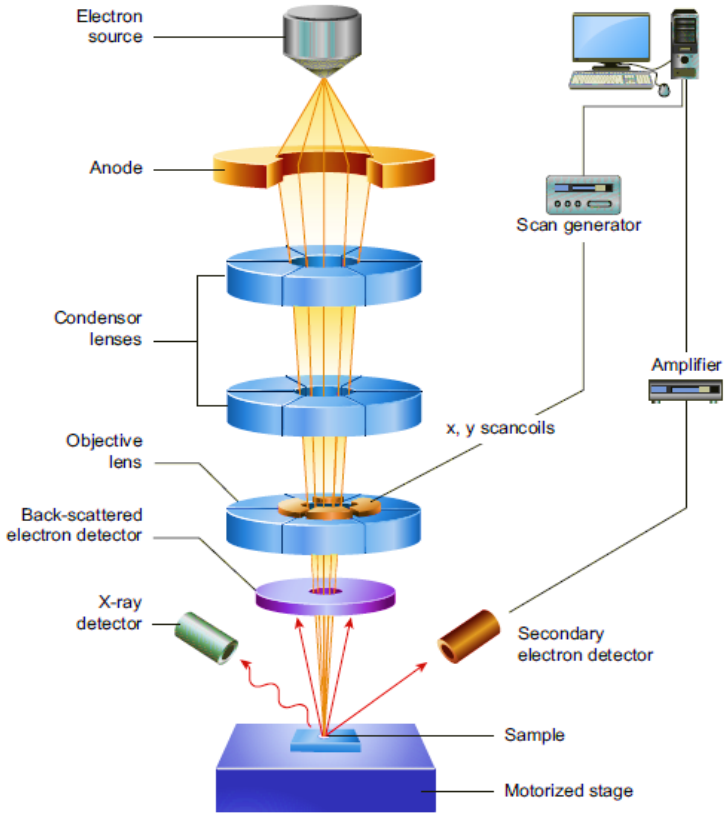

Figure 2.3 A Schematic diagram showing the main Components of a SEM Microscope.

2.2.9 Micro plate Reader

The absorbance of ligands and organotin (IV) complexes was measured at various times using a microplate reader (Type BioTek) as display in Fig. 2.4. Utilizing a plate reader can save operating time, lower reagent costs, and increase production. A small volume of blanks and samples were pipetted into a 96-well flat-bottom polystyrene plate and the absorbance was measured [109]. The measurements were carried out at the University of Babylon, College of Science, Department of Chemistry, Biochemistry Laboratory.

Figure 2.4 Micro plate Reader.

2.3 Synthesis of Organotin (IV) Complexes

2.3.1 Synthesis of Triorganotin (IV) Complexes [110]

The molar ratios (metal: ligand) to synthesize the complexes were 1:1, since the ligand was dissolved in 30 ml of methanol with an appropriate amount of sodium hydroxide then added to triorganotin (IV) chloride which was dissolved in 20 ml of methanol. The mixture was stirred at room temperature for 10 minutes and then refluxed for 5 hours. The resulting solution was filtered, washed, dried, and recrystallized to form the resulting precipitate. The weights and molar ratios of triorganotin (IV) complexes and ligands shown in Table 2.2.

Table 2.2 The weights and Molar ratios of Triorganotin (IV) Complexes and Ligands.

No. of Com.	Weights (g) of Triorganotin (IV) Chloride			Ligands	Weights (g) of Ligands	No. of Molar ratios
	Ph_3SnCl	Bu_3SnCl	Me_3SnCl			
1	**1.9273**	**1.6275**	**0.9964**	**Cephalexin**	**1.7369**	**1: 1**
2	**2.3128**	**1.9530**	**1.1956**	**L-tyrosine**	**1.0871**	**1: 1**

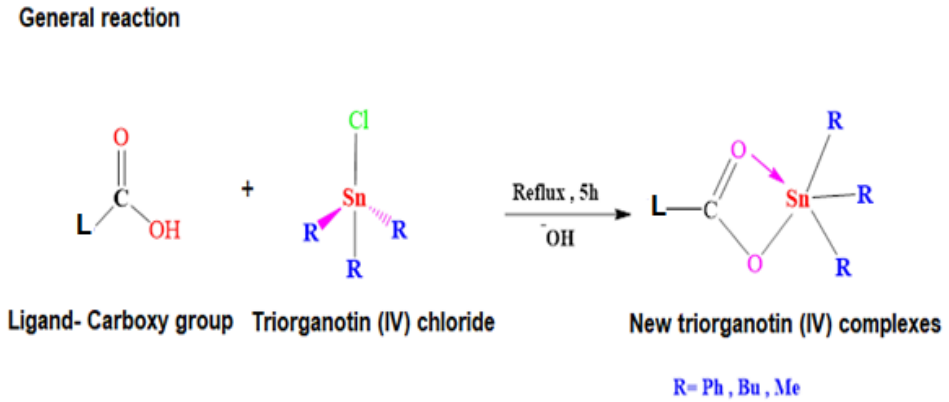

Scheme 2.1 Synthesis of Triorganotin (IV) Complexes.

2.3.2 Synthesis of Diorganotin (IV) Complexes [111]

The molar ratios (metal: ligand) to synthesize the complexes were 1:2, since the ligand was dissolved in 30 ml of methanol with an appropriate amount of sodium hydroxide then added to diorganotin (IV) dichloride which was dissolved in 20 ml of methanol. The mixture was stirred at room temperature for 10 minutes and then refluxed for 5 hours. The resulting solution was filtered, washed, dried, and recrystallized to form the resulting precipitate. The weights and molar ratios of diorganotin (IV) complexes and ligands shown in Table 2.3.

Table 2.3 The Weights and Molar ratios of diorganotin (IV) Complexes and Ligands.

No. of Com.	Weights (g) of diorganotin (IV) dichloride			Ligands	Weights(g) of Ligands	No. of Molar ratios
	Ph_2SnCl_2	Bu_2SnCl_2	Me_2SnCl_2			
1	**1.3752**	**1.2153**	**0.8787**	**Cephalexin**	**2.7791**	**1: 2**
2	**1.3752**	**1.2153**	**0.8787**	**L-tyrosine**	**1.4495**	**1: 2**

General reaction

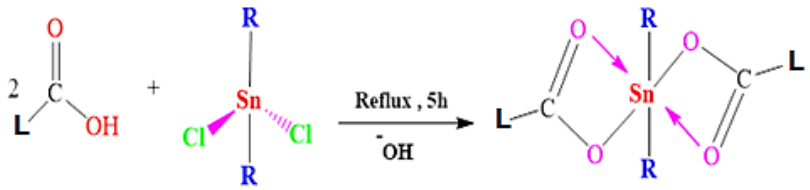

Ligand-Carboxyl group Diorganotin (IV) dichloride New diorganotin (IV) complexes

R= Ph , Bu , Me

Scheme 2.2 Synthesis of Diorganotin (IV) Complexes.

2.4 Experimental Procedures

2.4.1 Films Preparation

The polymer matrix used in this study was poly (vinyl chloride), (K value = 67, degree of polymerization = 800) supplied by Petkim (Turkey). Fixed concentrations of PVC solution 5 g per 100 ml of tetrahydrofuran (THF) were used to prepare polymer films with 40 µm thickness measured by a micrometer type 2610 A, (Germany). The prepared complexes of 0.5% by weight were added to the films. The films were prepared and left to dry at room temperature for 24 hours to remove the possible residual of THF solvent [112].

2.4.2 Films Irradiation

The QUV accelerated weathering device is a laboratory simulation of weather's damaging effects that is used to predict the relative durability of materials exposed to the outside. UV fluorescent lamps replicate the damaging effects of sunlight. The QUV can cause harm in a matter of days or weeks when outside exposure would generally take months or years. There was cracking, gloss loss, discoloration, strength loss and other defects discovered. PVC films were irradiated with UVB lamps (λ_{max} = 313 nm and light intensity = 6.43 x 10^{-9} ein.dm^{-3}.s^{-1}). The films were placed on stands and exposed to radiation. The thickness of the aluminum stand plate is 0.6 mm.

2.4.3 Evaluation the Stabilizing Efficiency for Poly (vinyl Chloride)

2.4.3.1 Photodegradation and Evaluation of PVC Stabilizing Efficiency Using the Weight Loss Method [113,114]

The stabilizing efficiency of the stabilizer was determined by measuring the percentage of weight loss of irradiated PVC films in absence and in presence of stabilizers. The weight loss measurements were carried out according to the following equation (2.1).

Weight loss % = (W_1 –W_2 /W_1) 100 ……... (2.1)

Where W_1 is the weight of the original sample (before irradiation) and W_2 is the weight of sample after irradiation.

2.4.3.2 FTIR Spectroscopy Method for Photodegradation and Evaluation of PVC Stabilizing Efficiency

Using an FTIR 4200 JASCO spectrophotometer, the photodegradation of PVC films was observed (4000-400 cm^{-1}). The chemical, mechanical and physical properties of polymeric materials are affected by UV light [115]. Because photooxidation of poly (vinyl chloride) creates carbonyl, conjugated double bonds and hydroxyl moieties, the changes in infrared absorption bands for polyene (1600 cm^{-1}) groups, carbonyl (1700 cm^{-1}) groups, and hydroxyl (3500 cm^{-1}) groups were recorded and compared to a reference peak (1328 cm^{-1}) [116,117]. The band index procedure equation (2.2) was used to calculate the indices for polyene ($I_{C=C}$), carbonyl ($I_{C=O}$) and hydroxyl (I_{OH}) groups. The absorbance of the peak under study (A_s) and the absorbance of the reference peak (A_r) both influence the functional group index (I_s) [118].

$$\mathbf{I_s = A_s / A_r} \quad \text{(2.2)}$$

The absorbance (A) is calculated from the reordered percentage transmittance (%T) using Beer-Lambent law by using the following equation (2.3).

$$\mathbf{A = 2 - \log \%T} \quad \text{(2.3)}$$

2.5 Evaluating of Antioxidant Activities

2.5.1 DPPH Free Radical Scavenging Assay

The ability of antioxidants to neutralize free radicals was used to evaluate their potential. The stable free radical DPPH, which was discovered by Goldsmith and Renn in 1922, is one of the most widely employed free radicals [119]. The radical scavenging activity was evaluated using the radical 2, 2-diphenyl-1-picrylhydrazyl (Sigma-Aldrich) by microplate reader spectrophotometry at λ_{max}=490 nm according to the known procedure. The reaction mixture contained DPPH (200 µg/ml) and a solution of the test complexes and tannic acid (50 µg/ml). The reaction was monitored for 15 minutes. The data were calculated using Microsoft Excel 2010 [120]. The % inhibition was calculated using the following formula equation (2.4).

$$\mathbf{I\%} = \frac{\boldsymbol{A\ Blank - A\ Sample}}{\boldsymbol{A\ Blank}} \times \mathbf{100} \quad \text{..... (2.4)}$$

Where **A blank** is the absorbance of the control reaction (all reagents except the test complex) and **A sample** is the absorbance of the test compound [121].

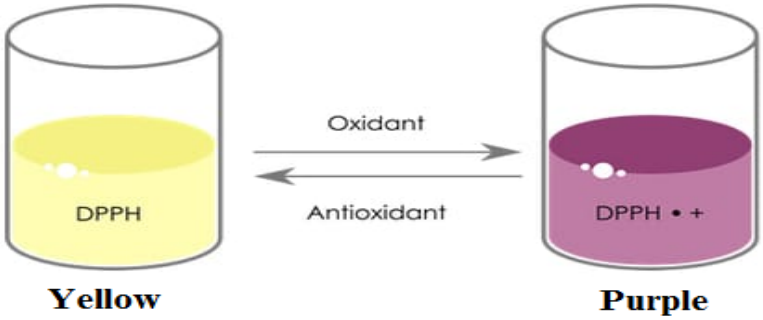

Figure 2.5 The Antioxidant Reaction of 2, 2-diphenyl-1-picrylhydrazyl with Organotin (IV) Complexes.

2.5.2 CUPRAC Free Radical Scavenging Assay

The capability of the compounds to undergo one electron transition was determined by a microplate reader spectrophotometry at λ_{max} = 450 nm using a complex of 2, 9-dimethyl-1, 10-phenanthroline (neocuproine, Sigma-Aldrich, 98%) with copper. The reaction mixture contained 100 µg/ml of ammonium acetate buffer (pH 7.0), 50 µg /ml of $CuCl_2$ solution in methanol, and 50 µg/ml of neocuproine solution in methanol. This reagent added to 20 µg/ml for each complexes solution (dissolved in methanol) also to tannic acid (dissolved in water) [122,123].

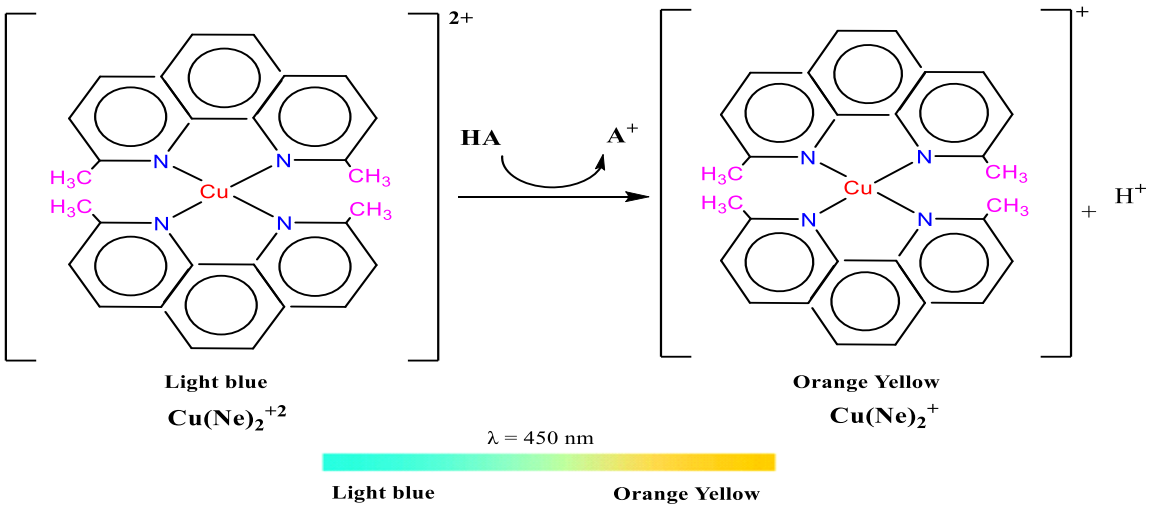

Figure 2.6 The Reaction of Cupric Reducing Antioxidant Capacity.

Chapter Three

Results and discussion

3.1 Synthesis and Identification of Organotin (IV)-Cephalexin Complexes

3.1.1 Synthesis of Organotin (IV) Cephalexin Complexes

Six organotin complexes, Ph_3SnL, Bu_3SnL, Me_3SnL, Ph_2SnL_2, Bu_2SnL_2, and Me_2SnL_2, were made using the ligand cephalexin reacted with triorganotin chloride and diorganotin dichloride, which were dissolved in methanol, and refluxed for five hours. Cephalexin formed new organotin (IV) complexes in the following molar ratios: 1:1 and 2:1 with triorganotin chlorides and diorganotin dichloride, respectively. In Schemes 3.1 and 3.2, this is depicted.

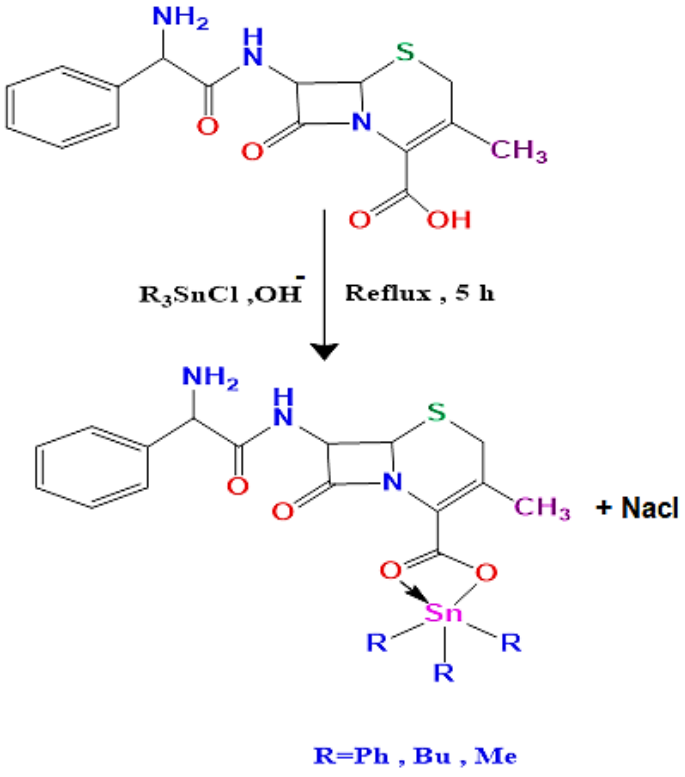

Scheme 3.1 Synthesis of Triorganotin (IV) - Cephalexin Complexes.

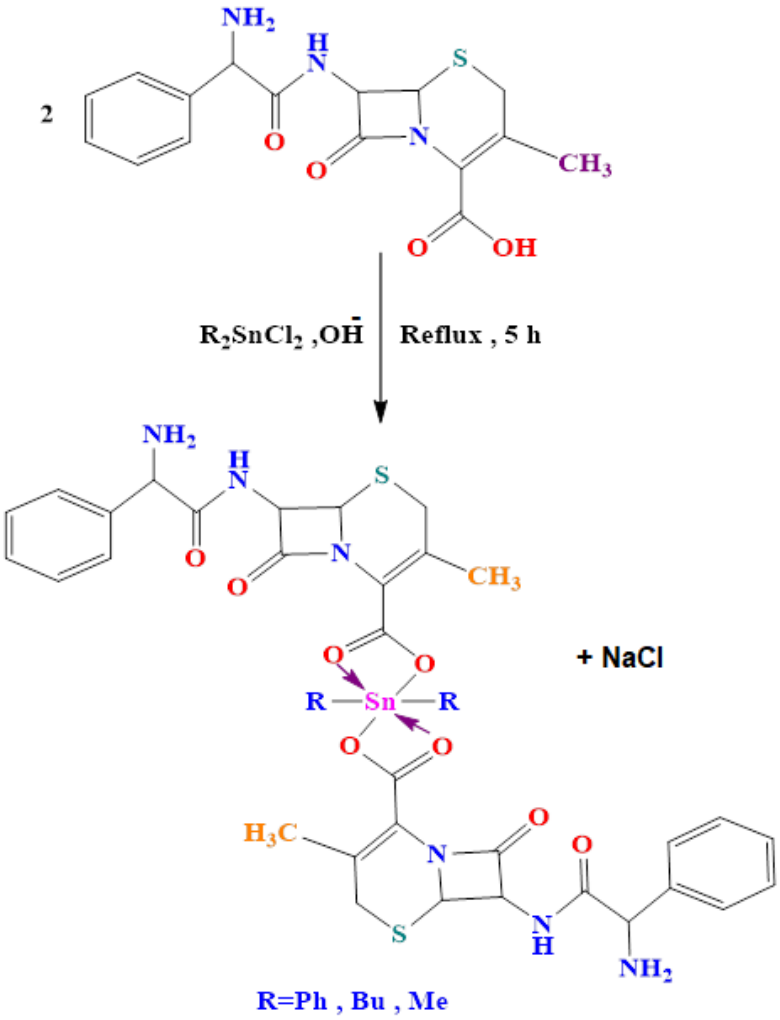

Scheme 3.2 Synthesis of Diorganotin (IV) - Cephalexin Complexes.

3.1.2 Physical Information

The elemental composition of the tri- and di-organotin (IV)- cephalexin complexes was determined using elemental analysis. The results agree with the calculated values of the ligand (Cephalexin) and its complexes in general (Ph_3SnL, Bu_3SnL, Me_3SnL, Ph_2SnL_2, Bu_2SnL_2 and Me_2SnL_2). Table 3.1 shows the elemental analysis data for (C, H, N and S %), colors, melting points and yields of organotin (IV) complexes along the ligand (L).

Table 3.1 Physical and Elemental Analysis Information for Cephalexin and its Complexes.

Compounds	Colors	Melting Points (°C)	Yields (%)	Calculated % (Measured %) C	H	N	S
Cephalexin (L)	Yellowish white	198-200	-----	55.32 (55.63)	4.93 (5.54)	12.10 (11.98)	9.23 (9.58)
Ph_3SnL	yellow	151-153	80	58.64 (57.34)	4.94 (4.35)	6.03 (6.93)	4.60 (5.02)
Bu_3Sn L	Dark red	101-103	87	52.84 (51.90)	6.81 (5.97)	6.60 (6.36)	5.04 (4.95)
Me_3Sn L	Pale yellow	147-149	91	44.73 (43.90)	4.94 (5.02)	8.24 (7.86)	5.04 (4.95)
Ph_2SnL_2	Yellowish orange	194 - 196	97	54.73 (53.95	4.38 (4.90)	8.70 (7.91)	6.64 (6.20)
Bu_2SnL_2	Reddish Orange	125 - 127	78	51.90 (51.35)	5.44 (4.95)	9.08 (9.60)	6.93 (7.03)
Me_2SnL_2	Orange	158 - 160	98	48.53 (47.78)	4.55 (5.20)	9.99 (10.13)	7.62 (7.15)

3.1.3 Fourier Transform Infrared Spectroscopy (FTIR)

FTIR spectroscopy can result in a positive identification of the substance since each material has a unique composition and consequently a specific arrangement of atoms [124]. The FTIR measurements (4000-400 cm^{-1}) were performed using the KBr disc. The information from the infrared spectra of cephalexin was compared with that of tri- and diorganotin (IV) complexes, as seen in Figs. 3.1–3.7. due to deprotonation occurs because of coordination between cephalexin and organotin (IV) compounds, the FTIR spectrum of the ligand (Cephalexin) displays a change in the fundamental frequency of the carboxylic acid's hydroxyl group. New frequencies of 1695 and 1260 cm^{-1}, respectively, were introduced in the positions of the C=O and C-O groups [125, 126]. The other indicators of coordination are the emergence of the new bands in complexes Sn-C and Sn-O in the regions 574-598 and 499-528 cm^{-1}, respectively [127]. The FTIR spectroscopy data for several of the synthesized organotin (IV) complexes and cephalexin groupings are shown in Table 3.2.

Table 3.2 Shows some of the FTIR Spectra for the Organotin (IV)-Cephalexin Complexes.

No.	Complexes	C=O	C-O	Sn-C	Sn-O
1	Ph_3Sn L	1653	1221	571	496
2	Bu_3Sn L	1655	1292	503	442
3	Me_3Sn L	1657	1292	544	451
4	Ph_2SnL_2	1616	1306	503	457
5	Bu_2SnL_2	1667	1246	511	419
6	Me_2SnL_2	1653	1395	513	459

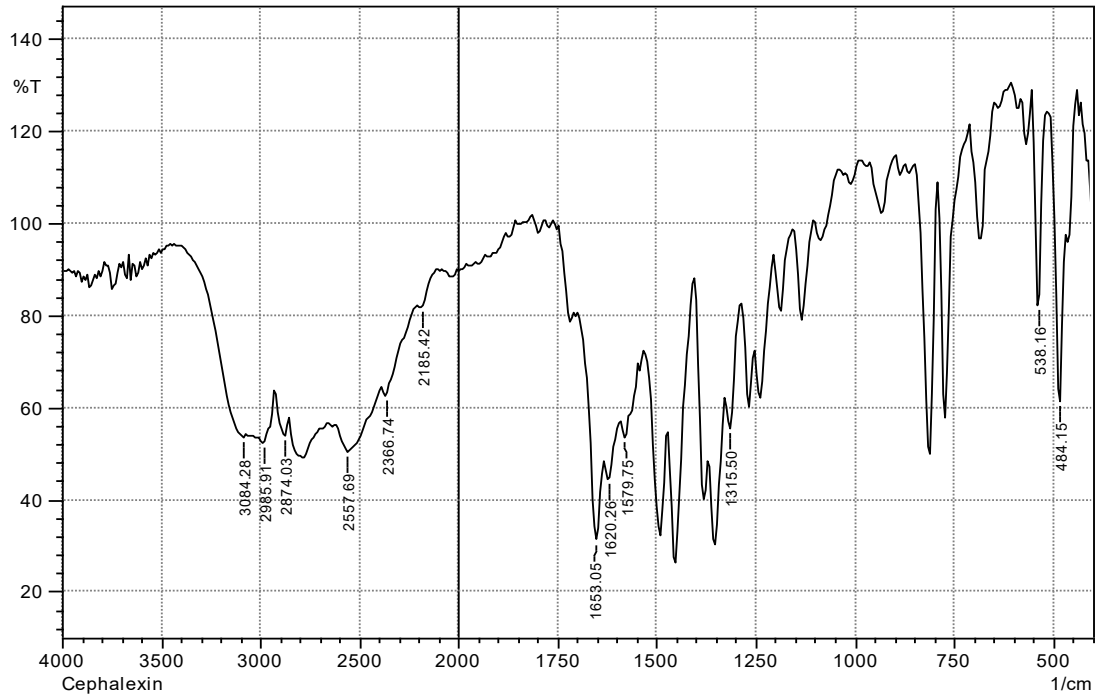

Figure 3.1 FTIR Spectrum of Cephalexin.

Figure 3.2 FTIR Spectrum of Ph_3SnL.

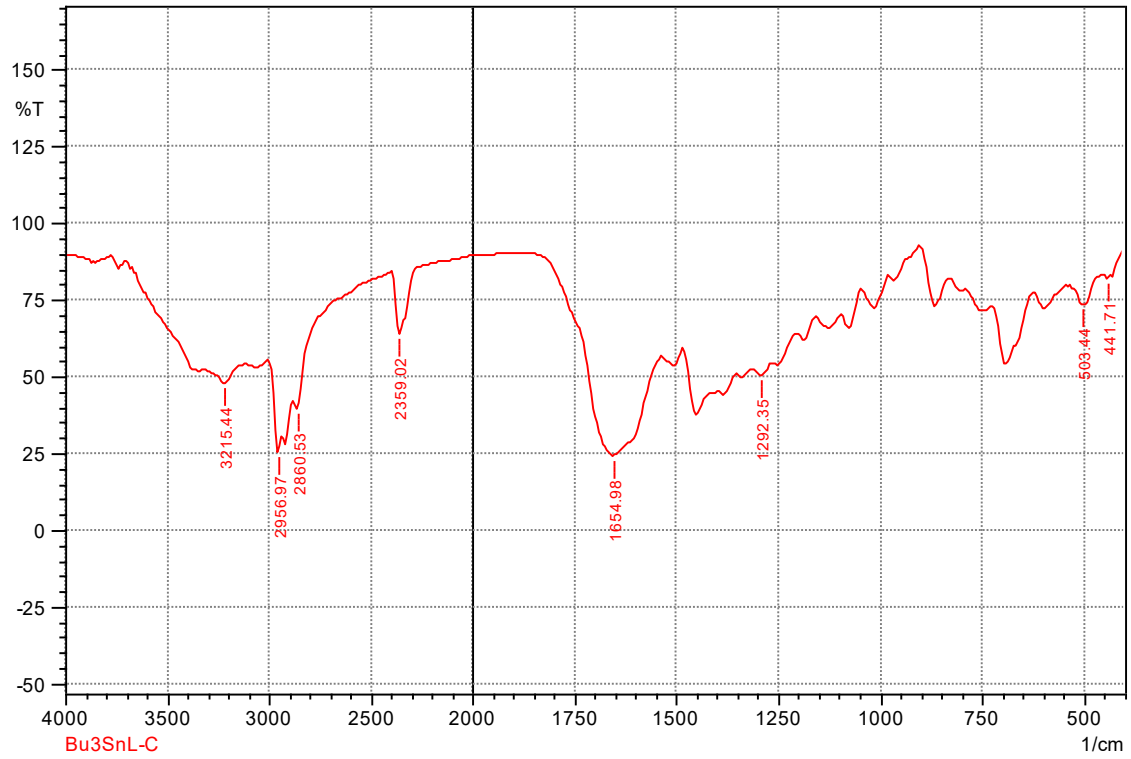

Figure 3.3 FTIR Spectrum of Bu_3SnL.

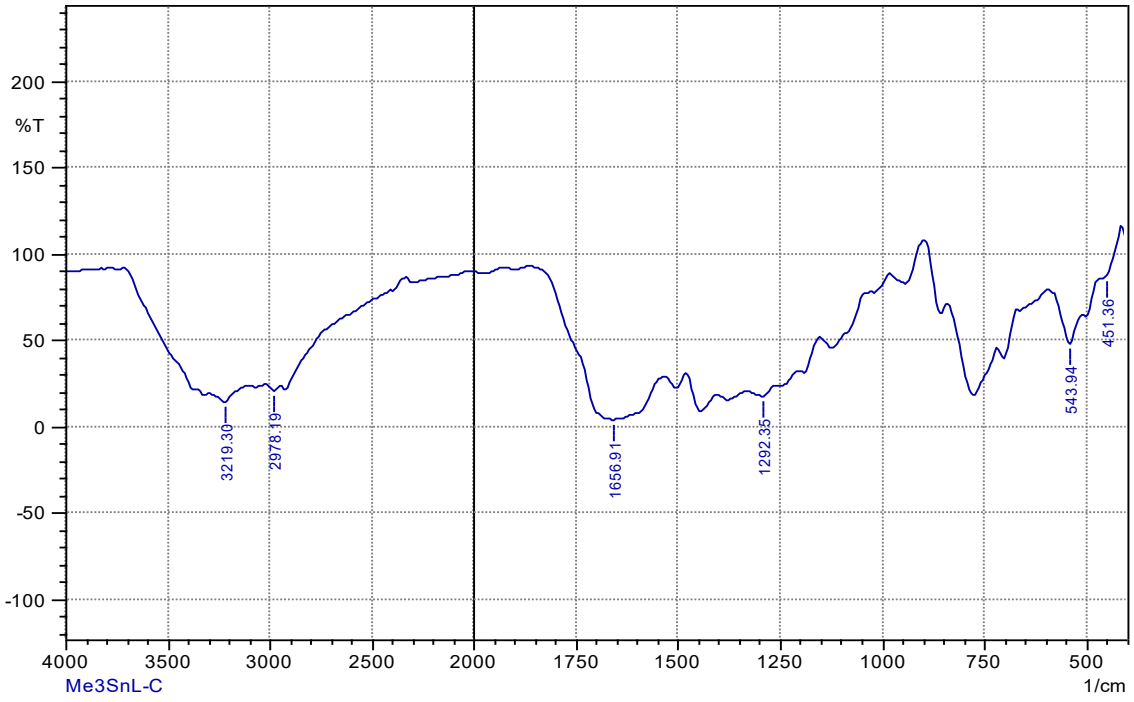

Figure 3.4 FTIR Spectrum of Me_3SnL.

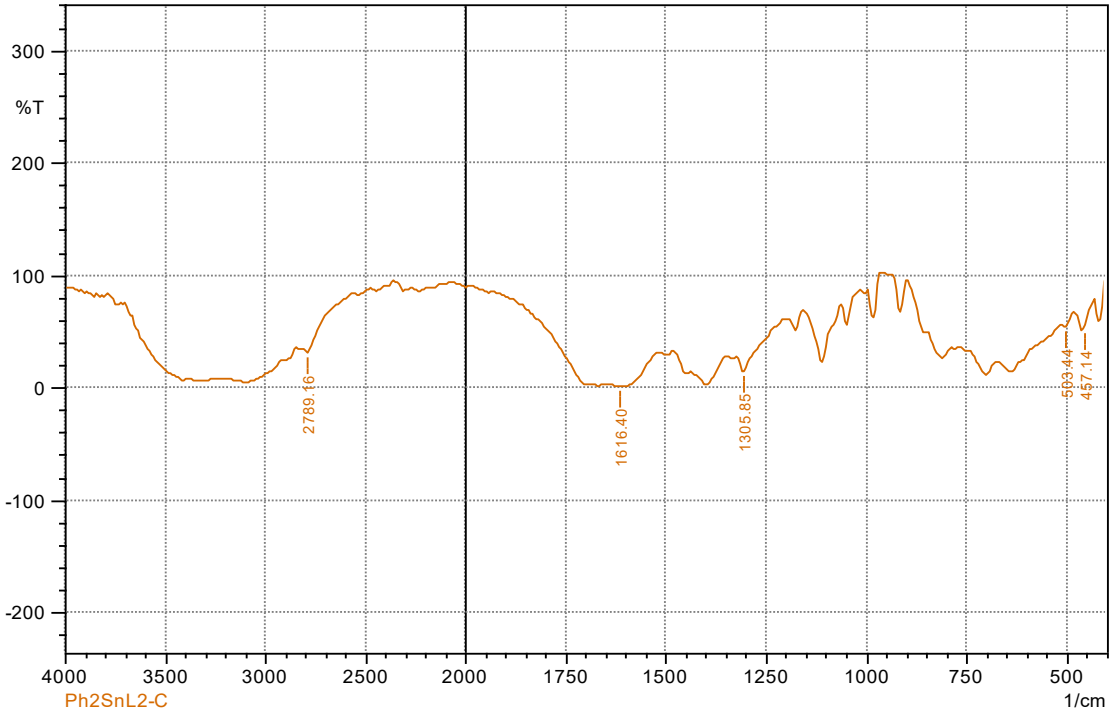

Figure 3.5 FTIR Spectrum of Ph_2SnL_2.

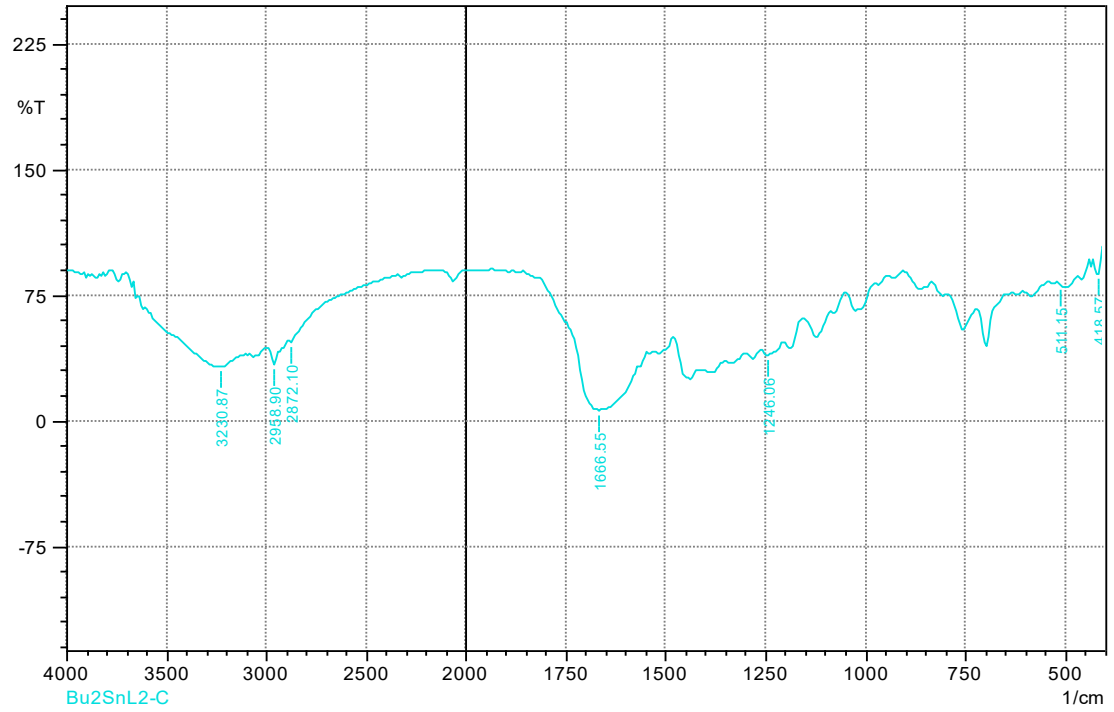

Figure 3. 6 FTIR Spectrum of Bu_2SnL_2.

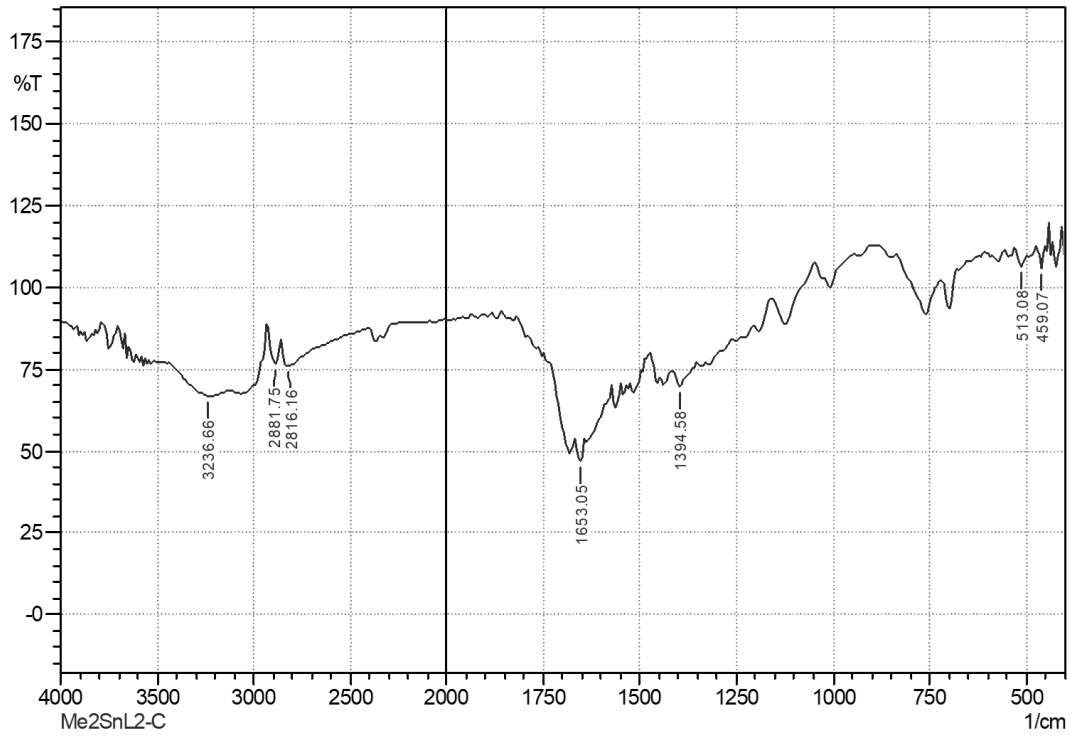

Figure 3.7 FTIR Spectrum of Me_2SnL_2.

3.1.4 Nuclear Magnetic Resonance Spectroscopy

Nuclear magnetic resonance spectroscopy (NMR) is an essential and commonly utilized analytical instrument in both academic and industrial applications. It enables the determination of the complete structure of molecules, even in mixtures [128].

3.1.4.1 ^{1}H-NMR Spectroscopy of Cephalexin and its Complexes

The ^{1}H (Proton) NMR spectrum, together with the chemical shift and coupling constants, provides the quantitative relationship between intramolecular and intermolecular resonances. The chemical change values between the ligand and its organotin (IV) complexes are significantly connected to the environment and can be used to prove coordination [129,130]. Cephalexin and organotin (IV) complexes were analyzed using ^{1}H-NMR spectroscopy in DMSO-d_6 solvent and tetramethyl silane serve as the internal reference standard. The spectra of ligand and organotin (IV) complexes indicated the elimination of the carboxylic group proton (-COOH), which shows as an exchangeable singlet in the ligand at 12.91 ppm, therefore ^{1}H-NMR spectra of the organotin (IV) complexes did not show this signal because the oxygen atoms of the carboxylate group combine with the tin atom. When the ligand coordinates with the organotin (IV) moiety, the up field shifting for complexes decreases [131]. Also, appearance new signals related to protons of phenyl, butyl, and methyl groups. When compared to the protons that are present in the ligand, the aromatic protons that are found in organotin (IV) complexes have a slight downfield shift due to resonance present in aromatic ring [132]. As the number of coordinated tin atoms increases, resulting increases in chemical shift [133]. In all complexes, the N-H proton appears as a singlet, suggesting that the nitrogen atom did not coordinate with the tin center. Cephalexin and its complexes are illustrated in Table 3.3. and Figs. 3.8-3.14.

Table 3.3 The ^{1}H-NMR Spectra (DMSO-d_6) of Cephalexin and its Complexes.

Ligand and Tin (IV) Complexes	^{1}H-NMR
Cephalexin	δ12.91(s,1H,COOH), 8.90 (s,1H,NH), 8.62 (d, J=9.6 Hz.2H,Ar), 8.47-7.30 (m,2H,Ar), 7.25 (t, J=8.5 Hz,1H,Ar), 5.41 (d, J=10.3 Hz,1H,N-CH), 5.25 (d, J=8.9 Hz ,1H,CO-CH), 5.02 (s,1H,PhCH-), 4.56-3.24 (br,2H,NH_2), 3.21(d, J=13.9 Hz,1H,S-CH), 3.16 (d, J=13.9 Hz ,1H,S-CH), 2.09 (s,3H,Me).
Ph_3SnL	δ9.58 (s,1H,NH), 8.85 (d,J=28.3,Hz,2H,Ar), 8.40-7.16 m,14H,Ar), 6.99 (t , J=11 Hz ,1H, Ar), 6.70 (t , J=11 Hz ,3H, Ar), 6.02 (d, J=10.8 Hz , 1H, N-CH), 5.50 (d, J=9.5 Hz ,1H, CO-CH), 4.97 (s,1H, PhCH-), 3.90-3.40 (br,2H, NH_2), 3.20 (d, J=14 Hz,2H, S-CH), 1.05 (s,3H, Me).
Bu_3SnL	δ8.46 (s,1H,NH), 8.30 (d,J=8.6Hz,2H,Ar), 8.20 (t,J=6.8Hz,1H,Ar), 8.07-6.50 (m,2H,Ar), 5.07 (d, J=14.5 Hz,1H, N-CH), 4.83 (d, J=12.5 Hz ,1H , CO-CH), 3.90 (s,1H, PhCH-) ,3.73 (d, J= 8.5 Hz ,2H, S-CH), 3.69-3.20 (br,2H,NH_2), 1.90 (s,3H, Me), 1.60 (qut, J= 7.5 Hz, 6H,3CH_2), 1.30 (sex, J=7.5Hz ,6H,3CH_2), 1.09 (t, J= 7.5Hz,9H,3Me), 0.87 (t, J=7.2 Hz,6H,3CH_2).
Me_3SnL	9.54 (s,1H,NH), 8.81(d,J=21.4,Hz,2H,Ar), 8.43-7.10 (m,2H,Ar), 6.67 (t , J=11 Hz ,1H, Ar), 5.98 (d, J=10.4 Hz , 1H, N-CH), 5.64 (d, J=7.5 Hz ,1H , CO-CH), 5.46 (s,1H, PhCH-), 3.95-3.40 (br,2H, NH_2), 3.20 (d, J=9.5 Hz ,1H, S-CH), 3.10(d, J=9.5 Hz ,1H, S-CH), 0.45(s,3H, Me),0.25(s,9H,3Me).
Ph_2SnL_2	δ 9.25 (s,2H,2NH),8.63 (d, J=9.5 Hz,4H,Ar), 8.54-7.10 (m,12H,Ar), 5. 88 (t, J=5.5 Hz,4H, Ar), 5.59 (d, J=5.0Hz,2H,2N-CH), 5.34 (d, J=7.5Hz,2H,2CO-CH),4.97 (s,2H,2PhCH-),4.45-3.26 (br,4H,2NH_2), 3.20 (d, J=9.5 Hz,4H, 2S-CH_2), 1.50 (s,3H,2Me).
Bu_2SnL_2	δ 9.15 (s,2H,2NH), 8.68 (d, J=22.8 Hz,4H,Ar), 8.59-6.92 (m,4H,Ar), 6.54 (t, J=11 Hz,2H,Ar),5.94 (d, J=10 Hz, 2H,2N-CH), 4.96 (d, J=23.5Hz,2H,2CO-CH),4.45 (s,2H,2PhCH-),4.18-3.23 (br,4H,2NH_2) 3.20 (d, J=9 Hz,4H,2S-CH_2), 1.93 (s ,6H,2Me),1.65 (qut, J=7.5 Hz, 4H,2CH_2),1.45 (sex,J=7.5 Hz,4H,2CH_2),1.20 (t, J=7.5 Hz,6H,2Me), 0.95 (t, J=7.3 Hz,4H,2CH_2).
Me_2SnL_2	δ 8.63 (s,2H,2NH), 8.06 (d, J=14.5 Hz,4H,Ar),7.98-6.84 (m,4H,Ar), 6.59 (t, J=6.5 Hz ,2H, Ar),6.05 (d, J=11 Hz, 2H,2N-CH), 5.49 (d, J=8.3 Hz,2H,2CO-CH),5.35(s,2H,2PhCH-),5.20-3.20 (br,4H,2NH_2), 3.10 (d, J=6.5 Hz,4H,2S-CH_2), 1.62 (s,6H,2Me), 0.85 (s,6H,2Me).

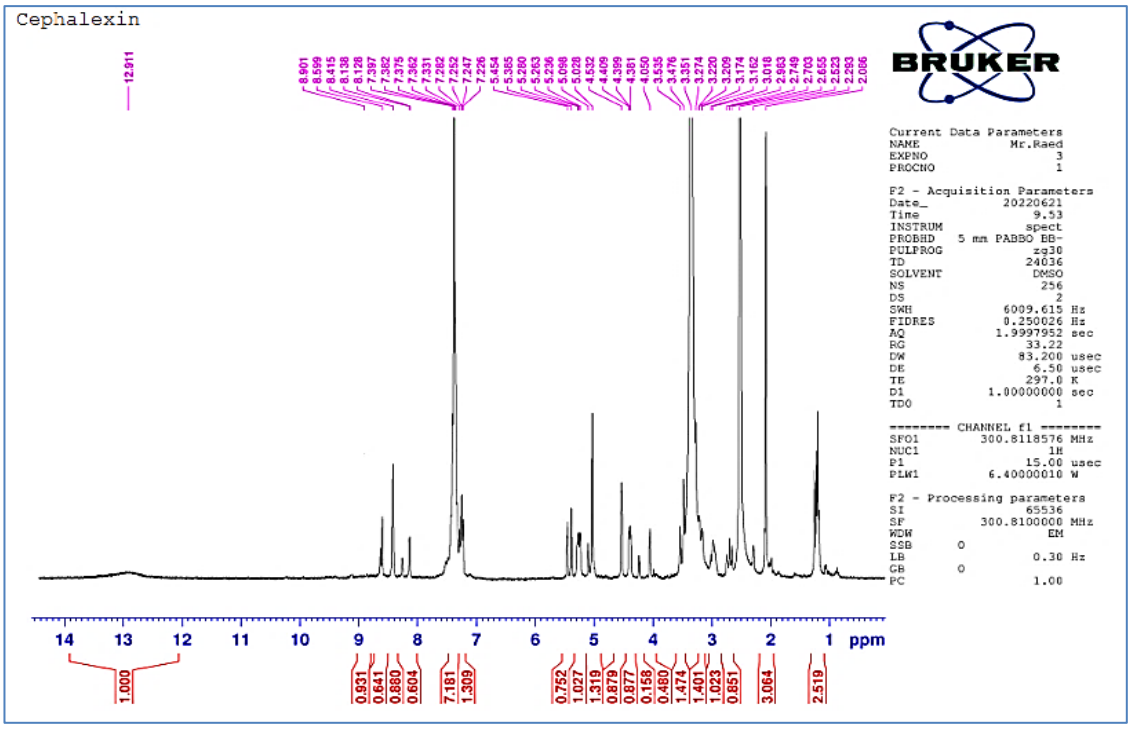

Figure 3.8 ^{1}H-NMR Spectrum of Cephalexin.

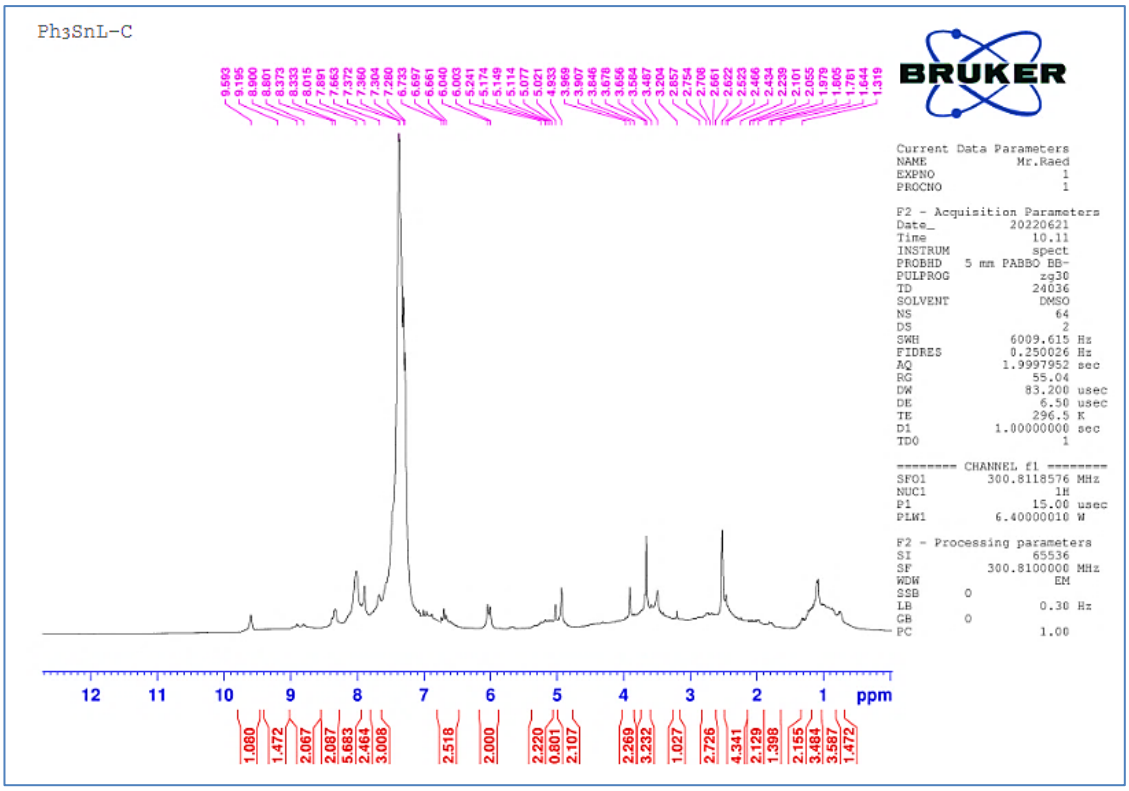

Figure 3.9 ^{1}H-NMR Spectrum of Ph_3SnL Complex.

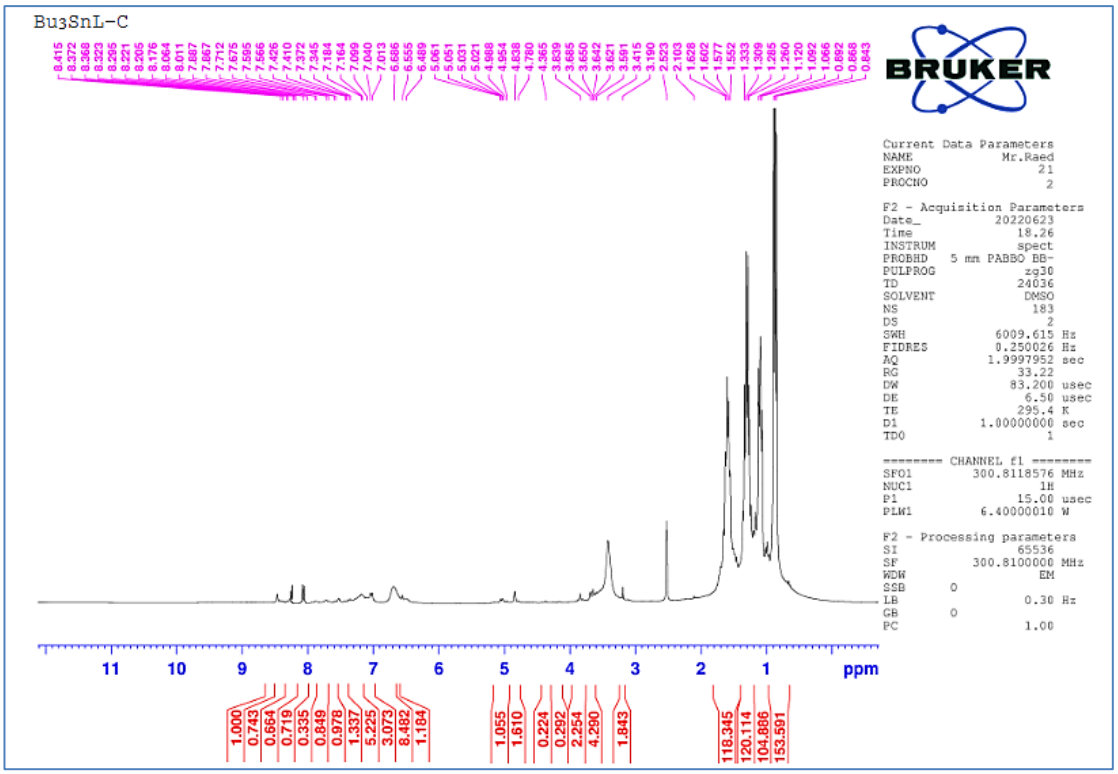

Figure 3.10 ^{1}H-NMR Spectrum of Bu_3SnL Complex.

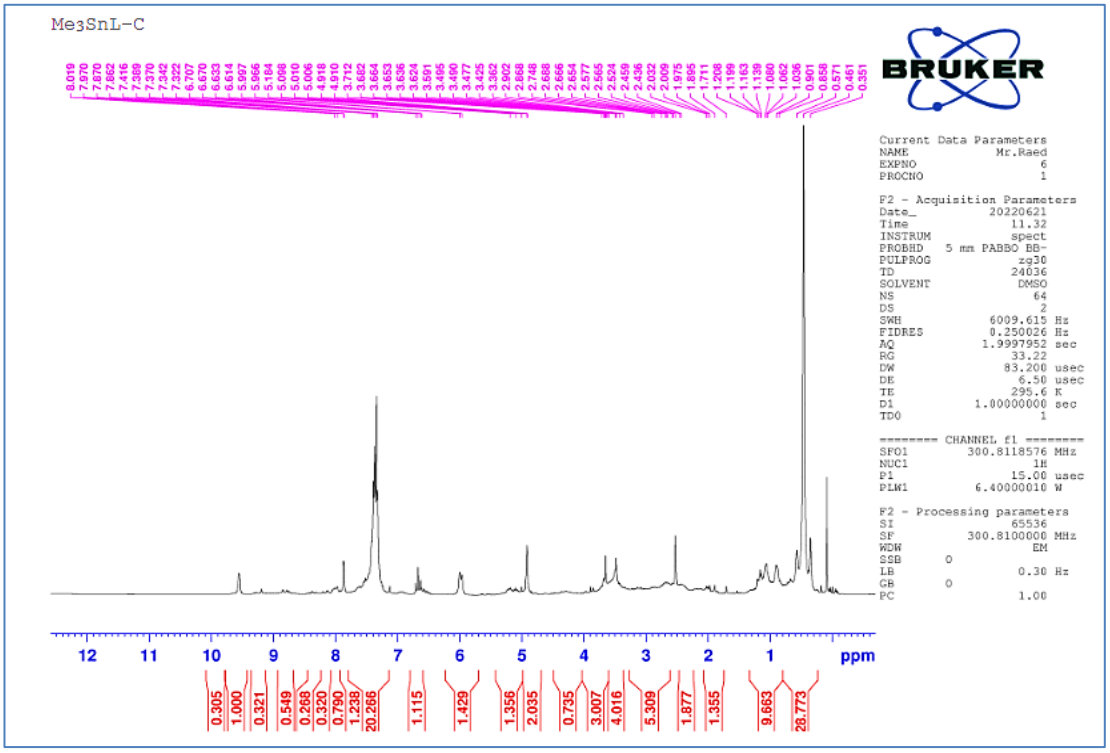

Figure 3.11 ^{1}H-NMR Spectrum of Me_3SnL Complex.

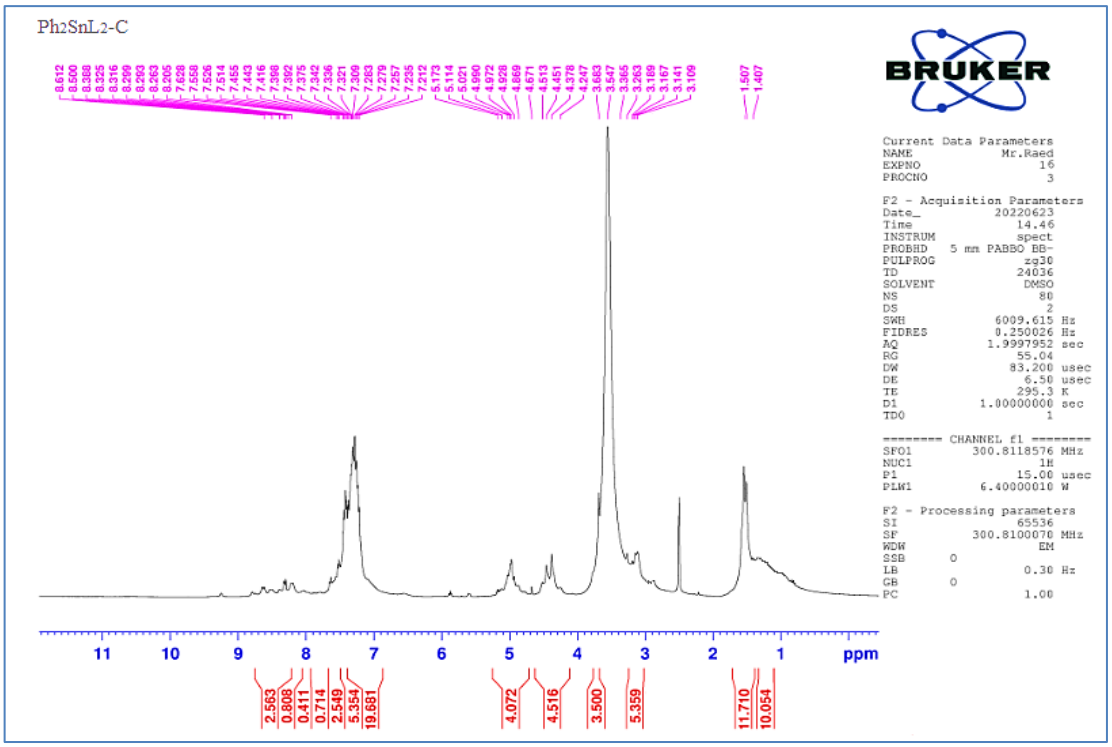

Figure 3.12 ^{1}H-NMR Spectrum of Ph_2SnL_2 Complex.

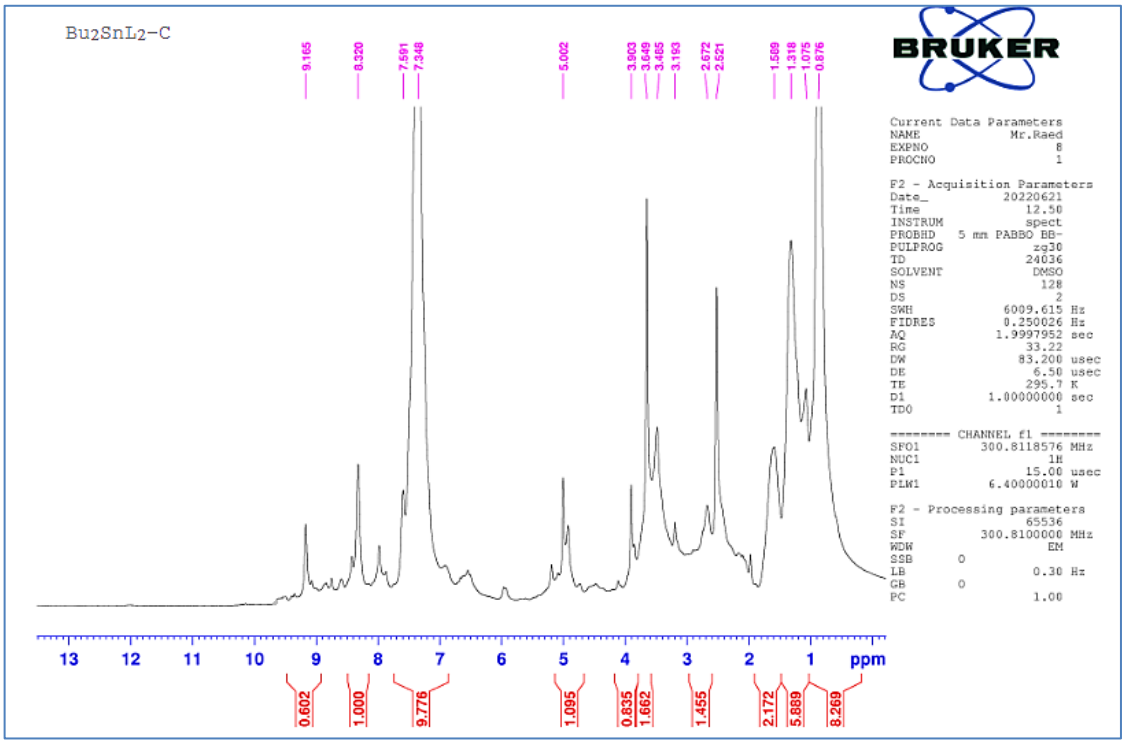

Figure 3.13 ^{1}H-NMR Spectrum of Bu_2SnL_2 Complex.

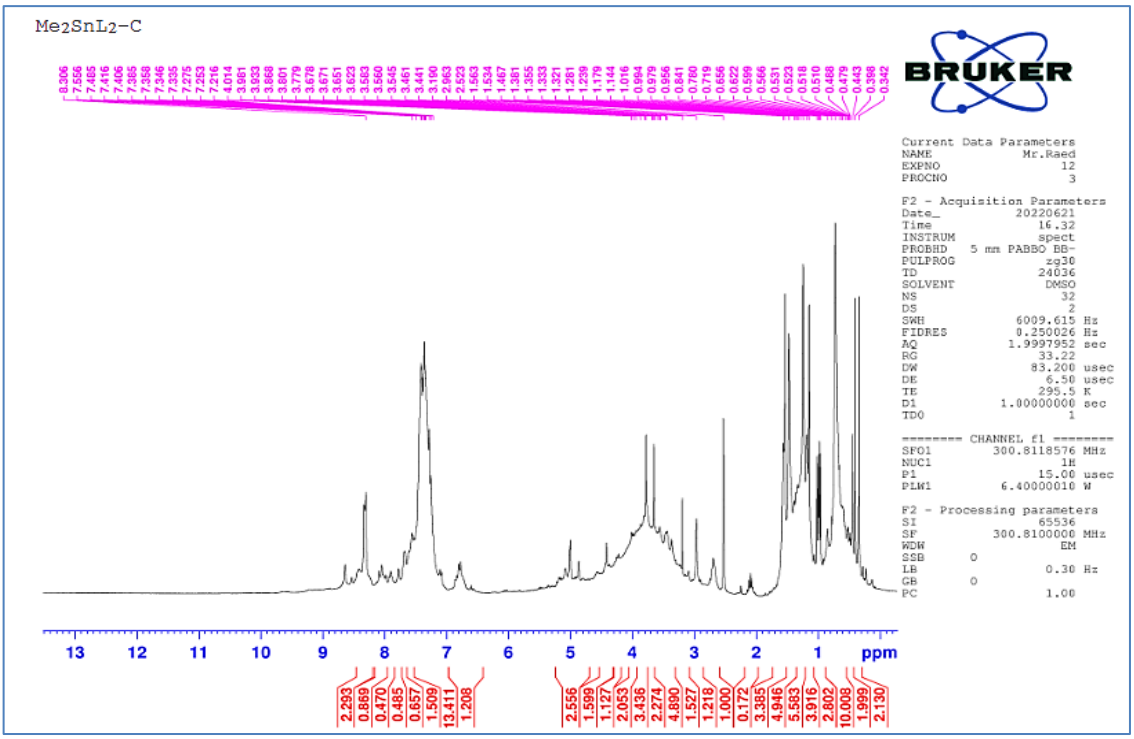

Figure 3.14 ^{1}H-NMR Spectrum of Me_2SnL_2 Complex.

3.1.4.2 ^{13}C- NMR Spectroscopy of Cephalexin and its Complexes

The^{13}C-NMR spectrum detects carbon atoms in different environments inside a molecule. Their spectra were recorded in deuterated DMSO-d_6. In organotin (IV) complexes the carboxylate carbon (C_{15}) showed a downfield chemical shift in the range 173.5-163.6 ppm compared with the position in the free ligand (Cephalexin) which appeared at position 183 ppm. Also, appearance new signals related to carbons of aryl and alkyl groups. It is most possible that shift is due to the decrease of electron density at carbon atoms when oxygen is coupled to an electropositive tin atom. This observation gives further evidence that the complexation occurred through the oxygen atoms of the carboxylate group [134,135]. Table 3.4 and Figs.3.15-3.21 display the ^{13}C- NMR data.

Table 3.4 Shows the ^{13}C-NMR Spectra (DMSO-d_6; ppm) of Cephalexin and its Complexes.

Ligand and organotin (IV) Complexes	^{13}C-NMR
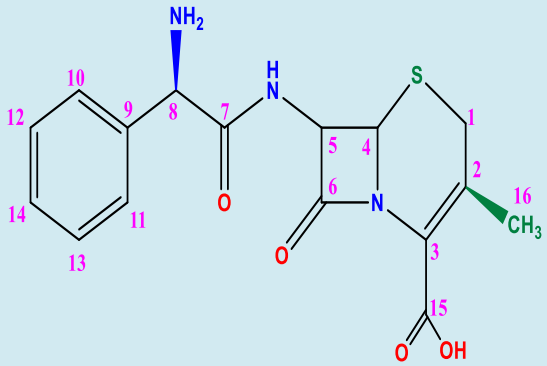 Ligand-Cephalexin	(C_{15}-Carboxyl, 183.0), (C_7 ,169.2), (C_6 ,168.2), (C_{14} ,142.6) , (C_{12},C_{13},138.3), (C_{10},C_{11} ,132.5), (C_9 ,130.1) ,(C_3 ,129.5), (C_2 ,128.3), (C_5 ,64.5), (C_4 ,58.3),(C_8 ,57.2), (C_1 ,22.3), (C_{16} ,18.5).
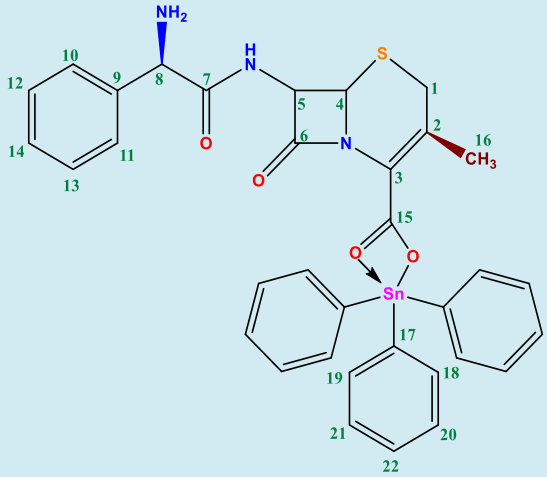	(C_{15},1C,163.7), (C_7,1C,162.4),(C_6,1C,162.2), (C_{17},3C,140.8),(C_{20},C_{21},6C,140.6),(C_{12},C_{13},2C,136.9) ,(C_{18},C_{19},6C,136.5),(C_{14},1C,129.6), (C_{22},3C,128.9),(C_{11},2C,128.4),(C_9,1C,128.0), (C_3,1C,127.2),(C_2,1C,127.0),(C_5,1C,59.7), (C_4,1C,59.5),(C_8,1C,59.0), (C_1,1C,32.1), (C_{16},1C,22.3).

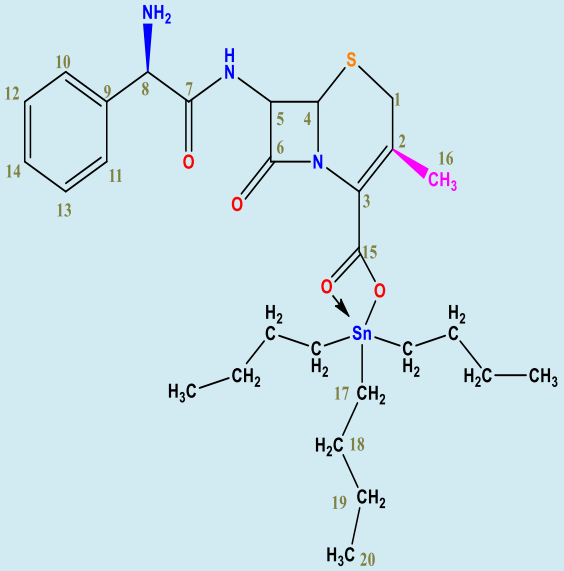	(C_{15},1C,171.9), (C_7,1C,167.9), (C_6,1C,167.4), (C_{12},C_{13},2C,131.9),(C_{14},1C,131.6),(C_{10},C_{11},2C,131.0),(C_9,1C,129.9),(C_3,1C,129.2),(C_2,1C,128.3),(C_5,1C,61.1),(C_4,1C,60.0),(C_8,1C,58.6),(C_1,1C,28.2),(C_{18},3C,27.5),(C_{19},3C,27.0), (C_{16},1C,26.5),(C_{17},3C,23.1), (C_{20}, 3C,19.9).
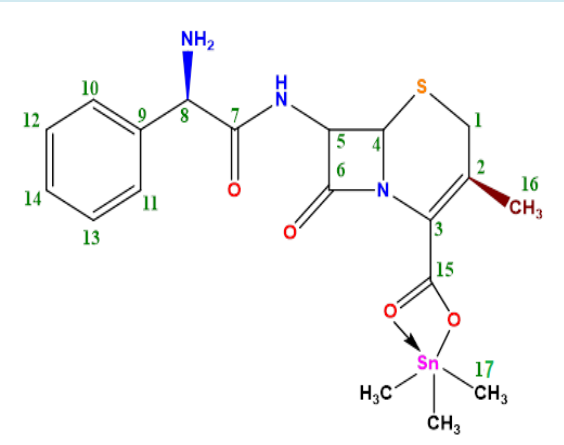	(C_{15},1C,163.8), (C_7,1C,162.2), (C_6,1C,155.3), (C_{12},C_{13},2C,140.8),(C_{14},1C,128.9),(C_{10},C_{11},2C,128.3),(C_9,1C,127.9),(C_3,1C,127.0),(C_2,1C,126.9),(C_5,1C,59.7),(C_4,1C,59.3),(C_8,1C,58.9),(C_1,1C,31.7),(C_{16},1C,21.7),(C_{17},3C,-8.5).
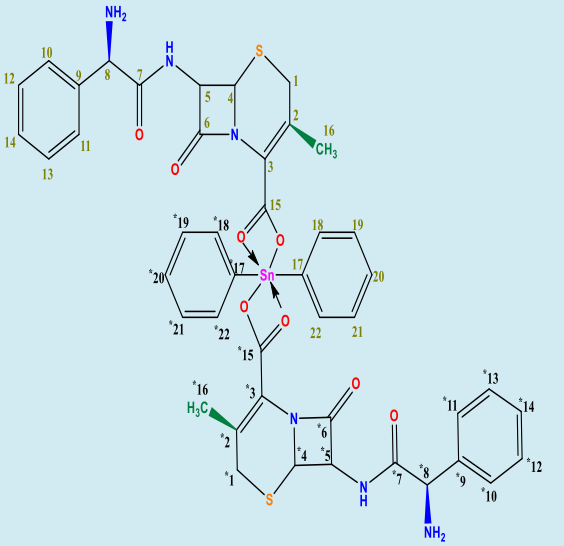	(C_{15},C_{15}*,2C,173.5),(C_7,C_7*,2C,172.8),(C_6,C_6*,2C,162.5),(C_{17},C_{17}*,2C,143.3),(C_{20},C_{20}*,C_{21} C_{21}*,4C,142.5),(C_{12},C_{12}*,C_{13},C_{13}*,4C,138.6),(C_{18},C_{18}*,C_{19},C_{19}*,4C,138.2),(C_{14},C_{14}*,2C,129.8),(C_{22},C_{22}*,2C,128.9),(C_{10},C_{10}*,C_{11},C_{11}*,4C,128.6),(C_9,C_9*,2C,128.2),(C_3,C_3*,2C,127.6),(C_2,C_2*,2C,127.2),(C_5,C_5*,2C,60.4),(C_4,C_4*,2C,59.5),(C_8,C_8*,2C,59.2),(C_1,C_1*,2C,32.6), (C_{16},C_{16}*,2C,25.4).

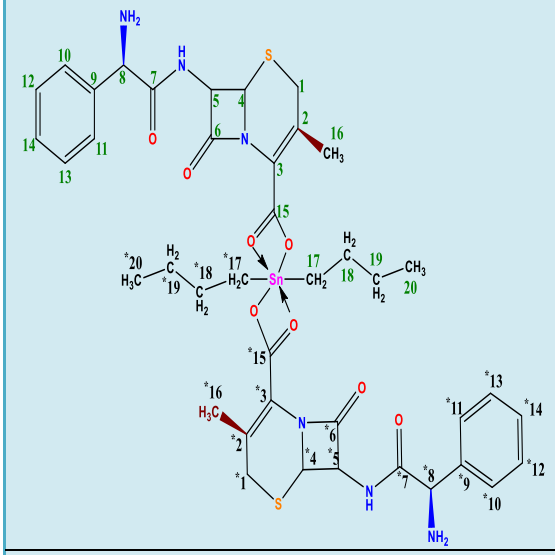	(C_{15},C_{15}*,2C,162.6),(C_7,C_7*,2C,162.3),(C_6, C_6*,2C,161.5),(C_{12},C_{12}*,C_{13},C_{13}*,4C,140.7), (C_{14},C_{14}*,2C,138.8),(C_{10},C_{10}*,C_{11},C_{11}*,4C, 136.5),(C_9,C_9*,2C,129.5),(C_3,C_3*,2C,128.9), (C_2,C_2*,2C,128.5),(C_5,C_5*,2C,59.8),(C_4,C_4* ,2C,58.3),(C_8,C_8*,2C,53.2),(C_1,C_1*,2C,28.2), (C_{18},C_{18}*,2C,27.5),(C_{19},C_{19}*,2C,26.4),(C_{16}, C_{16}*,2C, 26.1),(C_{17},C_{17}*,2C,22.5), (C_{20},C_{20}*.2C,14.0).
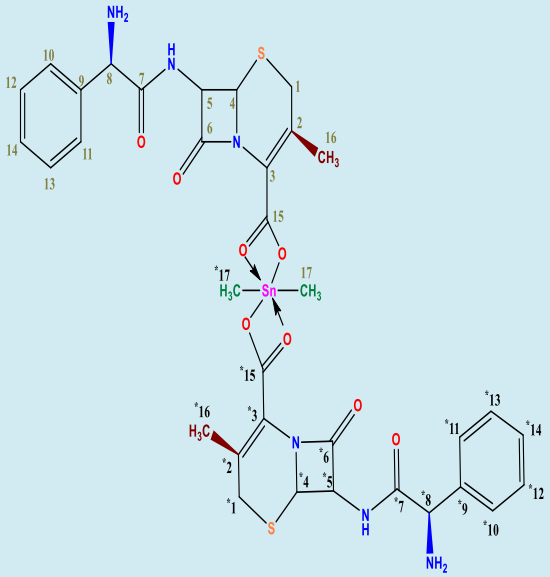	(C_{15}, C_{15}*,2C,176.9), (C_7, C_7*,2C,175.2), (C_6, C_6*,2C,163), (C_{12}, C_{12}*,C_{13},C_{13}*,4C,142.4), (C_{14},C_{14}*,2C,140.7),(C_{10},C_{10}*,C_{11},C_{11}*,4C, 139.7),(C_9,C_9*,2C,139.3),(C_3,C_3*,2C,128.6), (C_2,C_2*,2C,127.3),(C_5,C_5*,2C,66.7),(C_4,C_4* ,2C,59.8),(C_8,C_8*,2C,58.9),(C_1,C_1*,2C,19.3), (C_{17}, C_{17}*,2C, -2.2).

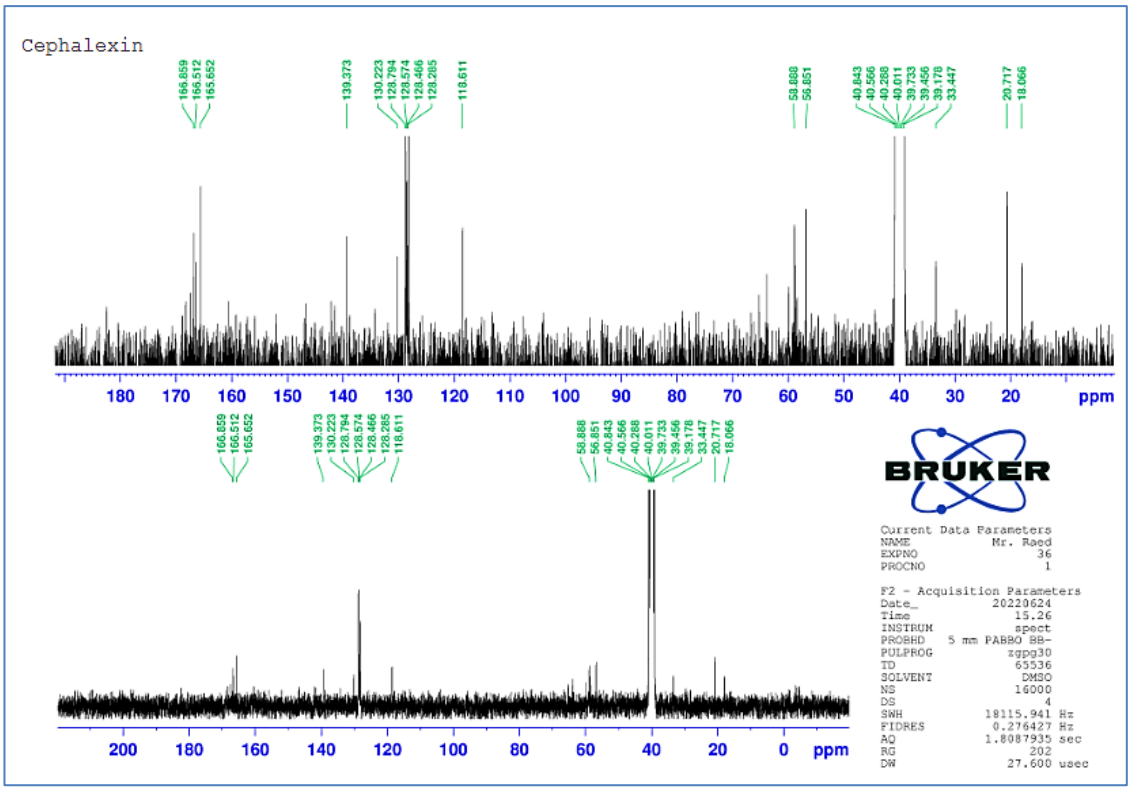

Figure 3.15 ^{13}C-NMR Spectra of Cephalexin.

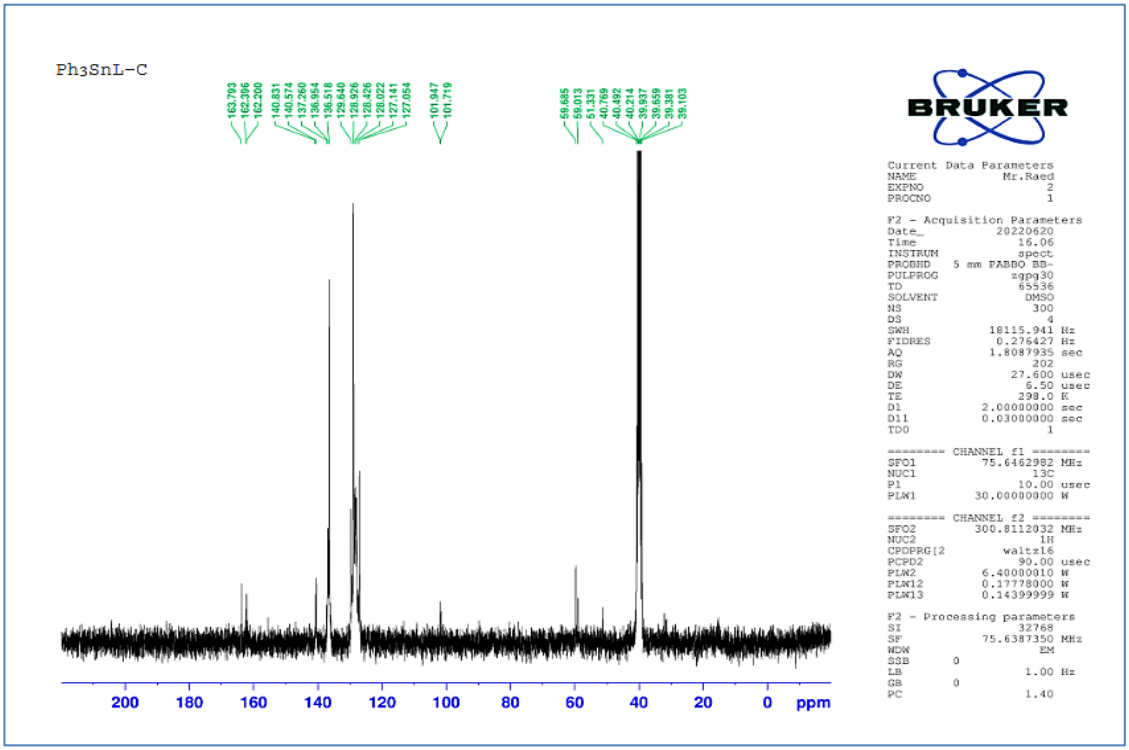

Figure 3.16 ^{13}C-NMR Spectrum of Ph_3SnL Complex.

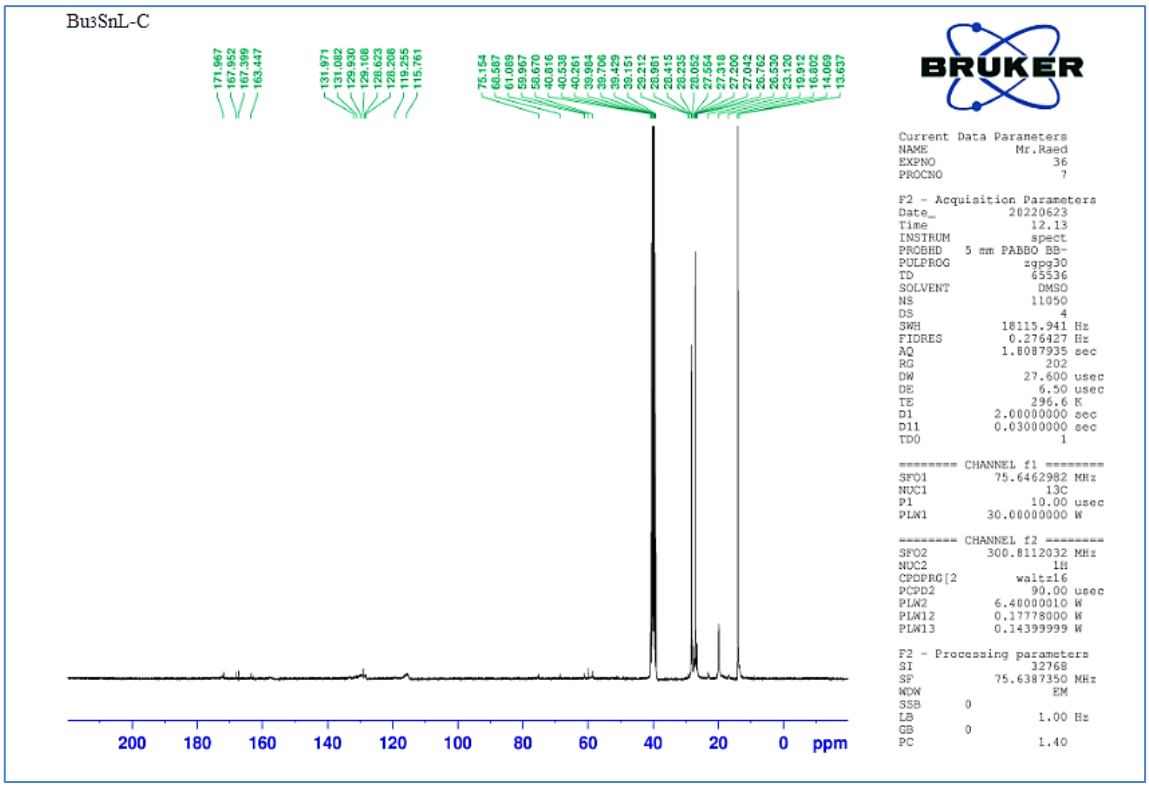

Figure 3. 17 ^{13}C-NMR Spectrum of Bu_3SnL Complex.

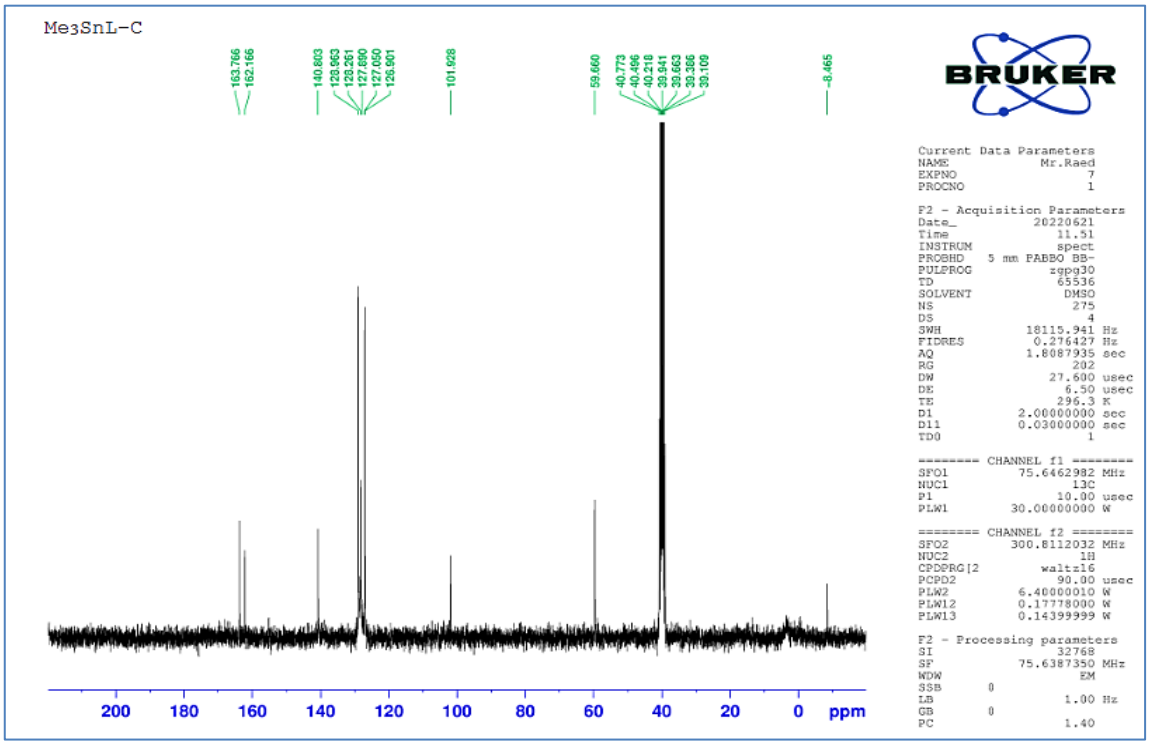

Figure 3. 18 ^{13}C-NMR Spectrum of Me_3SnL Complex.

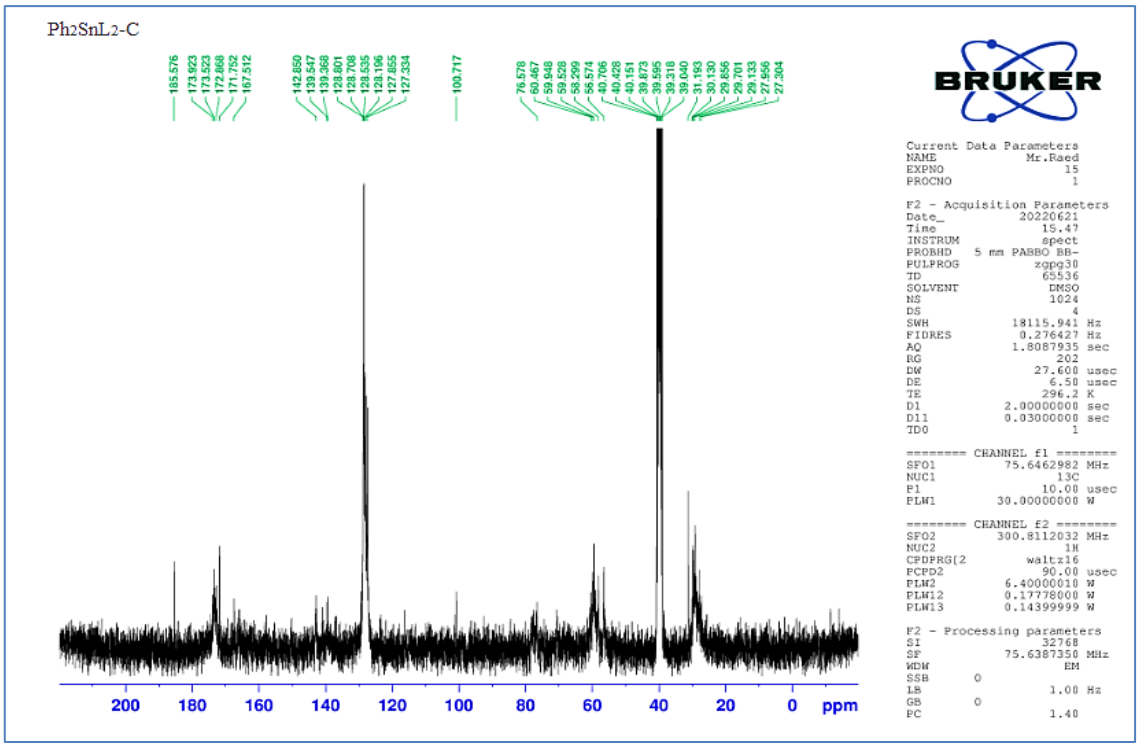

Figure 3.19 ^{13}C-NMR Spectrum of Ph_2SnL_2 Complex.

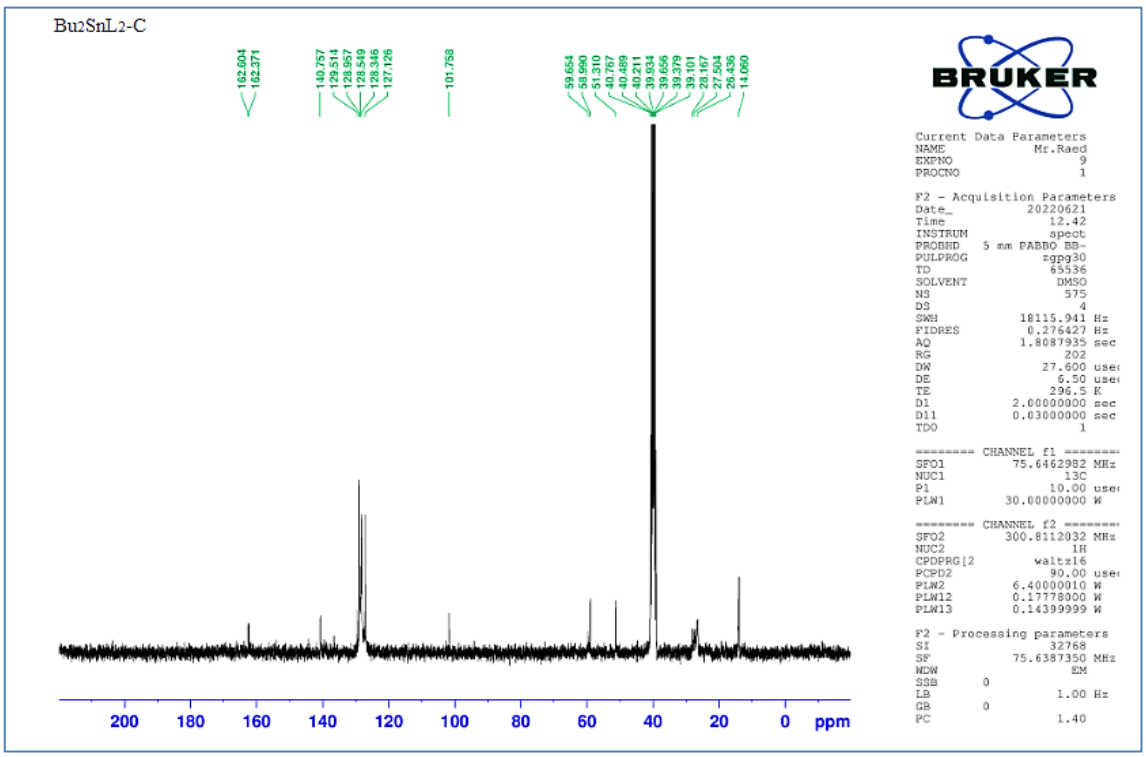

Figure 3.20 ^{13}C-NMR Spectrum of Bu_2SnL_2 Complex.

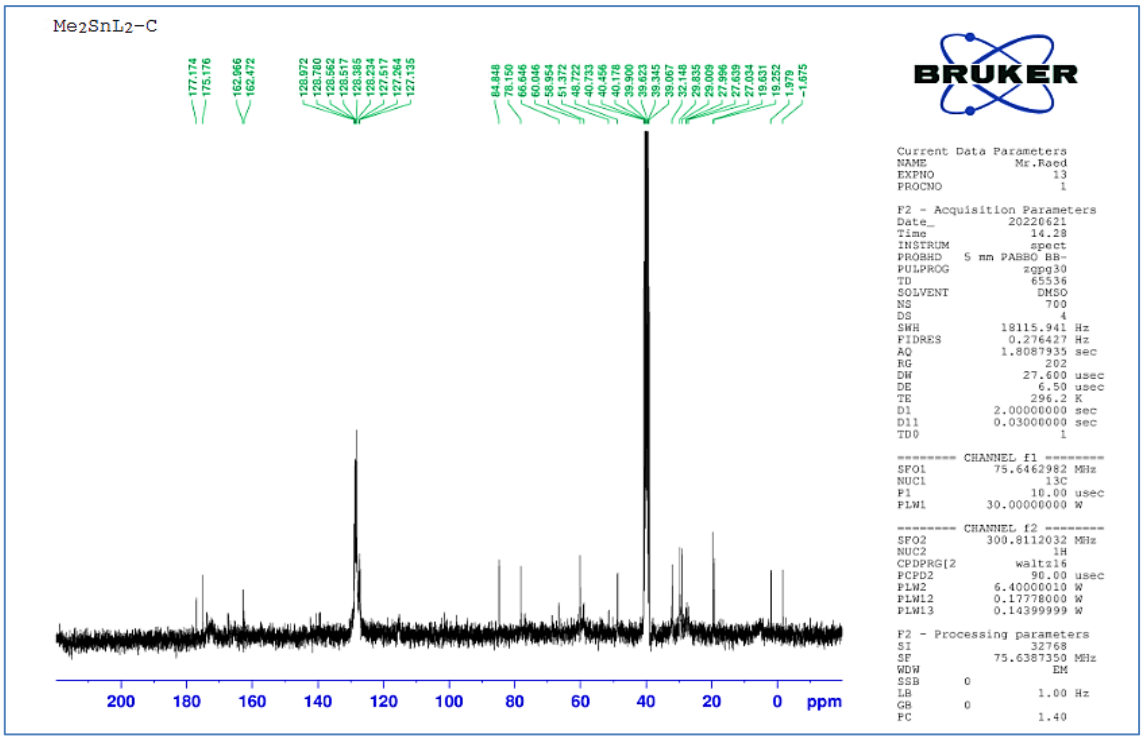

Figure 3.21 ^{13}C-NMR Spectrum of Me_2SnL_2 Complex.

3.1.4.3 ^{119}Sn-Nuclear Magnetic Resonance

The ^{119}Sn-NMR offers information that usually predicts probable geometry around the tin metal. The spectra for organotin (IV) complexes were recorded in DMSO-d_6. Different ^{119}Sn chemical shifts are present in complexes through tetra (+200 to - 60 ppm), penta (-90 to -190 ppm) and hexa (-210 to - 400 ppm) coordination numbers [136]. As shown in Table 3.5, the existence of a signals under -200 ppm indicates trigonal bipyramidal geometry, whereas the presence of a signals above -200 ppm indicates octahedral geometry. These results support coordination occurred between ligand and tin atom, leading to greater tin nuclear shielding [137]. Additionally, phenyl substituents result in greater chemical shifts than alkyl substituents [138]. As can be seen in Figs. 3.22-3.27.

Table 3.5 ^{119}Sn -NMR Spectral Information of Organotin (IV)-Cephalexin Complexes.

Complexes	δ (ppm)
Ph_3SnL	-158.34
Bu_3SnL	-143.51
Me_3SnL	-120.18
Ph_2SnL_2	-276.42
Bu_2SnL_2	-258.75
Me_2SnL_2	-209.97

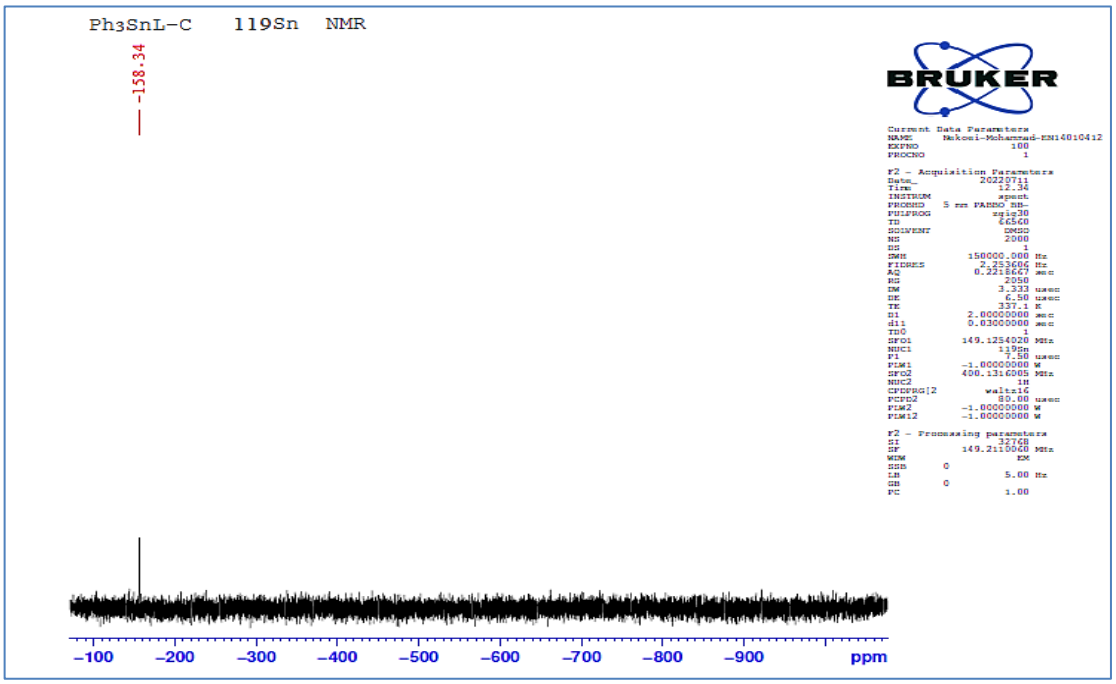

Figure 3.22 ^{119}Sn -NMR Spectrum of Ph_3SnL Complex.

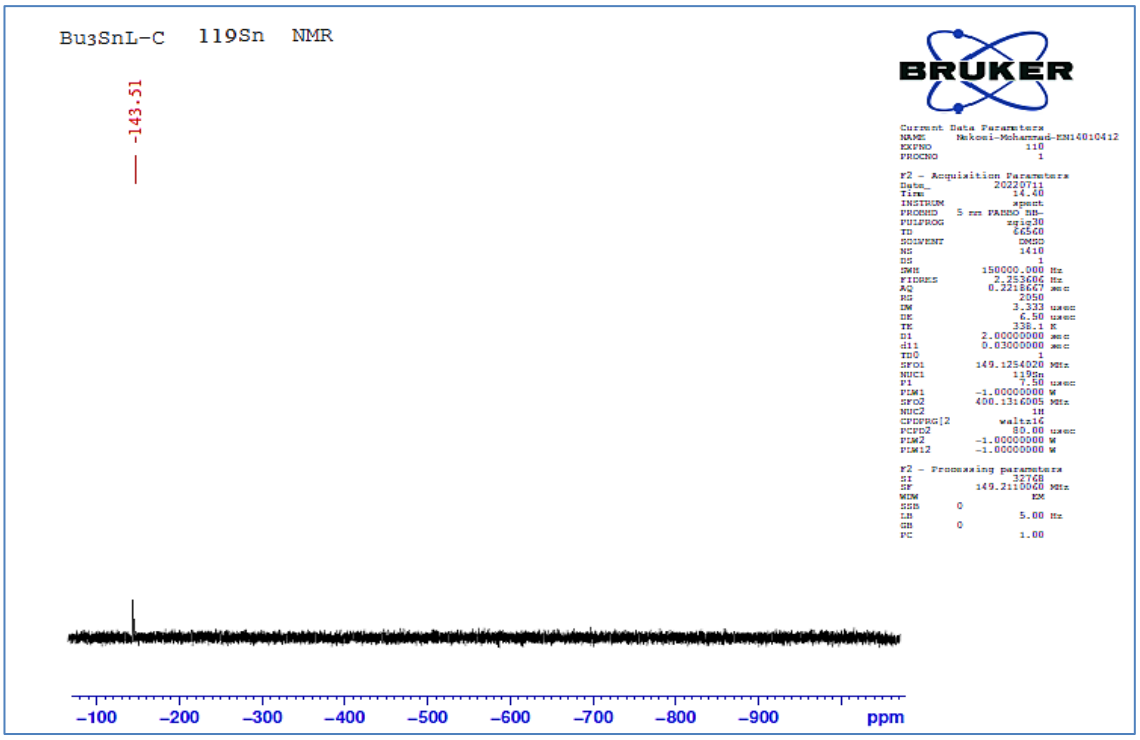

Figure 3.23 ^{119}Sn -NMR Spectrum of Bu_3SnL Complex.

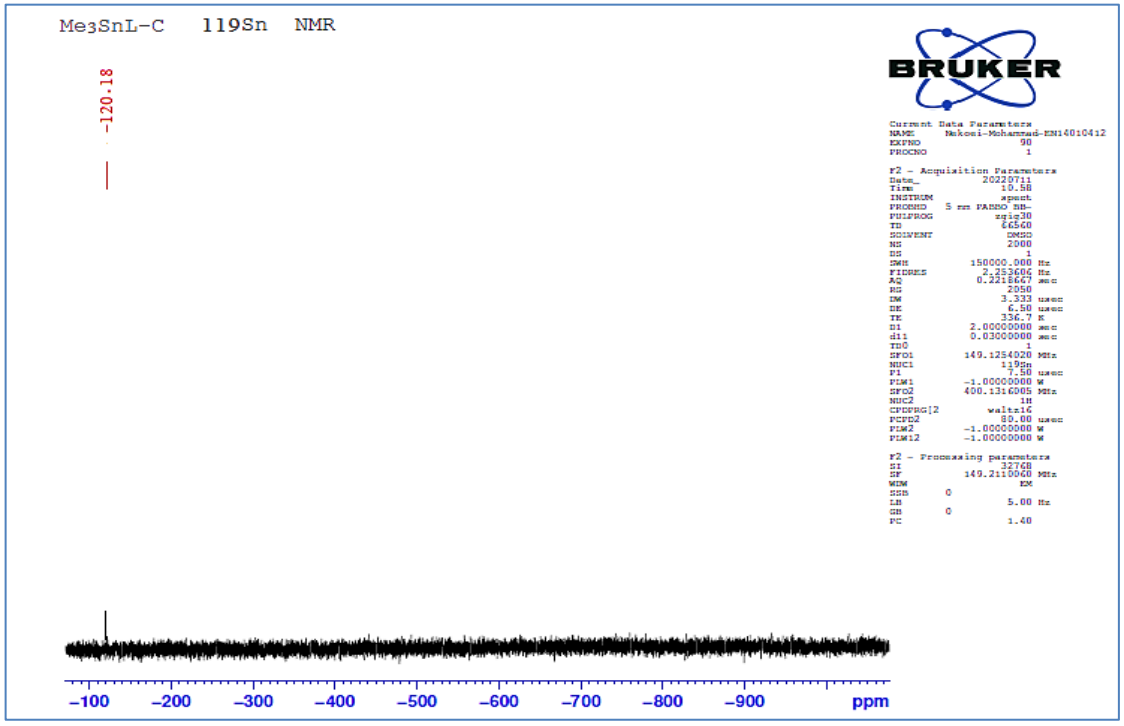

Figure 3.24 ^{119} Sn-NMR Spectrum of Me_3SnL Complex.

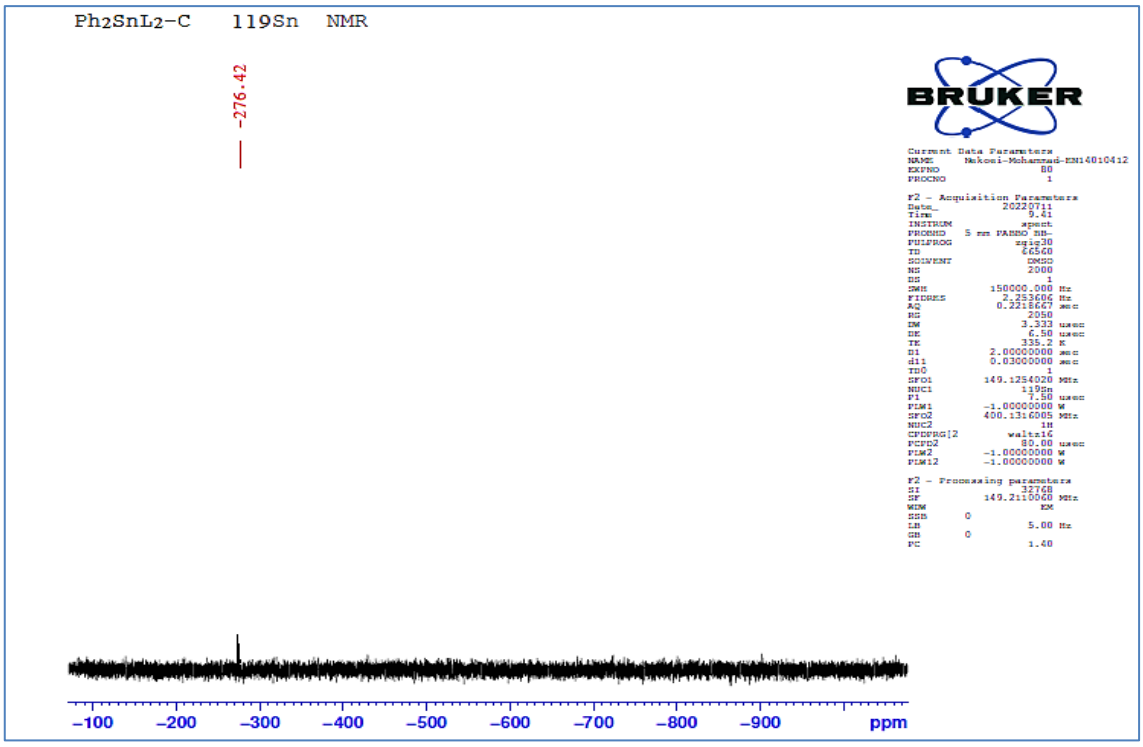

Figure 3.25 ^{119} Sn-NMR Spectrum of Ph_2SnL_2 Complex.

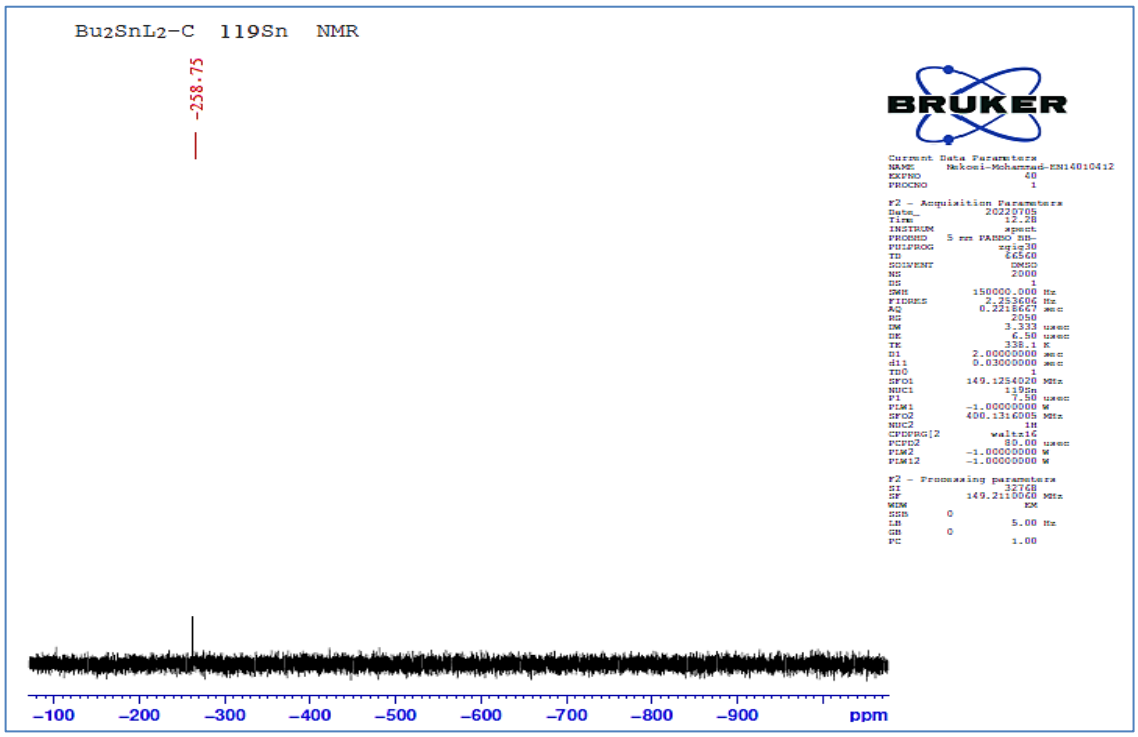

Figure 3.26 ^{119} Sn-NMR Spectrum of Bu_2SnL_2 Complex.

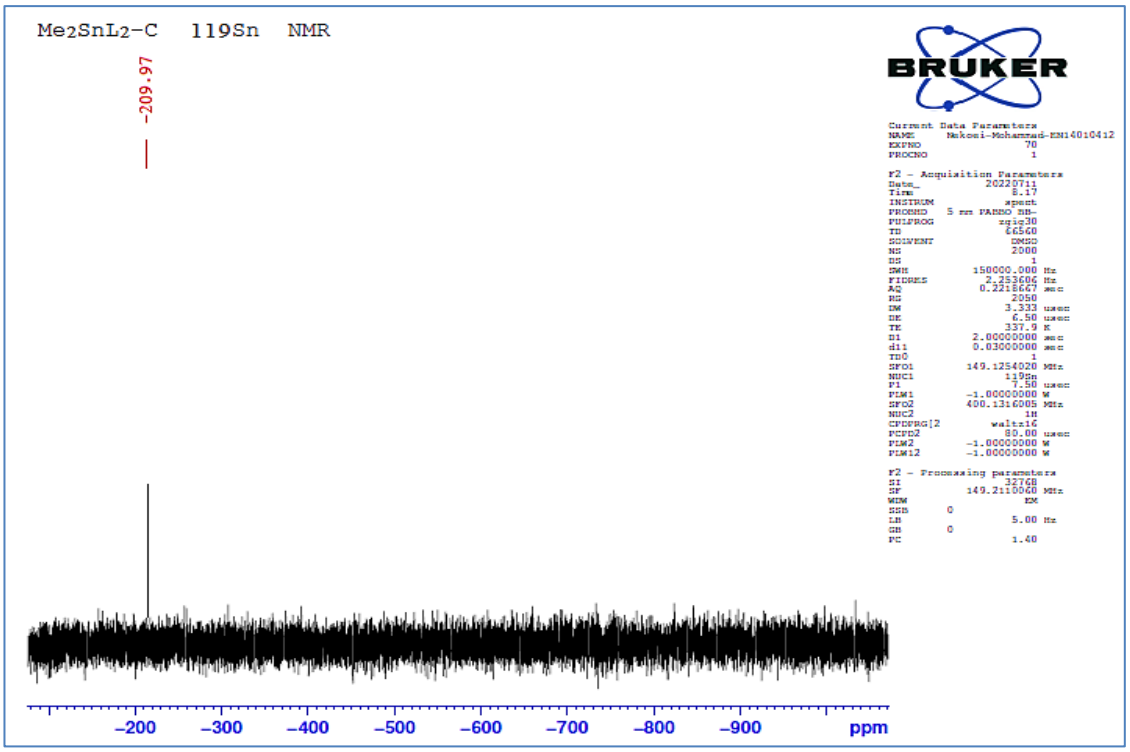

Figure 3.27 ^{119} Sn-NMR Spectrum of Me_2SnL_2 Complex.

3.2 Synthesis and Identification of Organotin (IV) L- Tyrosine Complexes

3.2.1 Synthesis of Organotin (IV) -Tyrosine Complexes

When all the components were dissolved in methanol and refluxed for five hours, the reaction between the ligand (L-Tyrosine), triorganotin (IV) chloride and diorganotin (IV) dichloride led to the formation of new organotin (IV) complexes, including Ph_3SnL, Bu_3SnL, Me_3SnL, Ph_2SnL_2, Bu_2SnL_2 and Me_2SnL_2, as shown in Schemes 3.3 and 3.4.

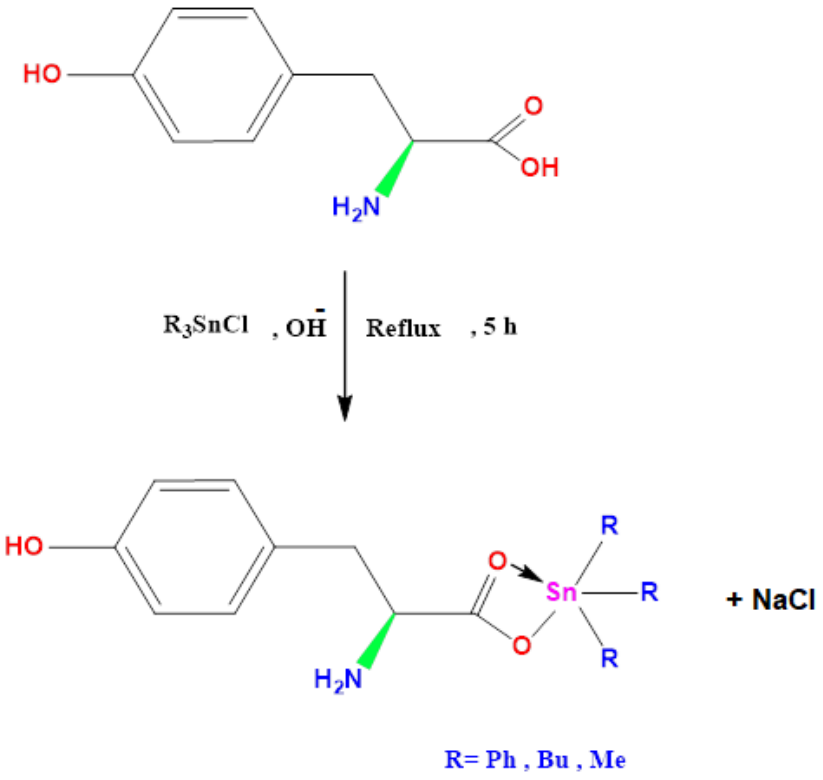

Scheme 3.3 Synthesis of Triorganotin (IV)-Tyrosine Complexes.

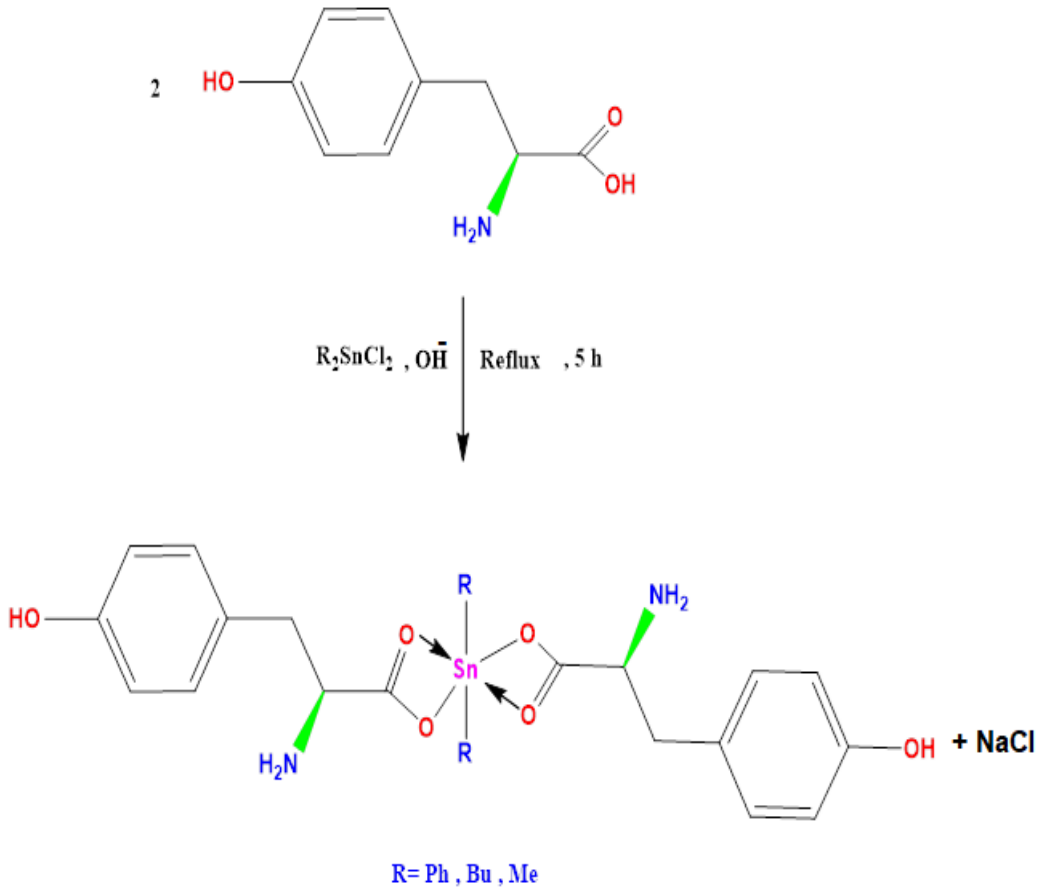

Scheme 3.4 Synthesis of Diorganotin (IV) -Tyrosine Complexes.

3.2.2 Physical Data

The chemical elements that exist in the tri and di Organotin (IV)-tyrosine complexes were determined using element analysis. The values of L-tyrosine and its complexes (Ph_3SnL, Bu_3SnL, Me_3SnL, Ph_2SnL_2, Bu_2SnL_2 and Me_2SnL_2) have been found to be associated with theoretical calculations. Table 3.6 includes the colours, melting points and yields of organotin (IV)-tyrosine complexes together with the percentages of carbon, hydrogen, and nitrogen.

Table 3.6 Physical and Elemental Analysis data of Ligand (Tyrosine) and Organotin (IV) Complexes.

Compounds	Colors	Melting Points (°C)	Yields (%)	Calculated % (Measured %) C	H	N
Tyrosine (L)	White	279-281	-------	59.66 (58.90)	6.12 (6.85)	7.73 (8.05)
Ph_3SnL	Off white	95-97	96	61.16 (62.25)	4.75 (5.05)	2.64 (2.25)
Bu_3Sn L	Greenish yellow	175-177	85	53.64 (52.95)	7.93 (8.02)	2.98 (3.25)
Me_3Sn L	Off white	245-247	97	41.90 (42.15)	5.57 (6.13)	4.07 (4.95)
Ph_2SnL_2	Grey	205-207	98	56.90 (55.85)	4.78 (5.05)	4.42 (4.95)
Bu_2SnL_2	Off white	230-232	98	52.63 (53.05)	6.46 (7.05)	4.72 (5.10)
Me_2SnL_2	Yellowish white	251-253	96	47.18 (48.05)	5.15 (5.95)	5.50 (6.05)

3.2.3 Fourier Transform Infrared Spectroscopy (FTIR)

Through the disappearance of some frequencies and the development of other frequencies, the frequency of significant groups in spectra offered strong evidence for newly formed compounds [139]. As a result of complexation by a tin atom, the bands that correspond to the stretching resonance of the O–H bonds for the ligand (L-tyrosine) were absent from the FTIR spectra of organotin (IV) -tyrosine complexes. As well as a change in the stretching frequencies in C-O and C=O groups for ligand which has the wave number 1263, 1613 cm^{-1} respectively evidences of the coordination between a metal ion and the ligand's carboxyl group. The FTIR spectra of the complexes showed new bands of absorption in the ranges 534-528 and 448-424 cm^{-1}, corresponding to the Sn-C and Sn-O groups [140,141] .

As shown in the Table 3.7 and Figs. 3.28-3.34. The amine group (NH_2) appears in ligand and all complexes in the position 3500-3300 cm^{-1} this indicated do not shared in complexation.

Table 3.7 Shows some of the FTIR Spectra for the Organotin (IV)-Tyrosine Complexes.

No.	Complexes	C=O	C-O	Sn-C	Sn-O
1	Ph_3Sn L	1597	1246	529	448
2	Bu_3Sn L	1598	1244	528	438
3	Me_3Sn L	1595	1242	534	436
4	Ph_2SnL_2	1615	1243	530	424
5	Bu_2SnL_2	1597	1242	529	428
6	Me_2SnL_2	1599	1244	528	434

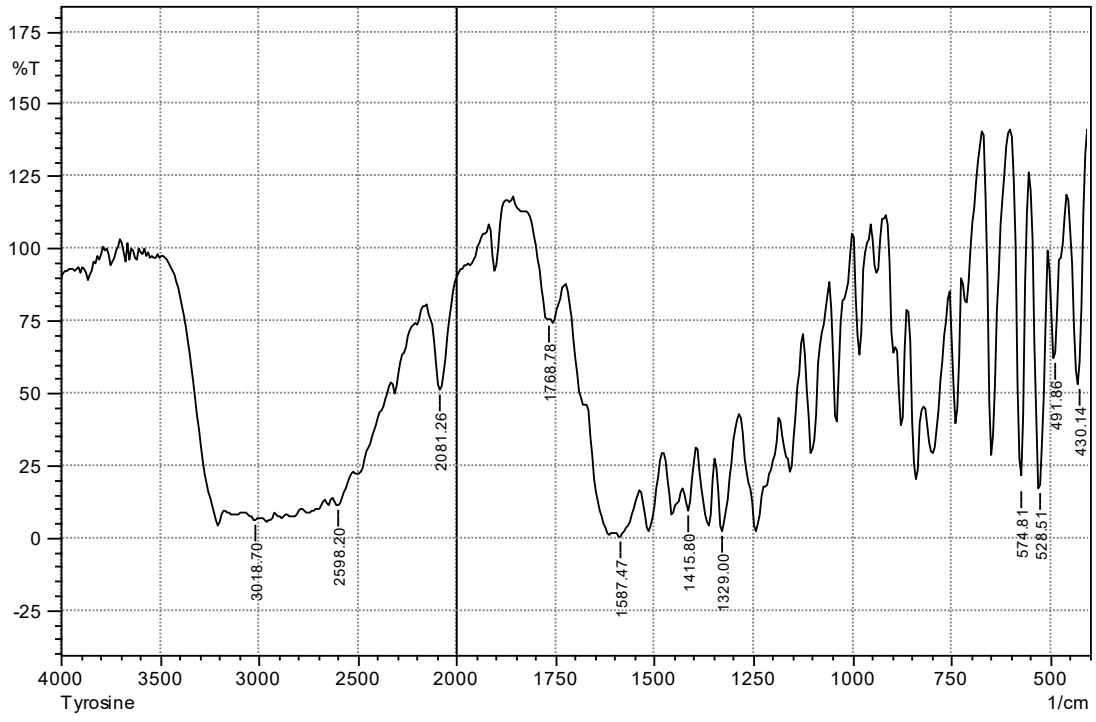

Figure 3.28 FTIR Spectrum of Tyrosine.

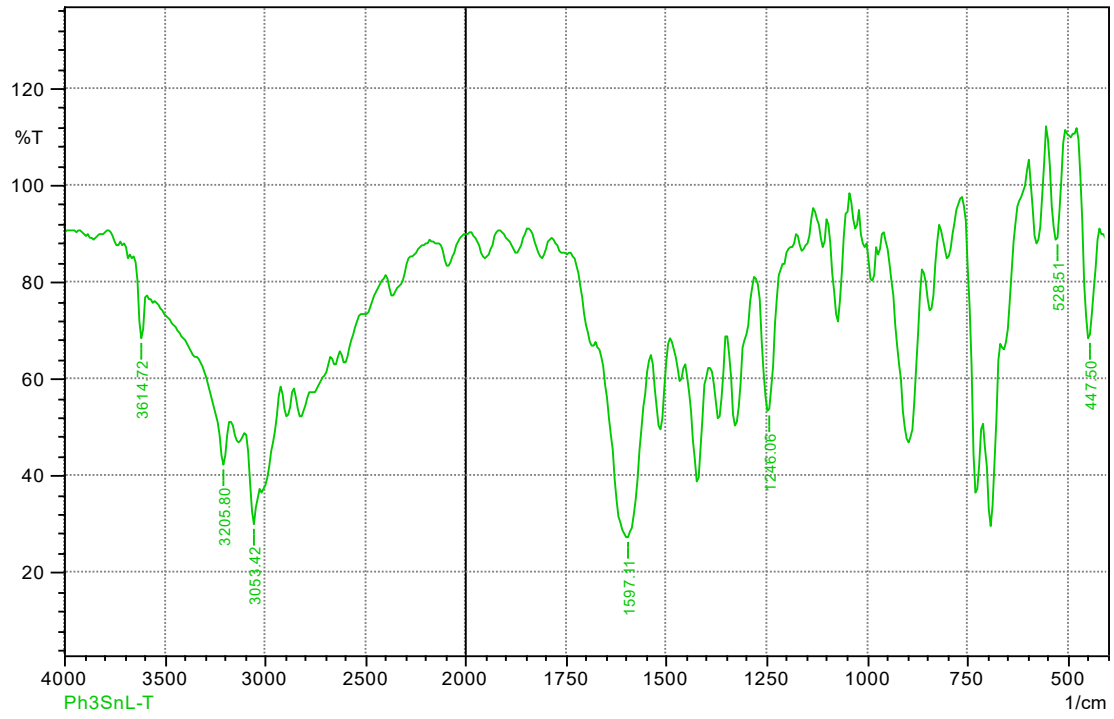

Figure 3.29 FTIR Spectrum of Ph_3SnL.

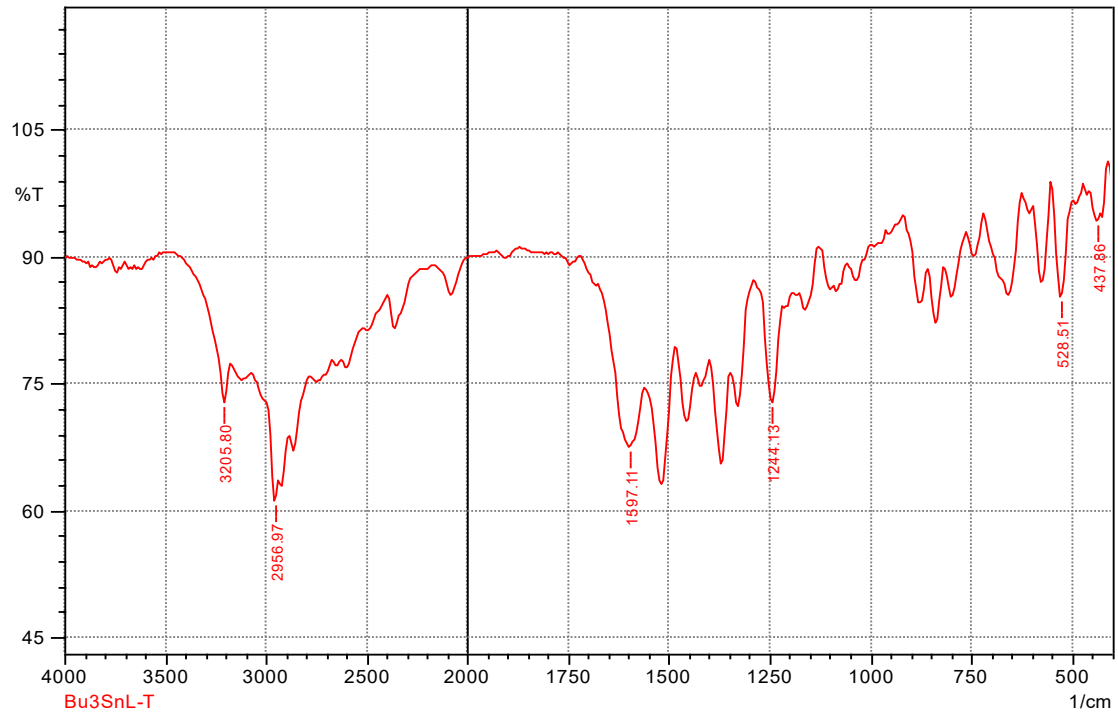

Figure 3.30 FTIR Spectrum of Bu_3SnL.

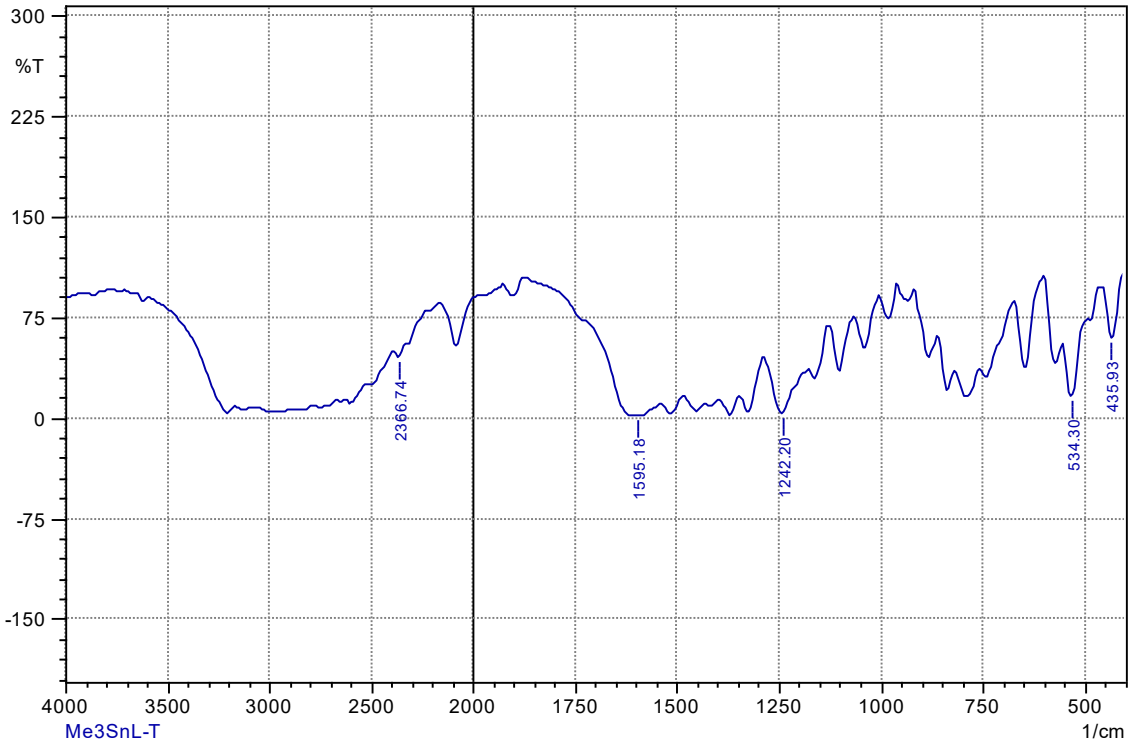

Figure 3.31 FTIR Spectrum of Me_3SnL.

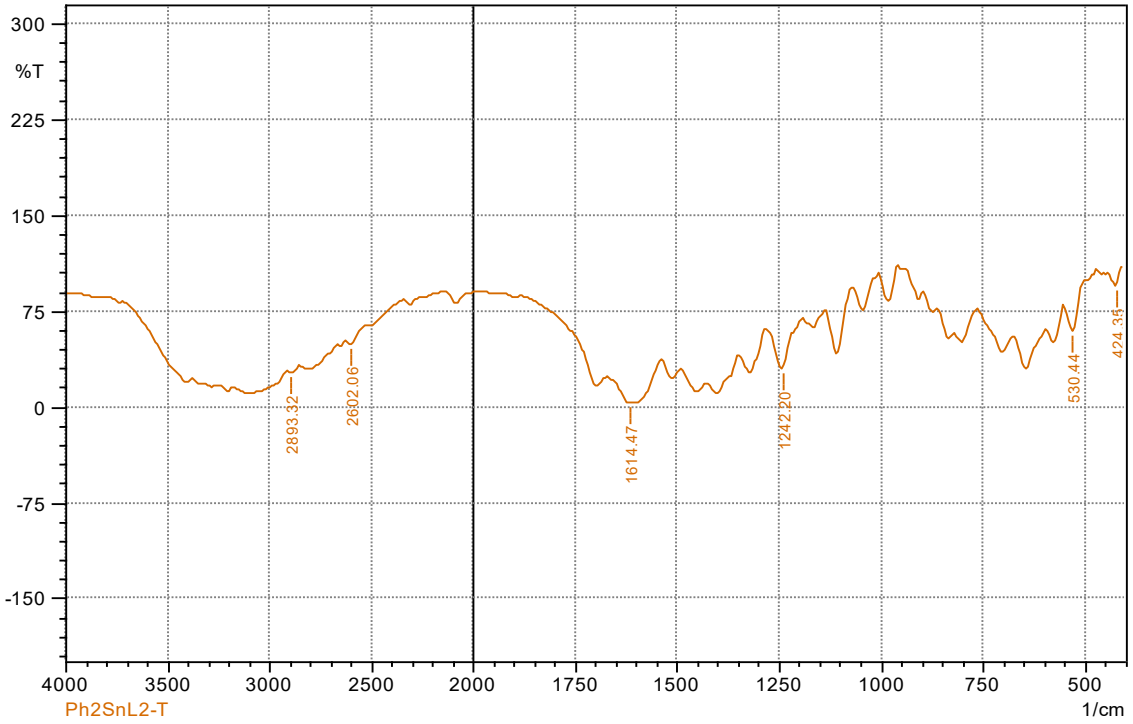

Figure 3.32 FTIR Spectrum of Ph_2SnL_2.

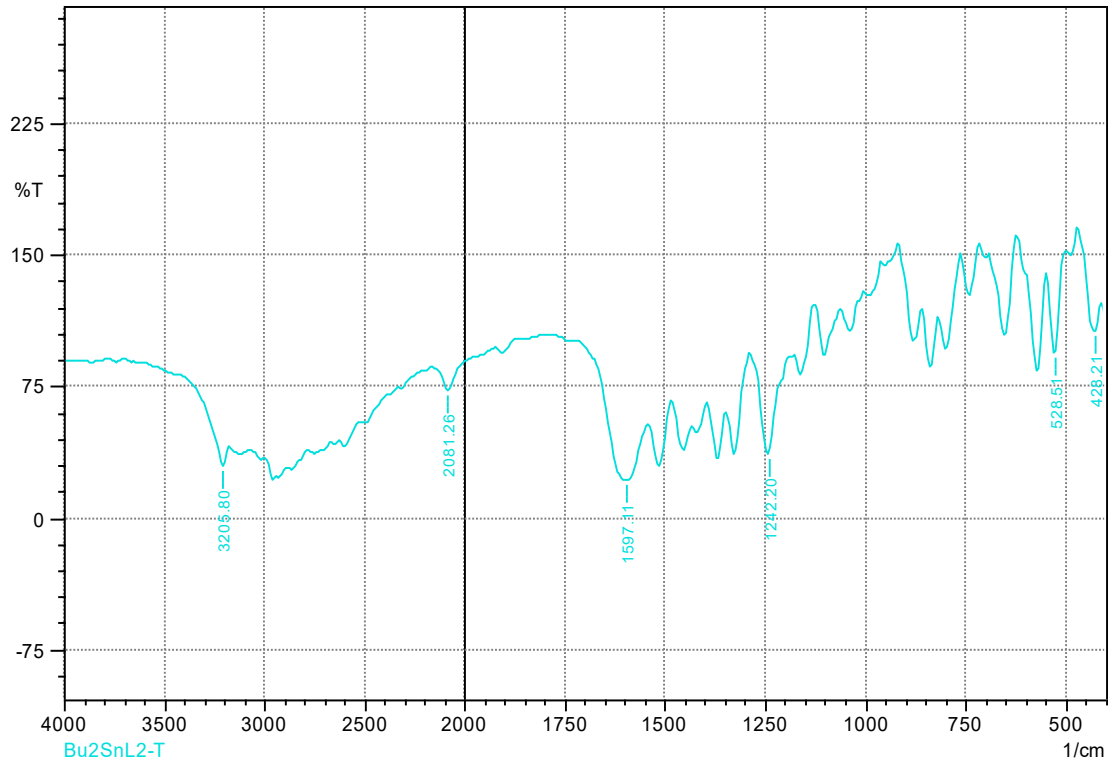

Figure 3.33 FTIR Spectrum of Bu_2SnL_2.

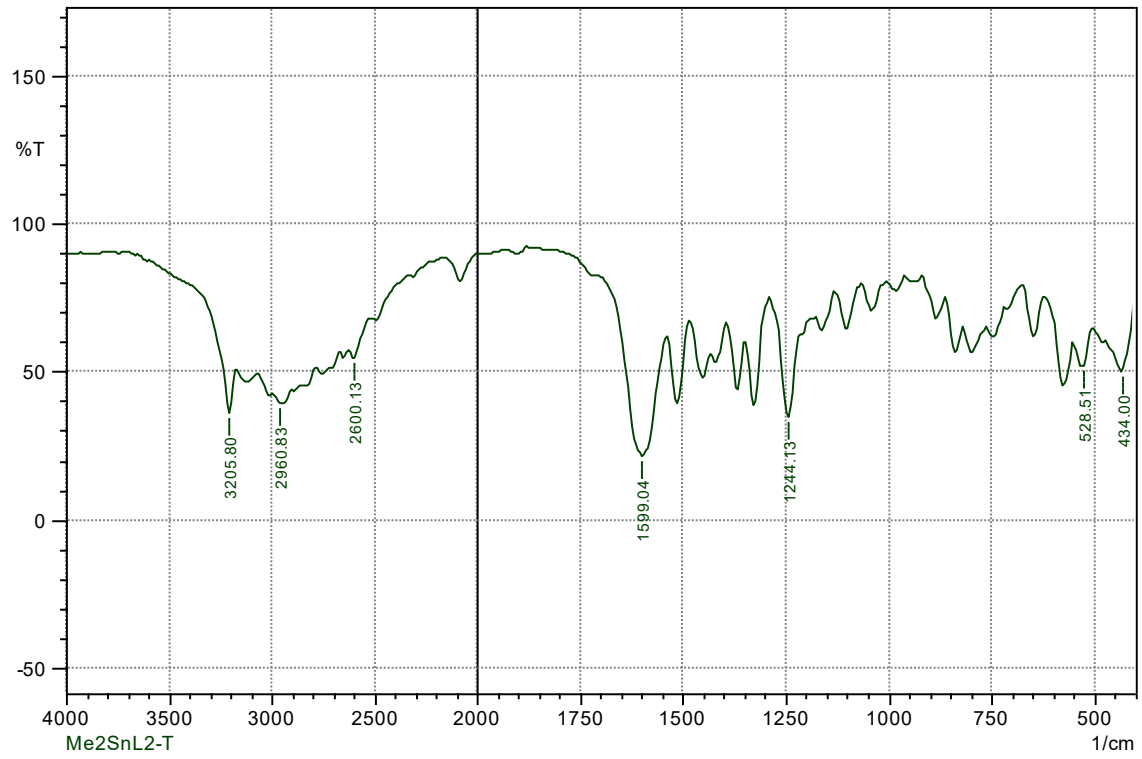

Figure 3.34 FTIR Spectrum of Me_2SnL_2.

3.2.4 Nuclear Magnetic Resonance Spectroscopy (NMR)

3.2.4.1 ^{1}H-NMR Spectroscopy of Tyrosine and its Complexes

Proton nuclear magnetic resonance spectroscopy, often known as ^{1}H-NMR, is one of the most important analytical methods in chemistry for figuring out how the hydrogen atoms are arranged in complex structures. The fundamental understanding is based on the chemical shift, which includes signal intensities that are influenced by the magnetic field employed and the interaction of the hydrogen atom with the atoms surrounding it. In DMSO-d_6 and utilizing TMS as an internal standard, ^{1}H-NMR was used to quantify the ligand (L-tyrosine) as well as its organotin (IV) complexes. The spectra of the organotin (IV) complexes do not include the proton of the carboxylic group (-CO_2H), which can be seen in the spectra of ligand (Tyrosine) as an exchangeable singlet at 12.40 ppm [142]. The signals corresponding to the phenol group proton (Ar-OH) in all compounds range between 9.43 and 7.99 ppm. The ^{1}H-NMR spectra that appeared in the range of 7.79–6.56 ppm was due to protons of the aryl moiety [143,144]. Also, appearance new signals in complexes related to protons of phenyl, butyl, and methyl groups. However, abroad signals in the 3.65-2.77 ppm range return to protons of the amine group (NH_2). As a result of comparing the ^{1}H-NMR ligand spectrum with its complexes, the shift in signal positions shows clear evidence of the loss of the carboxylic group proton and the achievement of complexity with the tin atom. As explained in Table 3.8 and Figs. 3.35–3.41.

Table 3.8 The ^{1}H-NMR Spectra (DMSO-d_6) of Tyrosine and its Complexes.

Ligand and Organotin(IV) Complexes	^{1}H-NMR
L-tyrosine	δ12.77 (s,1H, COOH), 9.24 (s,1H,Ar-OH), 7.05 (d, J=8.50 Hz.2H,Ar), 6.68 (d, J=8.50 Hz,2H,Ar), 3.51 (br, 2H,NH_2), 3.15 (t, J=4.0 Hz,1H, CO-CH-), 2.75 (m ,2H,2 PhCH-).
Ph_3SnL	δ7.99 (s,1H,Ar-OH), 7.88 (t,J=30Hz,3H,Ar), 7.64-7.58 (m,6H,Ar), 7.56 (d , J=2.36 Hz , 6H, Ar), 7.48 (d , J=1.07 Hz ,2H, Ar), 7.46 (d , J=2.07 Hz ,2H, Ar), 3.39 (br,2H, NH_2), 2.79 (t,J=8.09 Hz , 1H, CO-CH-), 2.35 (m, 2H, 2PhCH-).
Bu_3SnL	δ 9.10 (s,1H,Ar-OH), 6.99 (d , J=7.80 Hz ,2H, Ar), 6.88 (d , J=7.80 Hz ,2H, Ar), 3.41(br,2H, NH_2), 3.20 (t, J=5.20 Hz , 1H, CO-CH-), 2.76 (m, 2H, 2PhCH-), 1.60 (qut, J= 7.50 Hz, 6H,$3CH_2$), 1.29 (sex, J=7.50 Hz ,6H,$3CH_2$), 1.07 (t, J= 8.08 Hz,9H,3Me), 0.87 (t, J=7.5 Hz,6H,$3CH_2$).
Me_3SnL	δ 9.27 (s,1H, Ar-OH), 7.07 (d,J=7.5Hz,2H,Ar), 6.69 (d, J=7.5 Hz , 2H, Ar),3.30 (br,2H, NH_2), 3.01 (t, J=6.30 Hz ,1H , CO-CH), 2.86(d, J=12Hz,2H, PhCH-), 1.26 (s,9H,3Me).
Ph_2SnL_2	δ 7.94 (s,2H,Ar-OH),7.52 (d , J=2.24 Hz ,4H, Ar), 7.48(d , J=2.24 Hz ,4H, Ar), 7.18-7.01 (m,4H,Ar), 6.84 (t, J=28 Hz,2H,Ar), 6. 31 (d , J=1.20 Hz ,4H, Ar), 3.57 (br,4H,$2NH_2$) 3.43 (t,J=8.09 Hz , 2H, CO-CH-), 3.35 (m, 4H, 2PhCH-).
Bu_2SnL_2	δ 9.41 (s,2H,Ar-OH), 7.05 (d , J=8.40 Hz ,4H, Ar), 6.73 (d , J=8.40 Hz ,4H, Ar), 3.48 (br,4H, $2NH_2$), 3.12 (t , J=5.30 Hz ,2H,2 CO-CH-), 2.80 (m,4H, 2PhCH-), 1.42 (qut, J= 7.5 Hz, 4H,$2CH_2$), 1.22 (sex, J=7.30 Hz ,4H,$2CH_2$), 0.84 (t, J= 7.30 Hz,6H,2Me), 0.63 (t, J=7.30 Hz,4H,$2CH_2$).
Me_2SnL_2	δ 9.43 (s,2H, Ar-OH), 7.06 (d,J=8.25Hz,4H,Ar), 6.74 (d, J=8.25 Hz , 4H, Ar), 3.43 (br,4H, $2NH_2$), 3.15 (t , J=5.30 Hz ,2H,2 CO-CH-), 2.75 (m,4H, 2PhCH-), 0.41 (s,6H, 2Me).

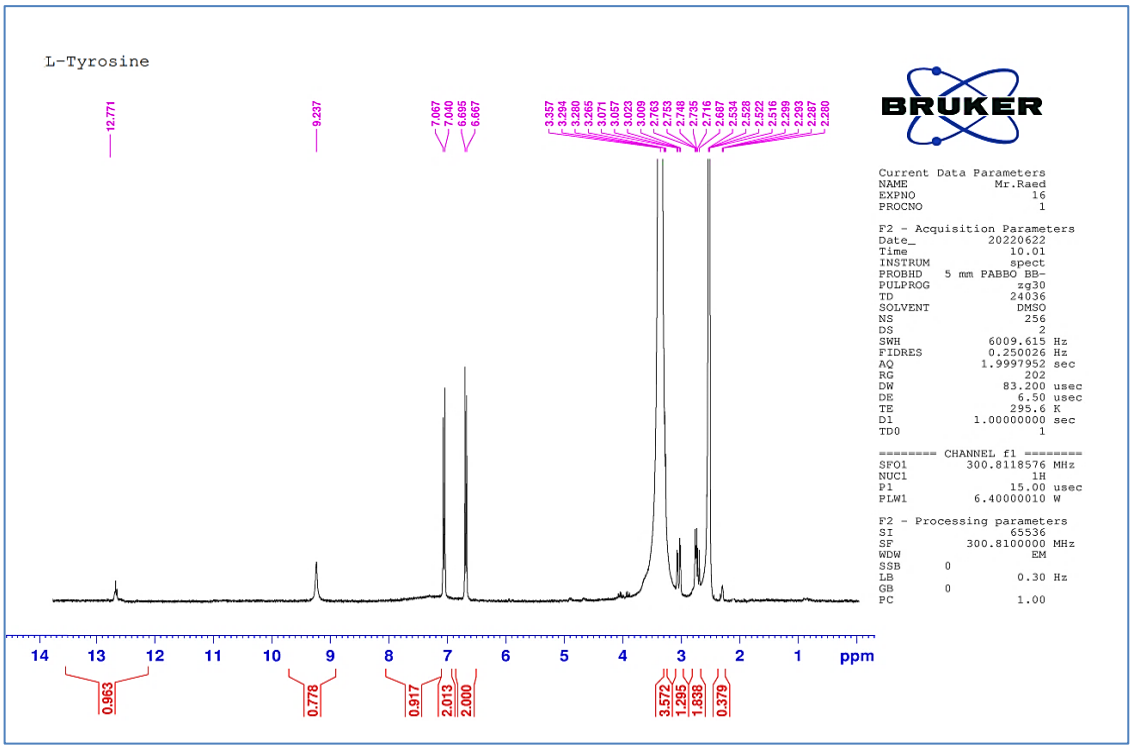

Figure 3.35 ^{1}H-NMR Spectrum of Tyrosine.

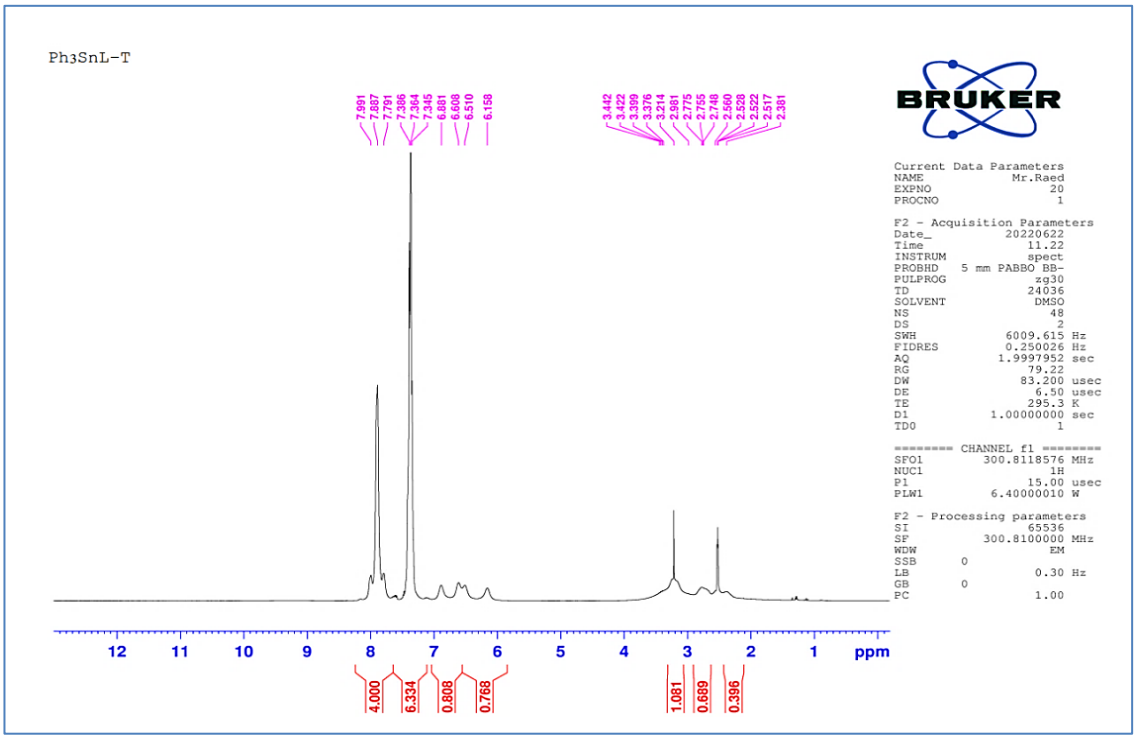

Figure 3.36 ^{1}H-NMR Spectrum of Ph_3SnL.

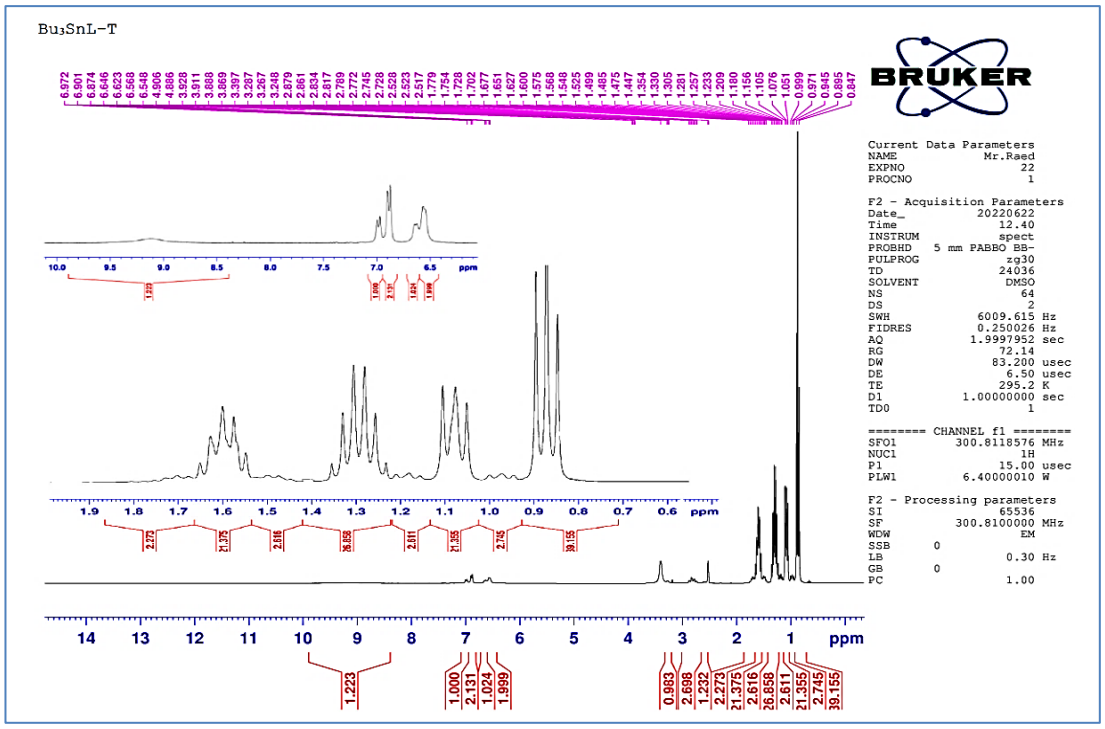

Figure 3.37 ^{1}H-NMR Spectrum of Bu_3SnL.

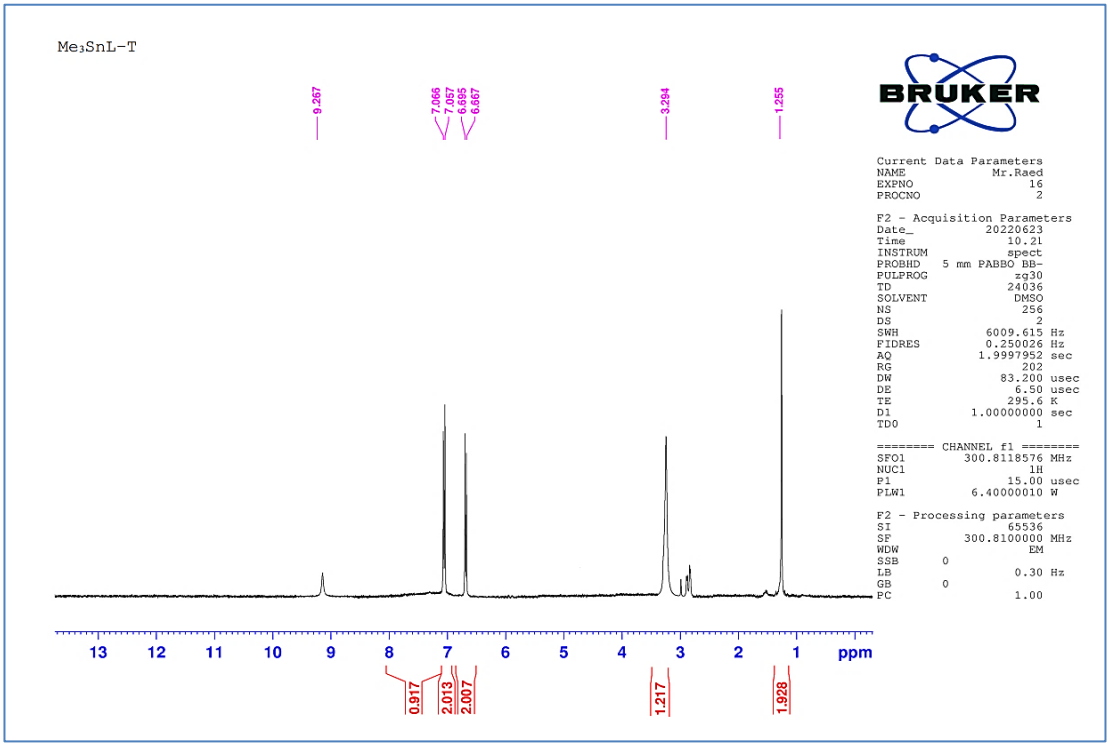

Figure 3.38 ^{1}H-NMR Spectrum of Me_3SnL.

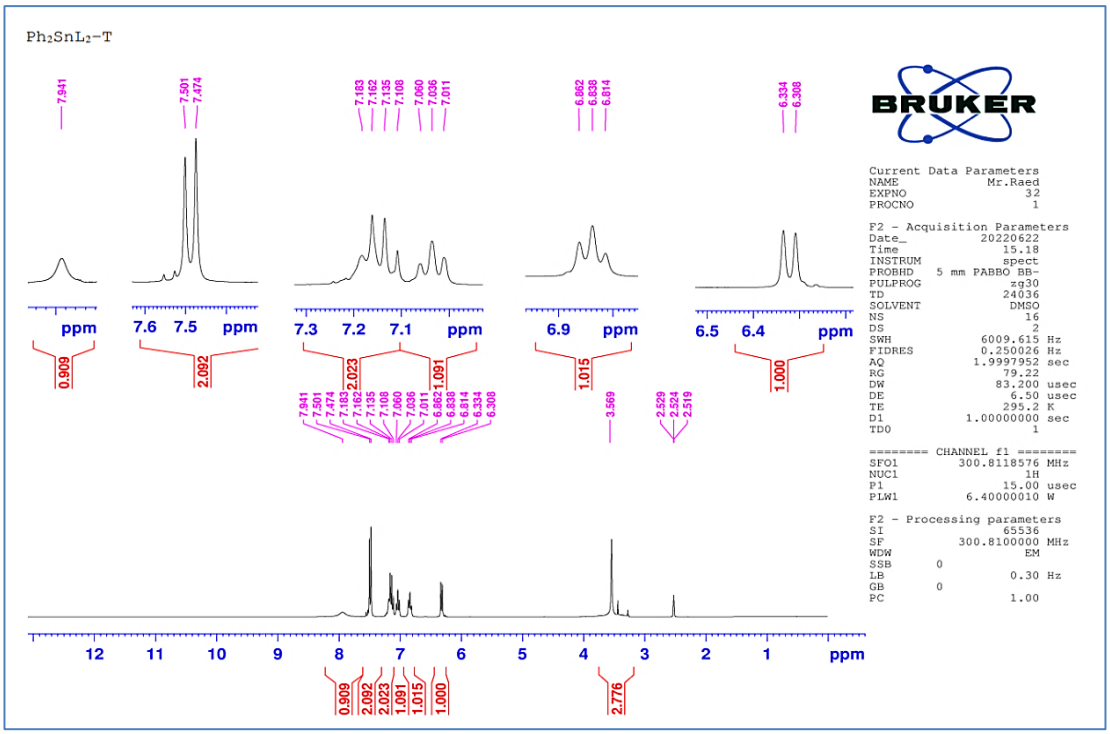

Figure 3.39 ^{1}H-NMR Spectrum of Ph_2SnL_2.

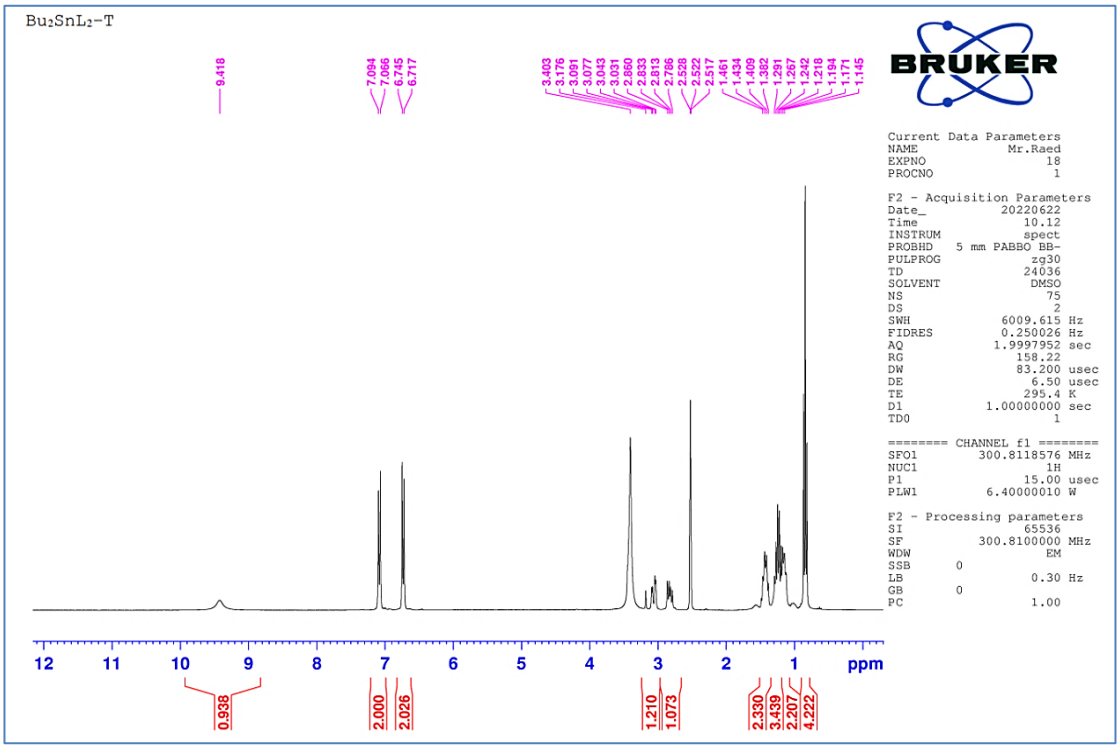

Figure 3.40 ^{1}H-NMR Spectrum of Bu_2SnL_2.

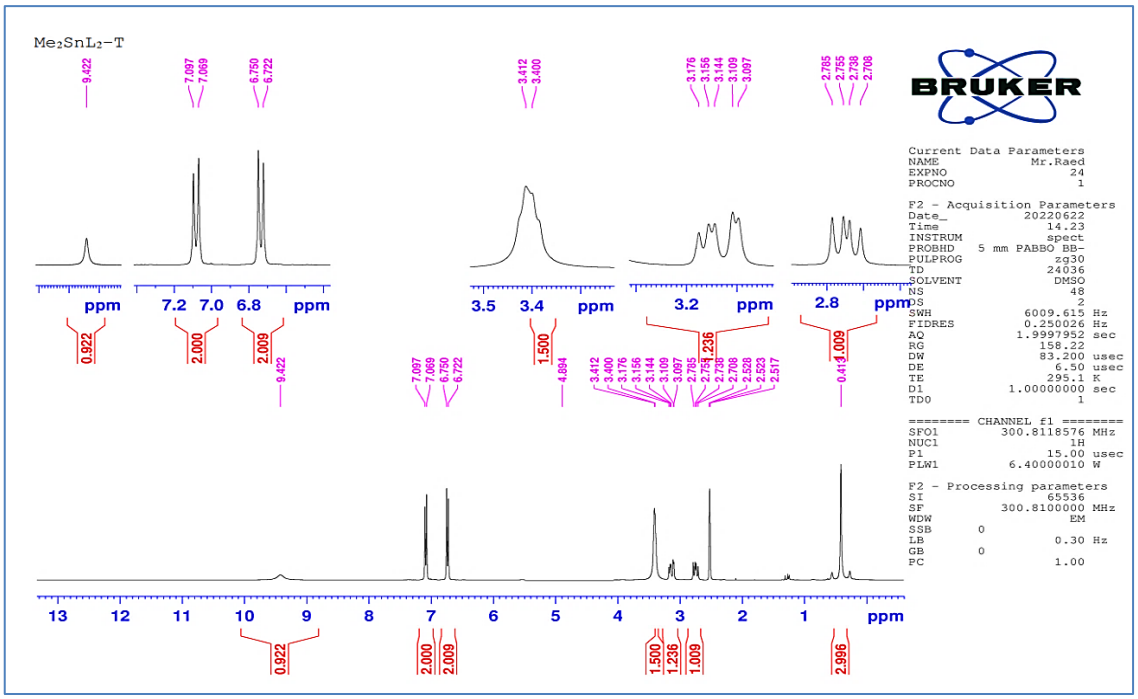

Figure 3.41 ^{1}H-NMR Spectrum of Me_2SnL_2.

3.2.4.2 ^{13}C NMR Spectroscopy of Tyrosine and its Complexes

The ^{13}C-NMR spectra showed the presence of all carbon atoms inside the complexes [145]. The ligand (L-tyrosine) and complexes spectra information matched with the ^{1}H-NMR and FTIR data for compounds generation. The complexes' C_1-carboxyl was moved downfield in range 177.3-174.2 ppm, compared to its position in the ligand that have signal in position 184.8 ppm, due to a decrease in electron density at carbon atoms when oxygen is linked to an electropositive tin atom, this discovery adds to the evidence that complexation occurred via the oxygen atoms of the carboxylic group [146].Also appearance new signals related to carbons of phenyl ,butyl and methyl groups. As displayed in Table 3.9 and Figs.3.42-3.48.

Table 3.9 Shows the ^{13}C-NMR Spectra (DMSO-d_6; ppm) of Tyrosine and its Complexes.

Ligand and Sn(IV) Complexes	^{13}C-NMR
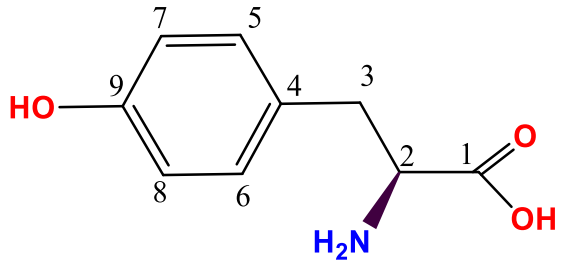	(C_1-Carboxyl, 1C, 184.8), (C_9-Phenolic, 1C,168.3), (C_4,1C,139.4), (C_5, C_6,2C,132.5), (C_7, C_8,2C 118.1),(C_2,1C,65.2) , (C_3,1C,21.8).
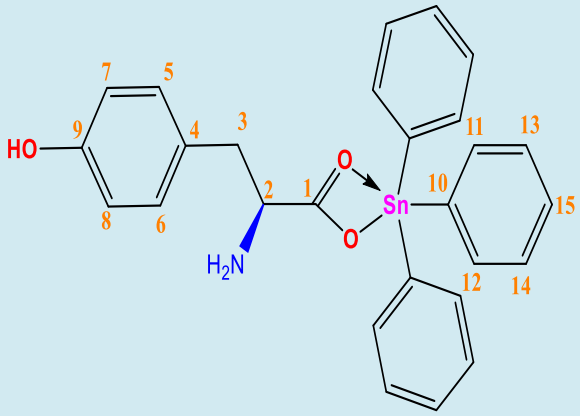	(C_1-Carbonyl,1C,177.3), (C_9-Phenolic,1C,145.9), (C_{10},3C,140.9), (C_4,1C, 137.2), (C_5, C_6,2C,129.5), (C_{13},C_{14},6C,128.3), (C_{11},C_{12},6C,127.8),(C_7,C_8,2C,120.0),(C_{15},3C, 115.4), (C_2,1C,57.8),(C_3,1C,38.8).
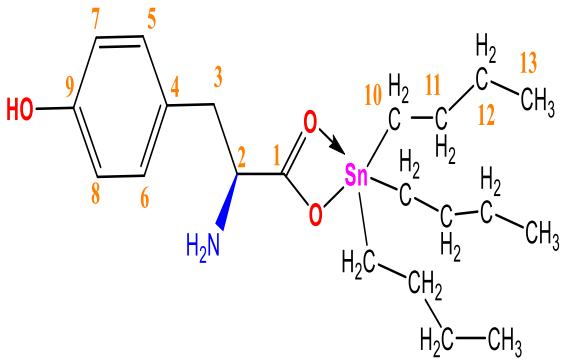	(C_1-Carbonyl,1C,177.4), (C_9-Phenolic,1C,160.2), (C_4,1C,130.7),(C_5,C_6,2C,115.0), (C_7,C_8,2C,103.5),(C_2,1C,57.2),(C_3, 1C,28.3),(C_{11},3C,27.0),(C_{12},3C,20.9) ,(C_{10},3C,16.6) ,(C_{13},3C,14.5).
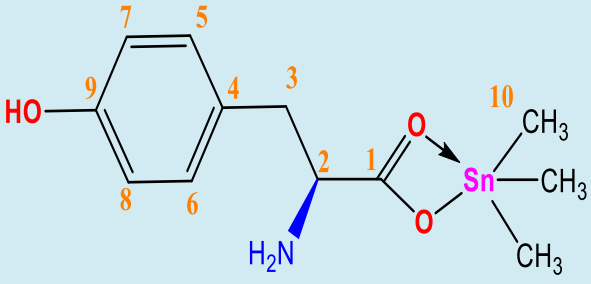	(C_1-Carbonyl,1C,176.4), (C_9-Phenolic,1C,157.5), (C_4,1C,132.1),(C_5,C_6,2C,129.8),(C_7,C_8,2C,11 6.3),(C_2,1C,57.7), (C_3, 1C,38.4),(C_{10},3C,10.1).

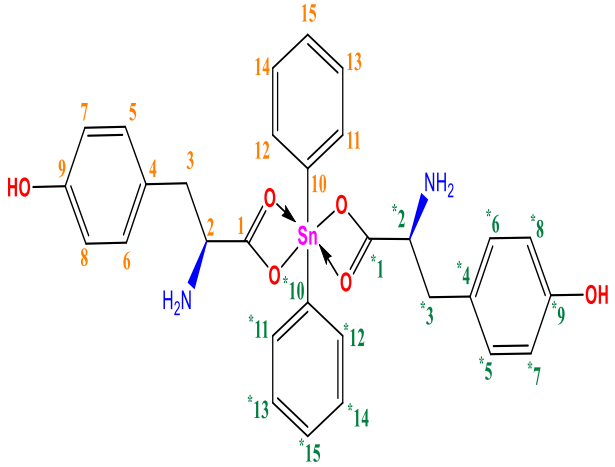	(C_1,C_1*-Carbonyl,2C,176.6),(C_9,C_9*-Phenolic,2C,161.3),(C_{10},C_{10}*,2C,145.8), (C_4,C_4*,2C,136.5),(C_5,C_5*,C_6,C_6*,4C,128.5), (C_{13},C_{13}*,C_{14},C_{14}*,4C,127.5),(C_{11},C_{11}*,C_{12},C_{12}*,4C,126.4),(C_7,C_7*,C_8,C_8*,4C,119.3), (C_{15},C_{15}*,2C,113.60),(C_2,C_2*,2C,55.7), (C_3,C_3*,2C,38.2).
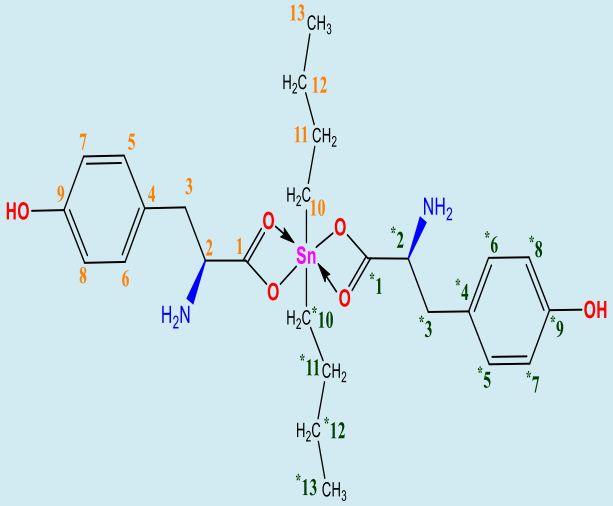	(C_1,C_1*-Carbonyl,2C,174.4),(C_9,C_9*-Phenolic,2C,156.7),(C_4,C_4*,2C,130.8),(C_5, C_5*,C_6,C_6*,4C,128.1),(C7,C7*,C_8,C_8*,4C, 115.8),(C_2,C_2*,2C,55.4),(C_3,C_3*,2C,37.3), (C_{11},C_{11}*,2C,27.5),(C_{12},C_{12}*,2C,26.7), (C_{10},C_{10}* ,2C,14.0), C_{13},C_{13}*,2C,-0.74).
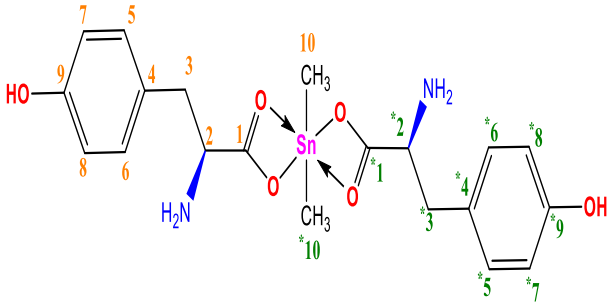	(C_1,C_1*-Carbonyl,2C,174.2),(C_9,C_9* -Phenolic,2C,156.9),(C_4,C_4*,2C,130.9), (C_5,C_5*,C_6,C_6*,4C,128.5),(C_7,C_7*,C_8,C_8*,4C, 115.8) (C_2,C_2*,2C,55.6),(C_3,C_3*,2C,37.5), (C_{10},C_{10}*,2C,-11.2).

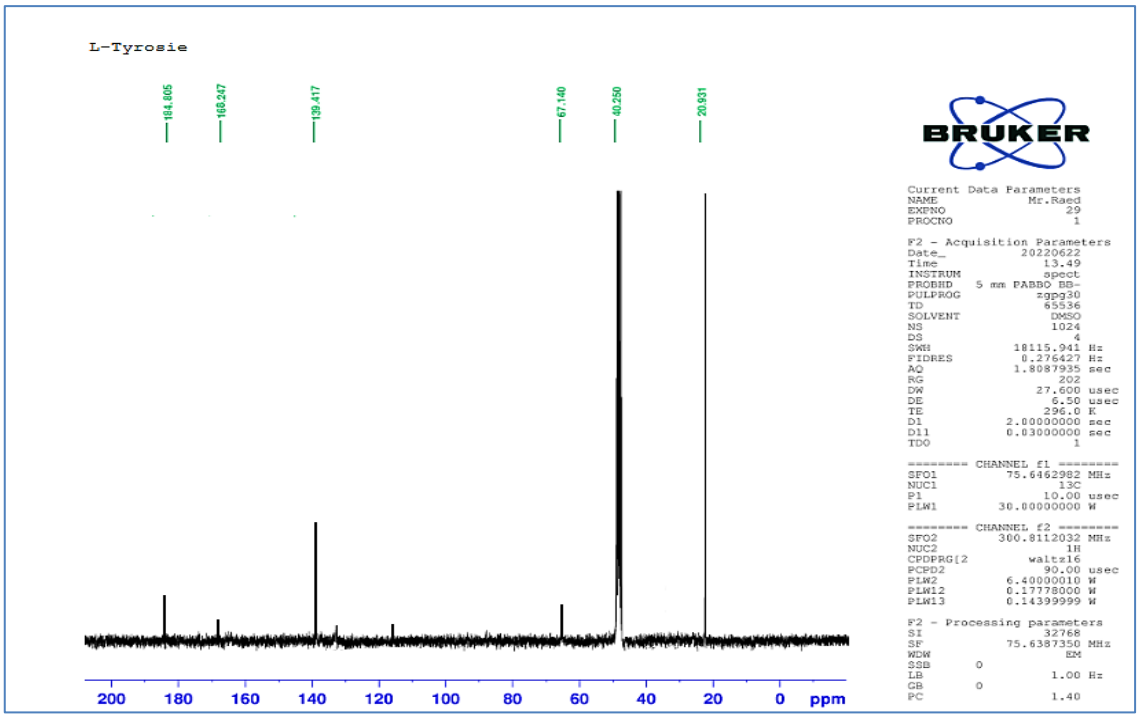

Figure 3.42 ^{13}C-NMR Spectrum of Tyrosine.

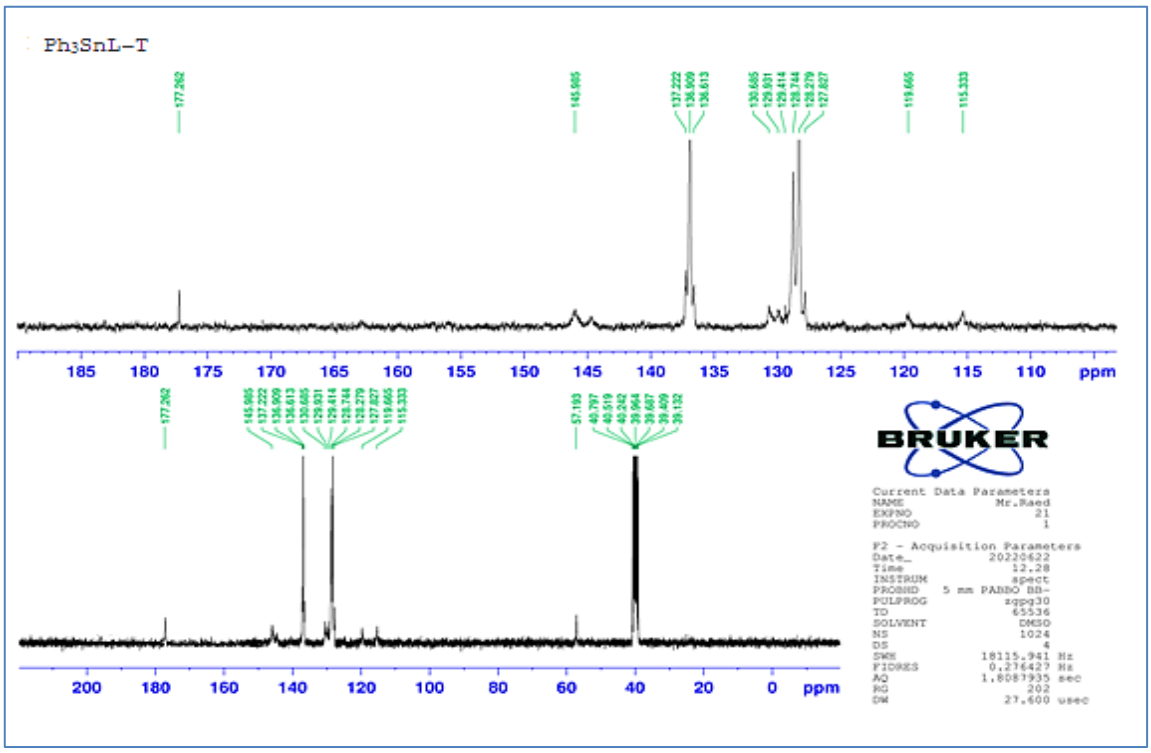

Figure 3.43 ^{13}C-NMR Spectrum of Ph_3SnL.

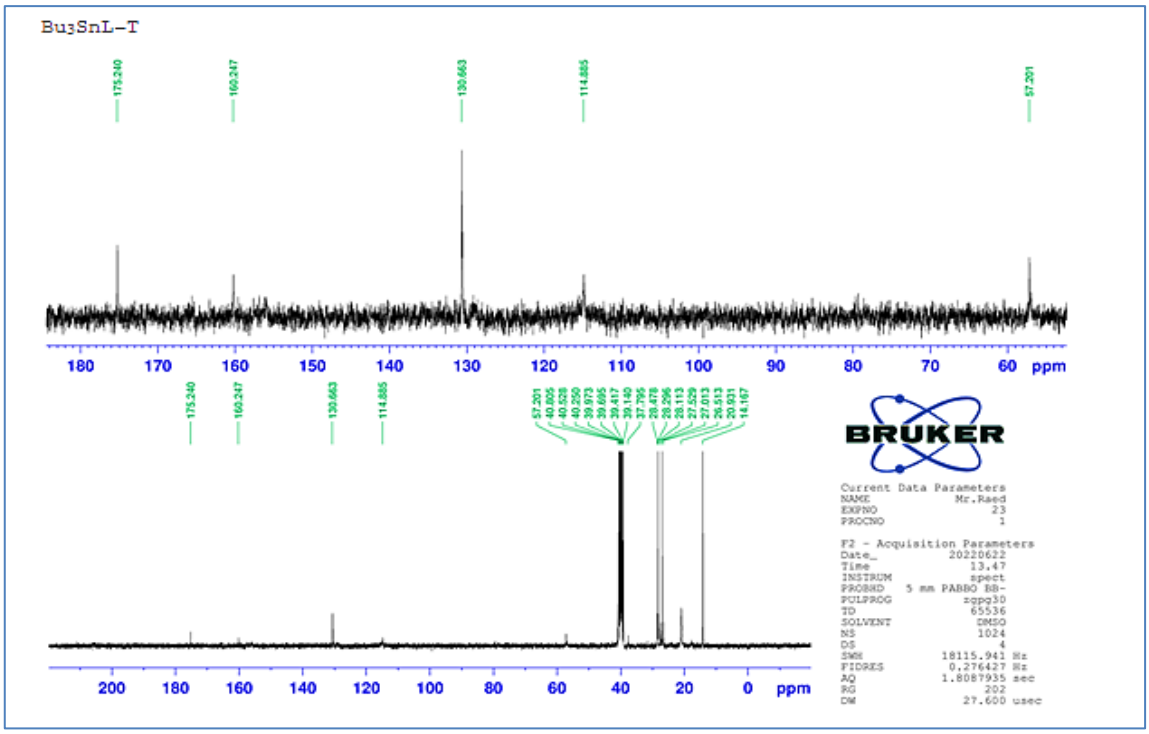

Figure 3.44 ^{13}C-NMR Spectrum of Bu_3SnL.

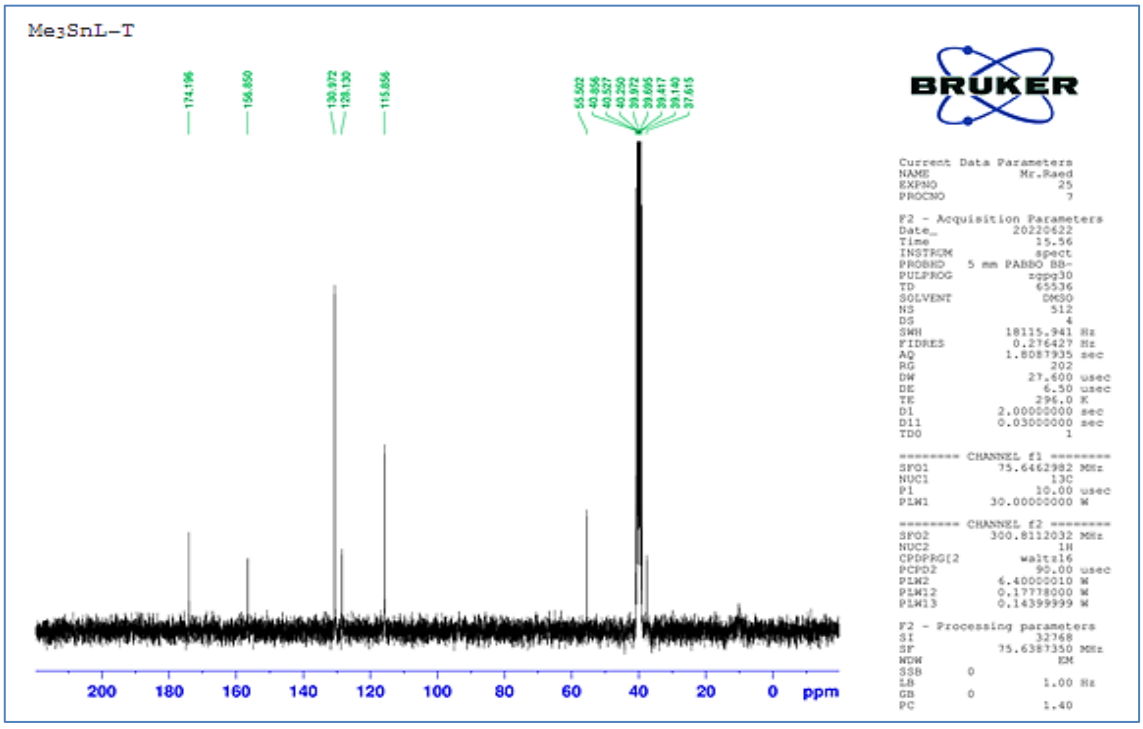

Figure 3.45 ^{13}C-NMR Spectrum of Me_3SnL.

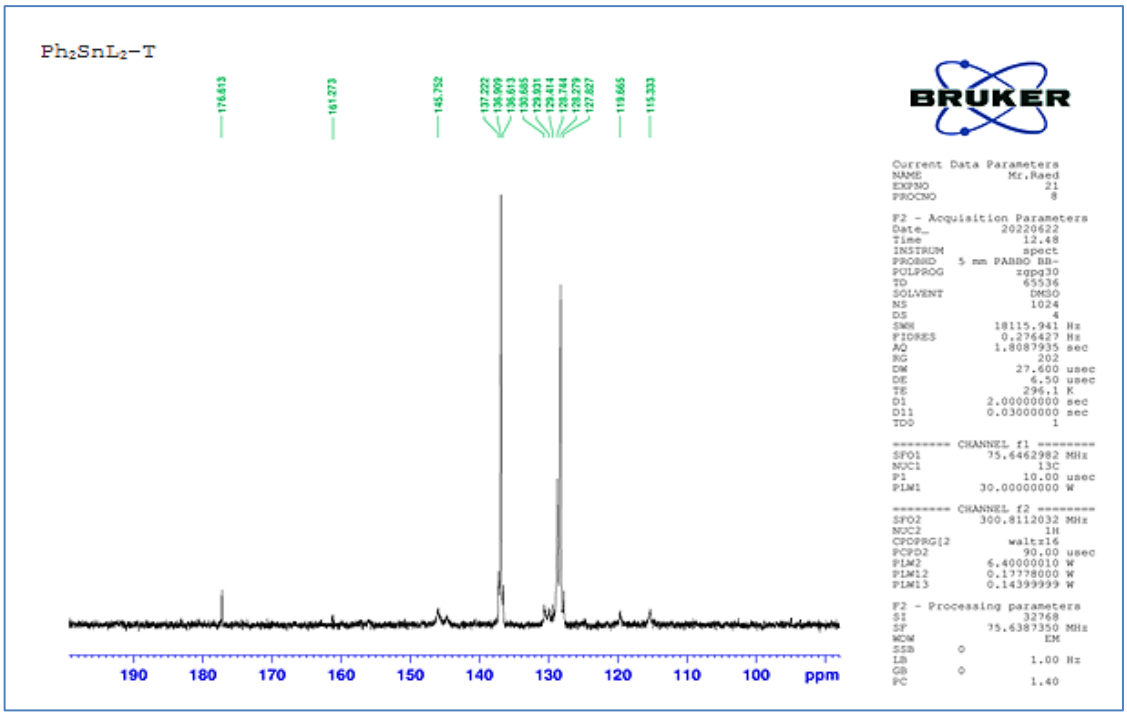

Figure 3.46 ^{13}C-NMR Spectrum of Ph_2SnL_2.

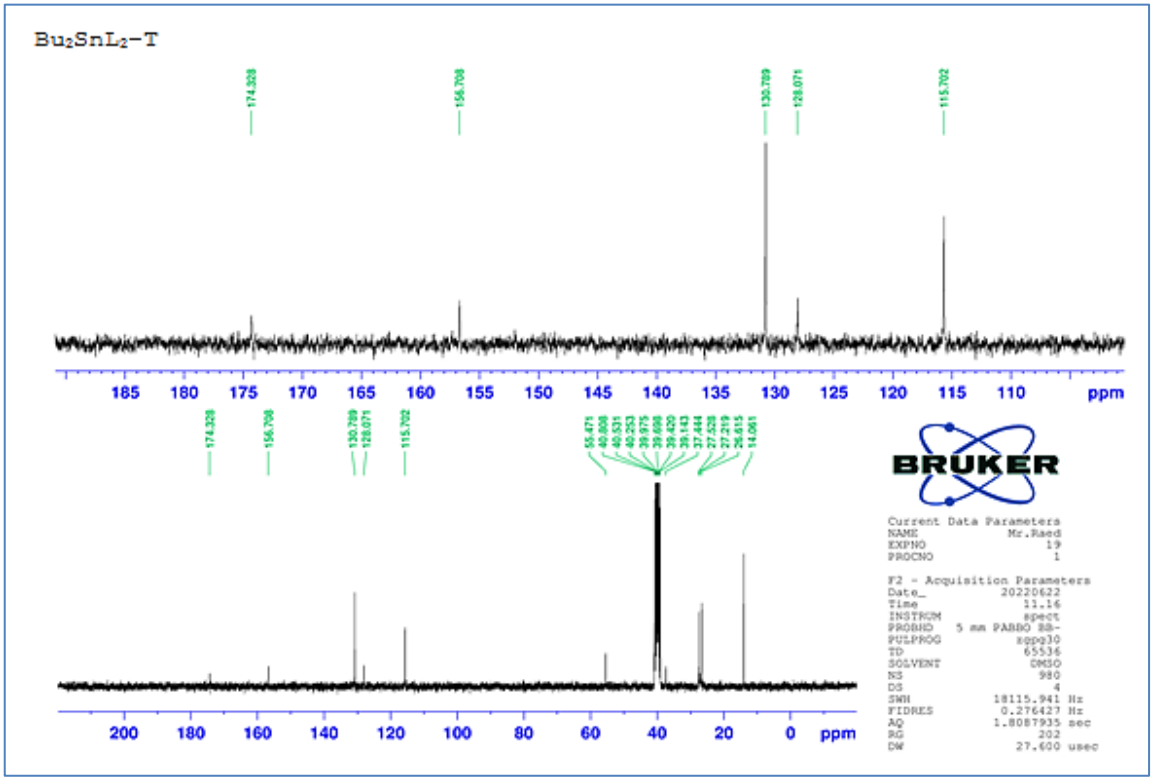

Figure 3.47 ^{13}C-NMR Spectrum of Bu_2SnL_2.

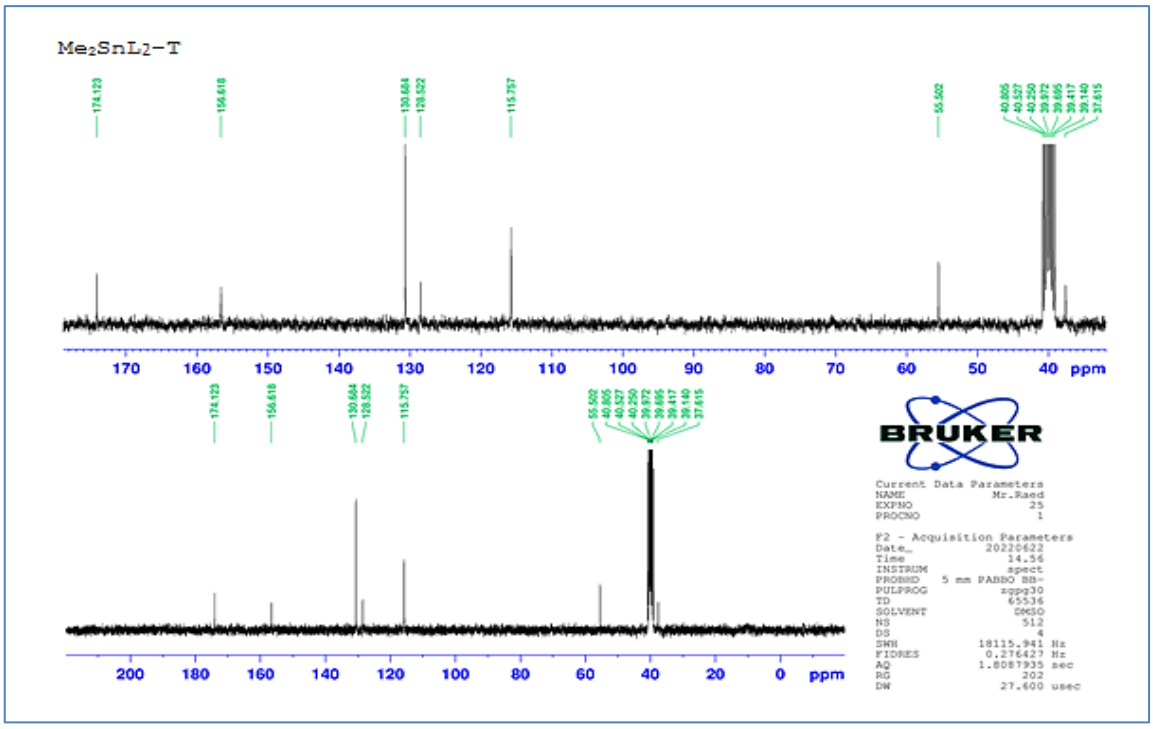

Figure 3.48 ^{13}C-NMR Spectrum of Me_2SnL_2.

3.2.4.3 ^{119}Sn NMR Spectroscopy for Complexes

Organotin (IV) complexes' ^{119}Sn- NMR spectra were obtained in DMSO-d_6 solvent using $SnCl_4$ as an internal standard. All complexes provide sharp signals. The ^{119}Sn chemical shifts are different for tetra (+200 to - 60 ppm), penta (-90 to -190 ppm) and hexa coordination number complexes (-210 to – 400 ppm), as indicated by previously published results [147]. The tin atom becomes increasingly more protected as the electron releasing power of the alkyl groups attached to tin increases and the ^{119}Sn chemical shift moves to a higher field compared to the phenyl group, which transfers to a lower field due to the increased influence of aromatic resonances [148].

The ^{119}Sn-NMR resonance of Ph_2SnL_2 appeared at a lower field region than in Bu_2SnL_2 and Me_2SnL_2, where resonance was at -380.51, -272.20 and -240.35 ppm, respectively, which is in agreement with the proposed hexa-coordinated octahedral geometry, while the resonance frequencies of Ph_3SnL, Bu_3SnL and Me_3SnL were at -190.03, -140.02 and -96.95 ppm, respectively, which is compatible with the hypothesized Penta coordinated trigonal bipyramidal geometry [149].As shown in Figs. 3.49–3.54.

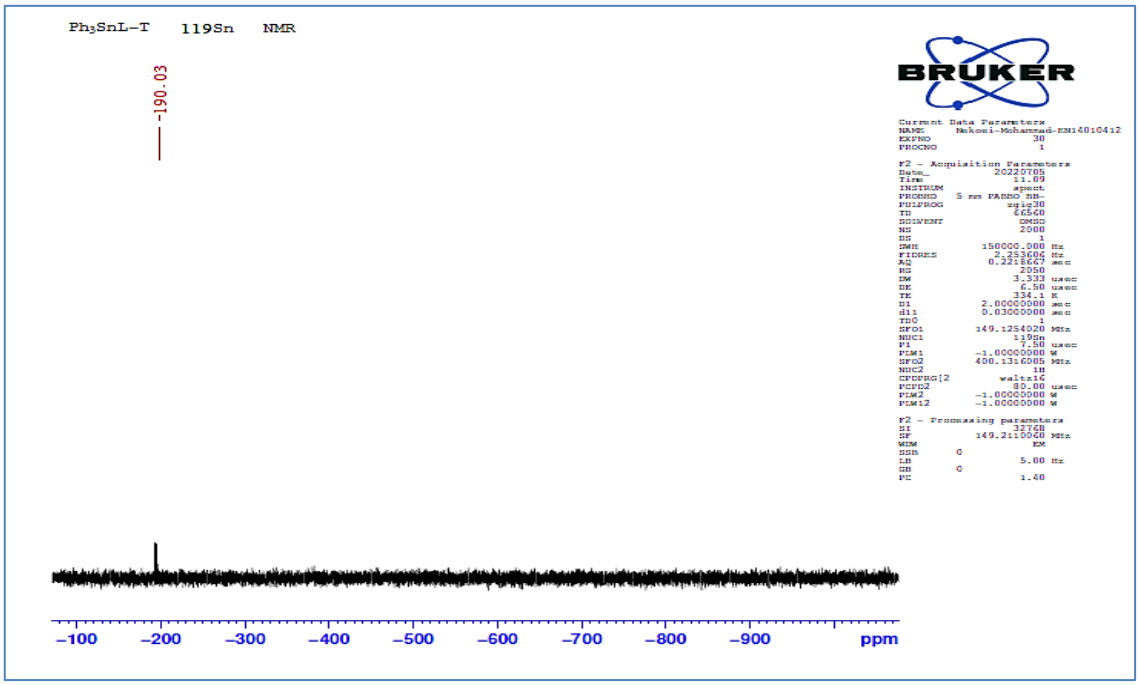

Figure 3.49 ^{119} Sn-NMR Spectrum of Ph_3SnL Complex.

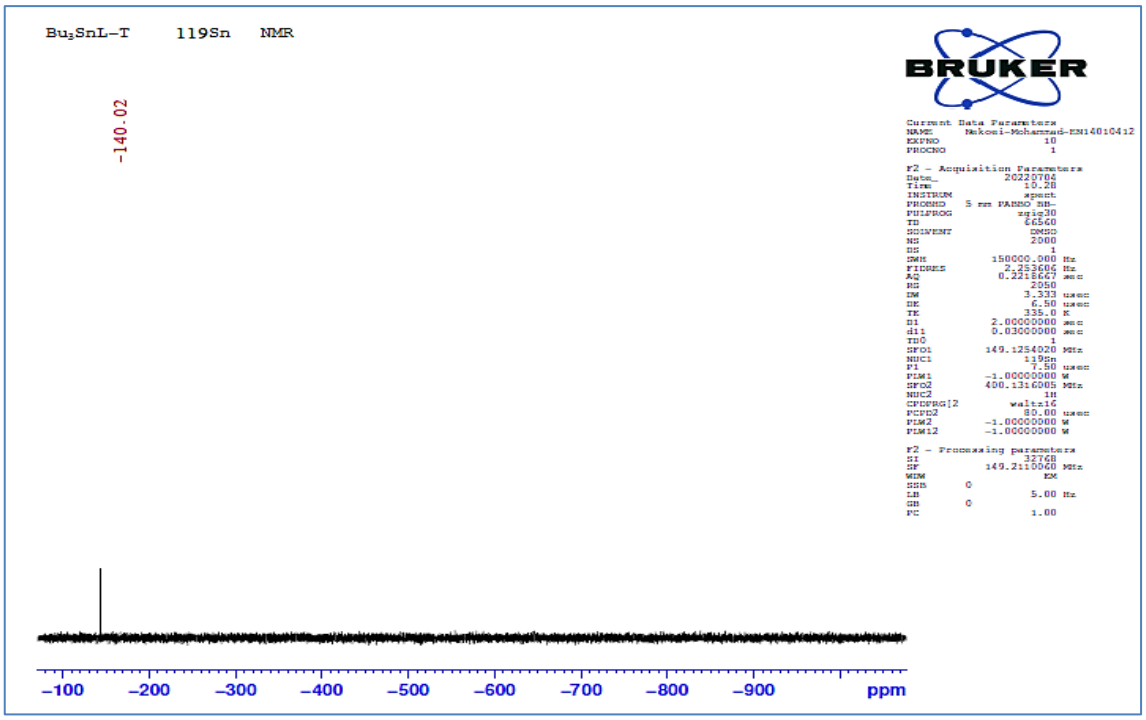

Figure 3.50 [119] Sn-NMR Spectrum of Bu_3SnL Complex.

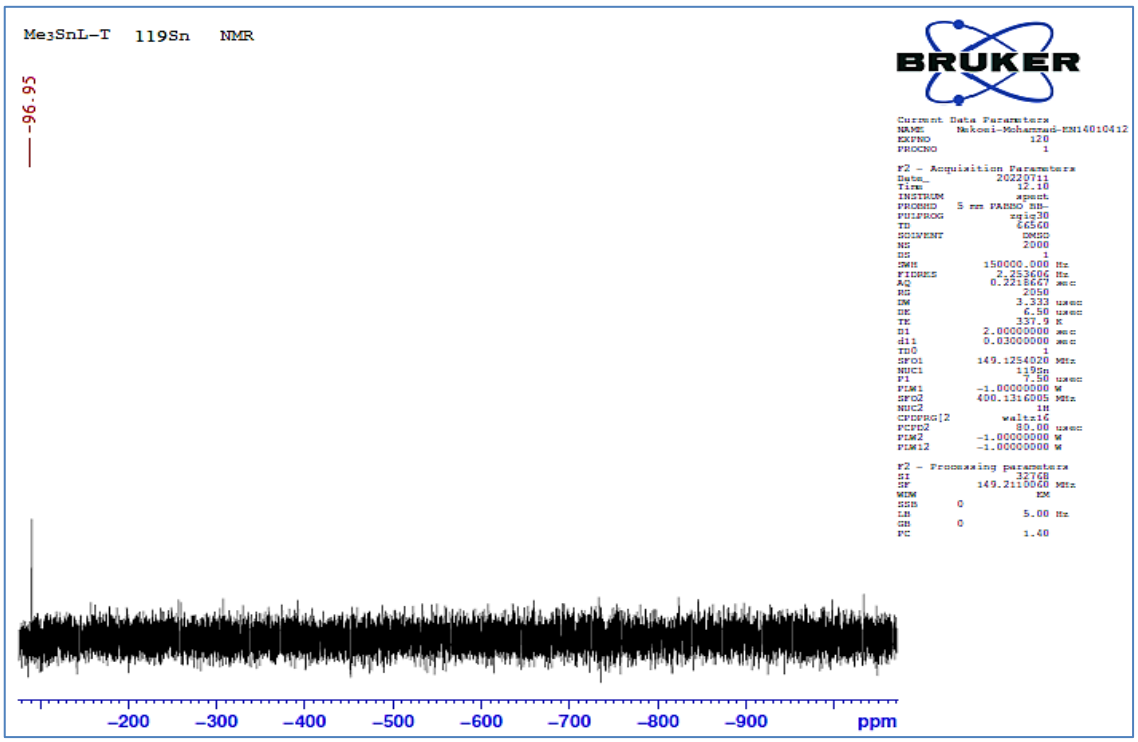

Figure 3.51 [119] Sn-NMR Spectrum of Me_3SnL Complex.

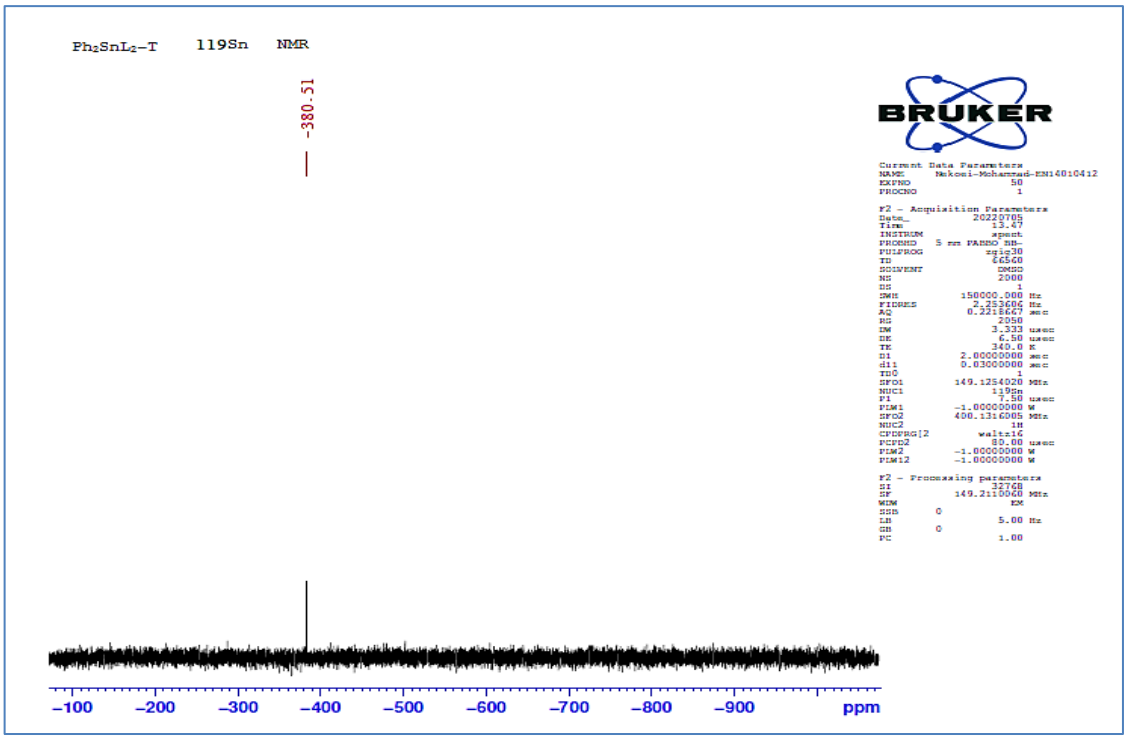

Figure 3.52 [119] Sn-NMR Spectrum of Ph_2SnL_2 Complex.

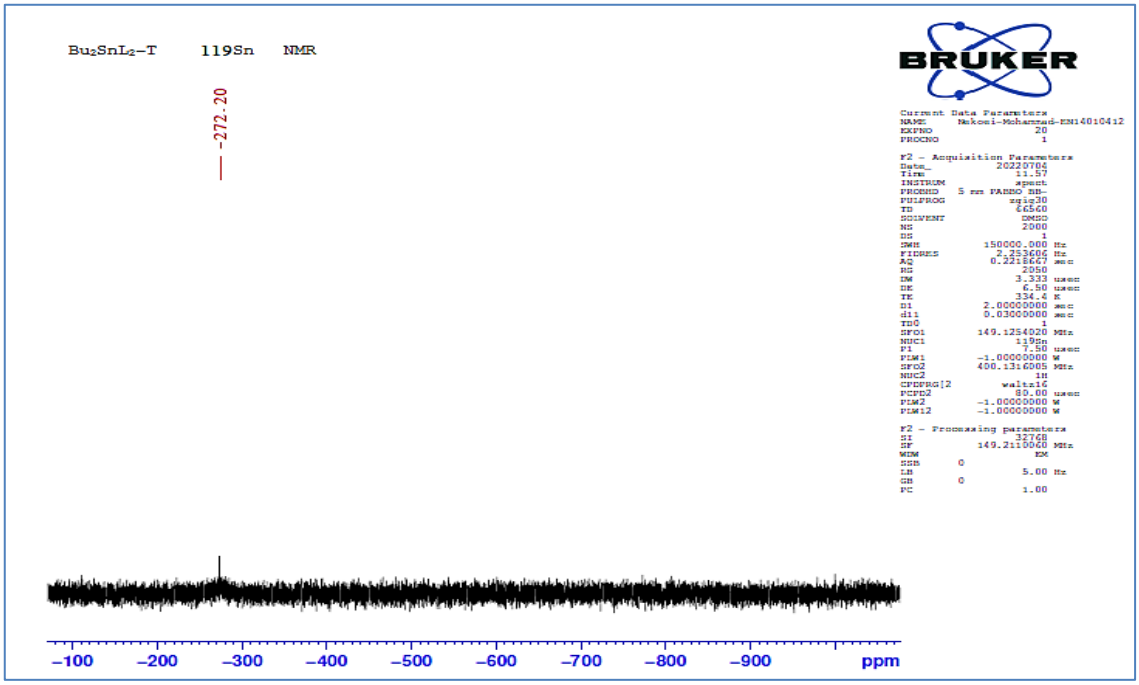

Figure 3.53 [119] Sn-NMR Spectrum of Bu_2SnL_2 Complex.

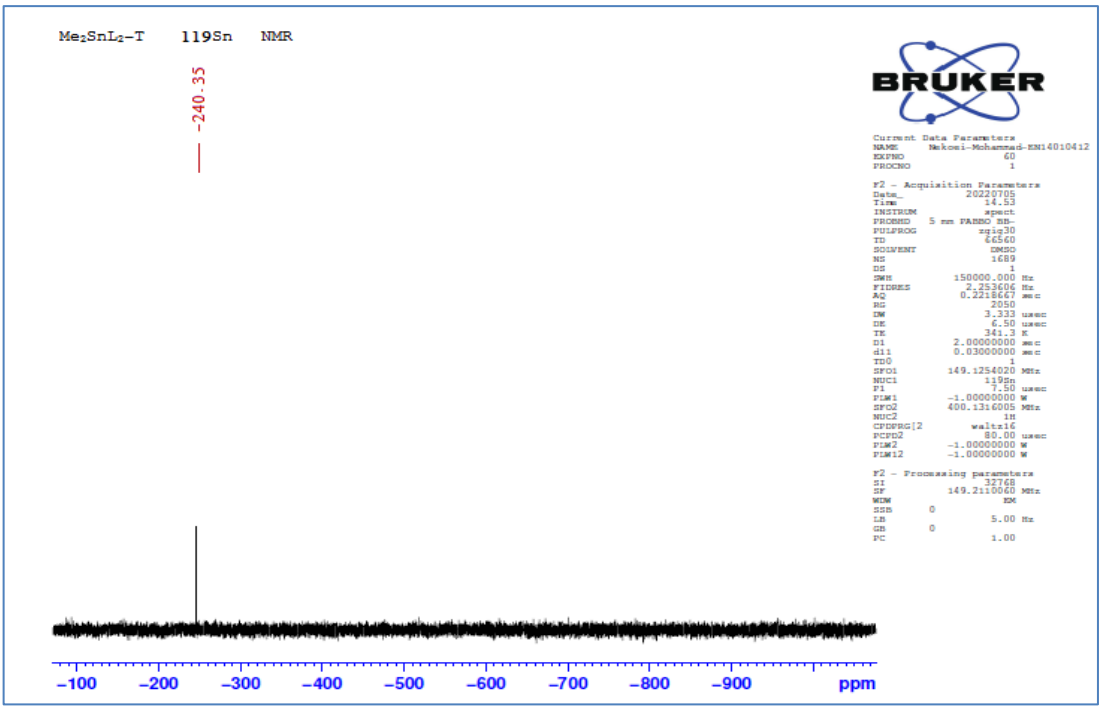

Figure 3.54 ^{119} Sn-NMR Spectrum of Me_2SnL_2 Complex.

Chapter Four

Applications

4. Applications

4.1 Photo Stabilizers of Poly (Vinyl Chloride) Films

4.1.1 Photodegradation of Organotin (IV) -Cephalexin Complexes

4.1.2 Weight Loss with Poly (Vinyl Chloride)

Poly (vinyl chloride) suffers autocatalytic dehydrochlorination after prolonged exposure to UV light and/or high temperatures [150]. Discoloration, significant changes in mechanical characteristics and the creation of unsaturated fragments and loss of mass as hydrogen chloride (HCl) result decrease in molecular weight. These undesirable alterations are mostly caused by cross-linking and chain scission. As a result, the amount of the damage may be measured by monitoring the weight loss [151-153]. Weight loss of PVC films (40µm thickness) containing organotin (IV) complexes (0.5% weight) during irradiation periods up to 300 h was determined and compared to blank PVC film, as shown in Table 4.1 and Fig. 4.1. When compared to a poly (vinyl chloride) blank, the weight loss of poly (vinyl chloride) films containing organotin (IV) complexes was significantly lower. The resulting complexes in the following order of their effectiveness in photo stabilizing PVC against irradiation: $Me_2SnL_2 > Me_3SnL > Ph_3SnL > Ph_2SnL_2 > Bu_2SnL_2 > Bu_3SnL$. Because it causes the least amount of steric hindrance compared to the other stabilizers that are used, the dimethyl tin (IV) complex functions as a more effective photo stabilizer than the other complexes. Before and after irradiation, both pure PVC film and films blend with organotin (IV)-cephalexin complexes were subjected to weighing to calculate the weight loss in percentage terms using equation (4.1).

Weight loss (%) = $[(W_0 - W_t) / W_0] \times 100$ ..... (4.1)

Where:

W_0: Weight of the Film before Irradiation.

W_t: Weight of the Film after Irradiation.

The films were damaged and became dark brown after 300 hours, thus no further attempts were made to explore the effects of irradiation.

Table 4.1 Measurements of Weight Loss % for PVC Films Containing 0.5% of Organotin (IV) - Cephalexin Complexes.

Compounds	Irradiation time (h)						
	0	50	100	150	200	250	300
PVC	0.00	1.23	2.11	2.61	3.03	3.26	3.48
Ph_3SnL	0.00	0.24	0.45	0.59	0.75	0.91	1.05
Bu_3SnL	0.00	0.51	0.82	1.08	1.31	1.53	1.75
Me_3SnL	0.00	0.16	0.31	0.46	0.59	0.72	0.85
Ph_2SnL_2	0.00	0.33	0.53	0.70	0.88	1.06	1.25
Bu_2SnL_2	0.00	0.46	0.65	0.95	1.12	1.34	1.57
Me_2SnL_2	0.00	0.12	0.24	0.35	0.41	0.54	0.63

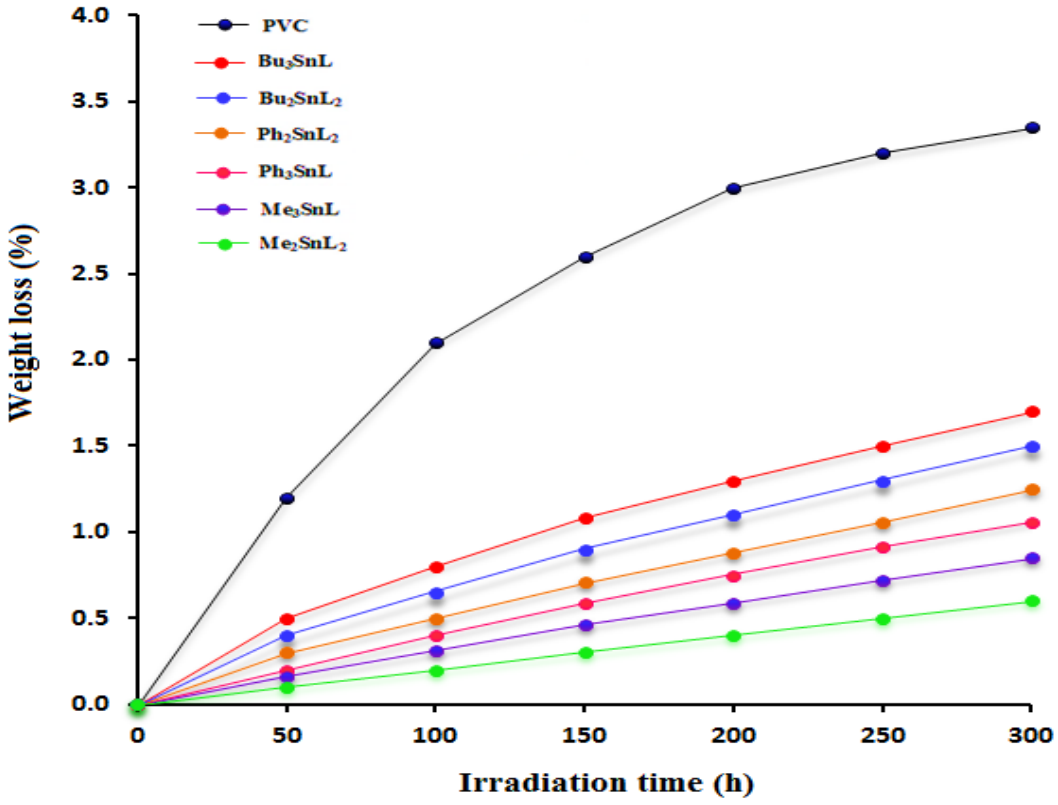

Figure 4.1 Effect of PVC Film Irradiation Time on Weight Loss (%).

4.1.3 FTIR Spectroscopy Evaluation of Poly (Vinyl Chloride) Stabilizing Effectiveness

When HCl is removed from poly (vinyl chloride), it breaks down into unstable polymeric chains and unsaturated (-CH=CH-, 1606 cm^{-1}) small fragments. After being exposed to oxygen, the radical-containing PVC fragments produced oxygenation groups including carbonyl (-C=O, 1732 cm^{-1}) and hydroxyl (-OH), respectively. Fig. 4.2 displays the difference in infrared spectroscopy of blank poly (vinyl chloride) films before and after being exposed to radiation for 300 hours.

By using FTIR spectroscopy can be determine the absorbance and intensity of the functional groups that comprise these components and then compare those results to a reference peak [154]. Because it is unaffected by the irradiation, the absorption peak at 1328 cm^{-1} that is created by the C-H bonds in the PVC may be utilized as a reference peak. Poly vinyl chloride films with and without organotin (IV)-cephalexin (0.5% weight) stabilizers have their I_{OH}, $I_{C=O}$, and $I_{C=C}$ calculated using equation (4.2). These measures were then graphed against the total irradiation duration for each film. The indices of PVC films containing organotin (IV) complexes were lower than those of blank PVC [155, 156]. As explained in Tables 4.2–4.4 and Figs. 4.3–4.5. Using equation (4.3) can be calculated the absorbance (A) for both the functional and reference groups by first determining the transmittance (T). For PVC films, the presence of more methyl groups, the lack of steric hindrance and the heteroatoms (such as N and O) of the stabilizers allowing done polar interactions make organotin (IV) complexes and Me_2SnL_2 in particular, promising candidates for photo stabilization. Conjugated systems are thought to absorb UV rays effectively, converting them into thermal energy [157].

$$\mathbf{I_s = A_s/A_r} \quad \text{(4.2)}$$

$$\mathbf{A = 2 - \log T\%} \quad \text{(4.3)}$$

Where

A_s: $A_{C=O}$, $A_{C=C}$ and A_{O-H}

A_r: A_{C-H}

I_s: $I_{C=O}$, $I_{C=C}$ and I_{O-H}

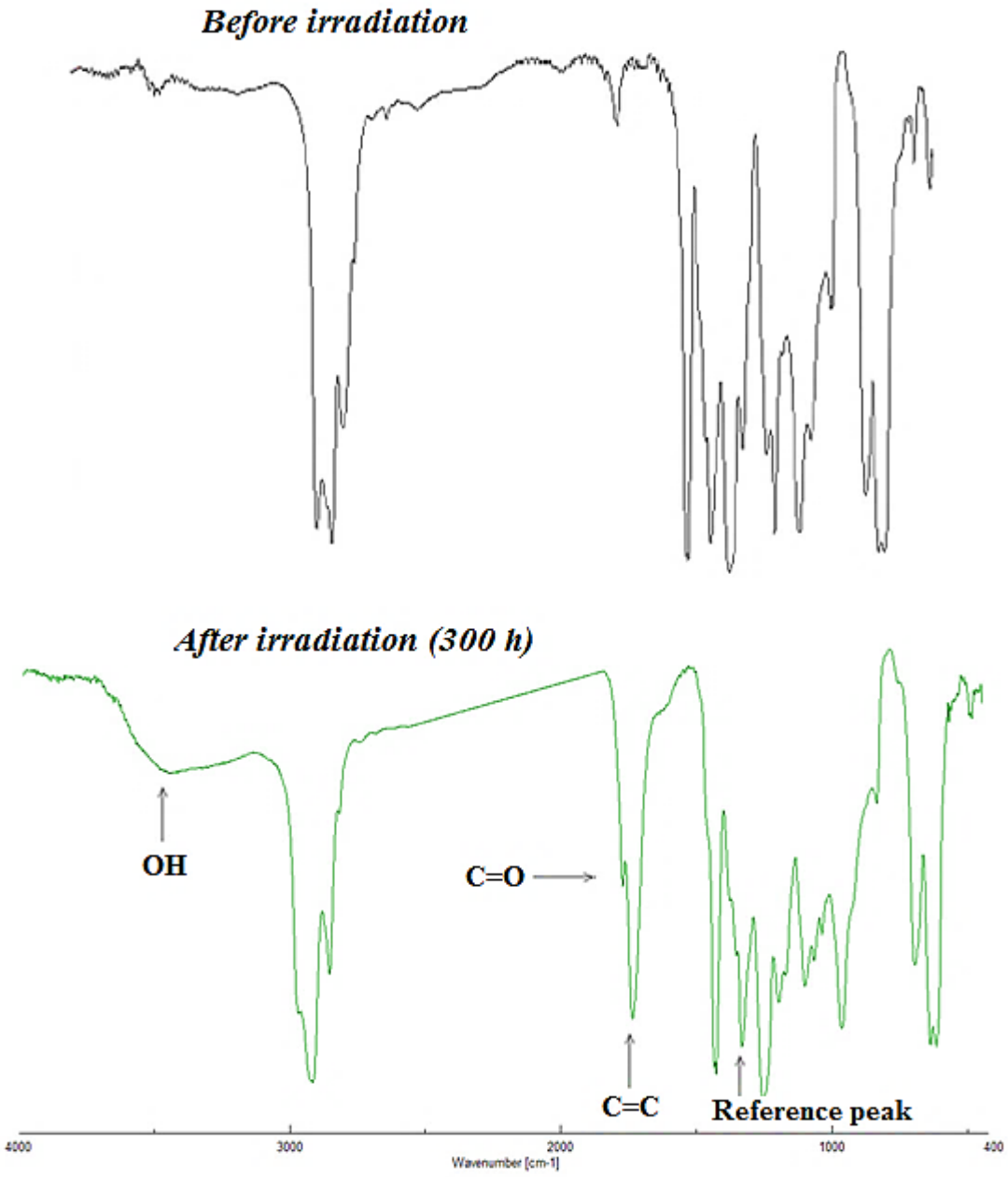

Figure 4.2 FTIR Spectra of PVC Film before and after Irradiation.

Table 4.2 Hydroxyl Index (I_{OH}) with Irradiation Time for PVC Films Containing 0.5% Stabilizers.

Compounds	Irradiation Time(h)						
	0	50	100	150	200	250	300
PVC	0.071	0.125	0.151	0.178	0.205	0.231	0.255
Ph_3SnL	0.065	0.087	0.101	0.113	0.121	0.127	0.132
Bu_3SnL	0.069	0.109	0.129	0.142	0.151	0.161	0.168
Me_3SnL	0.069	0.092	0.110	0.121	0.129	0.136	0.141
Ph_2SnL_2	0.064	0.098	0.116	0.129	0.137	0.144	0.149
Bu_2SnL_2	0.065	0.105	0.123	0.136	0.145	0.153	0.159
Me_2SnL_2	0.063	0.081	0.092	0.103	0.111	0.116	0.121

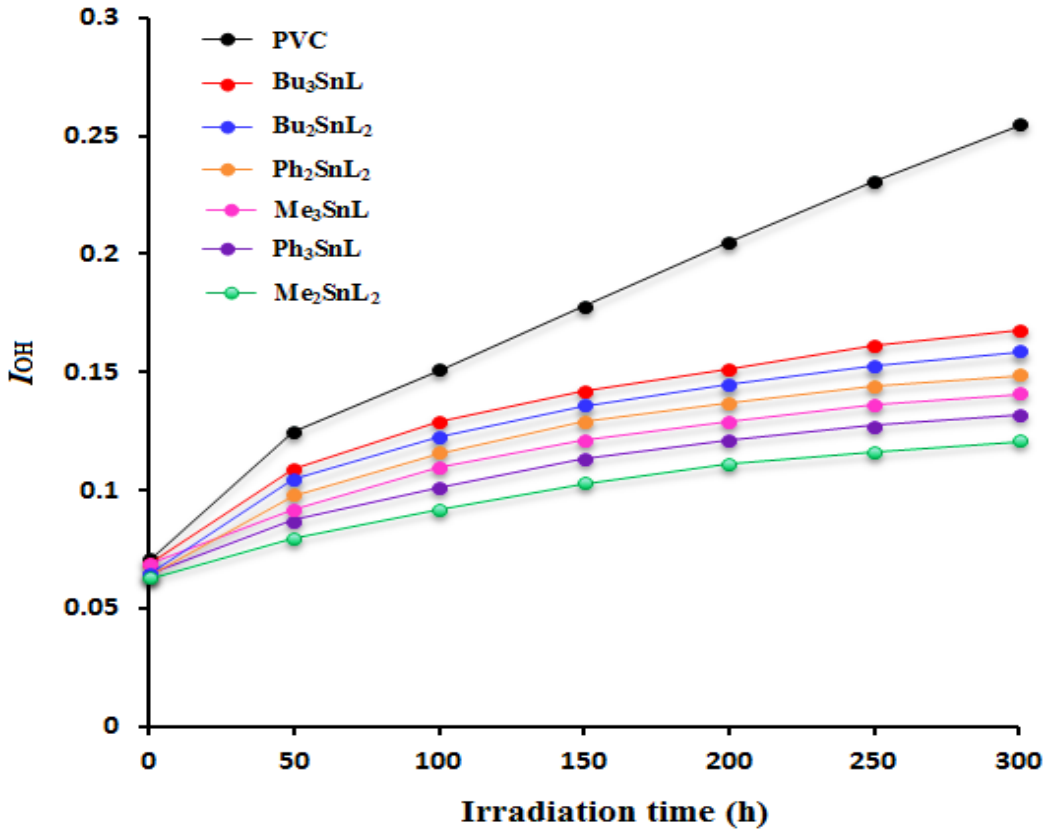

Figure 4.3 Effect of Irradiation on I_{OH} for PVC blank and Complexes Films.

Table 4.3 Carbonyl Index ($I_{C=O}$) with Irradiation Time for PVC Films Containing 0.5% Stabilizers.

Compounds	Irradiation Time (h)						
	0	50	100	150	200	250	300
PVC	0.873	1.531	1.971	2.351	2.582	2.751	2.883
Ph_3SnL	0.868	0.989	1.111	1.209	1.261	1.285	1.299
Bu_3SnL	0.869	1.191	1.392	1.518	1.611	1.689	1.746
Me_3SnL	0.858	1.060	1.179	1.278	1.342	1.369	1.399
Ph_2SnL_2	0.877	1.120	1.238	1.355	1.421	1.461	1.499
Bu_2SnL_2	0.858	1.15	1.311	1.419	1.499	1.563	1.599
Me_2SnL_2	0.823	0.914	1.011	1.111	1.166	1.201	1.211

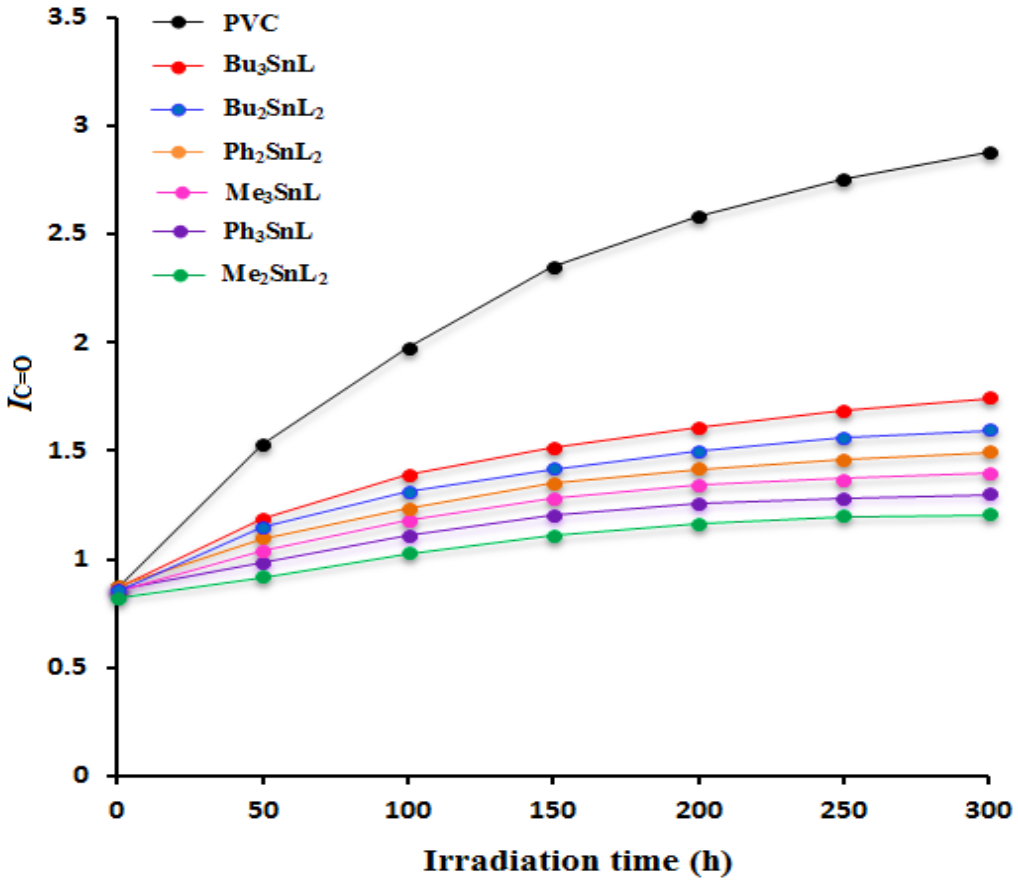

Figure 4.4 Effect of Irradiation on $I_{C=O}$ for PVC blank and Complexes Films.

Table 4.4 Polyene Index ($I_{C=C}$) with Irradiation Time for PVC Films containing 0.5% Stabilizers.

Compounds	Irradiation Time (h)						
	0	50	100	150	200	250	300
PVC	0.165	0.288	0.381	0.466	0.532	0.595	0.649
Ph_3SnL	0.162	0.193	0.222	0.249	0.284	0.311	0.339
Bu_3SnL	0.173	0.251	0.311	0.369	0.421	0.471	0.512
Me_3SnL	0.161	0.196	0.238	0.279	0.321	0.359	0.389
Ph_2SnL_2	0.159	0.221	0.261	0.31	0.359	0.399	0.439
Bu_2SnL_2	0.162	0.232	0.284	0.339	0.392	0.439	0.476
Me_2SnL_2	0.155	0.179	0.198	0.222	0.251	0.271	0.296

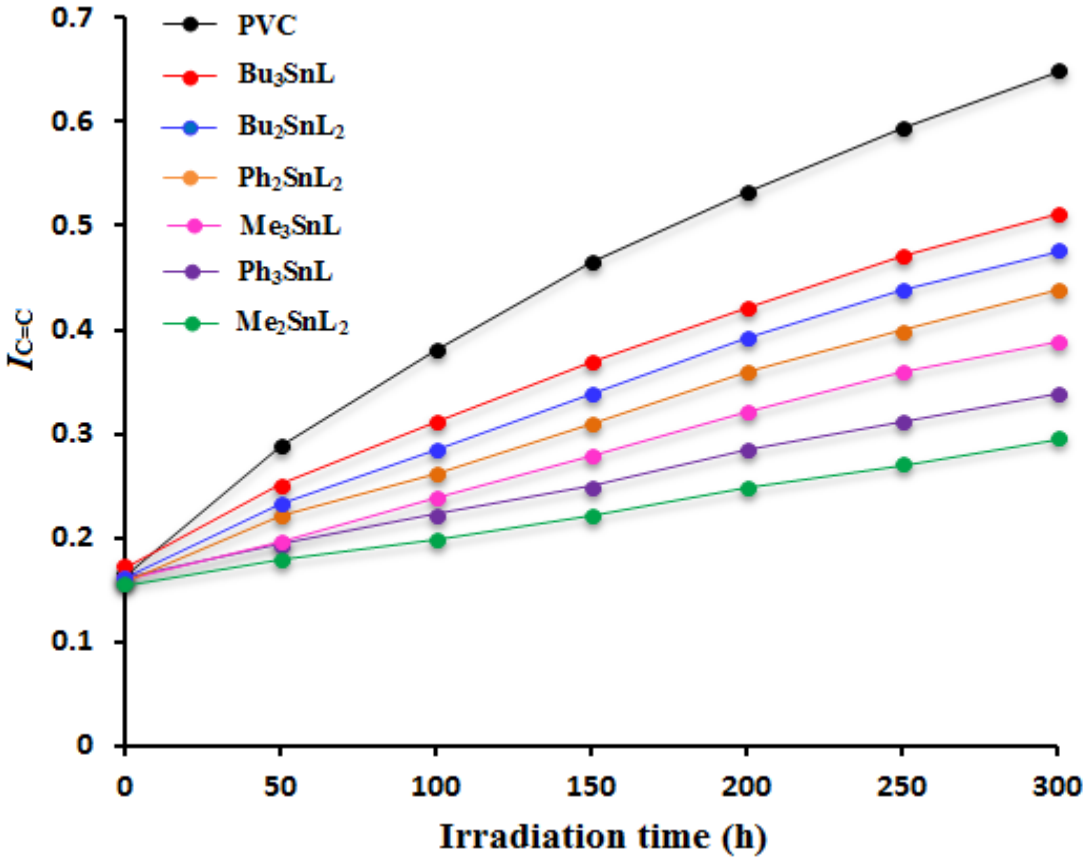

Figure 4.5 Effect of Irradiation on $I_{C=C}$ for PVC blank and Complexes Films.

4.2 Surface Morphology

4.2.1 Microscopic Analysis

The elimination of hydrogen chloride and the development of small unsaturated residues caused most of the surface degradation of poly (vinyl chloride) [158]. Optical microscopy at 400 x magnification may evaluate polymer surface crystallinity, smoothness, and roughness. The PVC films' surface after exposure to irradiation became rougher and had more cracks, spots and grooves compared with PVC that has organotin (IV) cephalexin complexes, which showed less surface damage. Therefore, the organotin (IV) complexes may be able to slow the dehydrochlorination process and increase the photo stability of irradiated PVC films [159–161]. After irradiation, the surface of poly (vinyl chloride) film containing Me_2SnL_2 complex was smoother and more transparent, with fewer defects and cracks, than the surfaces of other products containing complex as shown in Figs. 4.6 and 4. 7.

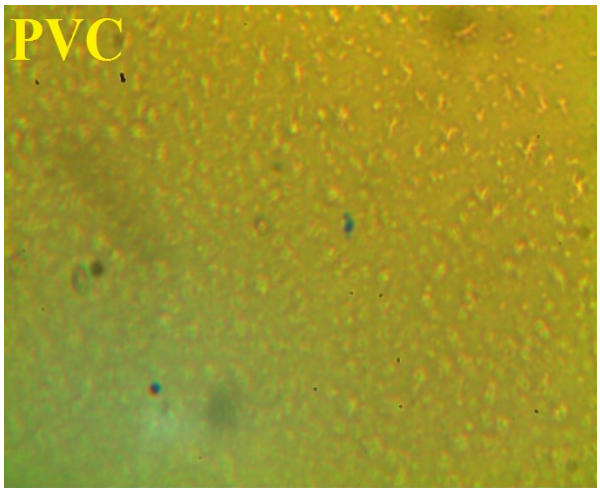

Figure 4.6 Microscope Images of PVC Film after 300 h Irradiation.

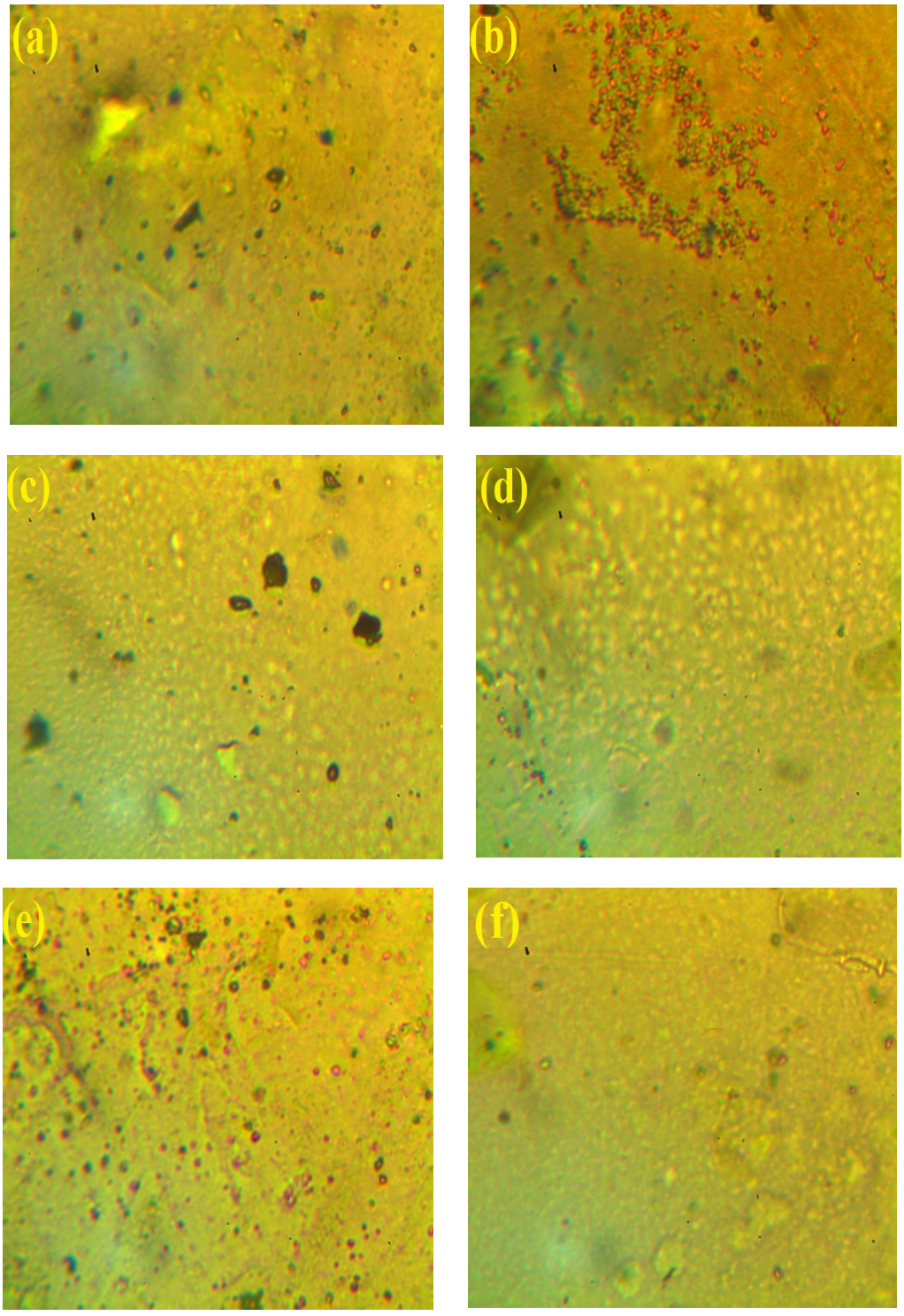

Figure 4.7 Microscope Images of PVC Films after Irradiation at 300 h in presence of (a) Ph_3SnL, (b) Bu_3SnL, (c) Me_3SnL, (d) Ph_2SnL_2, (e) Bu_2SnL_2 and (f) Me_2SnL_2 Complexes.

4.2.2 Atomic Force Microscopy (AFM) of PVC Films

Poly (vinyl chloride) film surface morphologies were examined using an atomic force microscope. It is a powerful microscopy technique for evaluating surface measurements that can image in both two and three dimensions [162]. The atomic force microscope provides valuable information on the properties and roughness of the PVC surface. Poly (vinyl chloride) bond breakdown after long-term irradiation for 300 hours, resulting in a rough and broken surface. The Two- and Three-dimensional images revealed that the PVC films containing organotin (IV)-cephalexin complexes, which act as photo stabilizers, had considerably fewer holes and smoother surfaces than the pure poly (vinyl chloride) film, as shown in Figs. 4.8–4.10. Also, Atomic force microscopy is used to evaluate the roughness factor (Rq) of polymer films. When Rq is high, dehydrochlorination and bond breakage result in rough surfaces [163, 164]. It appears that organotin (IV) complexes hinder the dehydrochlorination process. The values of Roughness Factor were listed in Table 4.5

Table 4.5 Roughness Factor (R_q) for PVC without and presence of Complexes after 300 h Irradiation.

PVC Film with Photo Irradiation (300 h)	Rq
PVC	316.2
PVC+Ph_3SnL	80.6
PVC+Bu_3SnL	87.1
PVC+Me_3SnL	67.6
PVC+Ph_2SnL_2	81.2
PVC+Bu_2SnL_2	86.3
PVC+Me_2SnL_2	67.2

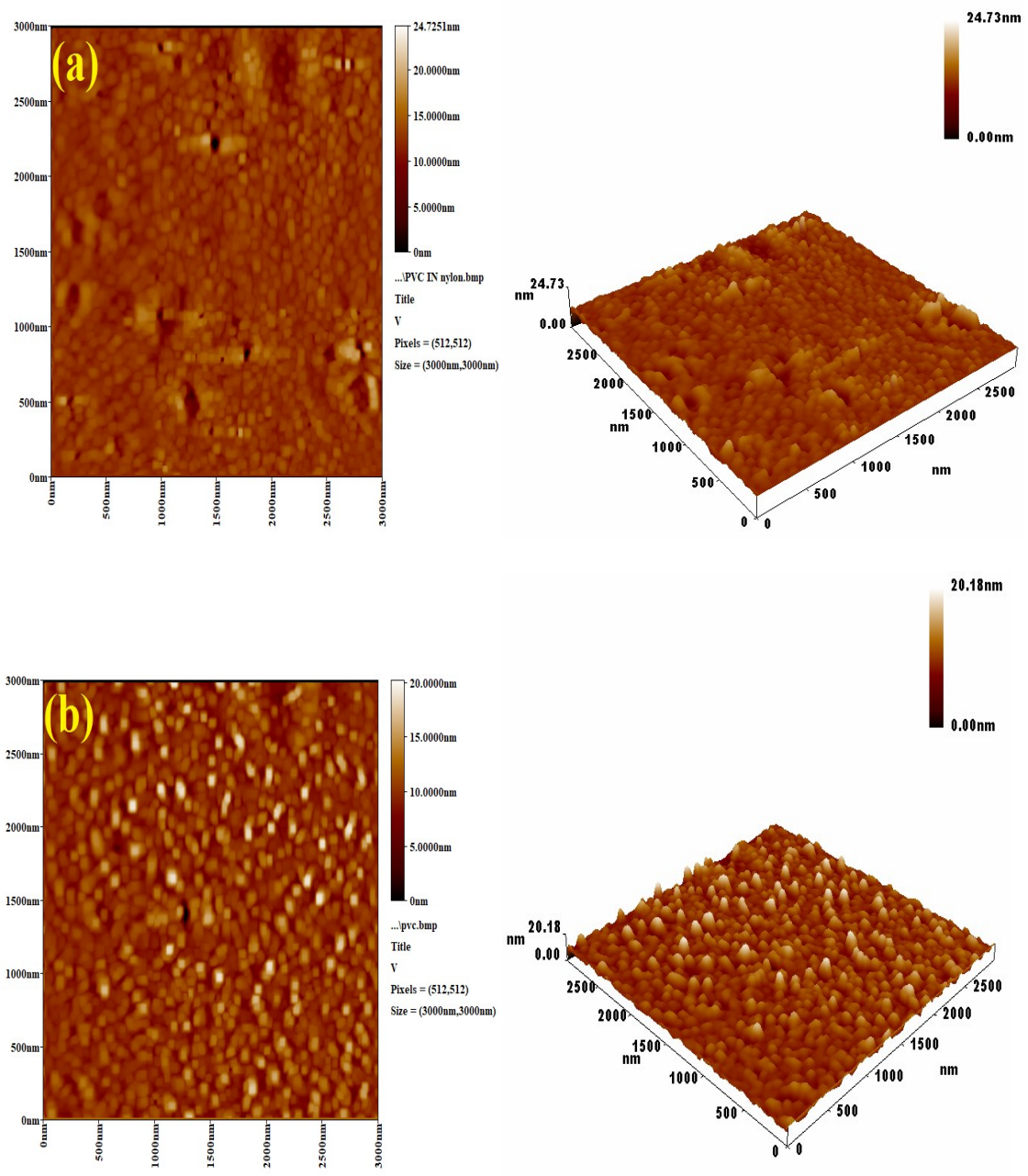

Figure 4.8 Two- and Three-dimensions AFM Images of PVC (a) Before and (b) After 300 h Irradiation.

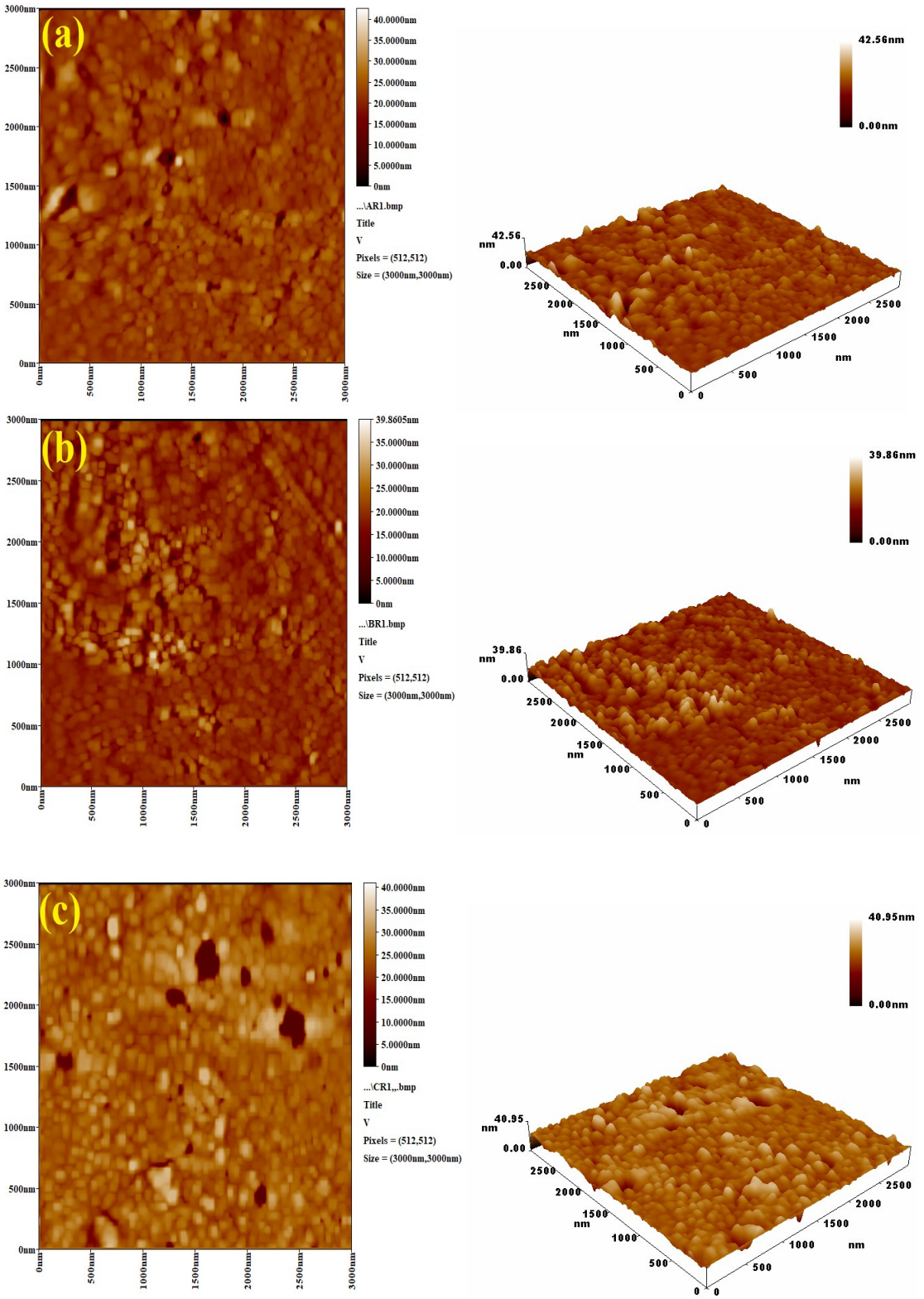

Figure 4.9 Two- and Three-dimensions AFM Images of PVC in presence of (a) Ph_3SnL, (b) Bu_3SnL and (c) Me_3SnL Complexes after Irradiation at 300 h.

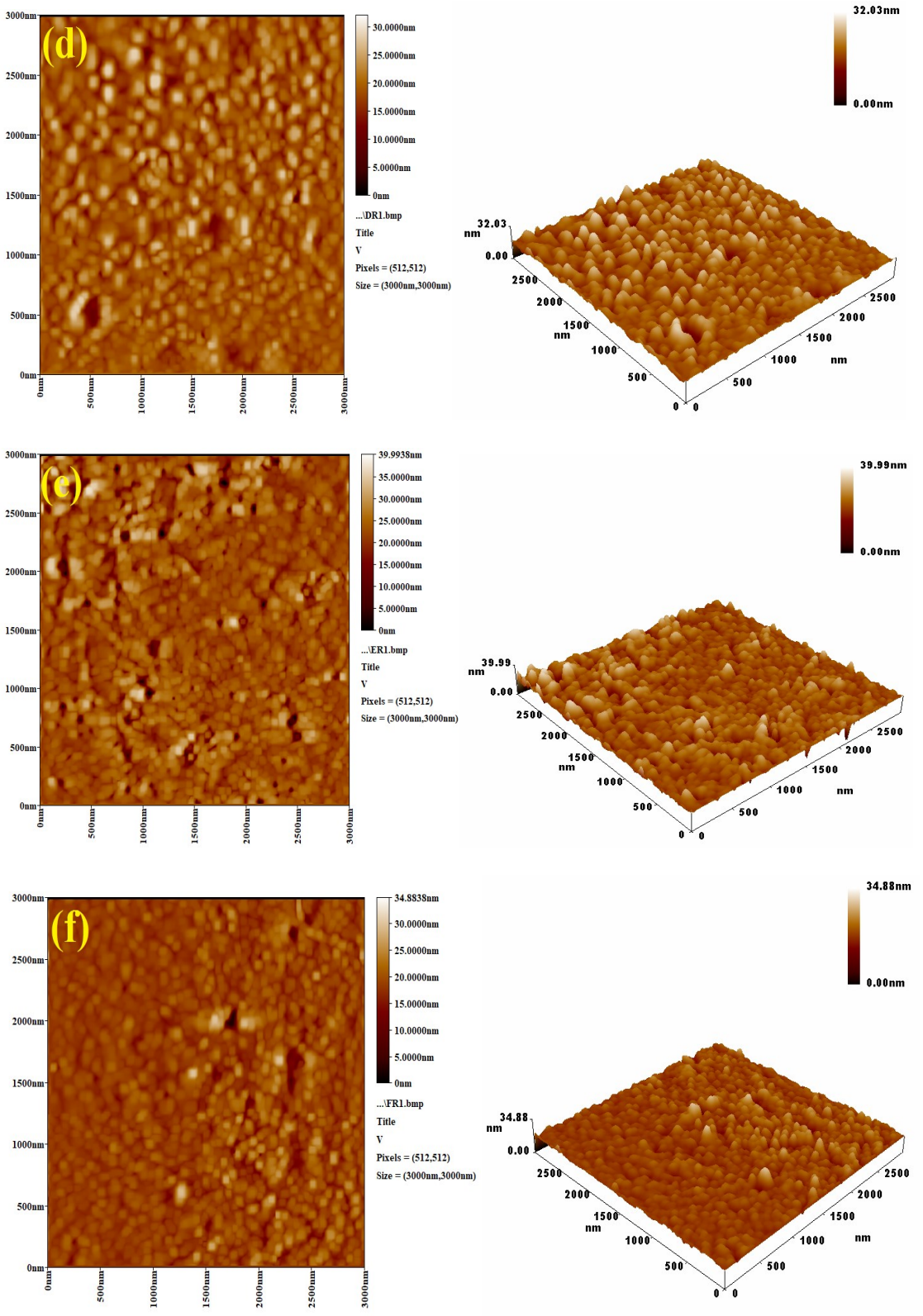

Figure 4.10 Tow and Three dimensions AFM Images of PVC in presence of (d) Ph_2SnL_2, (e) Bu_2SnL_2 and (f) Me_2SnL_2 Complexes after Irradiation at 300 h.

4.2.3 Scanning Electron Microscopy

Scanning electron microscopy (SEM) offers important information about the surface morphology of polymers, which in turn reflects their interior structures. Electron beams can be used to obtain clear, magnified pictures of the poly (vinyl chloride) surface. The surface of the PVC films was examined using a SEM and pictures were captured at various magnification powers [165-167]. In this study, the non-irradiated pure PVC film was smooth with a minimal number of grooves or white spots. In contrast, the irradiated pure PVC exhibited a large irregularity in the SEM picture, as seen by the presence of white spots, grooves, and lumps throughout the substance. Surface irregularities and damage were lower in PVC containing organotin (IV)-cephalexin complexes than blank PVC film. This is consistent with the organotin (IV)-cephalexin complex's less damaging effect on the released HCl from the PVC surface, as illustrated in Figs. 4.11–4.13.

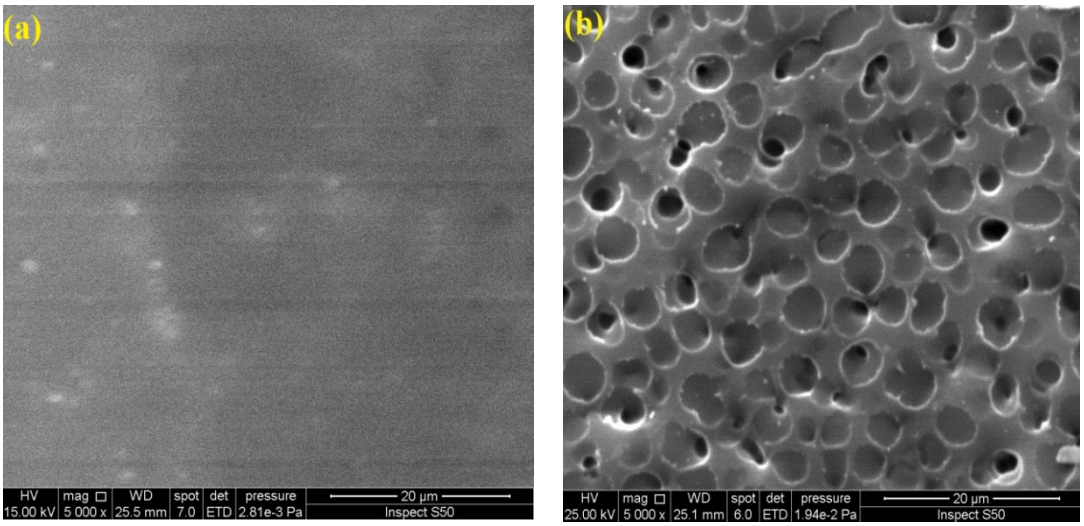

Figure 4.11 SEM Images for PVC Films (a) Before and (b) After Irradiation at 300 h.

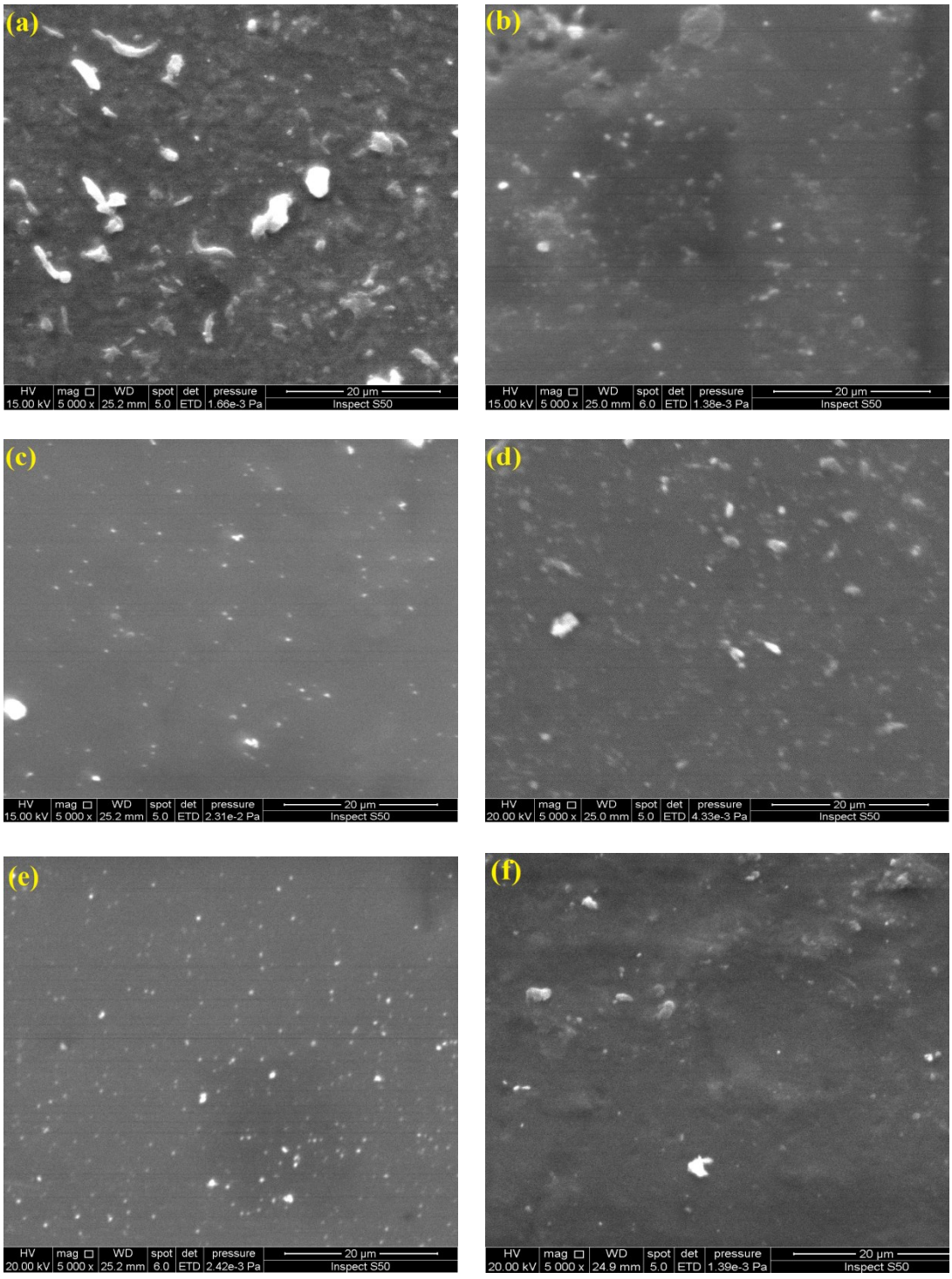

Figure 4.12 SEM Images for PVC in presence of (a) Ph_3SnL, (b) Bu_3SnL, (c) Me_3SnL, (d) Ph_2SnL_2, (e) Bu_2SnL_2 and (f) Me_2SnL_2 Complexes.

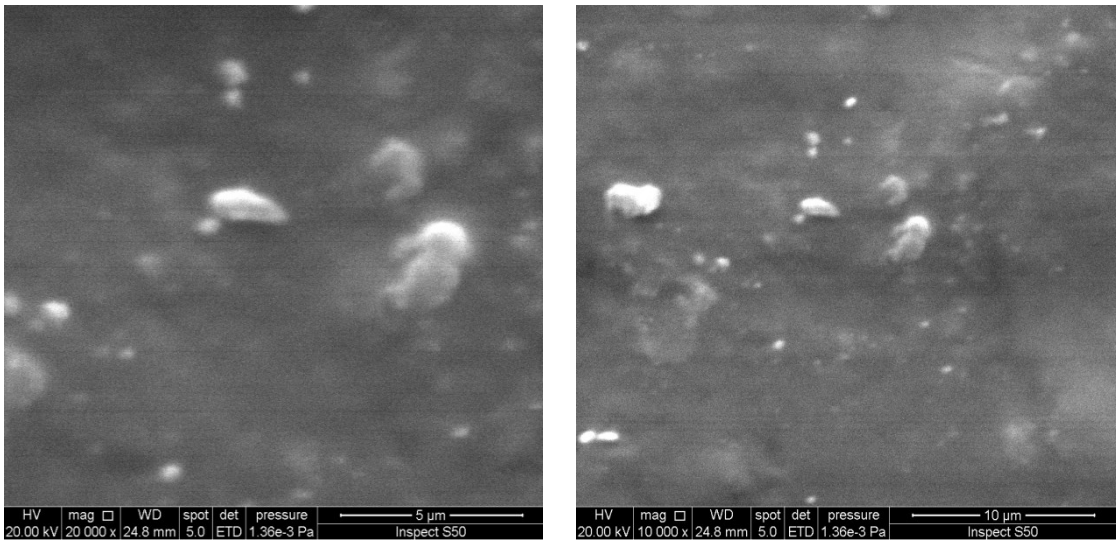

Figure 4.13 SEM Images for PVC in presence of Me_2SnL_2 in scale 5 and 10 µm.

4.3 Mechanisms of Photostabilization of PVC by Organotin (IV)-Cephalexin Complexes

The effectiveness of stabilizers as poly (vinyl chloride) photo stabilizers was evaluated by variations in the polyene, carbonyl, and hydroxyl group indices. Compared to PVC blank, the changes were less apparent in poly (vinyl chloride) films including organotin (IV)-cephalexin complexes. Tin (IV) is strong Lewis acid act as HCl scavenger. The oxygen atoms of the carboxylate groups that linked by tin (IV) atom can be substituted by the chlorine atoms in the PVC chain as shown in Scheme 4.1 [168, 169]. Polymeric chains would be shielded from the harmful effects of hydrogen chloride in this method [170]. These stabilizers give good photostabilizing characteristics for Poly (vinyl chloride) by serving as secondary stabilizers. The PVC photodegradation was significantly reduced by the organotin (IV)-cephalexin complexes used, but Me_2SnL_2 was the most successful.

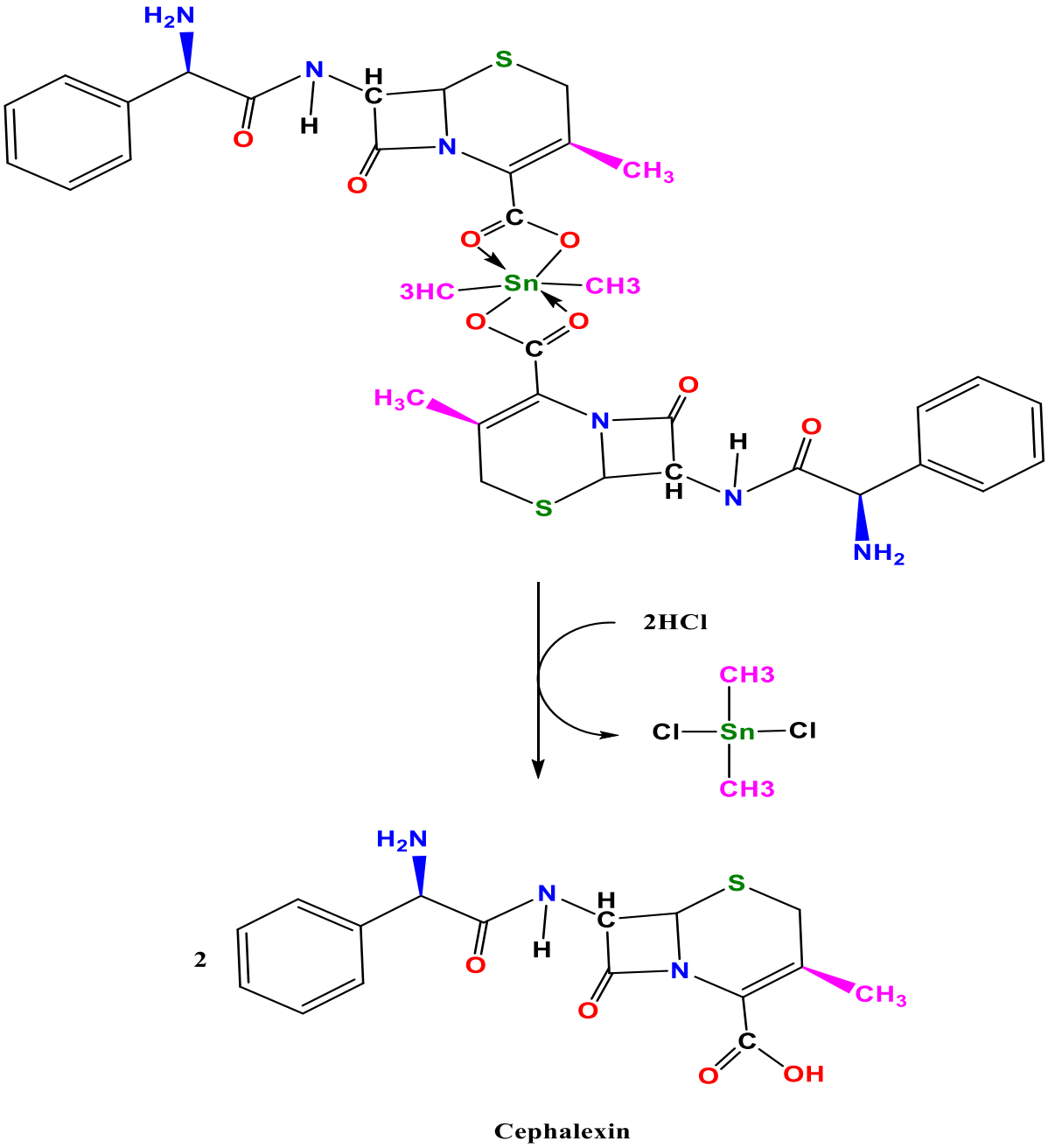

Cephalexin

Scheme 4.1 Dimethyltin (IV) -Cephalexin Complex as HCl Scavengers.

The coordination of polarized bonds between organotin (IV)-cephalexin complexes and C-Cl bonds within poly (vinyl chloride) chains might prevent polymeric photodegradation, as shown in Scheme 4.2.

This could help in the prevention of polymer photodegradation since these compounds act as major stabilizers by absorbing UV energy from the sun. The attraction between organotin (IV) and PVC can assist in the conversion of the PVC energy to one that doesn't harm the polymer [171, 172].

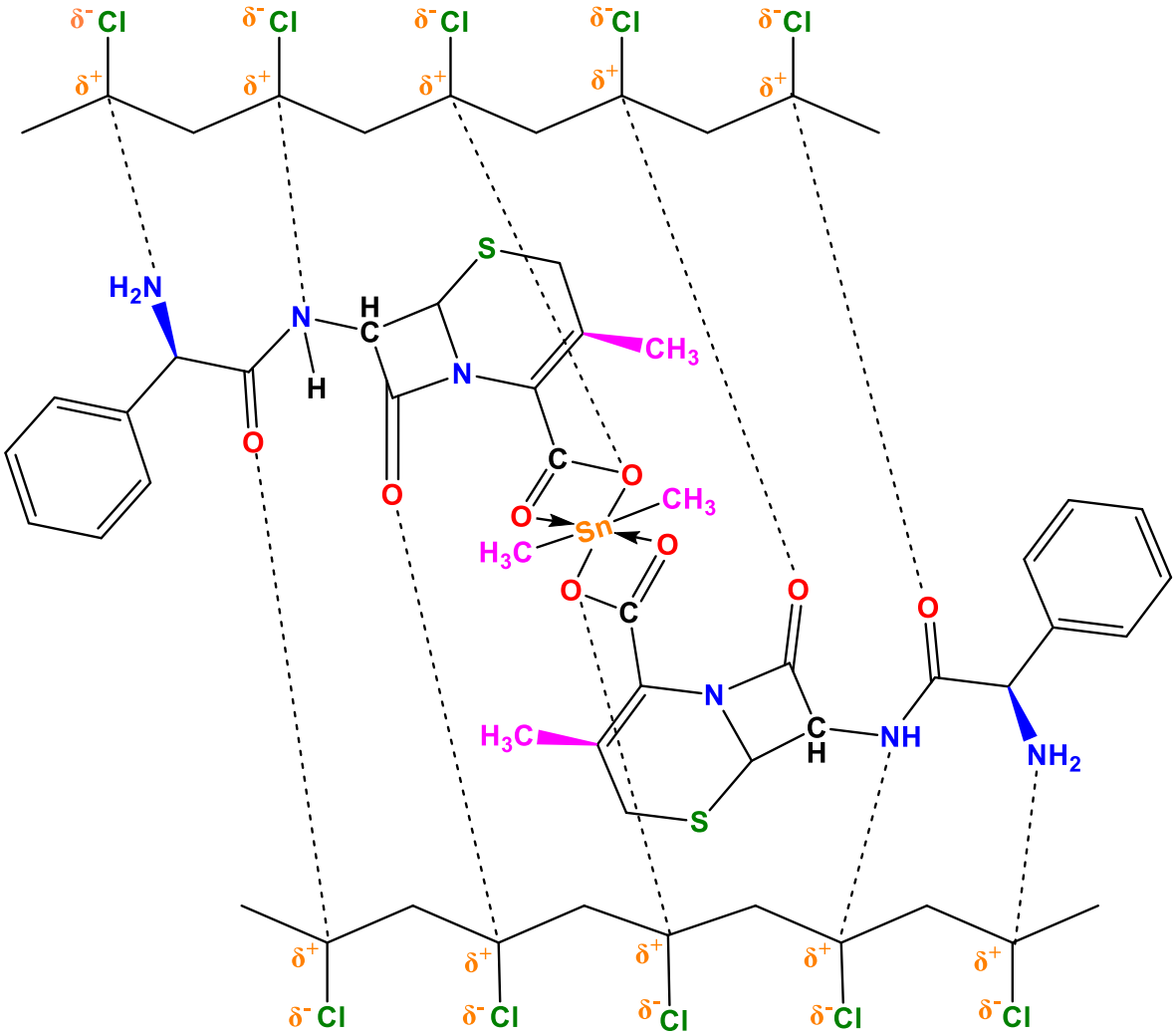

Scheme 4.2 Polarized Bonds between Dimethyltin (IV) - Cephalexin Complex and PVC.

PVC may be stabilized against photodegradation by using organotin (IV)-cephalexin complexes, which can act as peroxide decomposers. The photodegradation of PVC generates radicals when oxygen is present; these radicals combine with oxygen to create peroxide radicals [173].

As shown in Scheme 4.3, organotin (IV)-cephalexin complexes can interact with peroxides like hydroperoxides to increase the photostability of polymeric films during photooxidation.

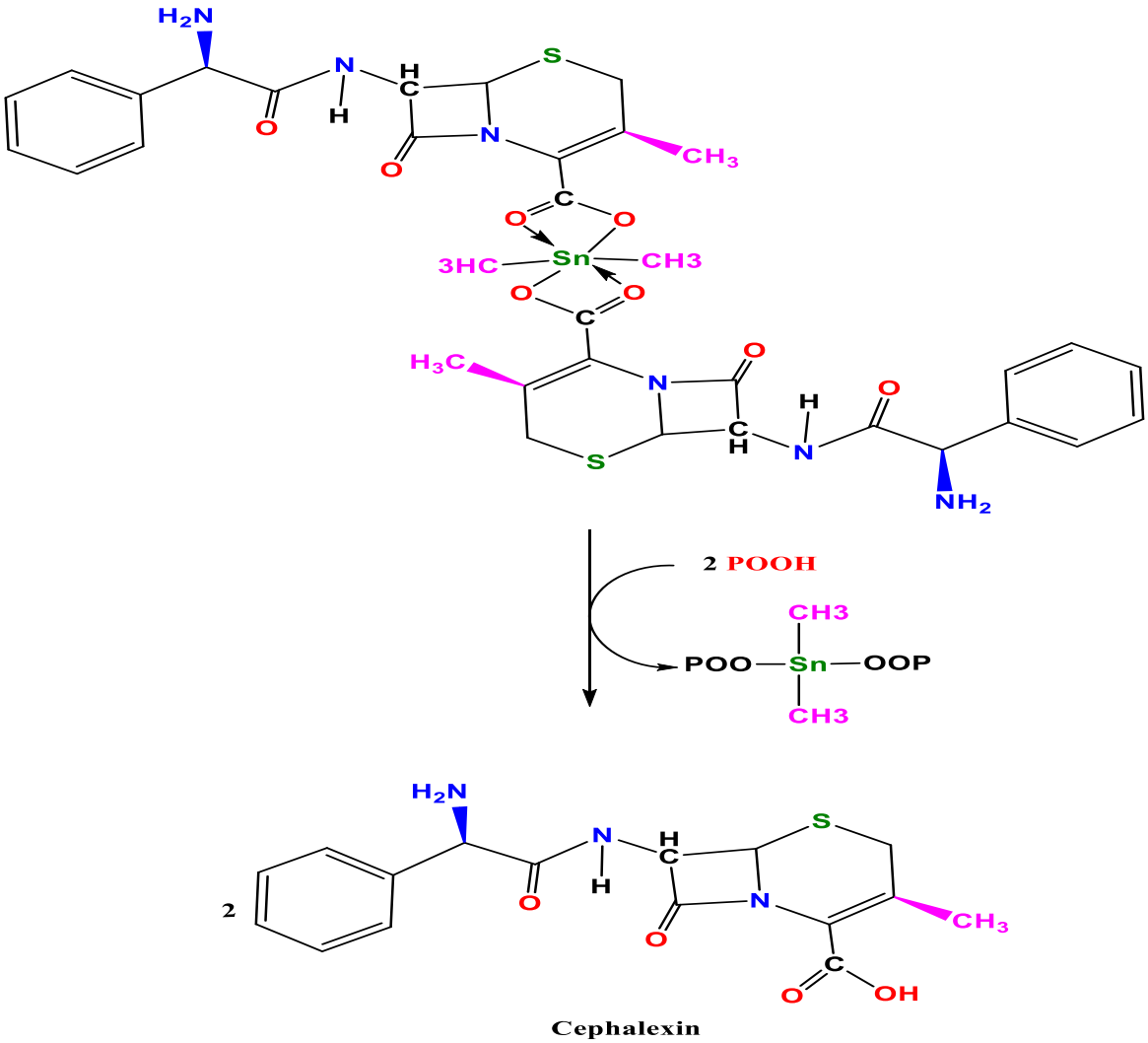

Scheme 4.3 Dimethyltin (IV) - Cephalexin Complex acting as a Peroxide decomposer.

Peroxide radicals (POO•), which continue to create other photooxidative products, are one of the most dangerous by products of the photooxidation of PVC.

As shown in scheme 4.4, the tin (IV) complexes could act as radical scavengers and produce intermediates that include peroxide radicals and aryl moieties in the additives. Through resonance, the intermediates are very stable [174, 175]. As a result, the complexes prevent PVC from oxidizing in sunlight and offer some irradiation stability.

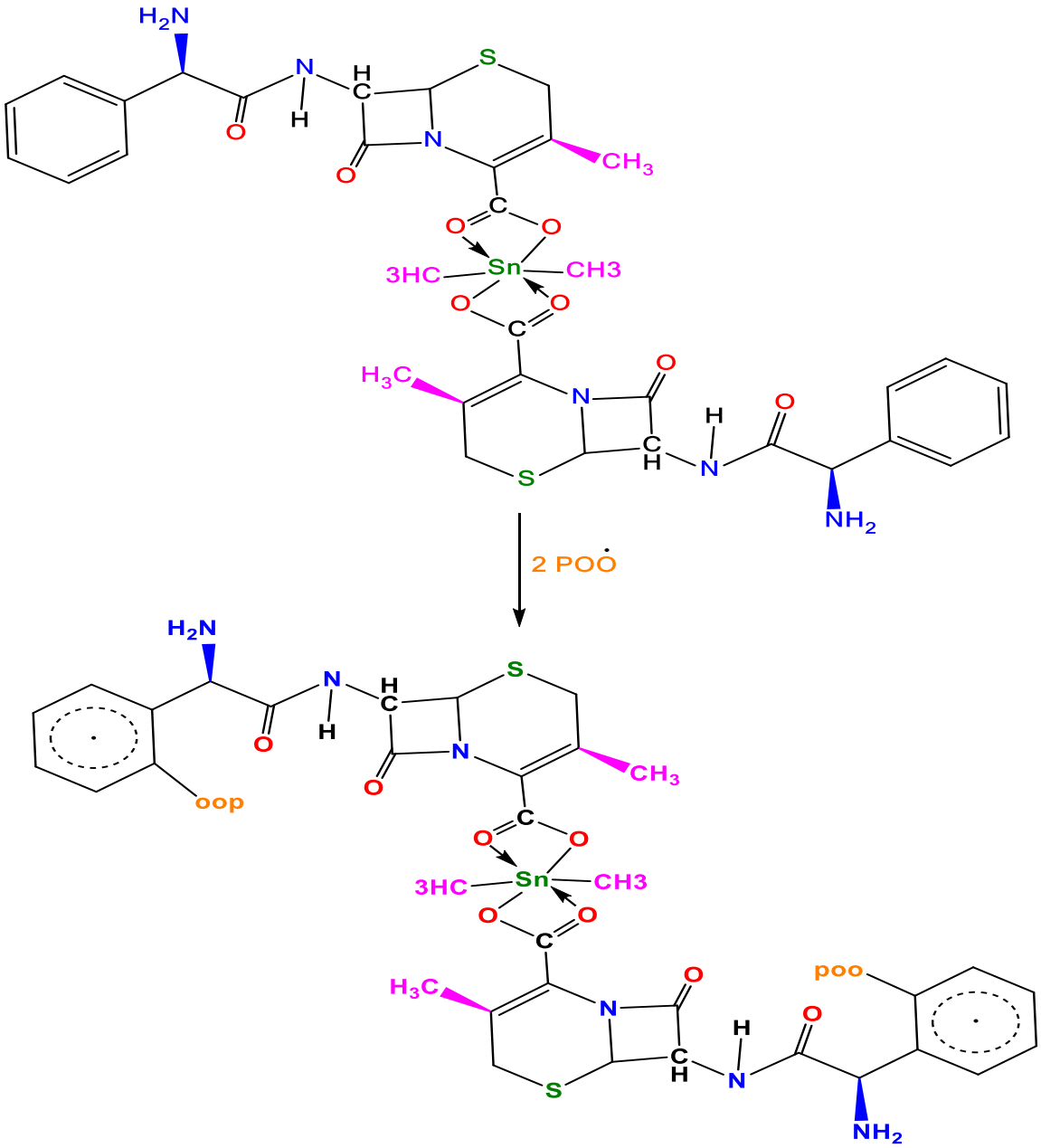

Scheme 4.4 Organotin (IV) Complexes as Radical Scavengers.

4.4 Photostabilizers of Poly (Vinyl Chloride) Films

4.4.1 Photodegradation of Organotin (IV) -Tyrosine Complexes

4.4.2 Impact of Irradiation on Weight of Poly (Vinyl Chloride)

PVC photodegradation leads to weight loss and linked to HCl gas estimation (dehydrochlorination process). The films (40 µm in thickness) were made by combining PVC with organotin (IV)-tyrosine complexes (0.5%). As a result, the degree of PVC photodegradation can be evaluated by the percentage of weight loss [176]. Fig. 4.14 and Table 4.6 illustrate the impact of irradiation duration on the percentage of PVC film weight loss. Obviously, compared to the blank PVC film, the weight loss in PVC was smaller in the presence of organotin (IV)-tyrosine complexes [177, 178]. The PVC films that blend with the dimethyl tin (IV) complex have the lowest weight loss. The addition of Me_2SnL_2, which has methyl group substitutions, lessens the steric hindrance of the organotin (IV)-tyrosine complexes, and facilitates the ability to form polarized bonds with PVC. The photodegradation of polymeric films was also significantly decreased by the presence of an aromatic ring in the structure of tyrosine, which promotes stability through resonance. Organotin (IV) complexes were discovered to have the following order of efficiency in the photostabilization of poly (vinyl chloride): $Me_2SnL_2 > Me_3SnL > Ph_3SnL > Ph_2SnL_2 > Bu_3SnL > Bu_2SnL_2$.

Table 4.6 Measurements of Weight Loss percent for PVC Films with 0.5% Organotin (IV)-Tyrosine Complexes.

Compounds	Irradiation time (h)						
	0	50	100	150	200	250	300
PVC	0.00	1.23	2.11	2.61	3.03	3.26	3.48
Ph_3SnL	0.00	0.75	1.00	1.21	1.42	1.63	1.82
Bu_3SnL	0.00	0.86	1.15	1.39	1.61	1.83	2.01
Me_3SnL	0.00	0.66	0.93	1.11	1. 33	1.48	1.67
Ph_2SnL_2	0.00	0.81	1.08	1.30	1.51	1.72	1.91
Bu_2SnL_2	0.00	0.95	1.25	1.50	1.72	1.90	2.15
Me_2SnL_2	0.00	0.55	0.76	0.97	1.15	1.32	1.48

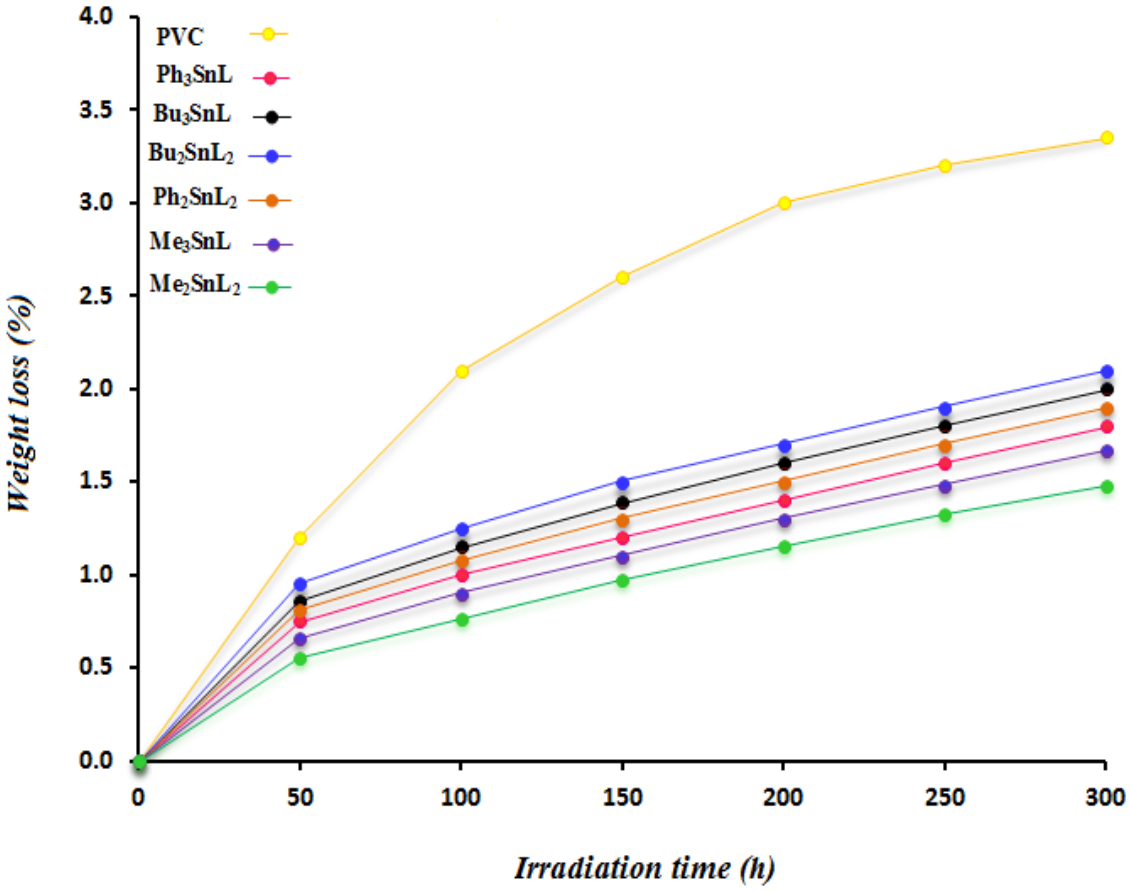

Figure 4.14 Effect of PVC Film Irradiation Time on Weight Loss (%).

4.4.3 Evaluation of Stabilizing Efficiency of PVC by FTIR Spectroscopy

PVC film functional group alterations were evaluated using Fourier transform infrared spectroscopy (4000-400 cm $^{-1}$). Several functional group moieties, including OH (3500 cm^{-1}), C=O (1724 cm^{-1}), and C=C (1603 cm^{-1}), occur when poly (vinyl chloride) films exposed to UV-Irradiation [179]. During the irradiation procedure, band intensities associated with these classes can be measured and compared to a constant reference peak C-H (1328 cm^{-1}) in poly (vinyl chloride). Results of calculating and plotting the carbonyl ($I_{C=O}$), polyene (Ic=c), and hydroxyl (I_{OH}) indices with irradiation time are presented in Tables 4.7- 4.9 and Figs. 4.16-4.18, respectively. PVC films containing organotin (IV)-tyrosine complexes had lower values for these indices compared to PVC blanks [180, 181]. The Me_2SnL_2 complex, followed by the Me_3SnL, Ph_3SnL, Ph_2SnL_2, Bu_3SnL and Bu_2SnL_2 complexes, was the most effective photo stabilizer for poly (vinyl chloride) due to the presence of methyl groups, which allowed complexing through polar interactions with poly (vinyl chloride) due to less steric hindrance and the presence of phenyl groups that absorb within the ultraviolet region because of their conjugation system. The infrared spectra of Me_2SnL_2 complex-containing PVC films before and after 300 hours of irradiation is shown in Fig. 4.15.

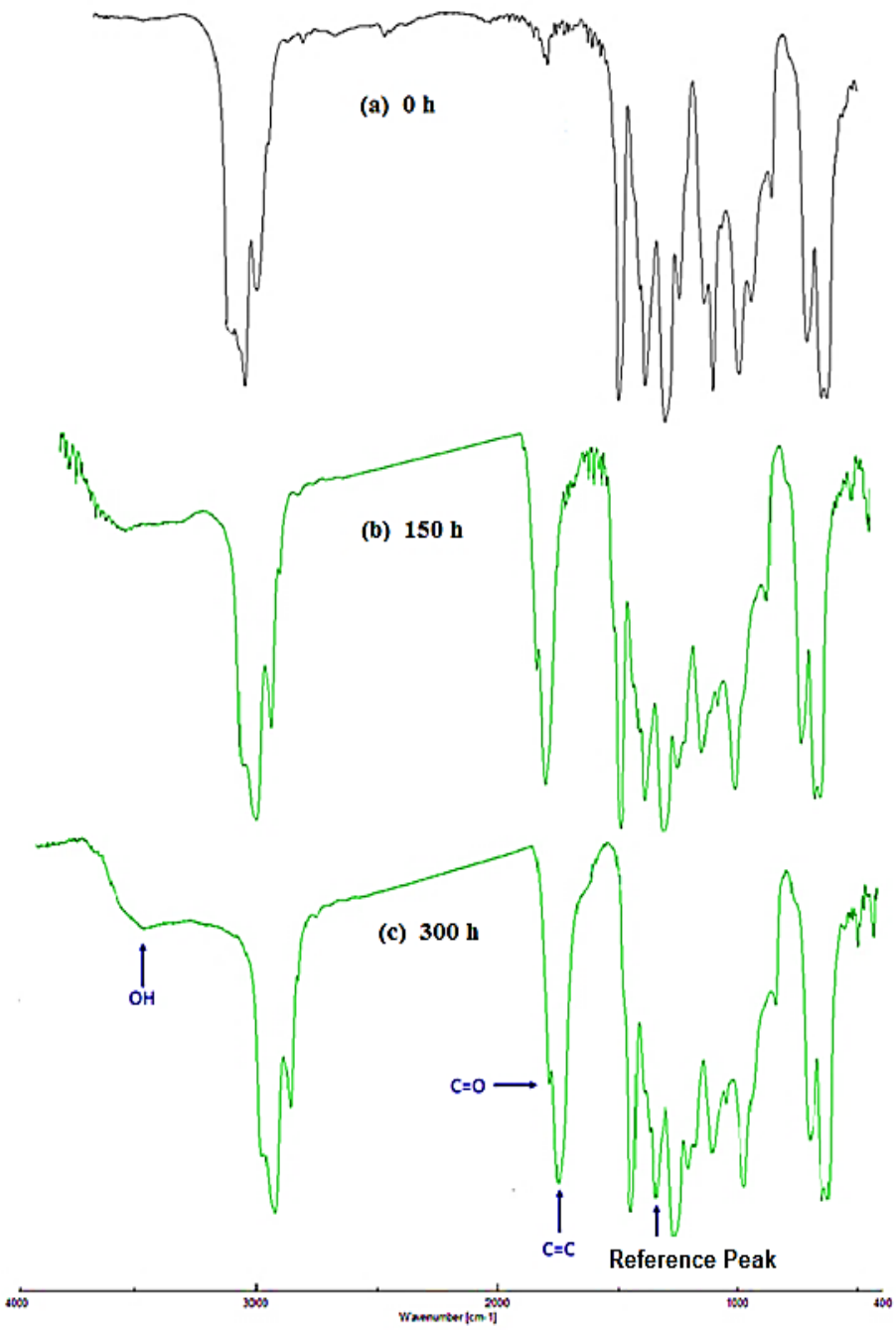

Figure 4.15 FTIR Spectra of PVC Film containing Me_2SnL_2 Complex at 0,150 and 300 hours of Irradiation.

Table 4.7 Hydroxyl Index (I_{OH}) with Irradiation Time for PVC Films containing 0.5% Stabilizers.

Compounds	Irradiation time(h)						
	0	50	100	150	200	250	300
PVC	0.074	0.135	0.157	0.179	0.198	0.217	0.235
Ph_3SnL	0.075	0.092	0.107	0.119	0.129	0.138	0.147
Bu_3SnL	0.079	0.109	0.125	0.139	0.151	0.161	0.171
Me_3SnL	0.078	0.087	0.099	0.109	0.118	0.126	0.134
Ph_2SnL_2	0.075	0. 101	0.115	0.127	0.137	0.148	0.157
Bu_2SnL_2	0.079	0.119	0.136	0.151	0.162	0.174	0.184
Me_2SnL_2	0.075	0.081	0.091	0.101	0.109	0.117	0.124

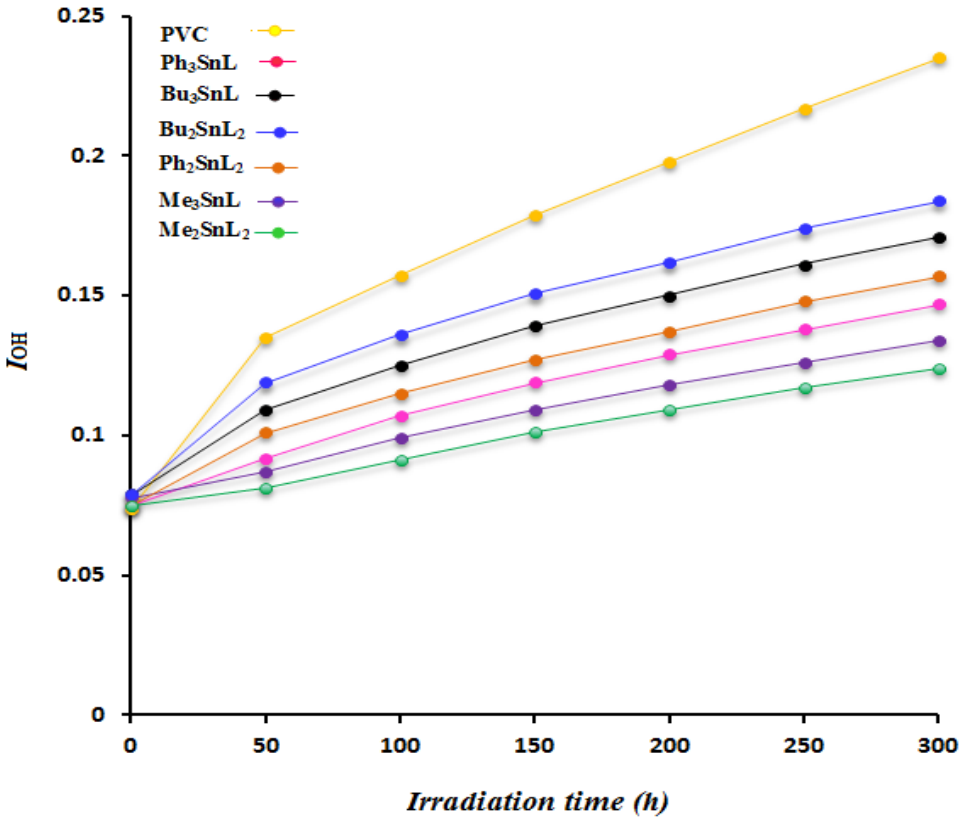

Figure 4.16 Effect of Irradiation on I_{OH} for PVC blank and Complexes Films.

Table 4.8 Carbonyl Index ($I_{C=O}$) with Irradiation Time for PVC Films containing 0.5% Stabilizers.

Compounds	Irradiation time (h)						
	0	50	100	150	200	250	300
PVC	0.875	1.531	1.971	2.353	2.582	2.750	2.881
Ph_3SnL	0.878	1.112	1.232	1.326	1.431	1.511	1.566
Bu_3SnL	0.877	1.291	1.442	1.578	1.681	1.745	1.798
Me_3SnL	0.871	1.171	1.293	1.398	1.494	1.569	1.628
Ph_2SnL_2	0.897	1.212	1. 384	1.498	1.597	1.681	1.733
Bu_2SnL_2	0.865	1.351	1. 521	1.642	1.742	1.812	1.869
Me_2SnL_2	0.843	1. 021	1.151	1.231	1.346	1.421	1.487

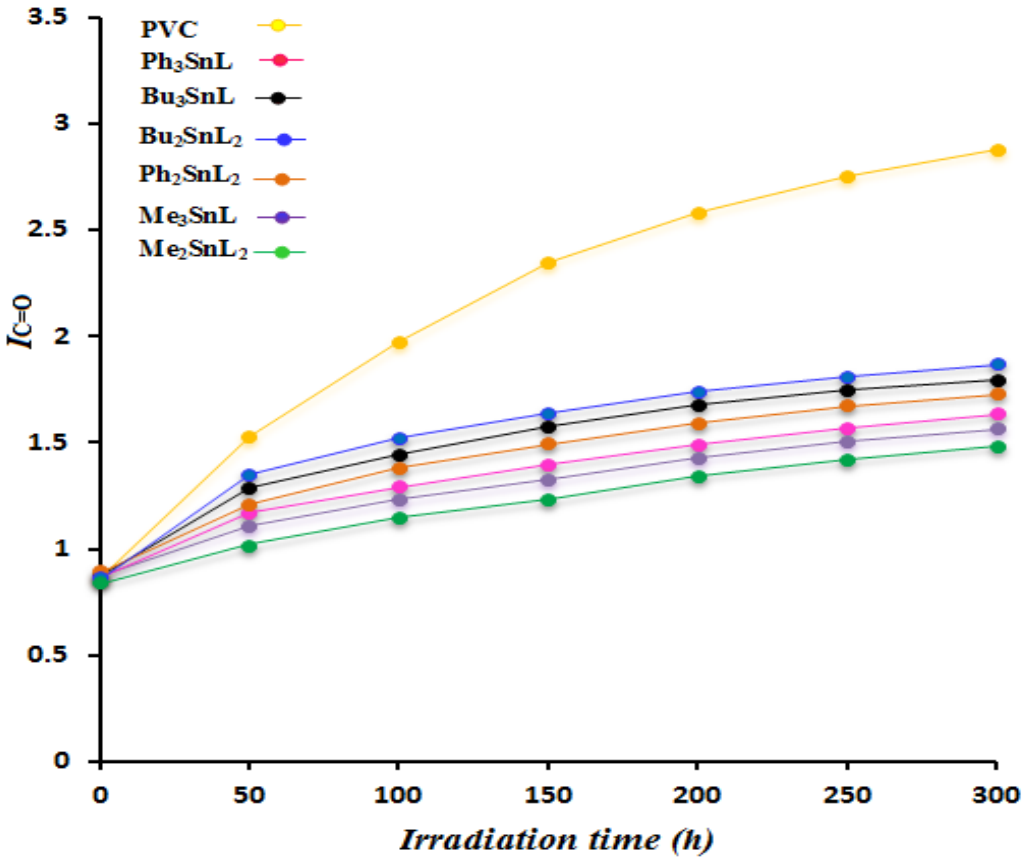

Figure 4.17 Effect of Irradiation on $I_{C=O}$ for PVC blank and Complexes Films.

Table 4.9 Polyene Index ($I_{C=C}$) with Irradiation Time for PVC Films containing 0.5% Stabilizers.

Compounds	Irradiation time(h)						
	0	50	100	150	200	250	300
PVC	0.177	0.289	0.381	0.466	0.532	0.595	0.649
Ph_3SnL	0.172	0.205	0.247	0.287	0.329	0.365	0.402
Bu_3SnL	0.178	0.245	0.301	0.349	0.396	0.441	0.483
Me_3SnL	0.177	0.198	0.227	0.265	0.301	0.334	0.367
Ph_2SnL_2	0.179	0.226	0.269	0.313	0.356	0. 399	0.441
Bu_2SnL_2	0.173	0.264	0.329	0.391	0.443	0.495	0.539
Me_2SnL_2	0.174	0.178	0.208	0.241	0.272	0.301	0.331

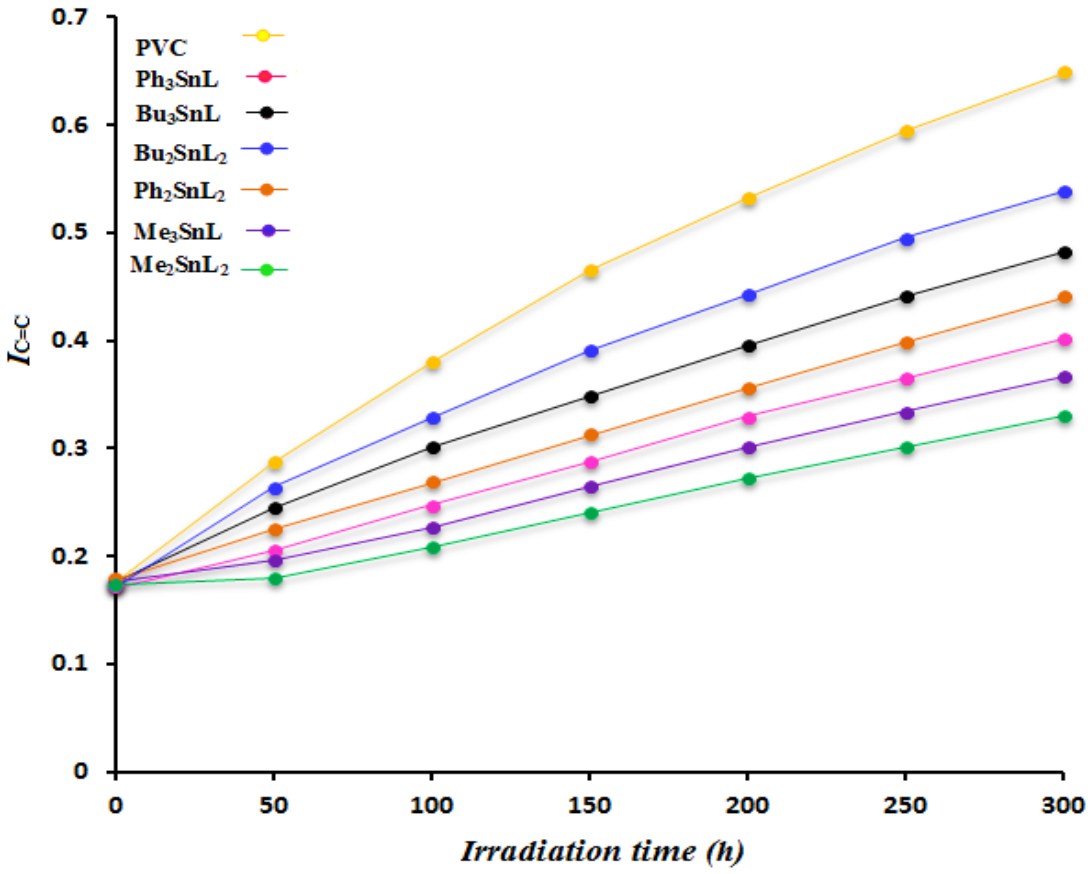

Figure 4.18 Effect of Irradiation on $I_{C=C}$ for PVC blank and Complexes Films.

4.5 Poly Vinyl Chloride Surface Morphological Study

4.5.1 Microscopic Analysis

Microscope can be used to provide useful information on the crystallinity, irregularities and defects that are present on the surface of polymers [182]. As a result, it may be employed to monitor the level of surface roughness as well as the appearance of black spots, cracks, and other forms of photodegradation-related damage in PVC. Before being exposed to ultraviolet radiation, optical microscope photographs of the poly (vinyl chloride) showed that it had a rather smooth surface, very few black spots and no visible cracks, as shown in Figs. 4.19 and 4.20 [183, 184]. Surface damage to poly (vinyl chloride) is most caused by the elimination of HCl. Films containing organotin (IV)-tyrosine complexes showed reduced surface damage because the tin atom helps in the scavenger of HCl, which in turn reduces the surface damage. After irradiation, the poly (vinyl chloride) with the Me_2SnL_2 complex had a smoother surface than the blank PVC.

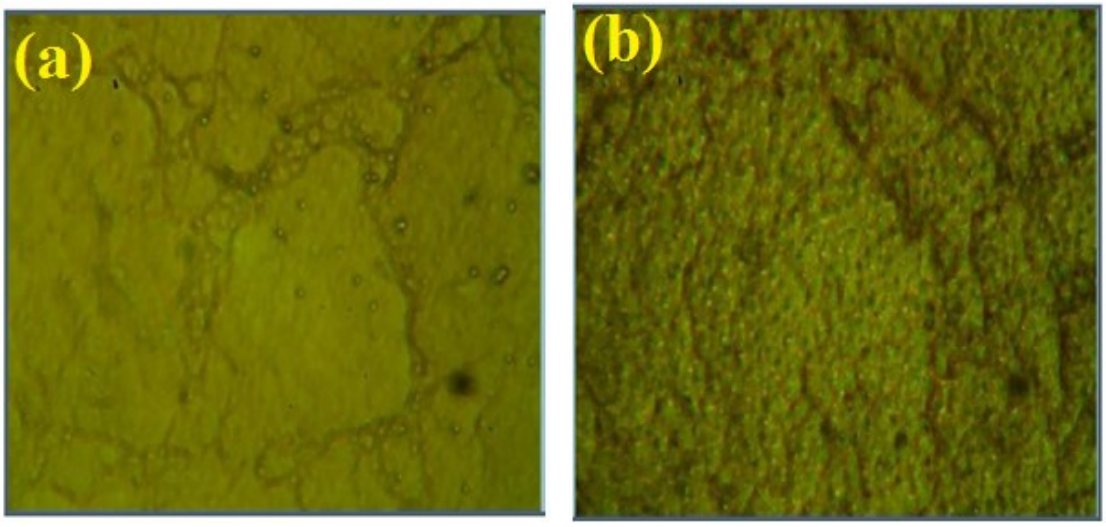

Figure 4.19 Microscope Images of PVC Films **(a)** before and **(b)** after irradiation at 300 h.

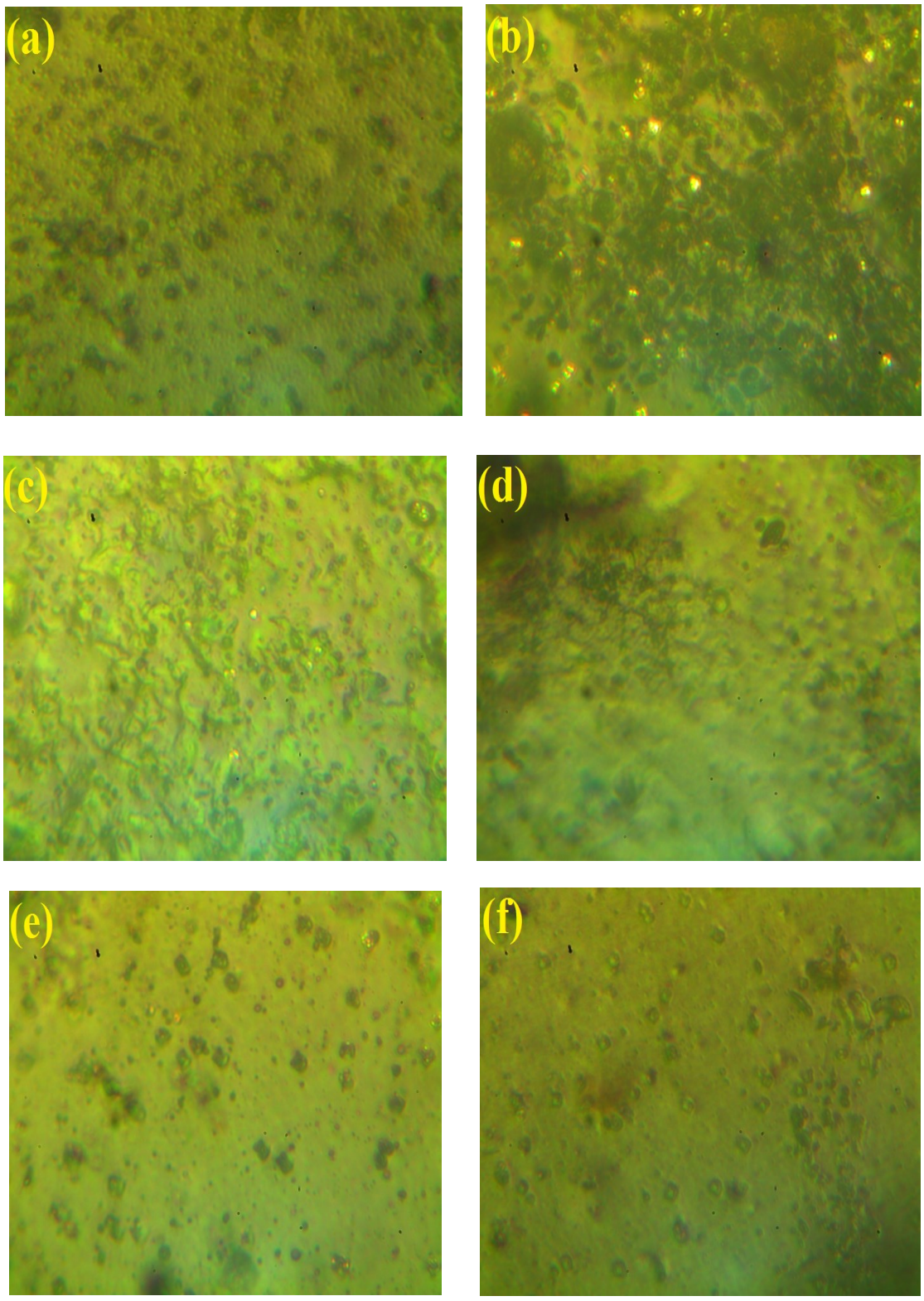

Figure 4.20 Microscope Images of PVC Films after Irradiation at 300 h in presence of **(a)** Ph_3SnL, **(b)** Bu_3SnL, **(c)** Me_3SnL, **(d)** Ph_2SnL_2, **(e)** Bu_2SnL_2 and **(f)** Me_2SnL_2 Complexes.

4.5.2 Atomic Force Microscopy (AFM)

The morphology of PVC films was investigated using the atomic force microscopy, which may produce two- and three-dimensional images of the films. Long-term irradiation causes bond breakage, resulting in a rough and cracked surface as illustrated in Figs.4.9, 4.21 and 4.22 [185, 186]. The roughness factor (R_q) for the surface of the irradiated PVC was usually high when compared to the values obtained for the films mixed [187, 188]. .as shown in Table 4.10. The roughness factor for the PVC blank was high after 300 hours of irradiation (R_q =316.2) compared to PVC containing the Me_2SnL_2 complex (R_q=70.5). Such an observation illustrates the critical function that stabilizers play in the stabilization of polymers after irradiation because of the harmless effect of ultraviolet due to aromatic conjugated resonance also because stabilizers that contain heteroatoms make polarized bonds with the polymeric chain of PVC.

Table 4.10 Roughness Factor (R_q) for PVC without and presence of Complexes after 300 h Irradiation.

PVC Film with Photo Irradiation (300 h)	Rq
PVC	316.2
PVC+Ph_3SnL	85.1
PVC+Bu_3SnL	91.8
PVC+Me_3SnL	72.3
PVC+Ph_2SnL_2	85.7
PVC+Bu_2SnL_2	89.4
PVC+Me_2SnL_2	70.5

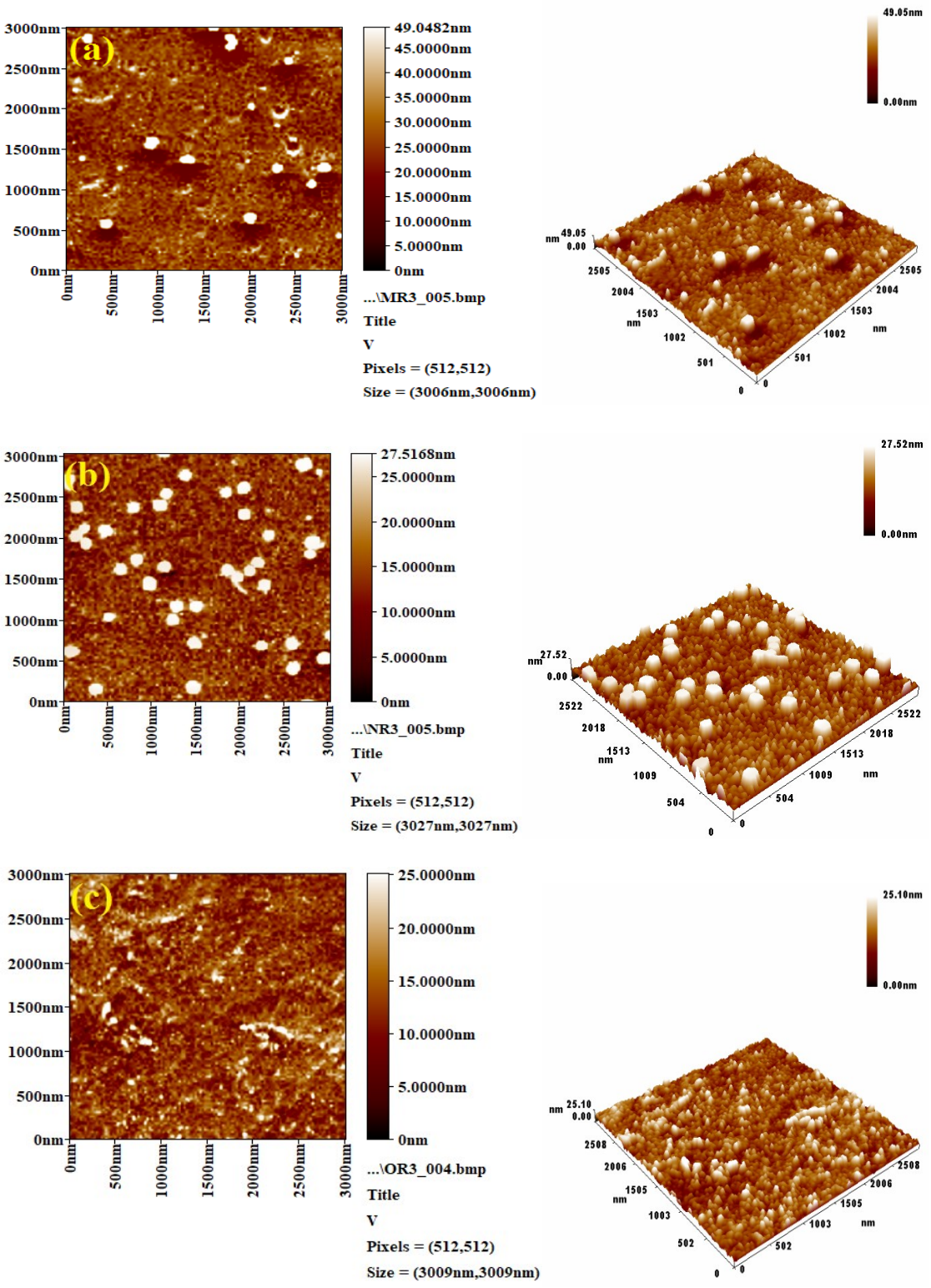

Figure 4.21 Two and Three dimensions AFM Images of PVC in presence of (a) Ph_3SnL, (b) Bu_3SnL and (c) Me_3SnL Complexes after Irradiation at 300 h.

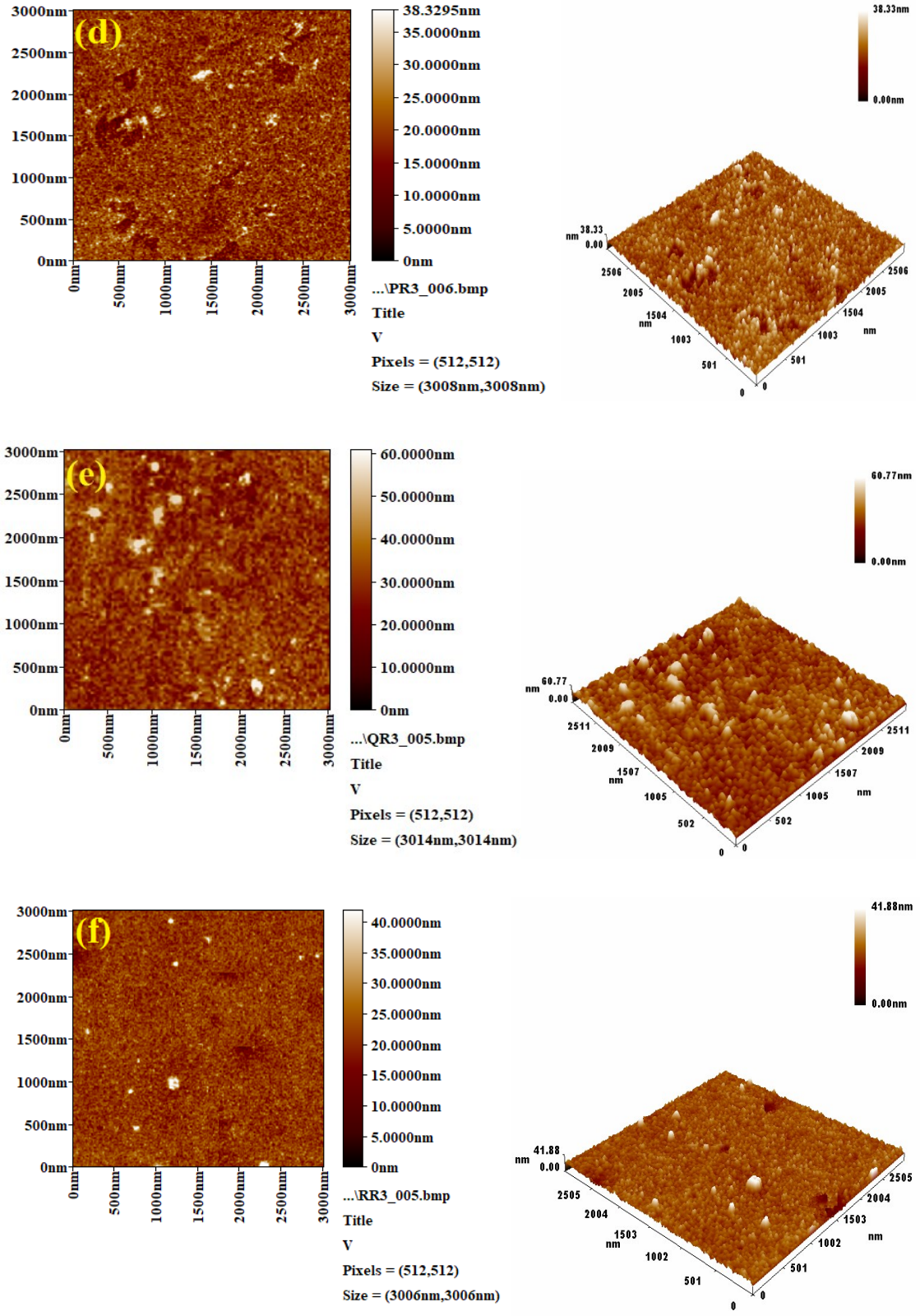

Figure 4.22 Two and Three dimensions AFM Images of PVC in presence of (d) Ph_2SnL_2, (e) Bu_2SnL_2 and (f) Me_2SnL_2 Complexes after Irradiation at 300 h.

4.5.3 Scanning Electron Microscope

Surface characterization by scanning electron microscopy (SEM) [189] was performed on irradiation pure poly (vinyl chloride) and mixes. When not exposed to irradiation, on the surface of the pure PVC film, there were no white spots or grooves, and the surface was regularly smooth. On the other hand, images obtained using scanning electron microscopy of irradiated pure PVC exhibited significant irregularities such as white spots, grooves, and lumps, all of which are suggestive of considerable photodegradation [190, 191]. As shown in Fig.4.11and Figs. 2.23–2.25. Irradiation improved the surface smoothness and reduced the number of cracks in the PVC containing the organotin (IV)-tyrosine complexes compared to the blank poly (vinyl chloride). loss of hydrogen chloride and other unstable degradation chemicals may contribute to the development of such cracks. The poly (vinyl chloride) films containing the Me_2SnL_2 complex were clearly the least damaged and rough on the surface.

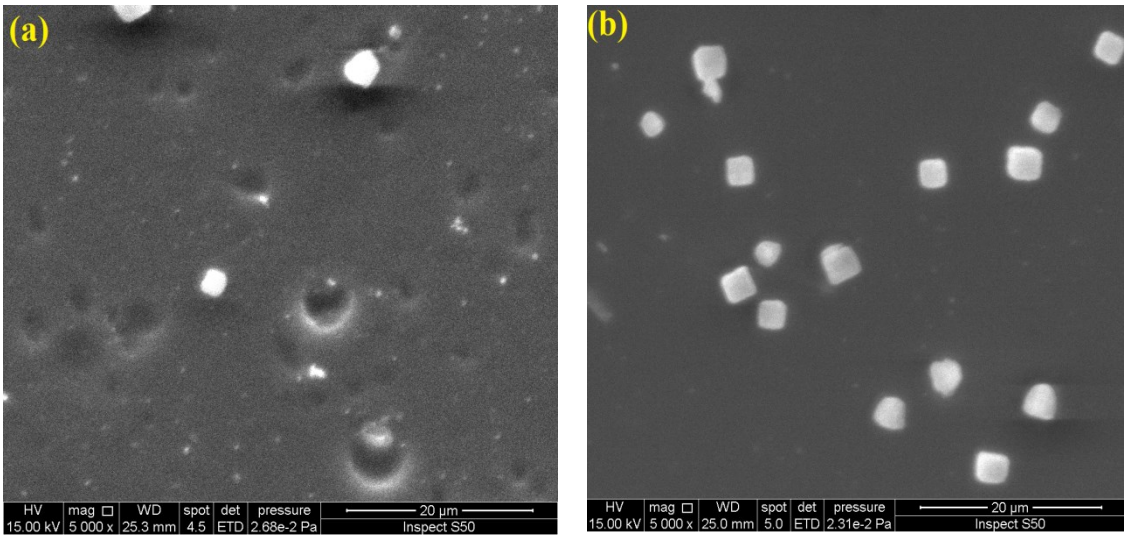

Figure 4.23 SEM Images for PVC in presence of (a) Ph_3SnL, (b) Bu_3SnLComplexes.

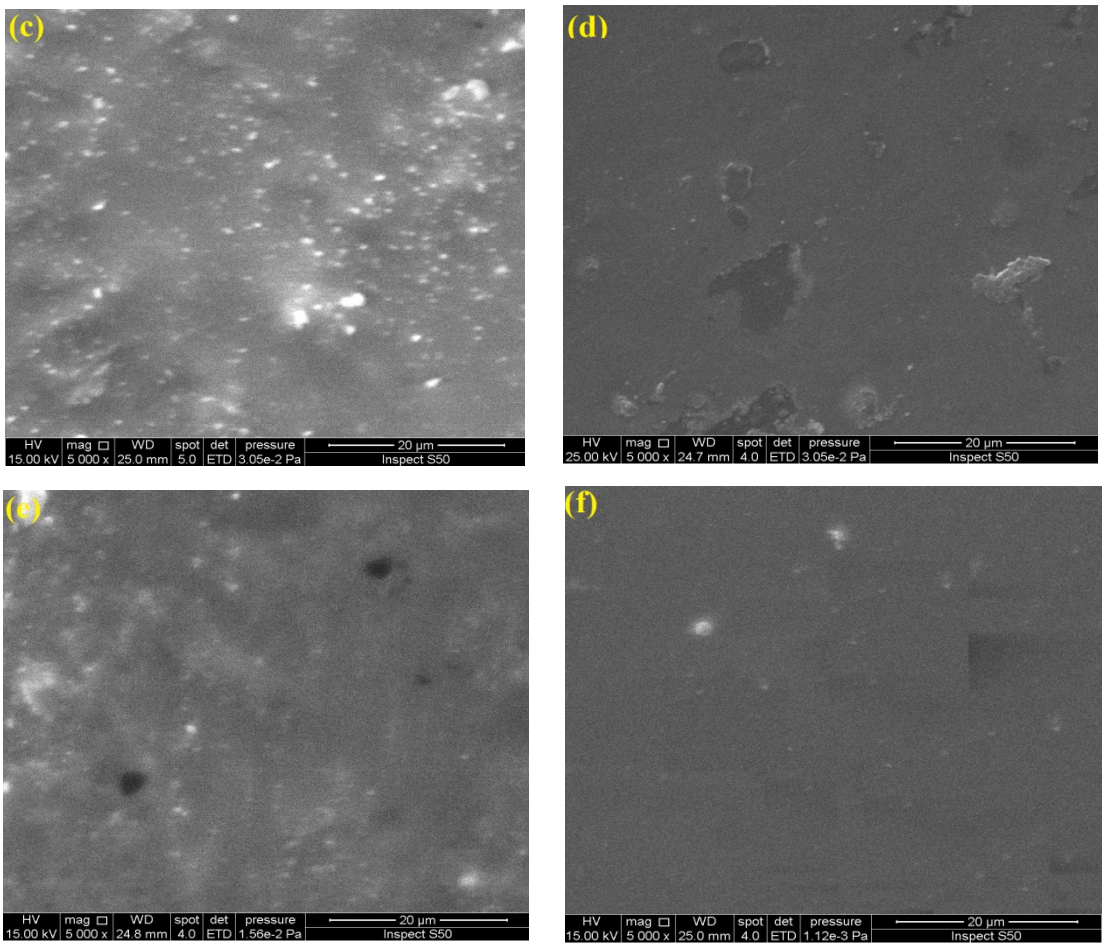

Figure 4.24 SEM Images for PVC in presence of (c) Me_3SnL, (d) Ph_2SnL_2, (e) Bu_2SnL_2 and (f) Me_2SnL_2 Complexes.

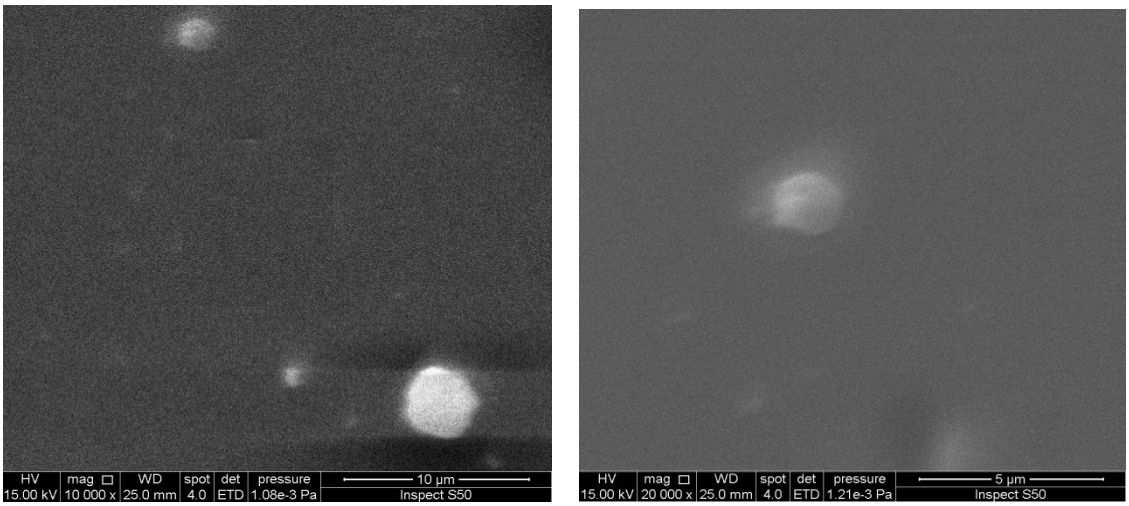

Figure 4.25 SEM Images for PVC in presence of Me_2SnL_2 in Scale 5 and 10 µm.

4.6 Proposed Mechanisms for Organotin (IV)-Tyrosine Complexes' Photostabilization of Poly(vinyl Chloride)

PVC is stabilized in many ways by organotin (IV)-tyrosine complexes, including by absorbing UV radiation and scavenging free radicals. as in Scheme 4.5. Among the compounds that stabilized PVC, dimethyl tin (IV) exhibits the most effective photostabilization [192].

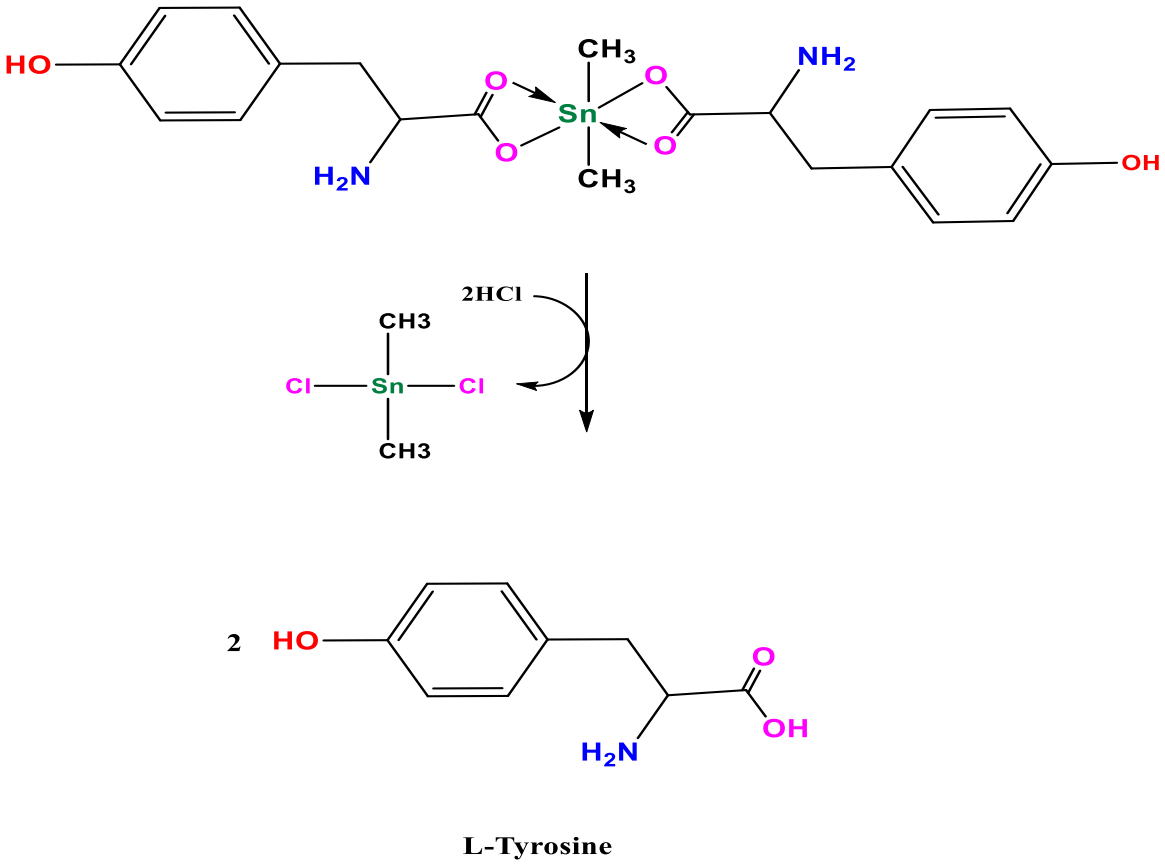

Scheme 4.5 Dimethyltin (IV) -Tyrosine Complex as HCl Scavengers.

Hydroperoxides are famous for having a detrimental effect on PVC chains, which results in photooxidation [193].

Because the produced organotin (IV) compounds may decompose hydroperoxides, they can shield PVC films from photooxidation as in scheme 4.6.

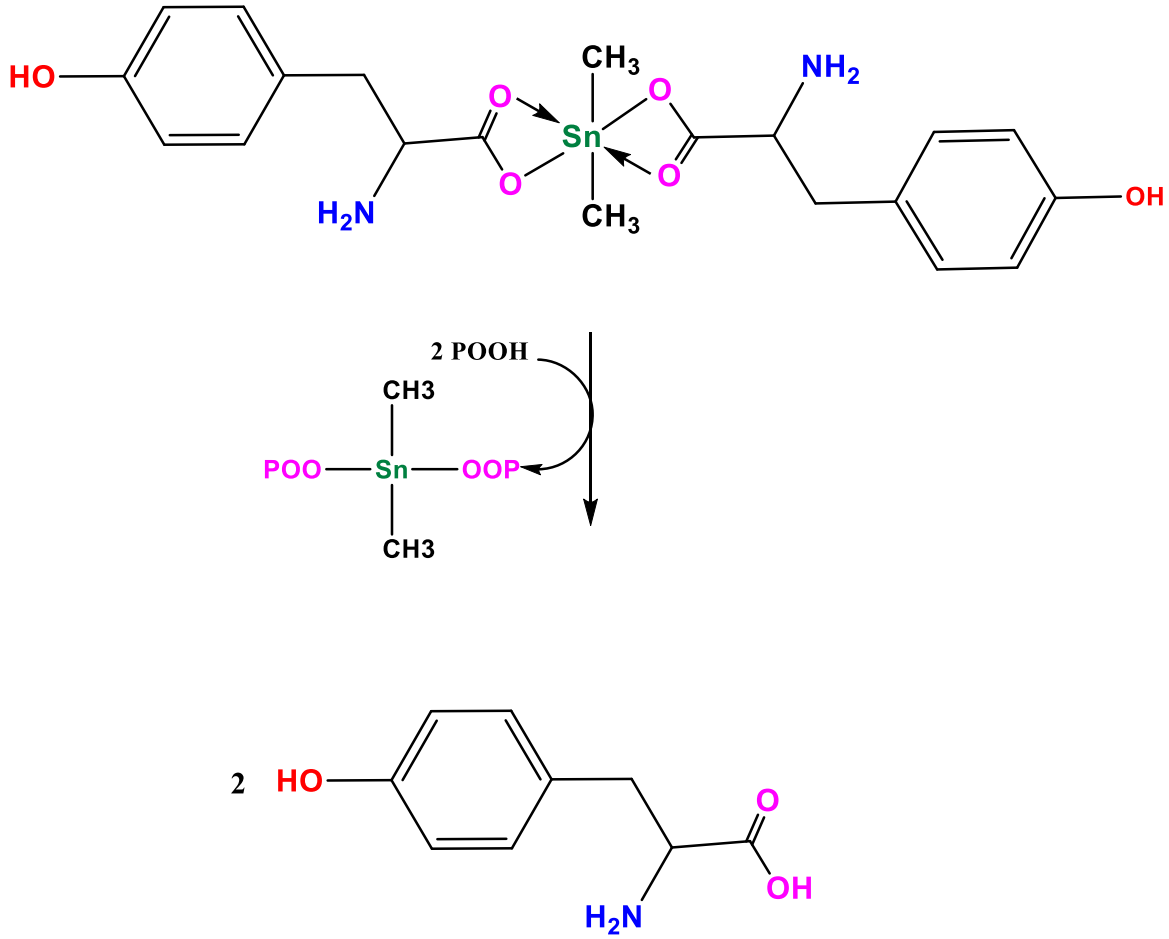

L-Tyrosine

Scheme 4.6 Dimethyltin (IV) -Tyrosine Complex Acting as a Peroxide Decomposer.

In the presence of organotin (IV) complexes could function as radical scavengers [194].

The polymeric proxy radicals POO· interact with dimethyl tin (IV) complexes [195]. Scheme 4.7 to create stable complexes. Through the resonance of aryl groups, the effect of the absorbed energy may be neutralized and distributed over a vast number of atoms.

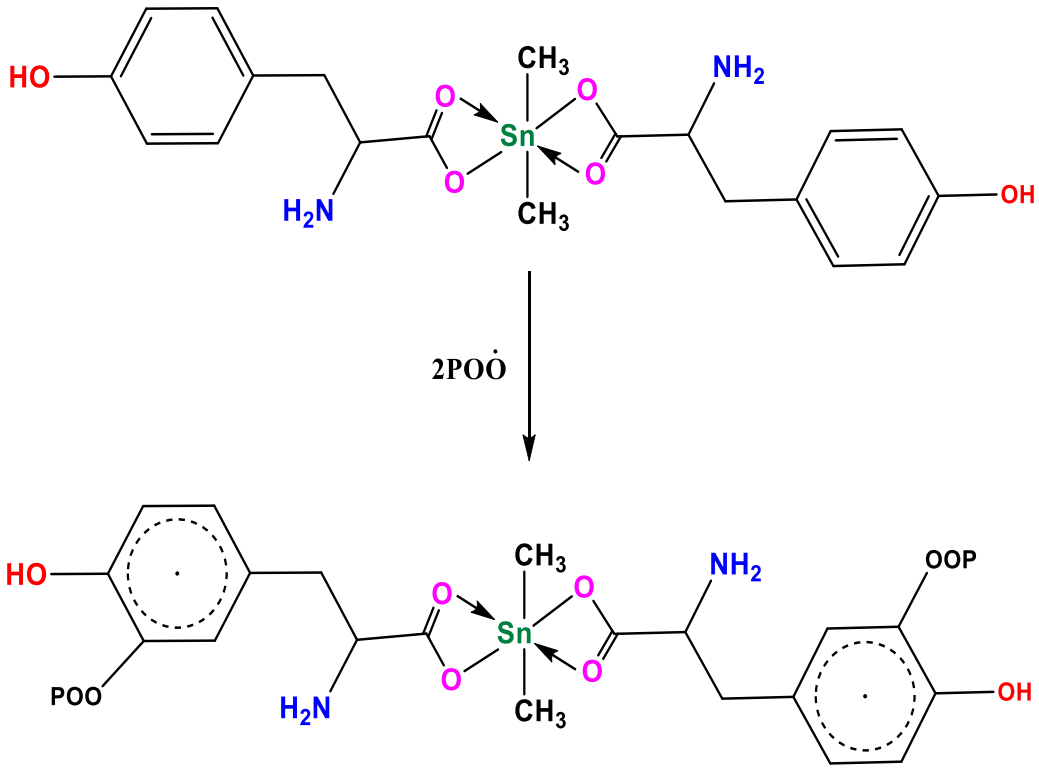

Scheme 4.7 Dimethyltin (IV) -Tyrosine complexes as radical scavengers.

The polarized N and O atoms of the amine, hydroxyl, and carboxylate moieties of the organotin (IV) complexes with carbons of the C-Cl bonds in PVC may coordinate to stabilize the polymeric materials, as explained in Scheme 4.8. This coordination makes it easier for the excited-state energy to be converted into a stable level in the polymeric chains [196, 197].

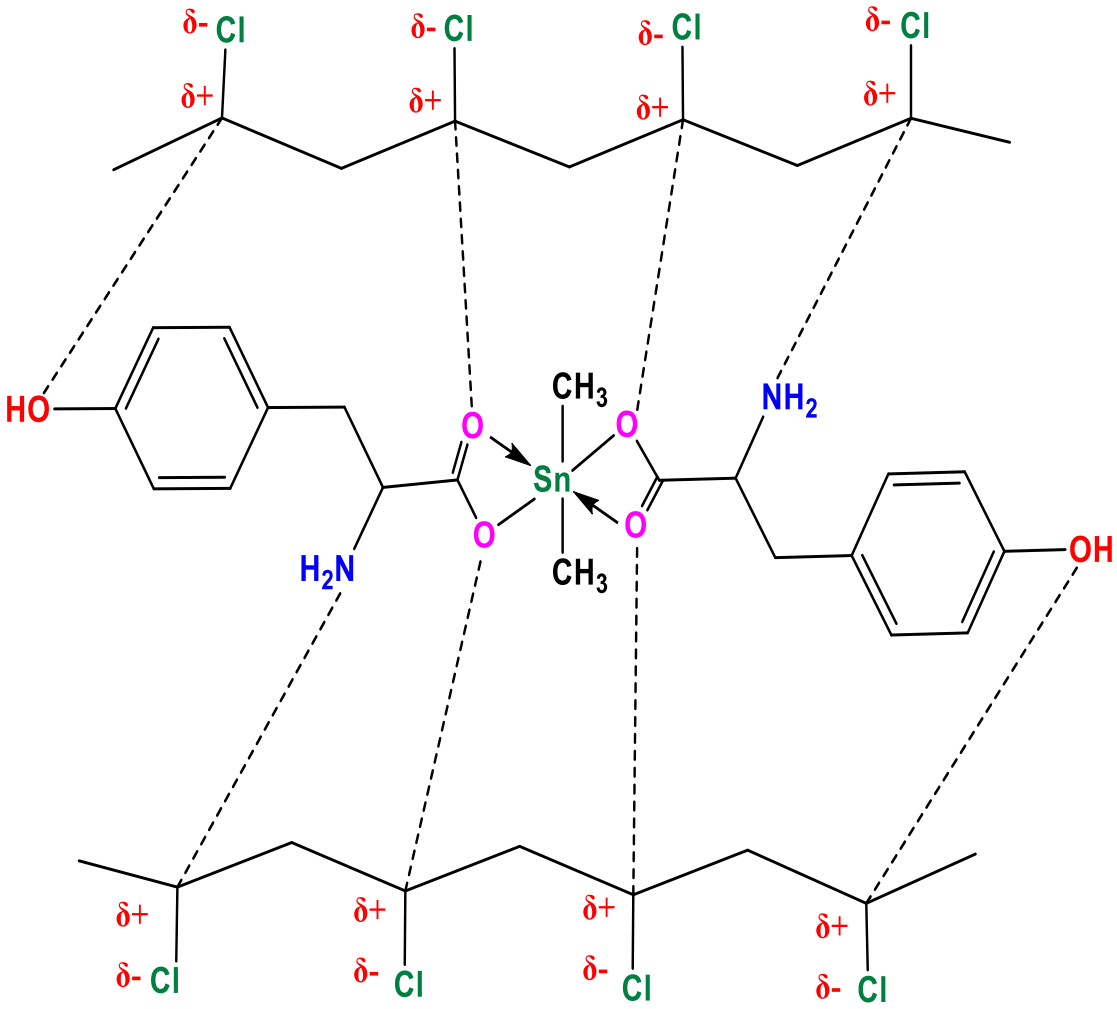

Scheme 4.8 Polarized bond between Dimethyl tin (IV) -Tyrosine Complexes and poly (vinyl chloride).

4.7 Determination of Antioxidant Activity of Organotin (IV) - Cephalexin Complexes

Several techniques, including 2, 2 -diphenyl-1-picrylhydrazyl (DPPH) and CUPRAC, can be used to determine whether cephalexin and its complexes have antioxidant activity [198].

4.7.1 DPPH Radical Scavenging Method

The most used approach for determining antioxidant activity was the DPPH method because it was fast, simple required a small sample and was sensitive enough to estimate the antioxidant activity of substances [199]. The organotin (IV)-cephalexin complexes were prepared at a concentration of 50 µg/ml then tested at intervals of 5, 10 and 15 minutes with the absorbance measured at λ_{max}= 490 nm. The % inhibition was calculated and the relationship between % inhibition and time was plotted to identify the best complexes given high inhibition by apply equation 2.4 [200]. As shown in Table 4.11 and Fig. 4.26. Organotin (IV) cephalexin complexes exhibit greater antioxidant activity than a ligand against the stable free radical DPPH because of the metal moiety present in the complexes [201, 202].

Table 4.11 The Results of the DPPH Method for Measuring the Antioxidant Activity of Ligand and their Complexes at different Times.

Control Absorbance = 0.378 λ = 490 nm						
Compounds	After Time 5 min		After Time 10 min		After Time 15 min	
	Sample Abs.	% Inhibition	Sample Abs.	% Inhibition	Sample Abs.	% Inhibition
Cephalexin	0.236	37.566	0.233	38.360	0.231	38.889
Ph_3Sn L	0.188	50.265	0.187	50.529	0.185	51.058
Bu_3Sn L	0.179	52.646	0.176	53.439	0.174	53.968
Me_3Sn L	0.169	55.291	0.168	55.556	0.166	56.085
Ph_2SnL_2	0.220	41.799	0.221	41.534	0.219	42.063
Bu_2SnL_2	0.201	46.825	0.199	47.354	0.198	47.619
Me_2SnL_2	0.211	44.180	0.207	45.238	0.205	45.767
Tannic acid	0.168	55.556	0.164	56.614	0.161	57.407

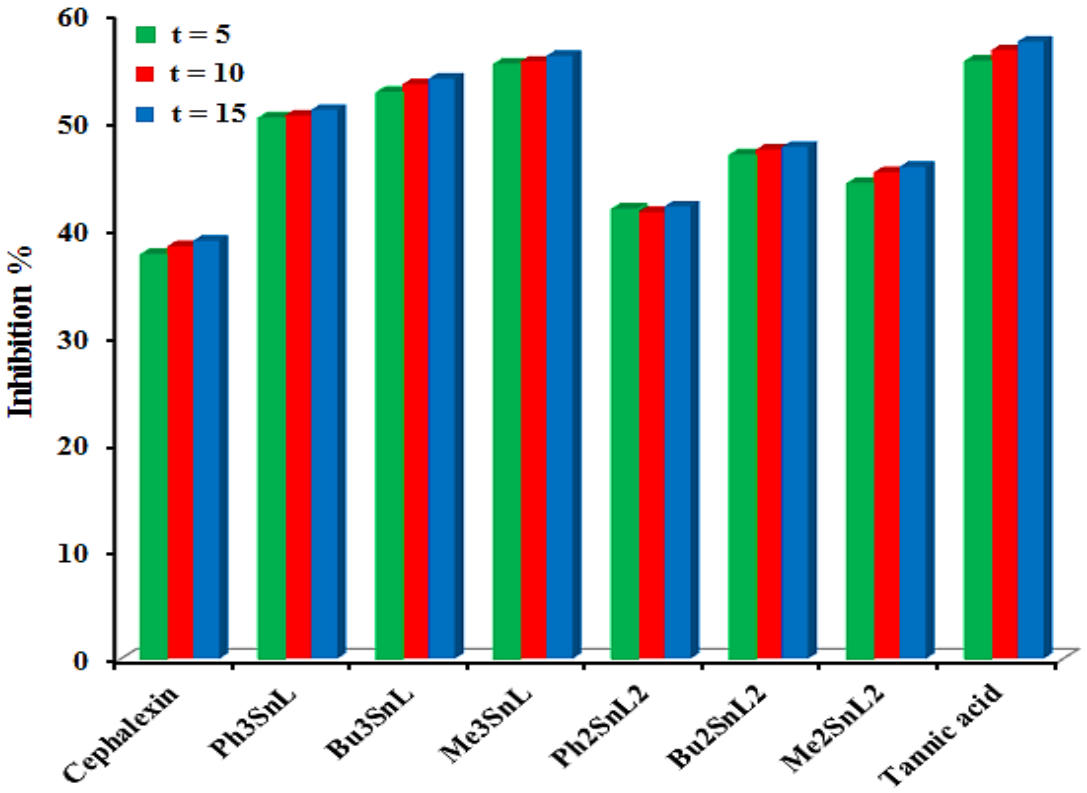

Figure 4.26 DPPH Assay for Cephalexin and its Complexes at Times 5, 10 and 15 min.

From the results in Table 4.11. The time factor does not significantly affect the inhibition ratio. The complexes Me_3SnL, Bu_3SnL and Ph_3SnL had higher scavenging percentages than the other complexes. The absorbance at the same maximum wavelength was measured for complexes prepared at concentrations of 25, 50 and 75 µg/ml; The best concentration that gave high inhibition was 50 µg/mL due to given highest percentage of inhibition. The complexes reduces DPPH, which has an unpaired valence electron at one nitrogen atom in the bridge [203]. At the same time, the % inhibition of complexes less activity than tannic acid (reference antioxidant). As shown in Fig. 4.27 and Tables 4.12 and 4.13.

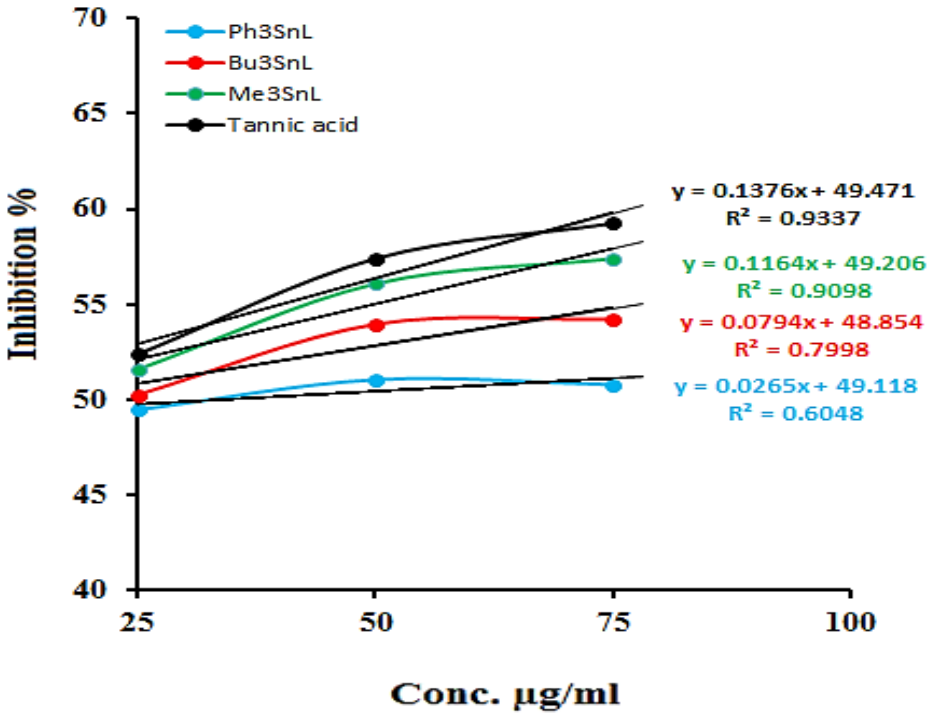

Figure 4.27 The Standard Calibration Curve of Organotin (IV)-Cephalexin Complexes and Tannic Acid.

Table 4.12 The Results of Absorbance at different Concentrations for Organotin (IV) - Cephalexin Complexes and Tannic acid.

Concentration (µg/mL)	Control Absorbance = 0.378 λ = 490 nm			
	Absorbance at different Concentration			
	Ph_3SnL	Bu_3SnL	Me_3SnL	Tannic acid
25 (µg/ml)	0.191	0.188	0.183	0.180
50 (µg/ml)	0.185	0.174	0.161	0.161
75 (µg/ml)	0.186	0.173	0.166	0.154

Table 4.13 The Results of % Inhibition at different Concentrations for Organotin (IV) - Cephalexin Complexes and Tannic acid.

Concentration (µg/mL)	% Inhibition			
	Ph_3SnL	Bu_3SnL	Me_3SnL	Tannic acid
25 (µg/ml)	49.471	50.265	51.587	52.381
50 (µg/ml)	51.058	53.968	57.407	57.407
75 (µg/ml)	50.794	54.233	56.085	59.259

4.7.1.1 Inhibitory Concentration Value 50% (IC_{50})

The IC_{50} (inhibitory concentration 50%) formula is used to determine radical capture activity. This number is the test compound concentration that can inhibit the DPPH oxidation process by 50%. The IC_{50} of samples was determined using the linear regression equation showed in Fig. 4.27. The percentage of inhibition was shown on the y-axis and the sample concentration on the x-axis [204]. From the equation **y = bx + a**, the value of IC_{50} was calculated using equation (4.4).

$$IC_{50} = \frac{50-a}{b} \quad \text{..... (4.4)}$$

Where **a** = Intercept

b = Slope

Table 4.14 shows the IC_{50} values and linear regression for complexes and tannic acid. As a result, the complex Me_3SnL classified as very strong antioxidant, While Bu_3SnL and Ph_3SnL were designated as active antioxidants. This is based on the classification proposed by Phongpaichit et al. Very active antioxidants have an IC_{50} value of less than 10 µg/mL, active antioxidants have an IC_{50} value between 10-50 µg/mL, moderate antioxidants have an IC_{50} value between 100-150 µg/mL, weak antioxidants have an IC_{50} value between 150-200 µg/mL and extremely weak antioxidants have an IC_{50} value greater than 200 µg/mL [205,206].

Table 4.14 Shows the IC_{50} Values and Linear Regression of Organotin (IV)-Cephalexin Complexes and Tannic acid.

Complexes	Linear Regression Equation	IC_{50} (µg/mL)
Me_3SnL	y = 0.1164x + 49.206 R^2 = 0.9098	6.821
Bu_3SnL	y = 0.0794x + 48.854 R^2 = 0.7998	14.433
Ph_3SnL	y = 0.0265x + 49.118 R^2 = 0.6048	33.283
Tannic acid	y = 0.1376x + 49.471 R^2 = 0.9337	3.844

4.7.2 Cuprac Activity Assay

Evaluation antioxidant capacity using the CUPRAC method is easy and flexible [207]. Bis(neocuproine) copper (II) cation (Cu (II)-Nc), which operated as an outer-sphere electron transfer agent, was the CUPRAC chromogenic oxidation reagent, and the CUPRAC chromophore was bis(neocuproine) copper (I) cation (Cu(I)-Nc), which was created by reducing this reagent with antioxidants equation (4.5). The CUPRAC reagent is most efficient at a pH of 7, and the absorbance of the Cu (I)-chelate formed in the redox reaction with reducing organotin (IV) complexes was measured at 450 nm for Cu (I)-Nc spectra [208].

n Cu $(Nc)_2^{2+}$ + n-electron reductant (AO) ↔ n Cu $(Nc)_2^{+}$ + n-electron oxidized product + n H^+ …… (4.5)

All complexes, ligand and tannic acid were measured for absorbance at a concentration of 20 µg/ml and a maximum wavelength of 450 nm. Using the following formula, the inhibition ratio (%) was determined: Inhibition ratio (%) = 100 $[(A_o - A)/A_o]$, where A_o and A were the absorbance in the absence and presence of scavengers, respectively [209].

Table 4.15 Results of Absorbance and % Inhibition at Concentration 20 µg/ml for Cephalexin, Complexes and Tannic acid.

Control Absorbance = 0.238		λ = 450 nm
Complexes	Absorbance at Concentration 20 µg/ml	% Inhibition
Cephalexin	0.171	28.151
Ph_3SnL	0.143	39.916
Bu_3SnL	0.138	42.017
Me_3SnL	0.128	46.218
Ph_2SnL_2	0.159	33.193
Bu_2SnL_2	0.161	32.353
Me_2SnL_2	0.153	35.714
Tannic acid	0.117	50.840

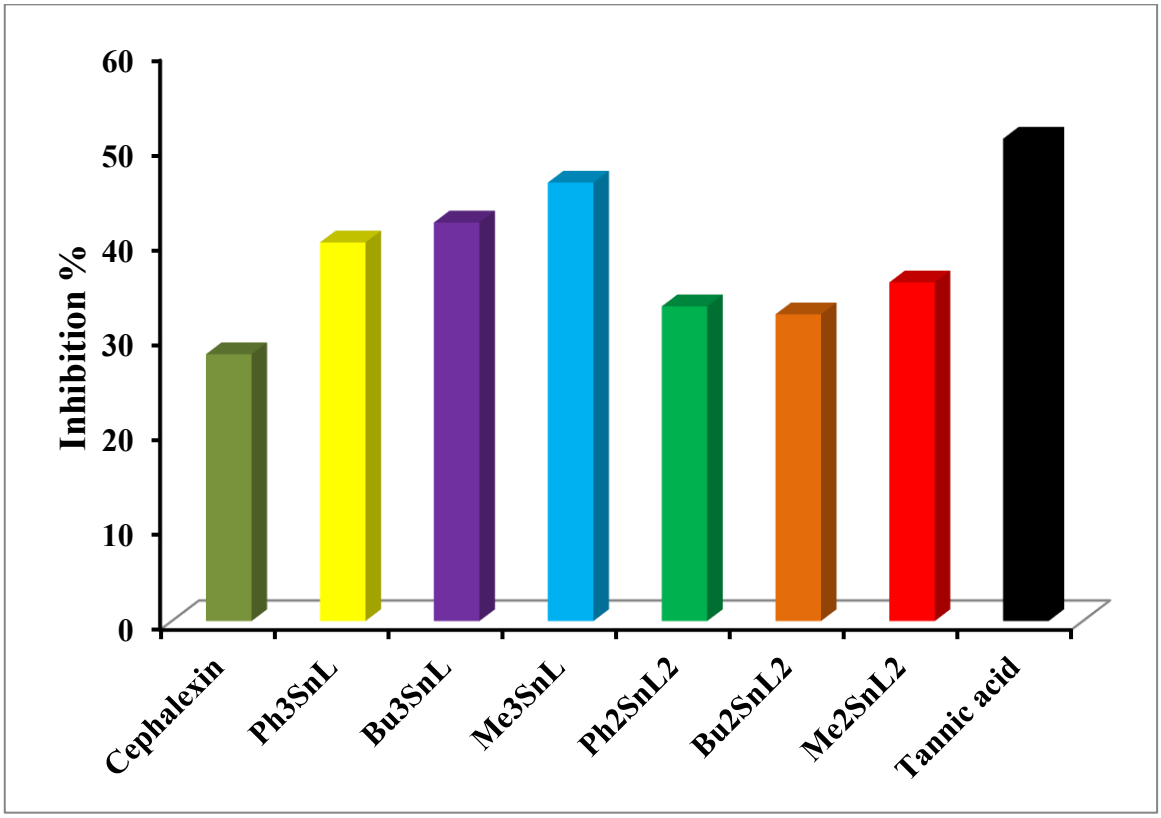

Figure 4.28 CUPRAC Assay at Concentration 20 µg/ml for Cephalexin, Complexes and Tannic Acid.

From precedent data in Table 4.15 and Fig. 4.28, it was clearly demonstrated that complexes Me_3SnL, Bu_3SnL, Ph_3SnL and Me_2SnL_2 have higher antioxidant activity than ligands and other complexes. Then the absorbance and inhibition ratio were measured at different concentrations of 20, 40 and 60 µg/ml as shown in Tables 4.16 and 4.17. The best concentration that gave high inhibition was 40 µg/mL.

Table 4.16 Results of Absorbance at different Concentration of Complexes and Tannic Acid.

Control Absorbance = 0.238 λ = 450 nm			
Complexes	Absorbance at different Concentration		
	20 µg/ml	40 µg/ml	60 µg/ml
Ph_3SnL	0.143	0.138	0.137
Bu_3SnL	0.138	0.129	0.127
Me_3SnL	0.128	0.116	0.117
Me_2SnL_2	0.153	0.143	0.144
Tannic acid	0.117	0.108	0.109

Table 4.17 Results of % Inhibition at different Concentration of Complexes and Tannic Acid.

Control Absorbance = 0.238 λ = 450 nm			
Complexes	% Inhibition at different Concentration		
	20 µg/ml	40 µg/ml	60 µg/ml
Ph_3SnL	39.916	42.017	42.437
Bu_3SnL	42.017	45.798	46.639
Me_3SnL	46.218	51.261	50.840
Me_2SnL_2	35.714	39.916	39.496
Tannic acid	50.840	54.622	54.202

The slope - intercept values of linear calibration curves are measured by plotting the relation between % inhibition and concentrations, as shown in Fig. 4.29.

The IC_{50} values of all substances in comparison to tannic acid were calculated using the linear regression equation in the calibration curve shown in Table 4.18.

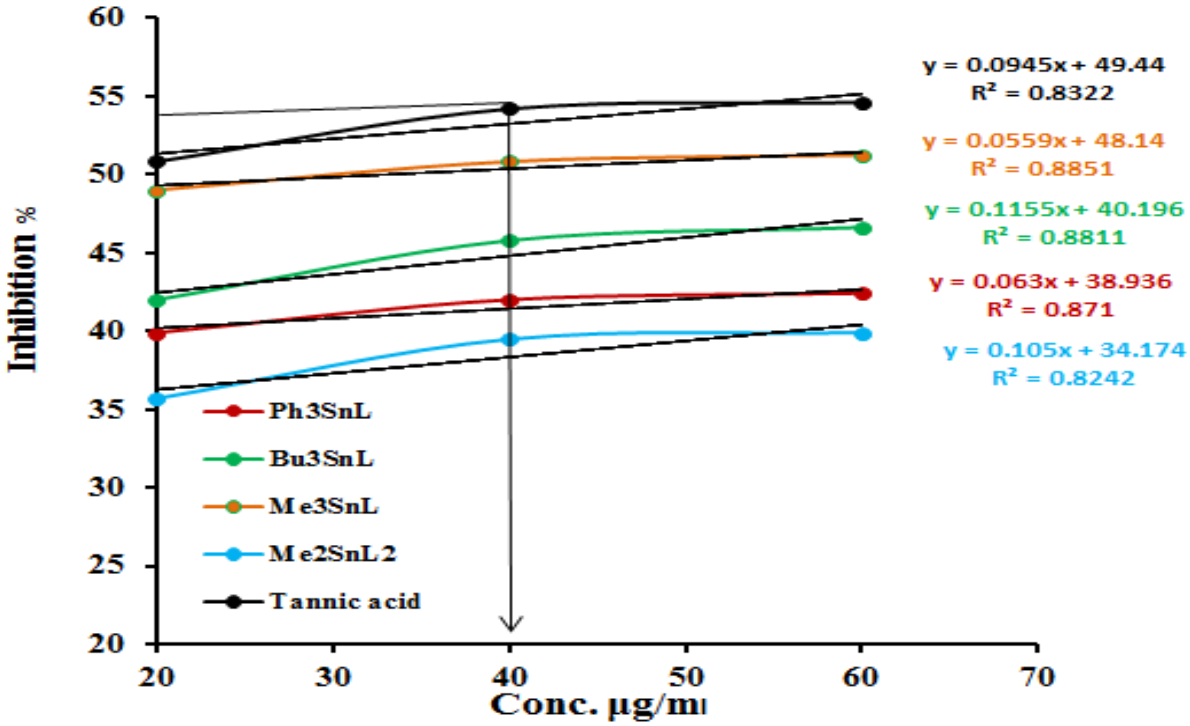

Figure 4.29 The Standard Calibration curve of Organotin (IV)-Cephalexin Complexes and Tannic Acid.

Table 4.18 Shows the IC_{50} Values and Linear Regression of Organotin (IV)-Cephalexin Complexes and Tannic acid.

Complexes	Linear Regression Equation	IC_{50} (µg/mL)
Ph_3SnL	y = 0.063x + 38.936 R^2 = 0.871	175.619
Bu_3SnL	y = 0.1155x + 40.196 R^2 = 0.8811	84.883
Me_3SnL	y = 0.0559x + 48.14 R^2 = 0.8851	33.273
Me_2SnL_2	y = 0.105x + 34.174 R^2 = 0.8242	150.723
Tannic acid	y = 0.0945x + 49.44 R^2 = 0.8322	5.925

The complex Me_3SnL was categorized as active antioxidants based on their values of IC_{50}, whereas Bu_3SnL exhibit moderate antioxidant activity while the complexes Ph_3SnL and Me_2SnL_2 were classified as weak antioxidants. However, the high antioxidant activity was shown by the low IC_{50} value [210]. However, the reported IC_{50} values of the complexes remained lower than those of tannic acid (reference antioxidant), which has an IC_{50} of 5.925 µg/mL.

4.8 Determination of Antioxidant Activity of Organotin (IV) -Tyrosine Complexes

To assess the antioxidant activity of tyrosine and the complexes it produces, two methods were used: 2, 2 -diphenyl-1-picrylhydrazyl (DPPH) and the CUPRAC assay.

4.8.1 DPPH Radical Scavenging Method

The organotin (IV) complexes to be evaluated were dissolved in methanol at a concentration of 50 µg/ml in each test solution and the absorbance was measured in a micro plate reader at a maximum wavelength of 490 nm after 5, 10 and 15 minutes. As shown in Table 4.19 and Fig. 4.30. Equation (2.4) was used to calculate antioxidant activity as the percentage of inhibition against DPPH. then plot the relation between the percentage of inhibition and time to identify the best complexes gives high inhibition. Due to the presence of the metal moiety, which increases their activity, organotin (IV) tyrosine complexes have higher antioxidant activity than a ligand [211].

Table 4.19 The Results for Evaluating the Antioxidant Activity of Tyrosine and its Complexes at Different Times.

Control Absorbance = 0.378			λ = 490 nm			
Compounds	**After Time 5 min**		**After Time 10 min**		**After Time 15 min**	
	Sample Abs.	**% Inhibition**	**Sample Abs.**	**% Inhibition**	**Sample Abs.**	**% Inhibition**
L-Tyrosine	0.298	21.16402	0.085	22.48677	0.291	23.016
Ph_3Sn L	0.261	30.95238	0.119	31.48148	0.257	32.011
Bu_3Sn L	0.209	44.70899	0.174	46.03175	0.201	46.825
Me_3Sn L	0.173	54.2328	0.208	55.02646	0.169	55.291
Ph_2SnL_2	0.229	39.41799	0.153	40.47619	0.221	41.534
Bu_2SnL_2	0.223	41.00529	0.158	41.79894	0.217	42.593
Me_2SnL_2	0.219	42.06349	0.164	43.38624	0.211	44.180

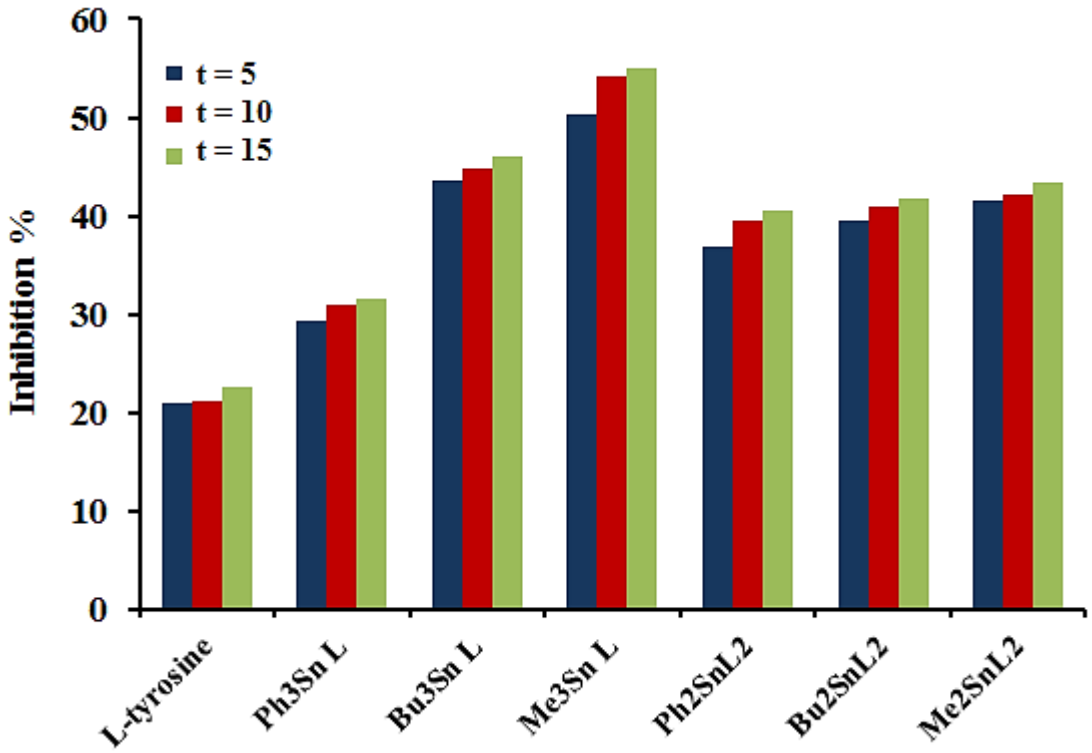

Figure 4.30 DPPH Assay for Tyrosine and its Complexes at Times 5, 10 and 15 min.

The scavenging percentages of the complexes Me_3SnL, Bu_3SnL and Me_2SnL_2 were higher than those of the other complexes and ligand (Tyrosine). Various concentrations of 25, 50 and 75 µg/ml were used to plot the concentration of these complexes against the percentage of inhibition. The optimal concentration was 50 µg/ml, due result high inhibition as in Tables 4.20, 4.21 and Fig. 4.31, tannic acid chosen as the reference antioxidant component has a higher percentage of scavenging than organotin (IV)-tyrosine complexes.

Table 4.20 The Results of Absorbance at different Concentrations for Organotin (IV) - Tyrosine Complexes and Tannic acid.

Concentration (µg/mL)	Control Absorbance = 0.378 λ = 490 nm			
	Absorbance at different Concentration			
	Me_3SnL	Bu_3SnL	Me_2SnL_2	Tannic acid
25 (µg/ml)	0.188	0.213	0.221	0.183
50 (µg/ml)	0.166	0.201	0.208	0.158
75 (µg/ml)	0.169	0.199	0.211	0.159

Table 4.21 The Result of Percentage Inhibition for Organotin (IV)-Tyrosine Complexes and Tannic Acid.

Concentration (µg/mL)	% Inhibition			
	Me_3SnL	Bu_3SnL	Me_2SnL_2	Tannic acid
25 (µg/ml)	50.265	43.651	41.534	51.587
50 (µg/ml)	56.085	46.825	44.974	58.201
75 (µg/ml)	55.291	47.354	44.180	57.937

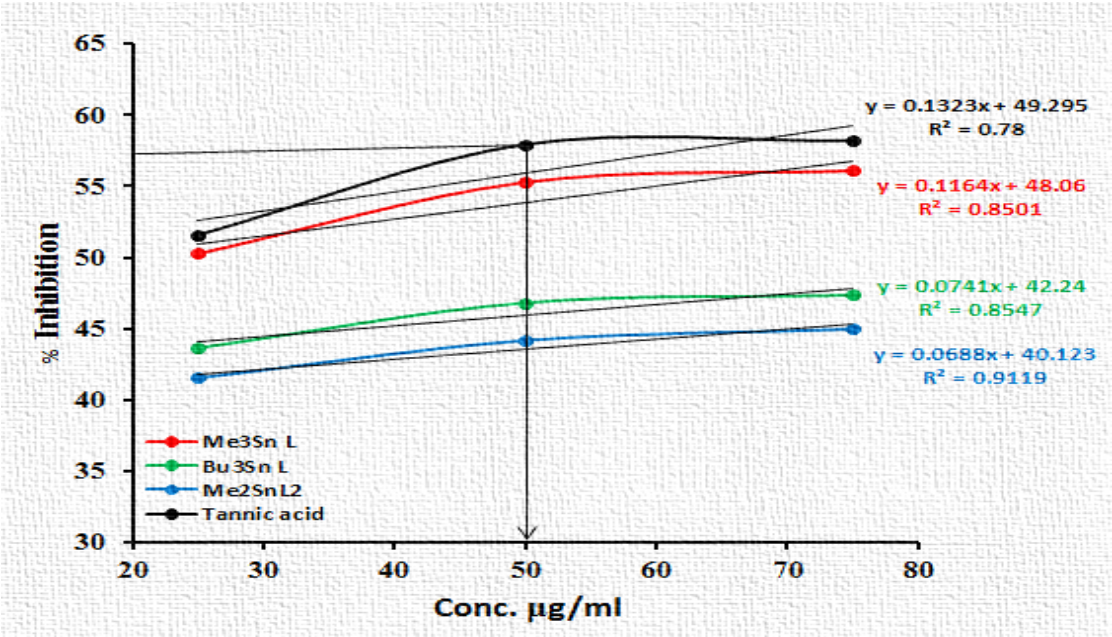

Figure 4.31 The Standard Calibration Curve of Organotin (IV)-Tyrosine Complexes and Tannic Acid.

The IC_{50} values can estimate from linear regression in calibration curve by applied slope and intercept values for complexes and tannic acid in equation (4.4) as shown in Table 4.22. Active antioxidant include the Me_3SnL-tyrosine complex while other complexes consider moderate antioxidant. Tannic acid is a very active antioxidant with an IC_{50} value of 5.328 µg/mL.

Table 4.22 Shows the IC_{50} values and Linear Regression of Organotin (IV)-Tyrosine Complexes and Tannic acid.

Complexes	Linear Regression Equation	IC_{50} (µg/mL)
Me_3SnL	y = 0.1323x + 49.259 R^2 = 0.78	16.666
Bu_3SnL	y = 0.1164x + 48.06 R^2 = 0.8501	104.864
Me_2SnL_2	y = 0.0741x + 42.24 R^2 = 0.8547	143.561
Tannic acid	y = 0.0688x + 40.123 R^2 = 0.9119	5.328

4.8.2 Cuprac Activity Assay

Based on the reduction of Cu^{2+} in the presence of neocuproine by a reducing agent, the CUPRAC test for assessing antioxidant activity produces a Cu^{+} complex with a maximum wavelength of 450 nm [212]. The ligand (Tyrosine), standard reference (Tannic acid) and all complexes were measured for absorbance and percentage inhibition at a concentration of 20 µg/ml. The complexes Me_3SnL, Bu_3SnL and Me_2SnL_2 have more antioxidant activity than their ligand (Tyrosine), as shown in Table 4.23 and Fig. 4.32.

Table 4.23 Results of Absorbance and % Inhibition at Concentration 20 µg/ml for Tyrosine, Complexes and Tannic acid.

Control Absorbance = 0.238		λ = 450 nm
Complexes	**Absorbance at Concentration 20 µg/ml**	**% Inhibition**
L-Tyrosine	0.193	18.908
Ph_3SnL	0.176	26.050
Bu_3SnL	0.148	37.815
Me_3SnL	0.125	45.798
Ph_2SnL_2	0.169	28.992
Bu_2SnL_2	0.168	29.412
Me_2SnL_2	0.157	34.034
Tannic acid	0.121	49.160

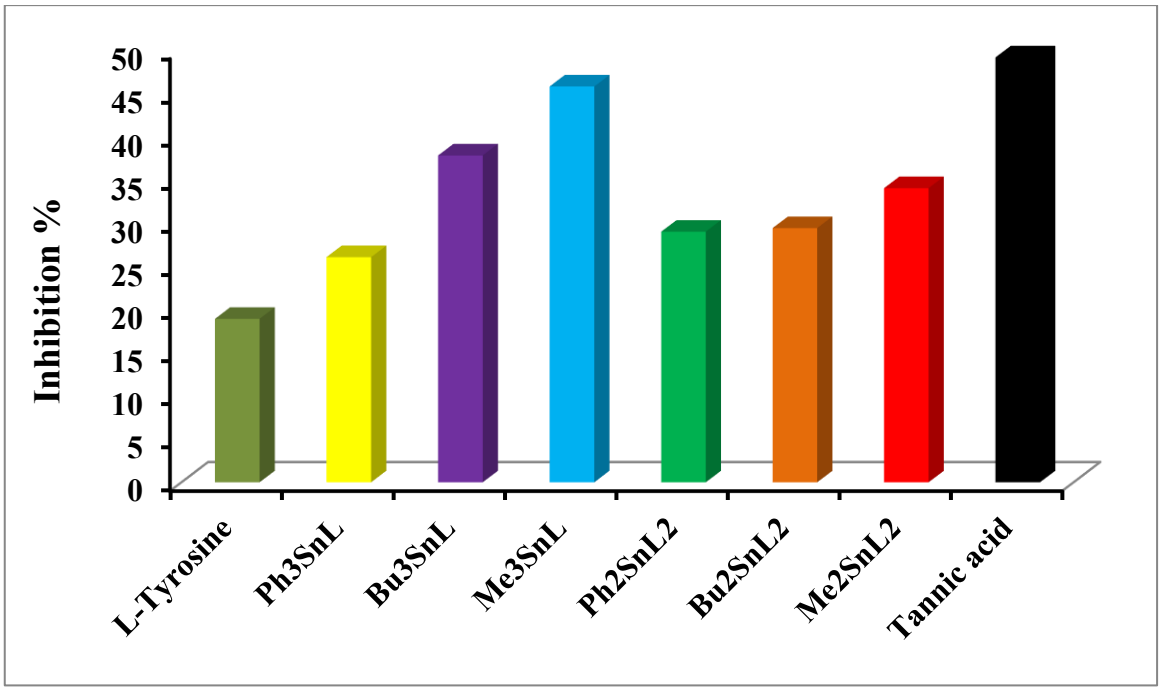

Figure 4.32 CUPRAC Assay at Concentration 20 µg/ml for Tyrosine, Complexes and Tannic Acid.

The organotin (IV)-tyrosine complexes with the highest antioxidants were taken in different concentrations of 20, 40 and 60 µg/ml. The absorbance and inhibition ratio were evaluated to determine the optimal concentration for high antioxidant activity, which was 40 µg/ml. Tables 4.24, 4.25 and Fig.4.33 demonstrate this.

Table 4.24 Results of Absorbance at different Concentration for Complexes and Tannic Acid.

Control Absorbance = 0.238 λ = 450 nm			
Complexes	**Absorbance at different Concentration**		
	20 µg/ml	**40 µg/ml**	**60 µg/ml**
Bu_3SnL	**0.148**	**0.135**	**0.136**
Me_3SnL	**0.125**	**0.115**	**0.117**
Me_2SnL_2	**0.157**	**0.140**	**0.142**
Tannic acid	**0.121**	**0.115**	**0.114**

Table 4.25 Results of % Inhibition at different Concentration for Complexes and Tannic Acid.

Control absorbance = 0.238 λ = 450 nm			
Complexes	**% Inhibition at different Concentration**		
	20 µg/ml	**40 µg/ml**	**60 µg/ml**
Bu_3SnL	**37.815**	**43.277**	**42.857**
Me_3SnL	**47.479**	**51.681**	**50.840**
Me_2SnL_2	**34.034**	**41.176**	**40.336**
Tannic acid	**49.160**	**51.681**	**52.101**

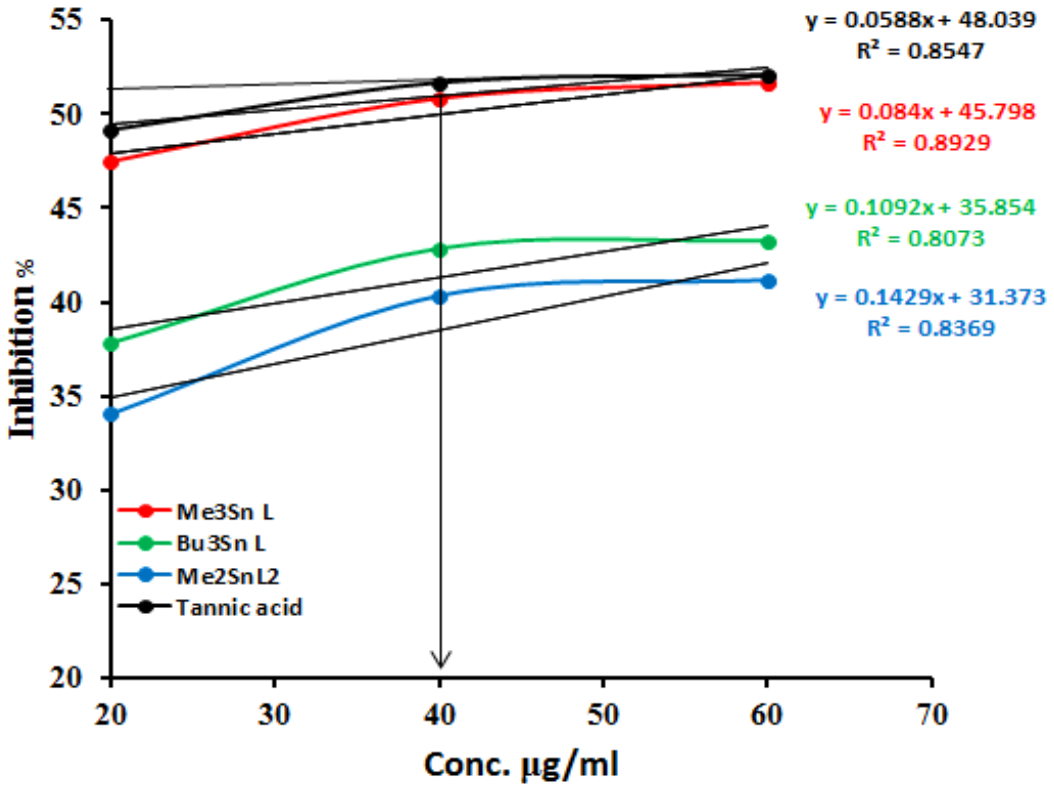

Figure 4.33 The Standard Calibration curve of Organotin (IV)-Tyrosine Complexes and Tannic Acid.

Table 4.26 Shows the IC_{50} Values and Linear Regression of Organotin (IV)-Tyrosine Complexes and Tannic acid.

Complexes	Linear Regression Equation	IC_{50} (µg/mL)
Bu_3SnL	y = 0.1092x + 35.854 R^2 = 0.8073	129.542
Me_3SnL	y = 0.084x + 45.798 R^2 = 0.8929	50.023
Me_2SnL_2	y = 0.1429x + 31.373 R^2 = 0.8369	130.349
Tannic acid	y = 0.0588x + 48.039 R^2 = 0.8547	33.350

The IC_{50} value was calculated using the linear regression equation y = ax + b as in Fig.4.33 and Table 4.26. By determining the slope and intercept via plotting the relationship between the percentage inhibition and different concentrations. The complex Me_3SnL was an active antioxidant, whereas others exhibit only moderate antioxidant activity [213]. Compared with tannic acid, which had an IC_{50} of 33.350 µg/mL.

4.9 Determination of Effective Antiradical Power (ARP)

Another factor that may be used to describe antioxidant activity is antiradical power (ARP). As this parameter is the reciprocal of IC_{50}, a greater IC_{50} value corresponds to a lower antiradical power [214].

$$\mathbf{ARP = 1/\ IC_{50}} \quad \text{..... (4.6)}$$

Reference standards like ascorbic acid and tannic acid are typically used when comparing the antioxidant activity of new compounds using the DPPH test.

Ascorbic acid and DPPH react extremely rapidly, ultimate the reaction in less than a minute [215]. Table 4.27 and Fig. 4.34 provide comprehensive data on the numerical values and percentage ratios of various antiradical factors. The complex Me_3SnL-Cefalexin was the most effective antiradical, whereas other complexes were taken in the following order: Bu_3SnL-C > Me_3SnL-T > Ph_3SnL-C > Me_2SnL_2-T and Bu_3SnL-T. This is because a high ARP value indicates stronger antioxidant activity.

Table 4.27 Result of Antiradical Power (ARP) for Organotin (IV) Complexes compared with Tannic acid and Ascorbic acid* by DPPH Assay.

DPPH Assay		
Comp.	**IC_{50} (µg/ml)**	**ARP**
Ph_3SnL-C	**33.283**	**0.030**
Bu_3SnL-C	**14.433**	**0.069**
Me_3SnL-C	**6.821**	**0.146**
Me_3SnL-T	**16.666**	**0.060**
Bu_3SnL -T	**104.864**	**0.009**
Me_2SnL_2-T	**143.561**	**0.007**
Tannic acid	**5.328**	**0.187**
***Ascorbic acid**	**5.400**	**0.185**

*Take from Reference [216].

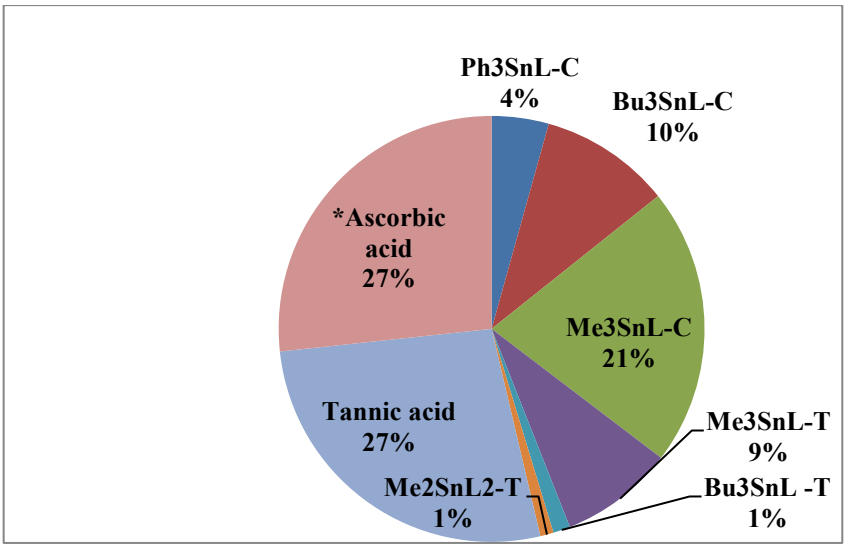

Figure 4.34 Percentage of Antiradical Power for Organotin (IV) Complexes compared with Tannic acid and Ascorbic acid* by DPPH Assay.

In cuprac assay by comparing the ARP values for tannic acid and organotin (IV) complexes also the complex Me_3SnL-C was the high antiradical power (ARP) than other complexes which take the following order Me_3SnL-T > Bu_3SnL-C > Bu_3SnL -T, Me_2SnL_2-T > Me_2SnL_2-C > Ph_3SnL-C as summarized in Table 4.28 and Fig.4.35.

Table 4.28 Result of Antiradical Power (ARP) for Organotin (IV) Complexes compared with Tannic acid by Cuprac Assay.

Cuprac Assay		
Comp.	**IC_{50} (µg/ml)**	**ARP**
Ph_3SnL-C	175.619	0.006
Bu_3SnL-C	84.883	0.012
Me_3SnL-C	33.273	0.030
Me_2SnL_2-C	150.723	0.007
Bu_3SnL -T	129.542	0.008
Me_3SnL-T	50.023	0.020
Me_2SnL_2-T	130.349	0.008
Tannic acid	19.637	0.050

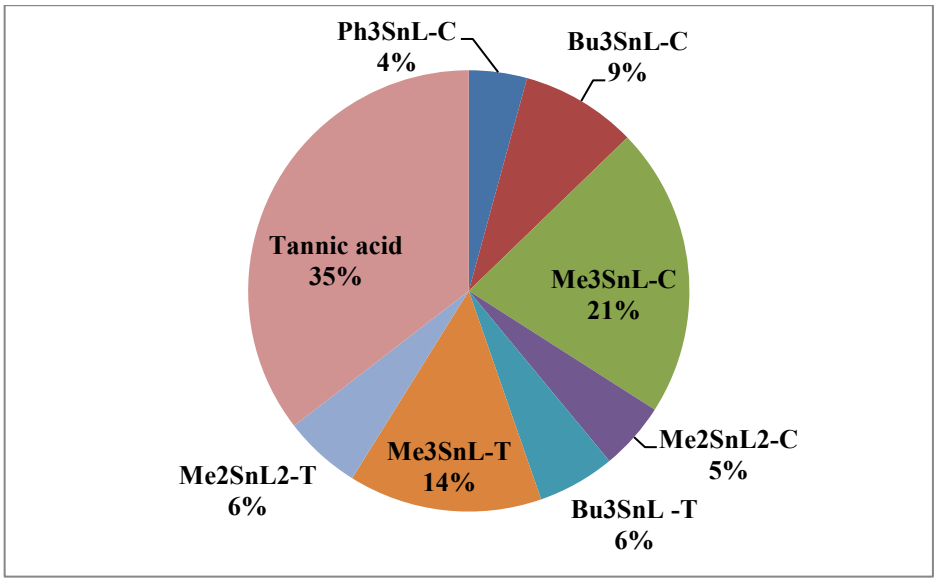

Figure 4.35 Percentage of Antiradical Power for Organotin (IV) Complexes compared with Tannic acid by Cuprac Assay.

The complex Me_3SnL-Cefalexin has a high antiradical power (ARP) and a low IC_{50} , as shown by the findings of the DPPH and Cuprac tests. Thus, at concentrations of 40 and 50 µg/mL, exhibits a larger percentage of scavenging activity.

This is attributed to the stability of the symmetric complex; also, the methyl complex has a higher tin content and less steric hindrance than other types, which increases its antioxidant activities [217].

5. Conclusions

- It is possible to easily (high yields %) synthesize organotin (IV) complexes and characterize them using various methods.
- Organotin (IV) complexes synthesized can be employed as photostabilizers for PVC (0.5% by weight) films.
- Using various techniques of assessment for their efficacy as photostabilizers, the organotin (IV) complexes demonstrated their usefulness in reducing photodegradation of PVC films.
- These techniques, which included tracking the development of specific functional groups such as carbonyl ($I_{C=O}$), polyene ($I_{C=C}$) and hydroxyl (I_{OH}) indexes and weight loss percentage during exposure to UV radiation, all demonstrated significant reductions in the effect of photodegradation for PVC films.
- The additives may stabilize PVC films by several methods, including primary stabilizers, HCl scavengers, peroxide decomposers, free radical scavengers, and UV absorbers.
- During photodegradation, Me_2SnL_2-cephalexin complexes were the most effective photostabilizers, supporting their usage as commercial PVC stabilizers.
- Organotin (IV) complexes exhibit greater antioxidant activity than a ligand against the stable free radical because of the metal moiety present in the complexes.
- The complex Me_3SnL-Cephalexin has a high antiradical power (ARP) and a low IC_{50}.
- Low concentrations of 40 and 50 µg/mL, exhibits a larger percentage of scavenging activity.

6. Suggestions for Future Work

- PVC has low heat stability; these additives can be used to test their efficiency as thermal stabilizers.

- Can be applied the current organotin (IV) complexes as photo stabilizers for other polymers such as polystyrene.

- Utilized the existing organotin (IV) complexes as an anticancer in mice.

- Employ Triorganotin (IV)-Cephalexin complexes as chemotherapy.

- Can be applied the organotin (IV) complexes as semiconductor.

References

References

1- Ghazi, D., Rasheed, Z., & Yousif, E. (2018). Review of organotin compounds: chemistry and applications. development, 3, 4.

2- Smith, P. J. (Ed.). (2012). Chemistry of tin. Springer Science & Business Media.

3- Gielen, M. (2008). Tin chemistry: fundamentals, frontiers, and applications. John Wiley & Sons.

4- Simanjuntak, W., Qudus, H. I., & Hadi, S. (2019, October). The potential of derivatives of organotin (IV) benzoate compounds in medicinal chemistry. In Journal of Physics: Conference Series (Vol. 1338, No. 1, p. 012014). IOP Publishing.

5- Maity, B., & Chakravarty, B. M. A. R. (2012). Photocytotoxic organometallic compounds.

6- Magami, S. M., Garba, Z. N., & Ibrahim, M. B. (2015). Properties, Characterizations and Applications of Organometallic Surfactants—A Review. Journal of Materials Science and Chemical Engineering, 3(10), 22.

7- Gasser, G., Ott, I., & Metzler-Nolte, N. (2011). Organometallic anticancer compounds. Journal of medicinal chemistry, 54(1), 3-25.

8- Hartinger, C. G., & Dyson, P. J. (2009). Bioorganometallic chemistry—from teaching paradigms to medicinal applications. Chemical Society Reviews, 38(2), 391-401.

9- Okoro, H. K., Fatoki, O. S., Adekola, F. A., Ximba, B. J., & Snyman, R. G. (2011). Sources, Environmental levels and toxicity of organotin in marine environment–a review.

10- Jain, R., Singh, R., & Kaushik, N. K. (2013). Synthesis, characterization, and thermal and antimicrobial activities of some novel organotin (IV): Purine base complexes. Journal of Chemistry, 2013.

11- Shah, S. S. A., Ashfaq, M., Waseem, A., Ahmed, M. M., Najam, T., Shaheen, S., & Rivera, G. (2015). Synthesis and biological activities of organotin (IV) complexes as antitumoral and antimicrobial agents. A review. Mini Rev. Med. Chem, 15(5), 406-426.

12- Adeyemi, J. O., & Onwudiwe, D. C. (2018). Organotin (IV) dithiocarbamate complexes: Chemistry and biological activity. Molecules, 23(10), 2571.

13- Olushola Sunday, A., Abdullahi Alafara, B., & Godwin Oladele, O. (2012). Toxicity and speciation analysis of organotin compounds. Chemical Speciation & Bioavailability, 24(4), 216-226.

14- Pellerito, C., Nagy, L., Pellerito, L., & Szorcsik, A. (2006). Biological activity studies on organotin (IV) n+ complexes and parent compounds. Journal of Organometallic Chemistry, 691(8), 1733-1747.

15- HadeerJasem, A. G. H. (2021). Enhanced the Antioxidant Activity of 1-Amino-2-naphthol-4-Sulfonic acid by Complexation with Organotin (IV) Compounds. Annals of the Romanian Society for Cell Biology, 25(6), 6182-6193.

16- Iqbal, H., Ali, S., & Shahzadi, S. (2015). Antituberculosis study of organotin (IV) complexes: A review. Cogent Chemistry, 1(1), 1029039.

17- Ghani, H., & Yousif, E. (2021). Chemistry of some organotin compounds. Al-Nahrain Journal of Science, 24(3), 9-15.

18- Davies, A. G. (2016). Industrial Applications of Organotin Compounds. Metal-Organics for Materials, Polymers & Synthesis, 2, 59.

19- Hadi, A. G., Jawad, K., Ahmed, D. S., & Yousif, E. (2019). Synthesis and biological activities of organotin (IV) carboxylates: a review. Systematic Reviews in Pharmacy, 10(1), 26-31.

20- Yousif, E. (2012). Synthesis, spectroscopic studies and fungicidal activity of some diorganotin (IV) with 2-[(phenylcarbonyl) amino] propanoato. Journal of King Saud University-Science, 24(2), 167-170.

21- Guan, R., Zhou, Z., Zhang, M., Liu, H., Du, W., Tian, X., ... & Tian, Y. (2018). Organotin (IV) carboxylate complexes containing polyether oxygen chains with two-photon absorption in the near infrared region and their anticancer activity. Dyes and Pigments, 158, 428-437.

22- Yousif, E., Mehdi, B. I., Yusop, R., Salimon, J., Salih, N., & Abdullah, B. M. (2014). Synthesis, structure, and antibacterial activity of some triorganotin (IV) complexes with a benzamidoalanine ligand. Journal of Taibah University for Science, 8(3), 276-281.

23- Adeyemi, J. O., Onwudiwe, D. C., Ekennia, A. C., Anokwuru, C. P., Nundkumar, N., Singh, M., & Hosten, E. C. (2019). Synthesis, characterization, and biological activities of organotin (IV) diallyldithiocarbamate complexes. Inorganica Chimica Acta, 485, 64-72.

24- Panhwar, Q. K., & Memon, S. (2013). Synthesis, characterization and antioxidant study of Tin (II)–rutin complex: Exploration of tin packaging hazards. Inorganica Chimica Acta, 407, 252-260.

25- Devi, J., Yadav, J., & Singh, N. (2019). Synthesis, characterisation, in vitro antimicrobial, antioxidant, and anti-inflammatory activities of diorganotin (IV) complexes derived from salicylaldehyde Schiff bases. Research on Chemical Intermediates, 45, 3943-3968.

26- Shahzadi, S., Shahid, K., Ali, S., Mazhar, M., & Khan, K. M. (2005). Organotin (IV) derivatives as biocides: An investigation of structure by IR, solution NMR, electron impact MS and assessment of structure correlation with biocidal activity. Journal of the Iranian Chemical Society, 2, 277-288.

27- Shahzadi, S., & Ali, S. (2008). Structural chemistry of organotin (IV) complexes. Journal of the Iranian Chemical Society, 5, 16-28.

28- Abbas, S. M., Ali, S., Hussain, S. T., & Shahzadi, S. (2013). structural diversity in organotin (IV) dithiocarboxylates and carboxylates. Journal of Coordination Chemistry, 66(13), 2217-2234.

29- Barbosa, A. S. L., de Siqueira Guedes, J., da Silva, D. R., Meneghetti, S. M. P., Meneghetti, M. R., da Silva, A. E., ... & Mendonça-Junior, F. J. B. (2018). Synthesis and evaluation of the antibiotic and adjuvant antibiotic potential of organotin (IV) derivatives. Journal of Inorganic Biochemistry, 180, 80-88.

30- Farina, Y., Graisa, A., Yousif, E., & Kassim, M. (2009). Synthesis and Structure of Some Diorganotin (IV) with N-methyl-mnitrobenzohydroxamic Acid. Australian Journal of Basic and Applied Sciences, 3(1), 291-294.

31- Yousif, E., Adil, H., Majeed, A., & Farina, Y. (2009). Synthesis, characterization, and fungicidal activity of some diorganotin (IV) with 2-thioacetic-5-phenyl-1, 3, 4-oxadiazole. Malaysian Journal of Fundamental and Applied Sciences, 5(2).

32- Hadi, A. G., Yousif, E., El-Hiti, G. A., Ahmed, D. S., Jawad, K., Alotaibi, M. H., & Hashim, H. (2019). Long-term effect of ultraviolet irradiation on poly (vinyl chloride) films containing naproxen diorganotin (IV) complexes. Molecules, 24(13), 2396.

33- Shaheen, F., Ali, S., & Shahzadi, S. (2017). Synthesis, Characterization, and Anticancer Activity of Organotin (IV) Complexes with Sodium 3-(1 H-Indol-3-yl) propanoate. Russian Journal of General Chemistry, 87, 2937-2943.

34-Watheq, B., Yousif, E., Al-Mashhadani, M. H., Mohammed, A., Ahmed, D. S., Kadhom, M., & Jawad, A. H. (2020). A surface morphological study, poly (vinyl chloride) photo-stabilizers utilizing ibuprofen tin complexes against ultraviolet radiation. Surfaces, 3(4), 579-593.

35- Ahmed, A., El-Hiti, G. A., Hadi, A. G., Ahmed, D. S., Baashen, M. A., Hashim, H., & Yousif, E. (2021). Photostabilization of poly (vinyl chloride) films blended with organotin complexes of mefenamic acid for outdoor applications. Applied Sciences, 11(6), 2853.

36-Elgharbawy, A. (2022). Poly Vinyl Chloride Additives and Applications-A Review. Journal of Risk Analysis and Crisis Response, 12(3).

37- Skelly, P. W., Li, L., & Braslau, R. (2022). Internal plasticization of PVC. Polymer Reviews, 62(3), 485-528.

38- Mulder, K., & Knot, M. (2001). PVC plastic: a history of systems development and entrenchment. Technology in Society, 23(2), 265-286.

39- El-Hiti, G. A., Ahmed, D. S., Yousif, E., Al-Khazrajy, O. S., Abdallh, M., & Alanazi, S. A. (2021). Modifications of polymers through the addition of ultraviolet absorbers to reduce the aging effect of accelerated and natural irradiation. Polymers, 14(1), 20.

40- Woo, E. M., & Chang, L. (2002). Tacticity in vinyl polymers. Encyclopedia of Polymer Science and Technology.

41- Huang, C. L., Chen, Y. C., Hsiao, T. J., Tsai, J. C., & Wang, C. (2011). Effect of tacticity on viscoelastic properties of polystyrene. Macromolecules, 44(15), 6155-6161.

42- Vohlídal, J. (2020). Polymer degradation: A short review. Chemistry Teacher International, 3(2), 213-220.

43- Ghazi, D., El-Hiti, G. A., Yousif, E., Ahmed, D. S., & Alotaibi, M. H. (2018). The effect of ultraviolet irradiation on the physicochemical properties of poly (vinyl chloride) films containing organotin (IV) complexes as photostabilizers. Molecules, 23(2), 254.

44- Ye, X., Pi, H., & Guo, S. (2010). A novel route for preparation of PVC sheets with high UV irradiation resistance. Journal of applied polymer science, 117(5), 2899-2906.

45- Shi, W., Zhang, J., Shi, X. M., & Jiang, G. D. (2008). Different photodegradation processes of PVC with different average degrees of polymerization. Journal of applied polymer science, 107(1), 528-540.

46- Feldman, D. (2002). Polymer weathering: photo-oxidation. Journal of Polymers and the Environment, 10, 163-173.

47- Kameda, T., Watanabe, Y., Grause, G., & Yoshioka, T. (2008). Dehydrochlorination behavior of polychloroprene during thermal degradation. Thermochimica acta, 476(1-2), 28-32.

48- Zheng, X. G., Tang, L. H., Zhang, N., Gao, Q. H., Zhang, C. F., & Zhu, Z. B. (2003). Dehydrochlorination of PVC materials at high temperature. Energy & fuels, 17(4), 896-900.

49- Dobashi, Y., & Ohkatsu, Y. (2008). Dependence of ultraviolet absorbers' performance on ultraviolet wavelength. Polymer degradation and stability, 93(2), 436-447.

50- Yousif, E., & Haddad, R. (2013). Photodegradation and photostabilization of polymers, especially polystyrene. SpringerPlus, 2(1), 1-32.

51- Yousif, E., Hameed, A., Rasheed, R., Mansoor, H., Farina, Y., Graisa, A., ... & Salimon, J. (2010). Synthesis and photostability study of some modified poly (vinyl chloride) containing pendant benzothiazole and benzimidozole ring. International Journal of Chemistry, 2(1), 65.

52- Kaavessina, M., Shohih, E. N., Distantina, S., & Fadilah, F. (2022). Photo-Oxidative Degradation and Hydrolytic Degradation of Micro-Graphite Filled Poly (lactic acid) Composites. ASEAN Journal of Chemical Engineering, 22(1), 72-81.

53- Folarin, O. M., & Sadiku, E. R. (2011). Thermal stabilizers for poly (vinyl chloride): A review. Int. J. Phys. Sci, 6(18), 4323-4330.

54- Arkış, E., & Balköse, D. (2005). Thermal stabilization of poly (vinyl chloride) by organotin compounds. Polymer Degradation and Stability, 88(1), 46-51.

55- Davies, A. G. (2010). Organotin compounds in technology and industry. Journal of Chemical Research, 34(4), 181-190.

56- Tomi, I. H. R., Ali, G. Q., Jawad, A. H., & Yousif, E. (2017). Synthesis and characterization of gallic acid derivatives and their utilized as organic photo-stabilizers for poly (vinyl chloride). Journal of Polymer Research, 24, 1-11.

57- Yousif, E., Ahmed, A., Abood, R., Jaber, N., Noaman, R., & Yusop, R. (2015). Poly (vinyl chloride) derivatives as stabilizers against photodegradation. Journal of Taibah University for Science, 9(2), 203-212.

58- Sabaa, M. W., & Mohamed, R. R. (2007). Organic thermal stabilizers for rigid poly (vinyl chloride). Part XIII: Eugenol (4-allyl-2-methoxy-phenol). Polymer degradation and stability, 92(4), 587-595.

59-Martins, L. M., Hazra, S., da Silva, M. F. C. G., & Pombeiro, A. J. (2016). A sulfonated Schiff base dimethyltin (IV) coordination polymer: Synthesis, characterization, and application as a catalyst for ultrasound-or microwave-assisted Baeyer–Villiger oxidation under solvent-free conditions. RSC advances, 6(81), 78225-78233.

60- Rabie, S. T., Ahmed, A. E., Sabaa, M. W., & Abd El-Ghaffar, M. A. (2013). Maleic diamides as photostabilizers for polystyrene. Journal of Industrial and Engineering Chemistry, 19(6), 1869-1878.

61- Alotaibi, M. H., El-Hiti, G. A., Yousif, E., Ahmed, D. S., Hashim, H., Hameed, A. S., & Ahmed, A. (2019). Evaluation of the use of polyphosphates as photostabilizers and in the formation of ball-like polystyrene materials. Journal of Polymer Research, 26, 1-14.

62- Crawford, C. B., & Quinn, B. (2017). The interactions of microplastics and chemical pollutants. Microplastic pollutants, 131-157.

63- Yu, J., Sun, L., Ma, C., Qiao, Y., & Yao, H. (2016). Thermal degradation of PVC: A review. Waste management, 48, 300-314.

64- Mohammed, A., & Majeed, A. (2019). The Trend of Additives for Poly (vinyl chloride) as Photostabilizers. Al-Nahrain Journal of Science, 22(4), 42-51.

65- Yousif, E., Salimon, J., & Salih, N. (2012). New stabilizers for polystyrene based on 2-thioacetic acid benzothiazol complexes. Journal of applied polymer Science, 125(3), 1922-1927.

66- Yousif, E., Salimon, J., & Salih, N. (2015). New photostabilizers for PVC based on some diorganotin (IV) complexes. Journal of Saudi Chemical Society, 19(2), 133-141.

67- Yousif, E., Salimon, J., Salih, N., & Yousif, E. (2011). Improvement of the photostabilization of PVC films in the presence of thioacetic acid benzothiazole complexes. MJAS, 15, 81-92.

68- Cui, K., Luo, X., Xu, K., & Murthy, M. V. (2004). Role of oxidative stress in neurodegeneration: recent developments in assay methods for oxidative stress and nutraceutical antioxidants. Progress in Neuro-Psychopharmacology and Biological Psychiatry, 28(5), 771-799.

69- Tvrdá, E., & Benko, F. (2020). Free radicals: what they are and what they do. In Pathology (pp. 3-13). Academic Press.

70- Lawson, M., Jomova, K., Poprac, P., Kuča, K., Musílek, K., & Valko, M. (2017). Free radicals and antioxidants in human disease. Nutritional Antioxidant Therapies: Treatments and Perspectives, 283-305.

71- Silva, J. P., & Coutinho, O. P. (2010). Free radicals in the regulation of damage and cell death--basic mechanisms and prevention. Drug Discoveries & Therapeutics, 4(3).

72- McCord, J. M. (2000). The evolution of free radicals and oxidative stress. The American journal of medicine, 108(8), 652-659.

73- Touyz, R. M., Rios, F. J., Alves-Lopes, R., Neves, K. B., Camargo, L. L., & Montezano, A. C. (2020). Oxidative stress: a unifying paradigm in hypertension. Canadian Journal of Cardiology, 36(5), 659-670.

74- Kunwar, A., & Priyadarsini, K. I. (2011). Free radicals, oxidative stress and importance of antioxidants in human health. Journal of Medical & Allied Sciences, 1(2).

75- Marchioli, R., Schweiger, C., Levantesi, G., Tavazzi, L., & Valagussa, F. (2001). Antioxidant vitamins and prevention of cardiovascular disease: epidemiological and clinical trial data. Lipids, 36(S1), S53-S63.

76- Lobo, V., Patil, A., Phatak, A., & Chandra, N. (2010). Free radicals, antioxidants, and functional foods: Impact on human health. Pharmacognosy reviews, 4(8), 118.

77- Phaniendra, A., Jestadi, D. B., & Periyasamy, L. (2015). Free radicals: properties, sources, targets, and their implication in various diseases. Indian journal of clinical biochemistry, 30, 11-26.

78- Fang, Y. Z., Yang, S., & Wu, G. (2002). Free radicals, antioxidants, and nutrition. Nutrition, 18(10), 872-879.

79- Halliwell, B. (2012). Free radicals and antioxidants: updating a personal view. Nutrition reviews, 70(5), 257-265.

80- Devasagayam, T. P. A., Tilak, J. C., Boloor, K. K., Sane, K. S., Ghaskadbi, S. S., & Lele, R. D. (2004). Free radicals and antioxidants in human health: current status and future prospects. Japi, 52(794804), 4.

81- Bardaweel, S. K., Gul, M., Alzweiri, M., Ishaqat, A., ALSalamat, H. A., & Bashatwah, R. M. (2018). Reactive oxygen species: The dual role in physiological and pathological conditions of the human body. The Eurasian journal of medicine, 50(3), 193.

82- Jeevan Kumar, S. P., Rajendra Prasad, S., Banerjee, R., & Thammineni, C. (2015). Seed birth to death: dual functions of reactive oxygen species in seed physiology. Annals of botany, 116(4), 663-668.

83- Min, D. B., & Boff, J. M. (2002). Chemistry and reaction of singlet oxygen in foods. Comprehensive reviews in food science and food safety, 1(2), 58-72.

84- Choe, E., & Min, D. B. (2006). Mechanisms and factors for edible oil oxidation. Comprehensive reviews in food science and food safety, 5(4), 169-186.

85- Martemucci, G., Costagliola, C., Mariano, M., D'andrea, L., Napolitano, P., & D'Alessandro, A. G. (2022). Free radical properties, source and targets, antioxidant consumption and health. Oxygen, 2(2), 48-78.

86- Zhang, C., Wang, X., Du, J., Gu, Z., & Zhao, Y. (2021). Reactive Oxygen Species-Regulating Strategies Based on Nanomaterials for Disease Treatment. Advanced Science, 8(3), 2002797.

87- Bienert, G. P., Schjoerring, J. K., & Jahn, T. P. (2006). Membrane transport of hydrogen peroxide. Biochimica et Biophysica Acta (BBA)-Biomembranes, 1758(8), 994-1003.

88- Bienert, G. P., Schjoerring, J. K., & Jahn, T. P. (2006). Membrane transport of hydrogen peroxide. Biochimica et Biophysica Acta (BBA)-Biomembranes, 1758(8), 994-1003.

89- Das, T. K., Wati, M. R., & Fatima-Shad, K. (2015). Oxidative stress gated by Fenton and Haber Weiss reactions and its association with Alzheimer's disease. Archives of Neuroscience, 2(2).

90- Collin, F. (2019). Chemical basis of reactive oxygen species reactivity and involvement in neurodegenerative diseases. International journal of molecular sciences, 20(10), 2407.

91- Sulekha, M., Satish, Y., Sunita, Y., & Nema, R. K. (2009). Antioxidants: a review. Journal of Chemical and Pharmaceutical Research, 1(1), 102-104.

92- Alzoghaibi, M. A. (2013). Concepts of oxidative stress and antioxidant defense in Crohn's disease. World journal of gastroenterology: WJG, 19(39), 6540.

93- Nimse, S. B., & Pal, D. (2015). Free radicals, natural antioxidants, and their reaction mechanisms. RSC advances, 5(35), 27986-28006.

94- Shahidi, F., & Zhong, Y. (2010). Novel antioxidants in food quality preservation and health promotion. European Journal of Lipid Science and Technology, 112(9), 930-940.

95- Flieger, J., Flieger, W., Baj, J., & Maciejewski, R. (2021). Antioxidants: Classification, natural sources, activity/capacity measurements, and usefulness for the synthesis of nanoparticles. Materials, 14(15), 4135.

96- Moharram, H. A., & Youssef, M. M. (2014). Methods for determining the antioxidant activity: a review. Alexandria Journal of Food Science and Technology, 11(1), 31-42.

97- Santos-Sánchez, N. F., Salas-Coronado, R., Villanueva-Cañongo, C., & Hernández-Carlos, B. (2019). Antioxidant compounds and their antioxidant mechanism. Antioxidants, 10, 1-29.

98- Shah, S. S. A., Ashfaq, M., Waseem, A., Ahmed, M. M., Najam, T., Shaheen, S., & Rivera, G. (2015). Synthesis and biological activities of organotin (IV) complexes as antitumoral and antimicrobial agents. A review. Mini Rev. Med. Chem, 15(5), 406-426.

99- Hadi, A. G., Hassen, T. F., & Mahdi, I. J. (2022). Synthesis, characterization, and antioxidant material activities of organotin (IV) carboxylates with tin-para methoxy benzoic acid. Materials Today: Proceedings, 49, 2797-2801.

100- Yousif, E., Mehdi, B. I., Yusop, R., Salimon, J., Salih, N., & Abdullah, B. M. (2014). Synthesis, structure, and antibacterial activity of some triorganotin (IV) complexes with a benzamidoalanine ligand. Journal of Taibah University for Science, 8(3), 276-281.

101- Win, Y. F., Teoh, S. G., Ha, S. T., Ong, L. G. A., & Tengku-Muhammad, T. S. (2011). Synthesis, characterization, and cytotoxic assay on human liver carcinoma cells (HepG2) of organodistannoxane dimer complexes derived from alkylaminobenzoic acids. International Journal of Physical Sciences, 6(6), 1463-1470.

102- Bhatt, P. M., Joshi, U. S., Shah, H. N., & Brahmbhatt, P. K. Low temperature Atomic Force Microscopy-A Review. IOSR Journal of Mechanical and Civil Engineering (IOSRJMCE) ISSN, 2278-1684.

103- Eaton, P., & West, P. (2010). Atomic force microscopy. Oxford university press.

104- Stokes, D. (2008). Principles and practice of variable pressure/environmental scanning electron microscopy (VP-ESEM). John Wiley & Sons.

105- Inkson, B. J. (2016). Scanning electron microscopy (SEM) and transmission electron microscopy (TEM) for materials characterization. In Materials characterization using nondestructive evaluation (NDE) methods (pp. 17-43). Woodhead publishing.

106- Akhtar, K., Khan, S. A., Khan, S. B., & Asiri, A. M. (2018). Scanning electron microscopy: Principle and applications in nanomaterials characterization. Handbook of materials characterization, 113-145.

107- Mohammed, A., & Abdullah, A. (2018, November). Scanning electron microscopy (SEM): A review. In Proceedings of the 2018 International Conference on Hydraulics and Pneumatics—HERVEX, Băile Govora, Romania (Vol. 2018, pp. 7-9).

108- Alyamani, A. M. O. L., & Lemine, O. M. (2012). FE-SEM characterization of some nanomaterial. In Scanning electron microscopy. IntechOpen.

109- Szymula, K. P., Magaraci, M. S., Patterson, M., Clark, A., Mannickarottu, S. G., & Chow, B. Y. (2018). An open-source plate reader. Biochemistry, 58(6), 468-473.

110- Yousif, E. (2013). Triorganotin (IV) complexes photo-stabilizers for rigid PVC against photodegradation. Journal of Taibah University for Science, 7(2), 79-87.

111- Mohammed, A., El-Hiti, G. A., Yousif, E., Ahmed, A. A., Ahmed, D. S., & Alotaibi, M. H. (2020). Protection of poly (vinyl chloride) films against photodegradation using various valsartan tin complexes. Polymers, 12(4), 969.

112- Yousif, E., Salimon, J., & Salih, N. (2014). Mechanism of photostabilization of poly (methy methacrylate) films by 2-thioacetic acid benzothiazol complexes. Arabian Journal of Chemistry, 7(3), 306-311.

113- Khalil, A. M., Rabie, S. T., Kapralkova, L., & Abd El Ghaffar, M. A. (2016). Itaconamide derivatives as organic stabilizers for poly (vinyl chloride) against photodegradation. Journal of Macromolecular Science, Part A, 53(2), 96-103.

114- Ali, M. M., El-Hiti, G. A., & Yousif, E. (2016). Photostabilizing efficiency of poly (vinyl chloride) in the presence of organotin (IV) complexes as photostabilizers. Molecules, 21(9), 1151.

115- Hadi, A. G., Baqir, S. J., Ahmed, D. S., El-Hiti, G. A., Hashim, H., Ahmed, A., ... & Yousif, E. (2021). Substituted organotin complexes of 4-methoxybenzoic acid for reduction of poly (vinyl chloride) photodegradation. Polymers, 13(22), 3946.

116- Yousif, E., Salimon, J., & Salih, N. (2012). New stabilizers for polystyrene based on 2-N-salicylidene-5-(substituted)-1, 3, 4-thiadiazole compounds. Journal of Saudi Chemical Society, 16(3), 299-306.

117- Almond, J., Sugumaar, P., Wenzel, M. N., Hill, G., & Wallis, C. (2020). Determination of the carbonyl index of polyethylene and polypropylene using specified area under band methodology with ATR-FTIR spectroscopy. e-Polymers, 20(1), 369-381.

118- Salam, B., El-Hiti, G. A., Bufaroosha, M., Ahmed, D. S., Ahmed, A., Alotaibi, M. H., & Yousif, E. (2020). Tin complexes containing an atenolol moiety as photostabilizers for poly (vinyl chloride). Polymers, 12(12), 2923.

119- Flieger, J., & Flieger, M. (2020). The [DPPH●/DPPH-H]-HPLC-DAD method on tracking the antioxidant activity of pure antioxidants and goutweed (Aegopodium podagraria L.) hydroalcoholic extracts. Molecules, 25(24), 6005.

120- Nikitin, E. A., et al. Antioxidant activity of modified 2, 6-Di-tert-butylphenols with pyridine moiety. Pharm. Pharmacol. Int. J, 2020, 8: 122-134.

121- Hadi, A. G., Zaooli, R. H., Ahmed, D. S., & Yousif, E. (2021). Antioxidant Activity of Naproxen and Its Diorganotin Complexes. INTERNATIONAL JOURNAL, 11(2), 383-385.

122- Bektaşoğlu, B., Özyürek, M., Güçlü, K., & Apak, R. (2008). Hydroxyl radical detection with a salicylate probe using modified CUPRAC spectrophotometry and HPLC. Talanta, 77(1), 90-97.

123- Bektaşoğlu, B., Celik, S. E., Özyürek, M., Güçlü, K., & Apak, R. (2006). Novel hydroxyl radical scavenging antioxidant activity assay for water-soluble antioxidants using a modified CUPRAC method. Biochemical and Biophysical Research Communications, 345(3), 1194-1200.

124- Dutta, A. (2017). Fourier transform infrared spectroscopy. Spectroscopic methods for nanomaterials characterization, 73-93.

125- Singh, H. L., & Singh, J. (2014). Synthesis, spectroscopic, molecular structure, and antibacterial studies of dibutyltin (IV) Schiff base complexes derived from phenylalanine, isoleucine, and glycine. Bioinorganic Chemistry and Applications, 2014.

126- Ghani, H., Yousif, E., Ahmed, D. S., Kariuki, B. M., & El-Hiti, G. A. (2021). Tin complexes of 4-(benzylideneamino) benzenesulfonamide: Synthesis, structure elucidation and their efficiency as PVC photostabilizers. Polymers, 13(15), 2434.

127- Joshi, A., Verma, S., Jain, A., & Saxena, S. (2004). Synthetic Pathway, Structural Chemistry and Structural Elucidation Based Upon Spectral Studies [IR, NMR (1H, 13C and 119Sn)] of Some Mixed Ligand Complexes of Diorganotin (IV) Derived from Sterically Demanding

Heterocyclic ß-Diketones and N-Protected Amino Acids. Main group metal chemistry, 27(2), 123-134.

128- Malz, F., & Jancke, H. (2005). Validation of quantitative NMR. Journal of pharmaceutical and biomedical analysis, 38(5), 813-823.

129- Bharti, S. K., & Roy, R. (2012). Quantitative 1H NMR spectroscopy. TrAC Trends in Analytical Chemistry, 35, 5-26.

130- Coşkun, A. (2006). The synthesis of 4-phenoxyphenylglyoxime and 4, 4'-oxybis (phenylglyoxime) and their complexes with Cu (II), Ni (II) and Co (II). Turkish Journal of Chemistry, 30(4), 461-469.

131- Masood, H., Ali, S., MAZHAR, M., Shahzadi, S., & Shahid, K. (2004). ^{1} H,^{13} C,^{119} Sn NMR, Mass, Mössbauer and Biological Studies of Tri-, Di-and Chlorodiorganotin (IV) Carboxylates. Turkish Journal of Chemistry, 28(1), 75-86.

132- Farina, Y., Adil, H., Ahmed, A., Graisa, A., & Yousif, E. (2009). Synthesis, structural and fungicidal studies of some diorganotin (IV) with benzamidoleucine. Australian Journal of Basic and Applied Sciences, 3(3), 1670-3.

133- Romero-Chávez, M. M., Pineda-Urbina, K., Pérez, D. J., Obledo-Benicio, F., Flores-Parra, A., Gómez-Sandoval, Z., & Ramos-Organillo, Á. (2018). Organotin (IV) compounds derived from ibuprofen and cinnamic acids, an alternative into design of anti-inflammatory by the cyclooxygenases (COX-1 and COX-2) pathway. Journal of Organometallic Chemistry, 862, 58-70.

134- Hussain, S., Ali, S., Shahzadi, S., Sharma, S. K., Qanungo, K., & Shahid, M. (2014). Synthesis, characterization, semiempirical and biological activities of organotin (IV) carboxylates with 4-piperidinecarboxylic acid. Bioinorganic Chemistry and Applications, 2014.

135- Yousif, E., Adil, H., Majeed, A., Graisa, A., & Farina, Y. (2009). Structure and fungicidal activity of some diorganotin (IV) with benzamidophenylalanine. J. Eng. Appl. Sci, 4, 39-42.

136- Mousa, O. G., El-Hiti, G. A., Baashen, M. A., Bufaroosha, M., Ahmed, A., Ahmed, A. A., ... & Yousif, E. (2021). Synthesis of carvedilol–

organotin complexes and their effects on reducing photodegradation of Poly (Vinyl Chloride). Polymers, 13(4), 500.

137- Rehman, W., Baloch, M. K., Badshah, A., & Ali, S. (2005). Synthesis and Characterization of Biologically Potent Di-organotin (IV) Complexes of Monomethyl Glutarate. Journal of the Chinese Chemical Society, 52(2), 231-236.

138- Choudhary, S., Varshney, S., & Varshney, A. (2015). Synthesis and Spectroscopic Characterization of New Coordination Compounds of Tin (IV) with Carbohydrazones. Iraqi National Journal Of Chemistry, 15(2).

139- Jawad, S. F., & Aljamali, N. M. (2021). Preparation, investigation and study of biological applications of tyrosine derivatives against breast cancer cells. NeuroQuantology, 19(9), 117.

140- Sharma, N., & Kumar, V. (2011). Synthesis, Characterization, and Antibacterial Activity of Diorganotin (IV) Complexes of 4-Methylphenol. Phosphorus, Sulfur, and Silicon and the Related Elements, 186(10), 2071-2085.

141- Yousefi, M., Safari, M., Torbati, M. B., Kazemiha, V. M., Sanati, H., & Amanzadeh, A. (2012). New mononuclear diorganotin (IV) dithiocarboxylates: synthesis, characterization and study of their cytotoxic activities. Applied Organometallic Chemistry, 26(8), 438-444.

142- Aljamali, N. M. (2021). Spectral and laboratory diagnostics of compounds. Nagham Mahmood Aljamali (Edt.)., Eliva Press, Europe.

143- Arafat, Y., Ali, S., Shahzadi, S., & Shahid, M. (2013). Preparation, characterization, and antimicrobial activities of bimetallic complexes of sarcosine with Zn (II) and Sn (IV). Bioinorganic chemistry and applications, 2013.

144- Ali, S., Ahmad, F., Mazhar, M., Munir, A., & Masood, M. T. (2002). Synthesis and spectral studies of di-and triorganotin (IV) complexes with 2-(6-methoxynaphthyl) propionic acid (naproxen). Synthesis and reactivity in inorganic and metal-organic chemistry, 32(2), 357-372.

145- Mousa, O. G., El-Hiti, G. A., Baashen, M. A., Bufaroosha, M., Ahmed, A., Ahmed, A. A., ... & Yousif, E. (2021). Synthesis of carvedilol–organotin complexes and their effects on reducing photodegradation of Poly (Vinyl Chloride). Polymers, 13(4), 500.

146- Hadi, A. G., Jawad, K., Yousif, E., El-Hiti, G. A., Alotaibi, M. H., & Ahmed, D. S. (2019). Synthesis of telmisartan organotin (IV) complexes and their use as carbon dioxide capture media. Molecules, 24(8), 1631.

147- Shahid, K., Ali, S., Shahzadi, S., Badshah, A., Khan, K. M., & Maharvi, G. M. (2003). Organotin (IV) complexes of aniline derivatives. I. Synthesis, spectral and antibacterial studies of di-and triorganotin (IV) derivatives of 4-bromomaleanilic acid. Synthesis and reactivity in inorganic and metal-Organic chemistry, 33(7), 1221-1235.

148- Rebolledo, A. P., de Lima, G. M., Gambi, L. N., Speziali, N. L., Maia, D. F., Pinheiro, C. B., ... & Beraldo, H. (2003). Tin (IV) complexes of 2-benzoylpyridine N (4)-phenyl-thiosemicarbazone: spectral characterization, structural studies and antifungal activity. Applied organometallic chemistry, 17(12), 945-951.

149- Mousa, O. G., El-Hiti, G. A., Baashen, M. A., Bufaroosha, M., Ahmed, A., Ahmed, A. A., ... & Yousif, E. (2021). Synthesis of carvedilol–organotin complexes and their effects on reducing photodegradation of Poly (Vinyl Chloride). Polymers, 13(4), 500.

150- Sabaa, M. W., Oraby, E. H., Naby, A. S. A., & Mohamed, R. R. (2006). N-phenyl-3-substituted 5-pyrazolone derivatives as organic stabilizers for rigid poly (vinyl chloride) against photodegradation. Journal of applied polymer science, 101(3), 1543-1555.

151- Pospıšil, J., & Nešpurek, S. (2000). Photostabilization of coatings. Mechanisms and performance. Progress in Polymer Science, 25(9), 1261-1335.

152- Jafari, A. J., & Donaldson, J. D. (2009). Determination of HCl and VOC emission from thermal degradation of PVC in the absence and presence of copper, copper (II) oxide and copper (II) chloride. E-Journal of Chemistry, 6(3), 685-692.

153- Ramzan, S., Rahim, S., Hussain, S. T., Holt, K. B., Cockcroft, J. K., Muhammad, N., ... & Shujah, S. (2023). Synthesis, characterization, X-ray structure, DNA binding, antioxidant and docking study of new organotin (IV) complexes. Applied Organometallic Chemistry, 37(8), e7161.

154- Chaochanchaikul, K., Rosarpitak, V., & Sombatsompop, N. (2013). Photodegradation profiles of PVC compound and wood/PVC composites under UV weathering. Express Polymer Letters, 7(2).

155- Nief, O. A. (2015). Photostabilization of polyvinyl chloride by some new thiadiazole derivatives. European Journal of Chemistry, 6(3), 242-247.

156- Pi, H., Xiong, Y., & Guo*, S. (2005). The kinetic studies of elimination of HCl during thermal decomposition of PVC in the presence of transition metal oxides. Polymer-Plastic Technology and Engineering, 44(2), 275-288.

157- Balakit, A. A., Ahmed, A., El-Hiti, G. A., Smith, K., & Yousif, E. (2015). Synthesis of new thiophene derivatives and their use as photostabilizers for rigid poly (vinyl chloride). International Journal of Polymer Science, 2015.

158- Mahmood, Z. N., Yousif, E., Alias, M., El-Hiti, G. A., & Ahmed, D. S. (2020). Synthesis, characterization, properties, and use of new fusidate organotin complexes as additives to inhibit poly (vinyl chloride) photodegradation. Journal of Polymer Research, 27, 1-12.

159- Yaseen, A. A., Al-Tikrity, E. T., Yousif, E., Ahmed, D. S., Kariuki, B. M., & El-Hiti, G. A. (2021). Effect of ultraviolet irradiation on polystyrene containing cephalexin Schiff bases. Polymers, 13(17), 2982.

160- Yousif, E., Haddad, R., & Noaman, R. (2014). Photostabilization of Polystyrene Films: Photostabilization Activity of Polystyrene. LAP LAMBERT Academic Publishing.

161- Schmitt, T., Guttmann, P., Schmidt, O., Müller-Buschbaum, P., Stamm, M., Schönhense, G., & Schmahl, G. (2000, May). Microscopy of thin polymer blend films of polystyrene and poly-n-butyl-methacrylate. In AIP Conference Proceedings (Vol. 507, No. 1, pp. 245-249). American Institute of Physics.

162- El-Hiti, G. A., Alotaibi, M. H., Ahmed, A. A., Hamad, B. A., Ahmed, D. S., Ahmed, A., ... & Yousif, E. (2019). The morphology and performance of poly (vinyl chloride) containing melamine Schiff bases against ultraviolet light. Molecules, 24(4), 803.

163- Yousif, E., Ahmed, D. S., El-Hiti, G. A., Alotaibi, M. H., Hashim, H., Hameed, A. S., & Ahmed, A. (2018). Fabrication of novel ball-like polystyrene films containing Schiff base microspheres as photostabilizers. Polymers, 10(11), 1185.

164- Fonseca, J. D., Grause, G., Kameda, T., & Yoshioka, T. (2015). Effects of steam on the thermal dehydrochlorination of poly (vinyl chloride) resin and flexible poly (vinyl chloride) under atmospheric pressure. Polymer Degradation and Stability, 117, 8-15.

165-Shi, W., Zhang, J., Shi, X. M., & Jiang, G. D. (2008). Different photodegradation processes of PVC with different average degrees of polymerization. Journal of applied polymer science, 107(1), 528-540.

166- Mousa, O. G., El-Hiti, G. A., Baashen, M. A., Bufaroosha, M., Ahmed, A., Ahmed, A. A., ... & Yousif, E. (2021). Synthesis of carvedilol–organotin complexes and their effects on reducing photodegradation of Poly (Vinyl Chloride). Polymers, 13(4), 500.

167- Yaseen, A. A., Yousif, E., Al-Tikrity, E. T., El-Hiti, G. A., Kariuki, B. M., Ahmed, D. S., & Bufaroosha, M. (2021). FTIR, weight, and surface morphology of poly (vinyl chloride) doped with tin complexes containing aromatic and heterocyclic moieties. Polymers, 13(19), 3264.

168- Folarin, O. M., & Sadiku, E. R. (2011). Thermal stabilizers for poly (vinyl chloride): A review. Int. J. Phys. Sci, 6(18), 4323-4330.

169- Zheng, X. G., Tang, L. H., Zhang, N., Gao, Q. H., Zhang, C. F., & Zhu, Z. B. (2003). Dehydrochlorination of PVC materials at high temperature. Energy & fuels, 17(4), 896-900.

170- Mohammed, A., El-Hiti, G. A., Yousif, E., Ahmed, A. A., Ahmed, D. S., & Alotaibi, M. H. (2020). Protection of poly (vinyl chloride) films against photodegradation using various valsartan tin complexes. Polymers, 12(4), 969.

171- Li, D., Zhou, M., Xie, L., Yu, X., Yu, Y., Ai, H., & Tang, S. (2013). Synergism of pentaerythritol-zinc with β-diketone and calcium stearate in poly (vinyl chloride) thermal stability. Polymer journal, 45(7), 775-782.

172- Mohammed, R., El-Hiti, G. A., Ahmed, A., & Yousif, E. (2017). Poly (vinyl chloride) doped by 2-(4-isobutylphenyl) propanoate metal complexes: Enhanced resistance to UV irradiation. Arabian Journal for Science and Engineering, 42, 4307-4315.

173- Khalaf, M., Fadhil, Z., Al-Mashhadani, M. H., Abdallh, M., Bufaroosha, M., Majeed, A., ... & Yousif, E. (2020, November). PVC films performance stabilized by dibutyltin (IV) complex for sustainable environment. In Journal of Physics: Conference Series (Vol. 1664, No. 1, p. 012072). IOP Publishing.

174- Sabaa, M. W., Oraby, E. H., Naby, A. S. A., & Mohamed, R. R. (2006). N-phenyl-3-substituted 5-pyrazolone derivatives as organic stabilizers for rigid poly (vinyl chloride) against photodegradation. Journal of applied polymer science, 101(3), 1543-1555.

175- Shyichuk, A. V., & White, J. R. (2000). Analysis of chain-scission and crosslinking rates in the photo-oxidation of polystyrene. Journal of Applied Polymer Science, 77(13), 3015-3023.

176- Jasem, H., Hadi, A. G., El-Hiti, G. A., Baashen, M. A., Hashim, H., Ahmed, A. A., ... & Yousif, E. (2021). Tin-naphthalene sulfonic acid complexes as photostabilizers for poly (vinyl chloride). Molecules, 26(12), 3629.

177- Mahmood, Z. N., Yousif, E., Alias, M., El-Hiti, G. A., & Ahmed, D. S. (2020). Synthesis, characterization, properties, and use of new fusidate organotin complexes as additives to inhibit poly (vinyl chloride) photodegradation. Journal of Polymer Research, 27, 1-12.

178- Ahmed, A., El-Hiti, G. A., Hadi, A. G., Ahmed, D. S., Baashen, M. A., Hashim, H., & Yousif, E. (2021). Photostabilization of poly (vinyl chloride) films blended with organotin complexes of mefenamic acid for outdoor applications. Applied Sciences, 11(6), 2853.

179- Ali, M. M., El-Hiti, G. A., & Yousif, E. (2016). Photostabilizing efficiency of poly (vinyl chloride) in the presence of organotin (IV) complexes as photostabilizers. Molecules, 21(9), 1151.

180- Ahmed, D. S., El-Hiti, G. A., Hameed, A. S., Yousif, E., & Ahmed, A. (2017). New tetra-Schiff bases as efficient photostabilizers for poly (vinyl chloride). Molecules, 22(9), 1506.

181- Hadi, A. G., Baqir, S. J., Ahmed, D. S., El-Hiti, G. A., Hashim, H., Ahmed, A., ... & Yousif, E. (2021). Substituted organotin complexes of 4-methoxybenzoic acid for reduction of poly (vinyl chloride) photodegradation. Polymers, 13(22), 3946.

182- Venkateshaiah, A., Padil, V. V., Nagalakshmaiah, M., Waclawek, S., Černík, M., & Varma, R. S. (2020). Microscopic techniques for the analysis of micro and nanostructures of biopolymers and their derivatives. Polymers, 12(3), 512.

183- Sawyer, L. C., Grubb, D. T., & Meyers, G. F. (2008). Emerging Techniques in Polymer Microscopy. Polymer Microscopy, 435-477.

184- Valko, L., Klein, E., Kovařík, P., Bleha, T., & Šimon, P. (2001). Kinetic study of thermal dehydrochlorination of poly (vinyl chloride) in the presence of oxygen: III. Statistical thermodynamic interpretation of the oxygen catalytic activity. European polymer journal, 37(6), 1123-1132.

185- Kara, F., Aksoy, E. A., Yuksekdag, Z., Hasirci, N., & Aksoy, S. (2014). Synthesis and surface modification of polyurethanes with chitosan for antibacterial properties. Carbohydrate Polymers, 112, 39-47.

186- Shinato, K. W., Huang, F., & Jin, Y. (2020). Principle and application of atomic force microscopy (AFM) for nanoscale investigation of metal corrosion. Corrosion Reviews, 38(5), 423-432.

187- Sabaa, M. W., Mohamed, R. R., & Oraby, E. H. (2009). Vanillin–Schiff's bases as organic thermal stabilizers and co-stabilizers for rigid poly (vinyl chloride). European polymer journal, 45(11), 3072-3080.

188- Shaalan, N., Laftah, N., El-Hiti, G. A., Alotaibi, M. H., Muslih, R., Ahmed, D. S., & Yousif, E. (2018). Poly (vinyl chloride) photostabilization

in the presence of Schiff bases containing a thiadiazole moiety. Molecules, 23(4), 913.

189- Venkateshaiah, A., Padil, V. V., Nagalakshmaiah, M., Waclawek, S., Černík, M., & Varma, R. S. (2020). Microscopic techniques for the analysis of micro and nanostructures of biopolymers and their derivatives. Polymers, 12(3), 512.

190- El-Hiti, G. A., Ahmed, D. S., Yousif, E., Al-Khazrajy, O. S., Abdallh, M., & Alanazi, S. A. (2021). Modifications of polymers through the addition of ultraviolet absorbers to reduce the aging effect of accelerated and natural irradiation. Polymers, 14(1), 20.

191- Shi, W., Zhang, J., Shi, X. M., & Jiang, G. D. (2008). Different photodegradation processes of PVC with different average degrees of polymerization. Journal of applied polymer science, 107(1), 528-540.

192- Fadhil, M., Yousif, E., Ahmed, D. S., Kariuki, B. M., & El-Hiti, G. A. (2022). Synthesis and application of levofloxacin–tin complexes as new photostabilizers for polyvinyl chloride. Polymers, 14(18), 3720.

193- Hadi, A. G., Jawad, K., El-Hiti, G. A., Alotaibi, M. H., Ahmed, A. A., Ahmed, D. S., & Yousif, E. (2019). Photostabilization of poly (vinyl chloride) by organotin (IV) compounds against photodegradation. Molecules, 24(19), 3557.

194- Yousif, E., & Haddad, R. (2013). Photodegradation and photostabilization of polymers, especially polystyrene. SpringerPlus, 2(1), 1-32.

195- Mohamed, S. H., Hameed, A. S., El-Hiti, G. A., Ahmed, D. S., Kadhom, M., Baashen, M. A., ... & Yousif, E. (2021). A process for the synthesis and use of highly aromatic organosilanes as additives for poly (vinyl chloride) films. Processes, 9(1), 91.

196- Balakit, A. A., Ahmed, A., El-Hiti, G. A., Smith, K., & Yousif, E. (2015). Synthesis of new thiophene derivatives and their use as photostabilizers for rigid poly (vinyl chloride). International Journal of Polymer Science, 2015.

197- Hadi, A. G., Jawad, K., Yousif, E., El-Hiti, G. A., Alotaibi, M. H., & Ahmed, D. S. (2019). Synthesis of telmisartan organotin (IV) complexes and their use as carbon dioxide capture media. Molecules, 24(8), 1631.

198- Ikhlas, N. (2013). Uji Aktivitas Antioksidan Ekstrak Herba Kemangi (Ocimum americanum Linn) dengan Metode DPPH (2, 2-Difenil-1-Pikrilhidrazil).

199- Cahyani, A. I. (2017). Uji Aktivitas Antioksidan Dari Ekstrak Kulit Batang Kayu Jawa (Lannea coromandelica) Dengan Metode DPPH (2, 2-Difenil-1-Pikrilhidrazil) (Bachelor's thesis, UIN Syarif Hidayatullah Jakarta: Fakultas Kedokteran dan Ilmu Kesehatan, 2017).

200- Nastasijević, B., Lazarević-Pašti, T., Dimitrijević-Branković, S., Pašti, I., Vujačić, A., Joksić, G., & Vasić, V. (2012). Inhibition of myeloperoxidase and antioxidative activity of Gentiana lutea extracts. Journal of pharmaceutical and biomedical analysis, 66, 191-196.

201- Gabrielska, J., Soczyńska-Kordala, M., & Przestalski, S. (2005). Antioxidative effect of kaempferol and its equimolar mixture with phenyltin compounds on UV-irradiated liposome membranes. Journal of agricultural and food chemistry, 53(1), 76-83.

202- Bukhari, S. B., Memon, S., Tahir, M. M., & Bhanger, M. I. (2008). Synthesis, characterization, and investigation of antioxidant activity of cobalt–quercetin complex. Journal of Molecular Structure, 892(1-3), 39-46.

203-Dawidowicz, A. L., Wianowska, D., & Olszowy, M. (2012). On practical problems in estimation of antioxidant activity of compounds by DPPH method (Problems in estimation of antioxidant activity). Food chemistry, 131(3), 1037-1043.

204- Gombert, M., Garcia, A. C., Luna, J. C., & Franch, P. C. (2018). A new procedure for the Antioxidant capacity dpph assessment in small samples.

205- Yuniarti, R., Nadia, S., Alamanda, A., Zubir, M., Syahputra, R. A., & Nizam, M. (2020, February). Characterization, phytochemical screenings and antioxidant activity test of kratom leaf ethanol extract (Mitragyna speciosa Korth) using DPPH method. In Journal of Physics: Conference Series (Vol. 1462, No. 1, p. 012026). IOP Publishing.

206-Phongpaichit, S., Nikom, J., Rungjindamai, N., Sakayaroj, J., Hutadilok-Towatana, N., Rukachaisirikul, V., & Kirtikara, K. (2007). Biological activities of extracts from endophytic fungi isolated from Garcinia plants. FEMS Immunology & Medical Microbiology, 51(3), 517-525.

207- Apak, R., Güçlü, K., Özyürek, M., Karademi˙ r, S. E. N., & Altun, M. (2005). Total antioxidant capacity assay of human serum using copper (II)-neocuproine as chromogenic oxidant: the CUPRAC method. Free radical research, 39(9), 949-961.

208- Özyürek, M., Güçlü, K., Tütem, E., Başkan, K. S., Erçağ, E., Çelik, S. E., ... & Apak, R. (2011). A comprehensive review of CUPRAC methodology. Analytical methods, 3(11), 2439-2453.

209- Özyürek, M., Güçlü, K., Tütem, E., Başkan, K. S., Erçağ, E., Çelik, S. E., ... & Apak, R. (2011). A comprehensive review of CUPRAC methodology. Analytical methods, 3(11), 2439-2453.

210- Abdel-Aty, A. M., Salama, W. H., Fahmy, A. S., & Mohamed, S. A. (2019). Impact of germination on antioxidant capacity of garden cress: new calculation for determination of total antioxidant activity. Scientia Horticulturae, 246, 155-160.

211- Hadi, A. G., Hassen, T. F., & Mahdi, I. J. (2022). Synthesis, characterization, and antioxidant material activities of organotin (IV) carboxylates with tin-para methoxy benzoic acid. Materials Today: Proceedings, 49, 2797-2801.

212- Munteanu, I. G., & Apetrei, C. (2021). Analytical methods used in determining antioxidant activity: A review. International Journal of Molecular Sciences, 22(7), 3380.

213- Fidrianny, I., Anggraeni, N. A. S., & Insanu, M. (2018). Antioxidant properties of peels extracts from three varieties of banana (Musa sp.) grown in West Java-Indonesia. International Food Research Journal, 25(1).

214- Flieger, J., Flieger, W., Baj, J., & Maciejewski, R. (2021). Antioxidants: Classification, natural sources, activity/capacity measurements, and usefulness for the synthesis of nanoparticles. Materials, 14(15), 4135.

215- Chelalba, I., Rebiai, A., Debbeche, H., Begaa, S., Messaoudi, M., & Benchikha, N. (2021). Total phenol and flavonoid content, antioxidant and cytotoxicity assessment of Algerian Launaea glomerata (Cass.) Hook. f. extracts. European Journal of Biological Research, 11(2), 168-176.

216- Egharevba, E., Chukwuemeke-Nwani, P., Eboh, U., Okoye, E., Bolanle, I. O., Oseghale, I. O., ... & Falodun, A. (2019). Evaluation of the antioxidant and hypoglycaemic potentials of the leaf extracts of Stachytarphyta jamaicensis (Verbenaceae). Tropical Journal of Natural Product Research, 3(5), 170-174.

217- Hashim, D. J., Falah, T. F., & Hadi, A. G. (2022). Enhanced Antioxidant Activity of Di-and Triorganotin Complexes Derived from Mefenamic Acid. Egyptian Journal of Chemistry, 65(5), 483-490.

الخلاصة:

تم تخليق اثنا عشر معقداً من القصدير العضوي (IV) بنجاح عن طريق تفاعلات تكثيف الليكاندات (السيفالكسين والتايروسين) مع مركبات القصدير العضوية (IV) الثنائية والثلاثية الذائبة في الميثانول. واستخدم التحليل الأولي لدراسة الصفات الفيزيائية و التحليل الطيفي للأشعة تحت الحمراء والرنين النووي المغناطيسي (^{119}Sn- NMR و ^{1}H,^{13}C) للمعقدات. استخدمت المعقدات المحضرة كمثبتات لمنع التكسير الضوئي لأفلام البولي فنيل كلورايد (بسُمك 40 مايكرومتر) عند تعرضها للأشعة فوق البنفسجية، مما يؤدي إلى فقدان الوزن، ونمو مجموعات وظيفية محددة (الهيدروكسيل والكربونيل والبوليين)، فضلا عن التغيرات في التركيب الكيميائي. اختبرت تضاريس السطح للأفلام باستخدام المجهر والفحص المجهري للقوة الذرية والمسح المجهري الإلكتروني. اذ أظهرت معقدات البولي فنيل كلورايد التي تحتوي على مركبات القصدير العضوية (IV) تشققات وأضرارًا سطحية أقل من الفلم النقي. وقد وجد ان المعقد Me_2SnL_2-Cephalexin هو المثبت الضوئي الأكثر تأثيرا على افلام البولي فنيل كلورايد بسبب وجود العديد من مجاميع الميثيل التي تمتلك أقل اعاقة فراغية بالإضافة الى الذرات غير متجانسة التي تسمح بتكوين تجاذبات قطبية مع البولي فنيل كلورايد. كان عامل الخشونة (Rq) للفلم النقي بعد 300 ساعة من التشعيع كبيرًا 316.2 مقارنة بالمركب Me_2SnL_2 حيث وجد انه يساوي 67.2. تم اجراء دراسة النشاط المضاد للأكسدة لمعقدات القصدير العضوية (IV) بطريقتين DPPH, CUPRAC من خلال المقارنة مع حامض التانيك (وهو مضاد أكسدة مرجعي) . تُظهر معقدات القصدير العضوية (IV) نشاطًا مضادًا للأكسدة أكبر من الليكاند ضد الجذور الحرة بسبب الشق الفلزي الموجود في المعقدات. وكانت قيم IC_{50} للمعقدات أقل من قيم حمض التانيك. يتمتع المعقد Me_3SnL -Cephalexin بقوة عالية ضد الجذور الحرة ، ويمتلك قوة مضادة للجذور الحره (ARP) و قيمة تركيز المثبط (IC_{50}) منخفضة ، كما يتضح من نتائج اختبارات DPPH و CUPRAC. اعطت التراكيز 40 و 50 µg/ml نسبة أكبر لمكافحة نشاط الجذور الحرة.

جمهورية العراق
وزارة التعليم العالي والبحث العلمي
كلية العلوم /جامعة بابل
قسم الكيمياء

تخليق مركبات قصدير جديدة ودراسة تطبيقاتها كمثبتات ضوئية للبولي فنيل كلورايد وكمضادات للأكسدة

أطروحة مقدمة الى

مجلس كلية العلوم – جامعة بابل

وهي جزء من متطلبات نيل درجة دكتوراه فلسفة في العلوم / الكيمياء

من قبل

رافد ريس عراك ضاحي

(بكالوريوس علوم كيمياء / جامعة بابل / كلية العلوم (2007)

(ماجستير علوم كيمياء لا عضوية /جامعة بابل / كلية العلوم (2019)

بإشراف

أ.م.د انغام غانم هادي

1445 هـ

2023 م